# The zebrafish as a model for *Epithelioid hemangioendothelioma* (EHE)

Eleanor R Markham

Submitted for the degree of
Doctor of Philosophy

School of Biosciences

November 2024

# Table of Contents

*I, Eleanor Markham, confirm that the Thesis is my own work. I am aware of the University's Guidance on the Use of Unfair Means (www.sheffield.ac.uk/ssid/unfair-means). This work has not previously been presented for an award at this, or any other, University.*

*Small sections from this thesis have been published online as part of Scientia News articles: https://www.scientianews.org/*

# Acknowledgements

Massive thanks to Freek, for everything.
Thanks to Will. Coward for the huge encouragement and Arunima Panda for further encouragement.
Thanks to my advisors**,** Vincent Cunliffe, and Henry Roehl, for experimental discussion and ideas.
Thanks to Rob. Wilkinson, Rosemary Kim, and Stone Elworthy, for solid Science training. Thanks to Maggie Glover, Pam Ellis, Nick Van Hateren, and Stone for training/generally facilitating my research.
Thanks also to Robin Young for the project and thanks to the EHE charity (UK) for funding.
Thanks to Stew for listening to it all.
Thanks to my parents.
Thanks.

Dedicated to Peggy Marsh.

"One day, hopefully many years in the future, we all get to look back on our lives and we'd better like what we see because by then, it'll be too late to do anything about it. The only time to do that is right now."

C. Gray

# Abbreviations

Ab – Antibody

ALL – Acute lymphoid leukaemia

ANKHD1 – Ankyrin-repeat and KH domain containing 1

AP-1 – Activator protein-1

ATAC – Ada2a-containing histone acetyltransferase

BAC – Bacterial artificial chromosome

bHLH – basic helix loop helix

BRD4 – Bromodomain-containing protein 4

CAMTA1 - Calmodulin binding transcription activator 1

CCL2 – C-C motif chemokine ligand 2

CCND1 – Cyclin D1

CDC25 – Cell division cycle 25

CDK1 – Cyclin-dependent kinase 1

CDK9 – Cyclin-dependent kinase 9

CDKN2a/b – Cyclin-dependent kinase inhibitor 2a/b

CFP – Cyan fluorescent protein

ChIP – Chromatin immunoprecipitation

CML – Chronic myeloid leukaemia

CPSF – Cleavage & polyadenylation specificity factor

CRISPR – Clustered regularly interspaced short palindromic repeats

CRY – Crystallin

CSC – Cancer stem cell

CstF – Cleavage stimulation factor

CTGF – Connective tissue growth factor

CXCL5 – C-X-C motif chemokine ligand 5

Cyr61 – Cysteine-rich angiogenic inducer

DA – Dominant active

DE – Differentially expressed

Dpf – Days post-fertilisation

ECM – Extracellular matrix

EGR2 – Early growth response gene 2

EHE – Epithelioid hemangioendothelioma

EMT – Epithelial to mesenchymal transition

ES – Enrichment score

ESC – Embryonic stem cell

EtOH - Ethanol

FPKM – Fragments per kilobase per million

GEMM – Genetically engineered mouse model

GFP – Green fluorescent protein

GSEA – Gene set enrichment analysis

HAT – Histone acetyltransferase

HCC – Hepatocellular cancer

Hif1α – Hypoxia inducible factor $1^{\alpha}$

HMEJ – Homology-mediated end joining

HR – Homologous recombination

IGV – Integrated genomics viewer

IHC – Immunohistochemistry

ILK – Integrin-linked kinase

IMS – Industrial methylated spirit

ISVs – Intersegmental vessels

ITGβ1 – Tumour integrin β1

KAT14 – Lysine acetyltransferase 14

LATS1/2 - Large tumour suppressor 1 and 2

LKB1 – Liver kinase B1

LPA – Lysophosphatidic acid

LZ – Leucine zipper

MAML1/2 – Mastermind like transcriptional coactivator 1/2

MAPK – Mitogen activated protein kinase

MCM – Minichromosome maintenance

MDS – Myelodysplastic syndrome

MED1 - Mediator of RNA polymerase II transcription subunit 1

MeOH - Methanol

MiTF – Microphthalmia-associated transcription factor

MOB1 – Mps one binder 1

NES – Normalised enrichment score

NLS – Nuclear localisation signal

PA – Poly A

PAR1 – Protease activated receptor 1

PAS – Polyadenylation site

PBS – Phosphate buffered saline

PBT – PBS Tween

PCA – Principal component analysis

PD-L1 – Programmed death ligand 1

PFA - Paraformaldehyde

PNST – Peripheral nerve sheath tumour

RFP – Red fluorescent protein

RMS - Rhabdomyosarcoma

RT – Room temperature

S1P – Sphingosine 1-phosphate

SAV1 – Salvador 1

SCLC – Small cell lung cancer

SEM – Standard error of the mean

Sib - Sibling

T-ALL - T-cell acute lymphoid leukaemia

TAD – Transactivation domain

TAZ - Transcriptional co-activator with a PDZ-motif

TBD – TEAD binding domain

TC – TAZ-CAMTA1

TEAD – Transcription enhanced associated domain

TFE3 – Transcription Factor binding to IGHM enhancer 3

TIG – Transcription factor immunoglobulin domain

TSS – Transcription start site

UTR – Untranslated region

WT – Wild type

WWTR1 - WW Domain-containing transcription regulator protein 1

YAP1 - Yes-associated protein 1

Yeats2 – Yeats containing domain 2

Yr - Year

YT – YAP1-TFE3

ZZZ3 – Zinc-finger zz-type containing 3

# List of Figures

# List of Tables

# 1 Abstract

*Epithelioid hemangioendothelioma* (EHE) is a rare sarcoma of the endothelial cells lining the blood vessels. 90% of cases show a translocation resulting in the TAZ-CAMTA1 fusion protein, and 10% have a translocation resulting in the YAP1-TFE3 fusion. Although EHE is rare, it is driven by constitutively activated YAP/TAZ signalling. Hippo is a vital pathway involved in many cancers, hence any breakthroughs here may also have significant implications for other cancers. As there are no specific treatments for EHE, there is a great need for *in vivo* models.

I aimed to create a TAZ-CAMTA1 and a YAP1-TFE3 zebrafish model to further characterise EHE. I initially created a TAZ-CAMTA1 model but found that although TAZ/CAMTA1 target genes were induced, expression levels of the oncogene were low, and unexpectedly, transcription stopped early in CAMTA1, exon 15. In an attempt to promote tumour formation in this line, CDKN2 mutations were induced in this background, as these are the most common secondary mutations in EHE disease. However, few tumours arose from this additional mutation. One potential issue was that the TAZ-CAMTA1 gene is extremely long, which may impair high levels of expression. Therefore, a much shorter YAP1-TFE3 model was created to overcome these issues. However, there were also problems with this as it was found, unexpectedly, that YAP1-TFE3 expression levels appeared to be reduced upon activation. In addition, I generated an alternative version of TAZ-CAMTA1 to attempt to address the poor expression encountered during this work, but this did not appear to solve these issues. However, this was not conclusive, as RNAseq was not performed on these transgenics. It can be concluded that the expression of these transgenes is surprisingly difficult, and the use of xenotransplants may be the way forward to create a preclinical model to test potential disease-modifying drugs, for treatment of EHE.

# 2 Introduction

## 2.1 Molecular basis of EHE disease

*Epithelioid hemangioendothelioma* (EHE) is an extremely rare soft tissue sarcoma of the endothelial cells lining the blood vessels (Sardaro et al., 2014). EHE prevalence is estimated to be around one in one million (Lau et al., 2011). It is most common in liver, lung, and bone (Sardaro et al., 2014), and is unusual as it can be indolent for years, or conversely highly active. Also, unusually, the course of the disease is unpredictable, with widespread disease unlinked to life expectancy. Most diagnoses are in middle age (Deyrup et al., 2008), and there is no standard treatment, owing to the rarity of the disease (Sardaro et al., 2014). EHE was characterised in 1982, when Weiss and Enzinger noted a vascular tumour of bone and soft tissue which exhibited features between *hemangioma* and *angiosarcoma*, naming it *epithelioid hemangioendothelioma* (Weiss and Enzinger, 1982).

A major breakthrough occurred in 2011, when it was discovered that specific gene fusions were present in EHE tumours (Errani et al., 2011, Tanas et al., 2011). It was found that 90% of cases show a translocation to create the Transcriptional co-activator with a PDZ-motif (TAZ)-Calmodulin binding transcription activator 1 (CAMTA1) fusion protein (Flucke et al., 2014), with 45% of EHE cases having this as a sole genetic aberration (Seavey et al., 2021). TAZ is officially known as WW Domain-containing Transcription Regulator Protein 1 (WWTR1), but it will be referred to as TAZ from hereon. The TAZ-CAMTA1 (TC) fusion gene is the result of a t(1;3)(p36;q25) translocation (Errani et al., 2011, Mendlick et al., 2001), with the N-terminus of TAZ bound to the C-terminus of CAMTA1 (Tanas et al., 2016). The Transcription enhanced associated domain (TEAD), containing a DNA binding domain, is bound to a 14-3-3 protein binding motif, bound to the majority of the WW domain (from TAZ), fused to a section of CAMTA1. CAMTA1 consists of the transactivation domain (TAD), transcription factor immunoglobulin (TIG) domain, ankyrin repeats, IQ (calmodulin-binding) domains, and nuclear localisation signal (NLS) (Tanas et al., 2016) (Fig. 1A). TC is comprised of exons 2/3/4 from TAZ, fused in frame to exon 8/9 from CAMTA1 (Tanas et al., 2011(Errani et al., 2011). In atypical cases, TAZ-MAML2 or TAZ-ACTL6A gene fusions have also been found in cardiac EHE (Suurmeijer et al., 2020).

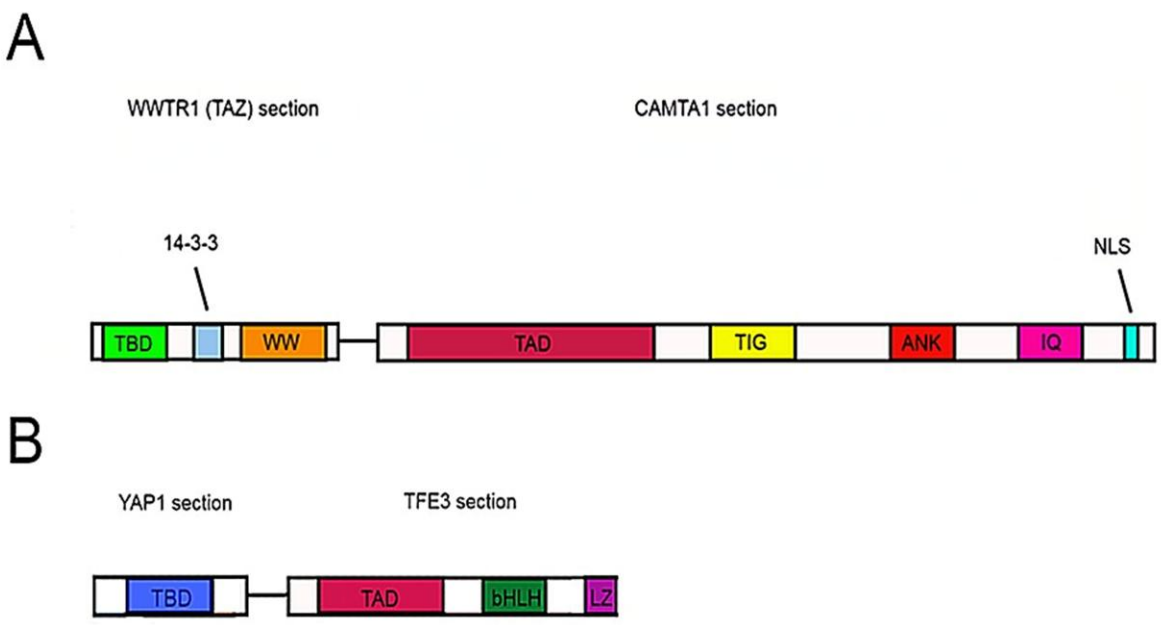


Fig. 1: TAZ-CAMTA1 and YAP1-TFE3 structure
A) TAZ-CAMTA1 structure. The TAZ section comprises a TEAD binding domain (TBD), 14-3-3, and a WW domain. This fuses to the CAMTA1 section, which comprises a transactivation domain (TAD), transcription factor immunoglobulin (TIG), IQ and nuclear localisation signal (NLS) domains.
B) YAP1-TFE3 structure. The YAP1 section comprises TBD. This fuses to the TFE3 section, which comprises a TAD, bHLH (basic helix loop helix), and LZ (leucine zipper) domain.

Subsequently, it was found that the remaining 10% derive from a Yes-associated Protein (YAP)-Transcription Factor binding to IGHM enhancer 3 (TFE3) fusion gene (Antonescu et al., 2013). YAP1-TFE3 consists of the TEAD-binding domain (TBD) from YAP1, and a transactivation domain (TAD), a basic helix loop helix (bHLH), and a leucine zipper (LZ) from TFE3 (Antonescu et al., 2013) (Fig. 1B). YAP1-TFE3 (YT) consists of exon 1 from YAP1, and exon 4-10 from TFE3 (Antonescu et al., 2013). It has been shown that the nuclear localisation of YAP1-TFE3 occurs via an NLS from TFE3 (Szulzewsky et al., 2020). In atypical cases, other YAP1 fusions have also been found, such as YAP1-MAMLD1, YAP1-SS18, and YAP1-FAM118B, YAP1-MAML2, but these cause cancers such as Supratentorial ependymoma, Cervical squamous cell carcinoma/Endocervical adenocarcinoma, and NF2-wild type meningioma/porocarcinoma, and not EHE (Pajtler et al., 2015, Pajtler et al., 2019, Hu et al., 2018) (Szulzewsky et al., 2021). Also, patients with YT fusion gene have been shown to have an

improved, 5-year survival rate (86%) than patients with TC (59%) (Rosenbaum et al., 2020). Therefore, Hippo signalling is a crucial pathway in EHE disease, as YAP and TAZ fusions have been found to cause EHE (Antonescu et al., 2013, Errani et al., 2011, Tanas et al., 2011), and YAP1 and TAZ are both transcriptional coactivators of the Hippo pathway, which is a tumour suppressor that also controls tissue growth in vertebrates (Dong et al., 2007, Wu et al., 2003, Varelas, 2014).

## 2.2 EHE morphology

EHE is usually characterised by strands, or nests of epithelioid cells, along with an eosinophilic cytoplasm and cytoplasmic vacuoles, in a myxohaline stroma (connective tissue) (Fig. 2, A&B). YAP-TFE3 EHE shows elements involved in blood vessel formation, however TC EHE does not (Stacchiotti et al., 2021a).

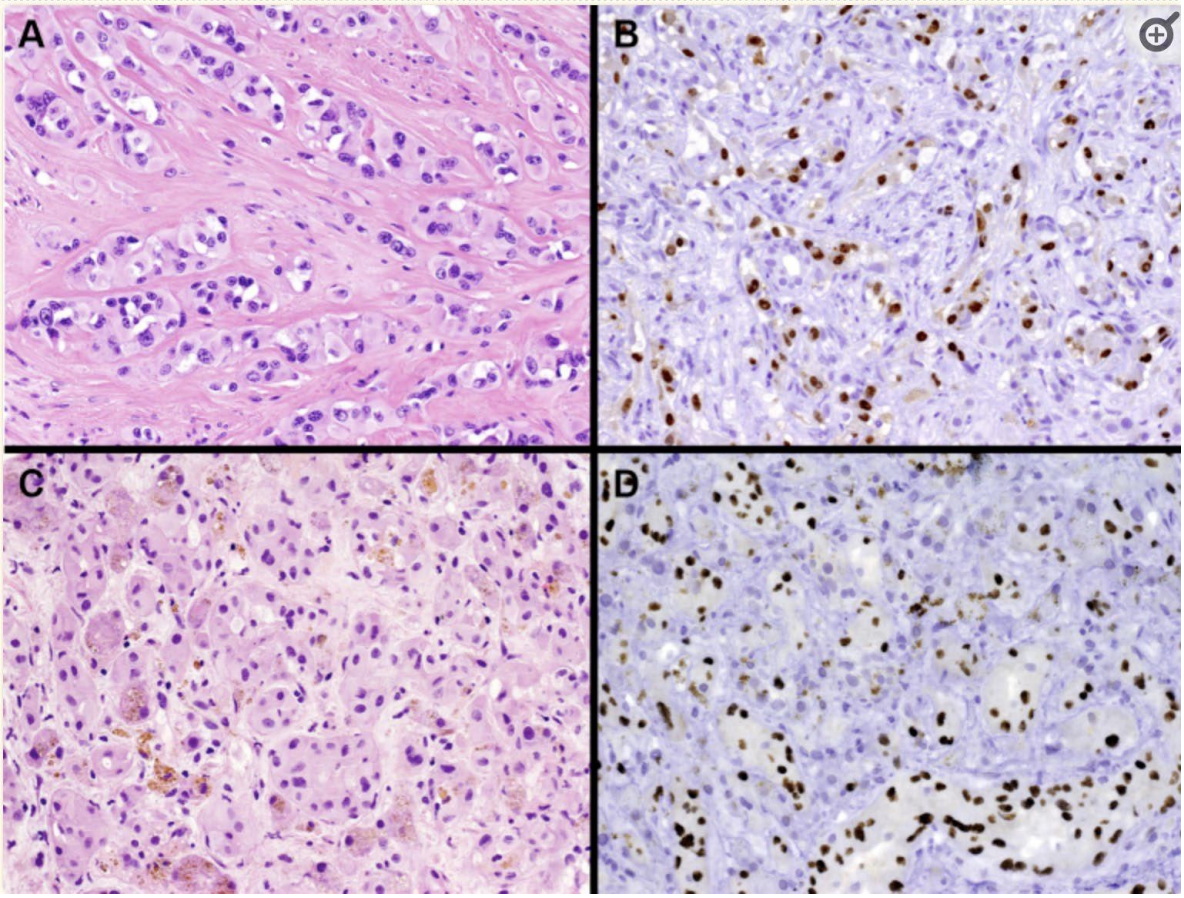


Fig 2: EHE morphology
A: H&E staining of TAZ-CAMTA1 EHE (nuclei in purple, epithelioid cells arranged in strands in pink)
B: CAMTA1 Ab staining of TAZ-CAMTA1
EHE (nuclei in brown)
C: H&E staining of YAP1-TFE3 EHE (nuclei in purple) D: TFE3 Ab staining of YAP1-TFE3 EHE (nuclei in brown)



## 2.3 Current EHE treatment

Currently, EHE has no standard treatment (Sardaro et al., 2014). For EHE in soft tissue, surgery is the favourable treatment (Stacchiotti et al., 2021a). Radiotherapy is occasionally used, as EHE is radiotherapy sensitive, but using this as a treatment for EHE disease has not been well studied (Stacchiotti et al., 2021a). Thalidomide (Soape et al., 2015), interferon (Moon et al., 2009, Radzikowska et al., 2008), mTOR inhibitors (Soape et al., 2015, Engel et al., 2020, Riou et al., 2012, Cohen et al., 2012, Bagan et al., 2006), and multi-tyrosine kinase/VEGF inhibitors (Shiba et al., 2018,

Saada et al., 2014, Kollar et al., 2017, Chevreau et al., 2013, Agulnik et al., 2013, Yousaf et al., 2015, Zheng et al., 2017), have all been used to some clinical effect for systemic treatment in EHE disease (Stacchiotti et al., 2021a). Liver transplant is used as a treatment for hepatic EHE, but disease has been shown to recur in some cases: out of 59 patients, 23.7% had recurrent disease, after a follow-up with a mean of 49 months (Lerut et al., 2007) (Rosenberg and Agulnik, 2018).

More recently the MEK inhibitor, Trametinib, has also been used in a phase II clinical trial: this showed that there was a median of 10.4 months for progression-free survival, and EHE-related pain decreased upon treatment (after 4 weeks, in patients also using opiates) (Schuetze et al., 2024). In a study with Sirolimus (mTOR inhibitor), there was stable disease in 75.7% patients. Patients were followed up at a 41.5 month median, with the median progression-free survival at 13 months, and median overall survival at 18.8 months (Stacchiotti et al., 2021b).

In addition, a patient-derived xenograft (PDX) model was created, which recapitulated the original tumour histologically, with TC gene fusion existence, and overall transcriptomic profile. This model was used to test drugs such as Doxorubicin and Sirolimus. Sirolimus gave 69-81% inhibition of tumour volume, in relation to drug dose (Stacchiotti et al., 2023).
TEAD inhibitors are also another avenue of possible treatment, with NCT04857372, NCT05228015, and NCT04665206 all currently being used in clinical trials for solid tumours (EHE inclusive) (Stacchiotti et al., 2023).

## 2.4 Hippo pathway

The identified protein fusions underlying EHE point to the Hippo pathway as a major driver (Tanas et al., 2011, Antonescu et al., 2013, Errani et al., 2011). The Hippo pathway is a serine/threonine kinase pathway, which regulates tissue growth via the control of cell proliferation, and apoptosis, and was discovered in a *Drosophila* genetic screen (Harvey and Tapon, 2007, Pan, 2010, Halder and Johnson, 2011, Yu et al., 2015b, Zheng and Pan, 2019, Wu et al., 2003). Loss of Hippo results in an overgrowth phenotype (Wu et al., 2003). In mammalian cell culture, contact inhibition occurs when cells cease proliferating on contact with other cells, forming a monolayer (Eagle and Levine, 1967). Hippo has been shown to control this (Zhao et al., 2007, Zhao et al., 2008, Aragona et al., 2013). When cells are at a low density/spread on a stiff extracellular matrix (ECM), YAP/TAZ move to the nucleus, where they are involved in transcription. When cells are at high density/spread on soft ECM, YAP/TAZ are

found inactive in the cytosol (Aragona et al., 2013, Dupont et al., 2011, Wada et al., 2011) (Pavel et al., 2018).

Genetic and molecular analysis has resulted in a Hippo signal transduction model, which shows how this pathway functions in cells (Fig. 2). When the Hippo pathway is activated, YAP and TAZ are inhibited by phosphorylation via the Hippo kinases, Large tumour suppressor 1 and 2 (LATS1/LATS2) (Wu et al., 2003, Justice et al., 1995). Sterile-20 related (MST) kinases are auto-phosphorylated (Deng et al., 2003, Praskova et al., 2004), which in turn phosphorylate LATS (Chan et al., 2005). LATS also auto-phosphorylate (Chan et al., 2005, Hergovich et al., 2006, Praskova et al., 2008), and it has been shown that both types of phosphorylation are vital to LATS1/2 activation (Galan and Avruch, 2016). LATS1/2 has been shown to be phosphorylated independently of MST1/2, via MAPK1/2/3/5 and MAPK4/6/8 (Zheng et al., 2015, Meng et al., 2015). TAZ has four serine residues which interact with LATS1, and YAP has five serine residues, which interact with LATS2 (Garcia et al., 2022). MOB1 and SAV1 are both known to be scaffold proteins, which also become phosphorylated and aid LATS1/2 activity (Ni et al., 2015, Callus et al., 2006, Chan et al., 2005, Hong et al., 2016). LATS1/2 phosphorylation causes phosphorylation of YAP/TAZ, which leads to cytoplasmic localisation, by YAP/TAZ binding to 14-3-3 proteins and ubiquitin-dependent degradation (Dong et al., 2007, Zhao et al., 2007, Kanai et al., 2000, Liu et al., 2010). This is further promoted through phosphorylation via casein kinase 1δ/ϵ, which causes SCF ubiquitin ligase to degrade YAP/TAZ (Liu et al., 2010, Zhao et al., 2010) (Meng et al., 2016).

YAP/TAZ bind to TEAD to enable transcription of target genes (Vassilev et al., 2001, Chan et al., 2009), such as connective tissue growth factor (CTGF), and cysteine-rich angiogenic inducer 61 (CYR61), (Zhao et al., 2008, Zhang et al., 2011, Zhang et al., 2009, Lai et al., 2011). There are also many other target genes, such as ANKRD1, CCND1, AREG, AMOT, AXL, MYC, and ADAMTS1, which are associated with migration, proliferation, ECM remodelling, and angiogenesis (Mokhtari et al., 2023, Ehmer and Sage, 2016, Boopathy and Hong, 2019). Also, the Hippo pathway is able to crosstalk with Notch, Wnt, TGFβ, Shh, BMP4, and EGFR pathways (Yu et al., 2015a, Zinatizadeh et al., 2021, Varelas and Wrana, 2012).

YAP and TAZ are paralogues, and both have a WW domain, a coil-coil domain, a transcription activation domain, and a TEAD-binding domain (Kanai et al., 2000, Zhang et al., 2009, Komuro et al., 2003, Lamar et al., 2012). However, although YAP and TAZ can both bind RUNX (Cui et al., 2003,

Vitolo et al., 2007), they also have their own specific transcription factor binding partners, such as ErbB4, Smad1 and p73 (YAP), and PPARγ, TBX5, TTF-1, and Pax3 (TAZ) (Strano et al., 2001, Komuro et al., 2003, Alarcon et al., 2009, Omerovic et al., 2004, Murakami et al., 2005, Murakami et al., 2006, Park et al., 2004, Hong et al., 2005) (Lu et al., 2020).

YAP/TAZ has also been shown to activate transcription of YAP/TAZ regulators, such as LATS1/2, NF2, and AMOT, in a negative feedback loop (Dai et al., 2015, Moroishi et al., 2015b) (Luo et al., 2023). As EHE is driven by constitutively activated YAP/TAZ signalling (Tanas et al., 2016), negative regulators of the pathway are of significant interest. YAP-TEAD binding has been shown to be supressed by vestigial-like family member 4 (VGLL4) and verteporfin (Deng and Fang, 2018, Liu-Chittenden et al., 2012). VGLL4 is a transcriptional cofactor and tumour suppressor. It binds to TEADs, competing with YAP (Deng and Fang, 2018), and also supports degradation of TEAD1 (Lin et al., 2016). Verteporfin is a chemical which acts as a photosensitizer (Henney, 2000), and has been shown to interrupt YAP-TEAD binding, and impede YAP-induced oncogenic growth by preventing YAP activation (Liu-Chittenden et al., 2012). It downregulates cyclinD1 and cyclinE1, activates PARP, and regulates Bcl-2 proteins, resulting in apoptosis (Wei et al., 2017). It also suppresses Angiopoietin-2 (Ang2), which is a growth factor involved in angiogenesis (Wei et al., 2017, Maisonpierre et al., 1997, Akwii et al., 2019).

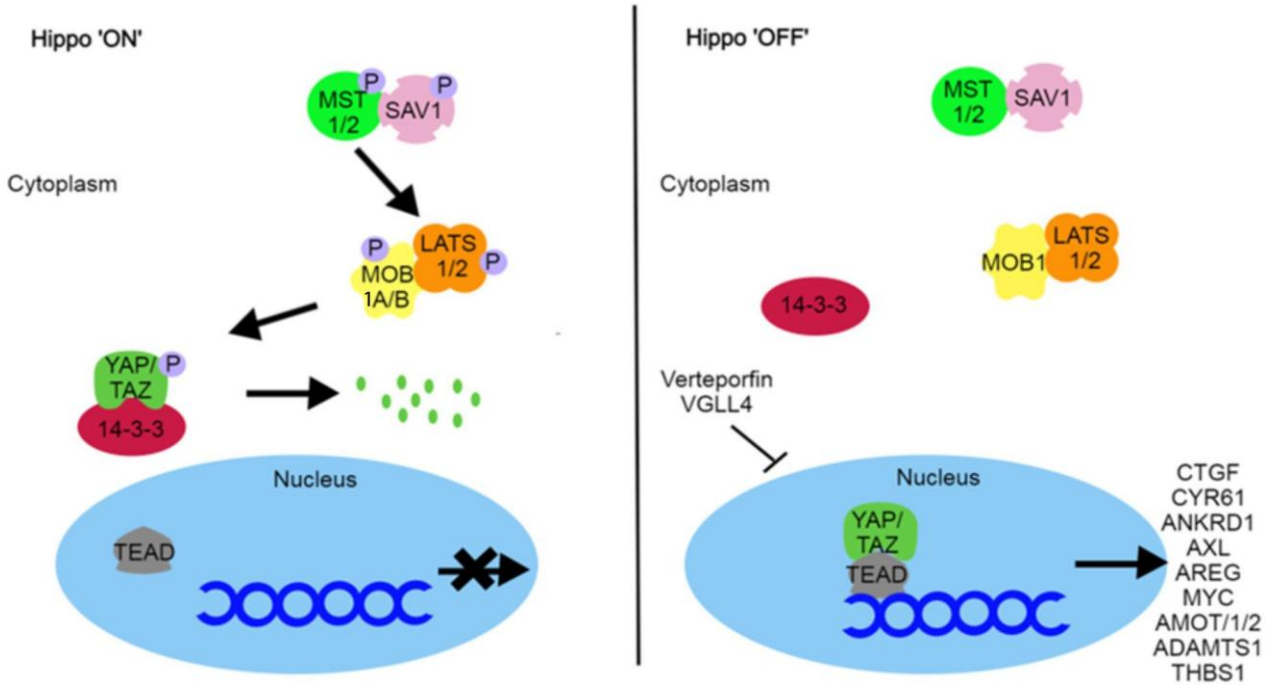


Fig. 3: The Hippo pathway when 'on' and 'off'
When the Hippo pathway is 'on' (left), MST1/2 causes phosphorylation of LATS1/2, which in turn causes phosphorylation of YAP/TAZ. YAP/TAZ is phosphorylated and degraded in the cytoplasm.
When the Hippo pathway is 'off' (right), YAP/TAZ move into the nucleus, where TEAD is bound, then this complex is involved in transcription of several different genes, such as CTGF (connective tissue growth factor). VGLL4 and Verteoporfin have both been shown to suppress YAP/TEAD binding.

## 2.5 Hippo pathway in EHE disease

Mutations in YAP/TAZ which lead to tumours usually arise from gene fusions, as opposed to point mutations, which are very rare (Zanconato et al., 2016b, Garcia et al., 2022). As previously stated, EHE is primarily caused by TC and YT fusion genes (Errani et al., 2011, Tanas et al., 2011, Antonescu et al., 2013). TAZ and YAP are usually phosphorylated on vital serine residues, TAZ-S89, TAZ-S311, YAP-S127 and YAP1-381 (Lei et al., 2008, Zhao et al., 2010, Zhao et al., 2012, Zhao et al., 2007). Phosphorylation would usually lead to degradation in the cytoplasm by YAP/TAZ binding to 14-3-3 proteins and ubiquitin-dependent degradation (Dong et al., 2007, Zhao et al., 2007, Kanai et al., 2000,

Liu et al., 2010), but in EHE disease, even though TAZ-S89 is phosphorylated (Tanas et al., 2016, Tanas et al., 2011, Seavey et al., 2021, Driskill et al., 2021), TC is still able to move to the nucleus and is involved in aberrant transcription (Tanas et al., 2016). TC is able to bind LATS1 (Merritt et al., 2021, Driskill et al., 2021), and, importantly, it has been found to bind more strongly to TEAD than TAZ alone (Chan et al., 2009) (Garcia et al., 2022). However, in EHE disease caused by YT, YAP-S127 and YAP-S381 are not present (Szulzewsky et al., 2020, Merritt et al., 2021). Although it is possible other residues could still be phosphorylated, YT has a presumed NLS from the bHLH TFE3 domain, which would allow it to be drawn into the nucleus nonetheless (Kauffman et al., 2014).

In EHE disease, even though TC is phosphorylated, it is still bound to TEAD in the nucleus, where it is involved in aberrant gene transcription (Tanas et al., 2016) (Fig. 4). The N-terminal section of TAZ is constitutively activated through its fusion to CAMTA1 protein, and hence freed from negative regulation of the Hippo pathway (Tanas et al., 2016). 90% of TC comprises CAMTA1, but it is TAZ which mainly drives transcription, and it is this which contains the TEAD binding domain (Tanas et al., 2016). TEAD transcription factors bind TC to DNA, hence activating transcription, and the CAMTA1 section donates the strong nuclear localisation signal (NLS) (Tanas et al., 2016). The TAZ WW domain has been shown to interact with transcription factors such as TBX5 (Murakami et al., 2005), Runx2, PPAR-γ (Hong et al., 2005), and SMADs (Varelas et al., 2008), but is not essential for functional TC, unlike TEAD (Merritt et al., 2018). Auto-palmitoylation on the sulfhydryl of a conserved cysteine is a prerequisite for TEAD activation (Chan et al., 2016, Noland et al., 2016), hence drugs which inhibit TEAD auto-palmitoylation could be examined for therapeutic treatment of EHE (Chan et al., 2016). CAMTA1 provides an NLS signal, but otherwise its role in EHE is much less well-defined (Tanas et al., 2011). It is known to be a transcription factor, which, surprisingly, is thought to act as a tumour suppressor involved in neural cancers, but otherwise it is not extensively characterised (Barbashina et al., 2005, Henrich et al., 2011, Henrich et al., 2012, Schraivogel et al., 2011).

In SW872 cell culture, from chromatin immunoprecipitation (ChIP) peak data, and also from unbiased motif enrichment analysis, TC has been shown to be enriched for the transcription factor, early growth response gene 2 (EGR2) binding motif, which is involved in neural development, and YT for microphthalmia-associated transcription factor (MiTF) binding motif (Szulzewsky et al., 2020, Merritt et al., 2021, Warner et al., 1998). Also, EGR2 was enriched in CAMTA1-bound regions and MiTF was enriched in TFE3-bound regions (Szulzewsky et al., 2020, Merritt et al., 2021). TFE3 belongs to

the MiTF family, which has a role in proliferation and the cell cycle (La Spina et al., 2020). This suggests that both CAMTA1 and TFE3 may create further DNA-binding abilities when fused to TAZ and YAP1, respectively (Garcia et al., 2022), and also gives reason as to why TC and YT transcriptomes were found to be distinctive from TAZ and YAP1 transcriptomes alone (20-47% difference, from RNA-seq. data in SW872 and NIH3T3 cells) (Szulzewsky et al., 2020, Merritt et al., 2021) (Garcia et al., 2022). Thus, although activated YAP/TAZ transcriptomes are thought to be most important in EHE, the fusion partner may also be a contributor in the process of driving EHE.

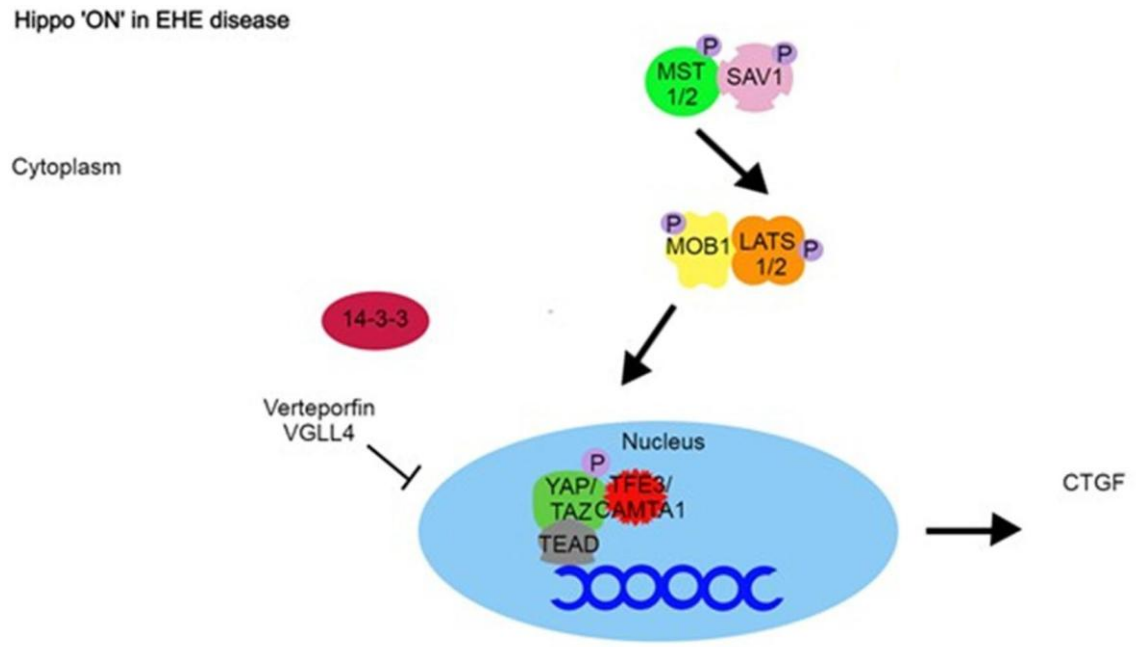


Fig. 4: The Hippo pathway when 'on' in EHE disease
Even though the Hippo pathway is 'on,' MST1/2 causes phosphorylation of LATS1/2, YAP/TAZ are bound to TFE3/CAMTA1 and phosphorylated, but remain in the nucleus, and are involved in transcription of different genes, such as CTGF (connective tissue growth factor).

## 2.6 Regulation of the Hippo pathway

The Hippo pathway is regulated in a variety of ways; it is possible that inappropriate activation of YAP/TAZ (in EHE disease) could mimic the dysregulation of upstream regulators. Many pathways have been implicated in the regulation of the Hippo pathway, in cancer cells: Wnt, AMPK, TGF-β,

KARS, MAPK/ERK have all been identified (Han, 2019). Hippo signalling is modulated by tight /adherens junctions, mechanical signals, and growth factors/receptors (Boopathy and Hong, 2019) (Fig. 5). Tight junctions exist where there is a permeability barrier between adjoining cells, and proteins associate with these membranes for different functions (Anderson et al., 2004, Matter et al., 2005). Angiomotin (AMOT) is primarily found in endothelial cells, which are the cells at the basis of EHE (Tanas et al., 2011). It is an important regulator of YAP/TAZ and is a member of the motin angiostatin-binding proteins (Bratt et al., 2002, Lv et al., 2017, Zhao et al., 2011). Angiostatin is a known inhibitor of angiogenesis and is also known to control the migration of endothelial cells, and to cause apoptosis (O'Reilly et al., 1994, Ji et al., 1998, Claesson-Welsh et al., 1998, Lucas et al., 1998) (Bratt et al., 2002). AMOT was found to sequester YAP/TAZ in the cytoplasm, or cause it to move to the tight junctions, hence acting as a negative regulator of YAP/TAZ (Chan et al., 2011, Wang et al., 2011). AMOT has also been shown to inhibit YAP by activating NF2/Merlin and causing LATS-dependent phosphorylation through LATS kinase (Li et al., 2015). Also, AMOT has been shown to detach from YAP when under shear stress (Nakajima and Mochizuki, 2017) and has been shown to aid *hemangioendothelioma* invasion in murine aortic endothelial cells (Levchenko et al., 2004).

Neurofibromatosis2 (NF2) is a syndrome which can cause nerve tumours and also ependymomas/multiple meningiomas (Tamura, 2021). It is caused by mutation/deletion of the neurofibromin 2 gene (Rouleau et al., 1993, Trofatter et al., 1993, Evans, 2009), which encodes the protein Merlin: this is a cytoskeletal protein (Morrison et al., 2001) from the ezrin, radixin, and moesin (ERM) protein family (Xu and Gutmann, 1998). Merlin was found to connect the actin cytoskeleton to cell-surface glycoproteins (Algrain et al., 1993, Tsukita et al., 1994). Baia *et al*., showed that in loss-of-NF2 meningiomas, YAP1 was found to be highly expressed, and that expression of Merlin is linked to YAP1 phosphorylation (Baia et al., 2012). NF2/Merlin is an upstream regulator of the Hippo pathway, well known as a tumour suppressor (Hamaratoglu et al., 2006, Zhao et al., 2007, Harvey et al., 2013) and vital component involved in contact inhibition during proliferation (Petrilli and Fernandez-Valle, 2016). The specific mechanism by which the regulation and contact inhibition occurs is still unknown (Hong et al., 2020, Cui et al., 2019). Merlin is known to interact with adherens junction proteins in confluent cells, and loss of Merlin causes a lack of development of adherens junctions (Lallemand et al., 2003) (Karaman and Halder, 2018). Adherens junction proteins are also crucial for regulation of the Hippo pathway: Loss of α-catenin, β-catenin, or E-cad results in YAP being sequestered to the nucleus, hence activated, in cultured endothelial cells and breast cancer cells (Kim et al., 2011, Choi et al., 2015). Another crucial cytoskeletal protein is Spectrin, which supports

the structure of the cell (Machnicka et al., 2012). When α- and β-spectrin are knocked down, this results in the nuclear localisation of YAP in mammalian cell culture (Wong et al., 2015, Deng et al., 2015).

Fluid shear stress is the frictional force between flowing blood and endothelial cells lining the blood vessels (Hahn and Schwartz, 2009), and is known to cause vascular growth, remodelling and maintenance (Nakajima and Mochizuki, 2017). Shear stress can result in changes to endothelial cell shape, and cause the activation of transcription factors, leading to gene expression (Chiu and Chien, 2011). YAP is known to be a mechanotransducer (Piccolo et al., 2014), which responds to shear stress (Nakajima and Mochizuki, 2017), along with TAZ (Low et al., 2014). In cell cultured endothelial cells, it has been shown that YAP/TAZ move to the nucleus and activate transcription of CTGF, CYR61, and ANKRD1 upon disturbed flow (Wang et al., 2016b). Other mechanical signals also regulate YAP: YAP moves to the nucleus via changes in the filamentous actin (F-actin) cytoskeleton (Nakajima and Mochizuki, 2017).

Growth factors, such as Sphingosine 1-phosphate (S1P) and lysophosphatidic acid (LPA) are both part of the phospholipids growth factor family (Panetti, 2002). They bind to the S1P receptor and LPA receptor respectively, inhibiting LATS, causing activation of YAP/TAZ (Yu et al., 2012). Whereas molecules such as glucagon and epinephrine have been shown to suppress YAP/TAZ (Yu et al., 2012, Zhou et al., 2015) (Ma et al., 2019). Molecules such as cytokines, vascular endothelial growth factors (VEGF), epidermal growth factors (EGF), insulin, Wnt, bone morphogenic protein (Bmp), and transforming growth factor β (TGF-β) have also been shown to regulate the Hippo pathway (Azad et al., 2018, Wang et al., 2017, Sorrentino et al., 2017, Miranda et al., 2017) (Ma et al., 2019). RhoA GTPase activates actin polymerisation and causes stress fibers to be produced, which regulates YAP/TAZ in response to cell stiffness (Wada et al., 2011). GPCRs, such as the Protease activated receptor 1 (PAR1), have been shown to promote YAP activation via dephosphorylation, involving RhoA GTPase and F-actin, which is also thought to be involved in both kinase-dependent and independent YAP activation (Regue et al., 2013). Par1 is able to cause tumour proliferation and metastasis, and is upregulated in different cancers (Eck et al., 2009, Bar-Shavit et al., 2011, Zigler et al., 2011, Regue et al., 2013).

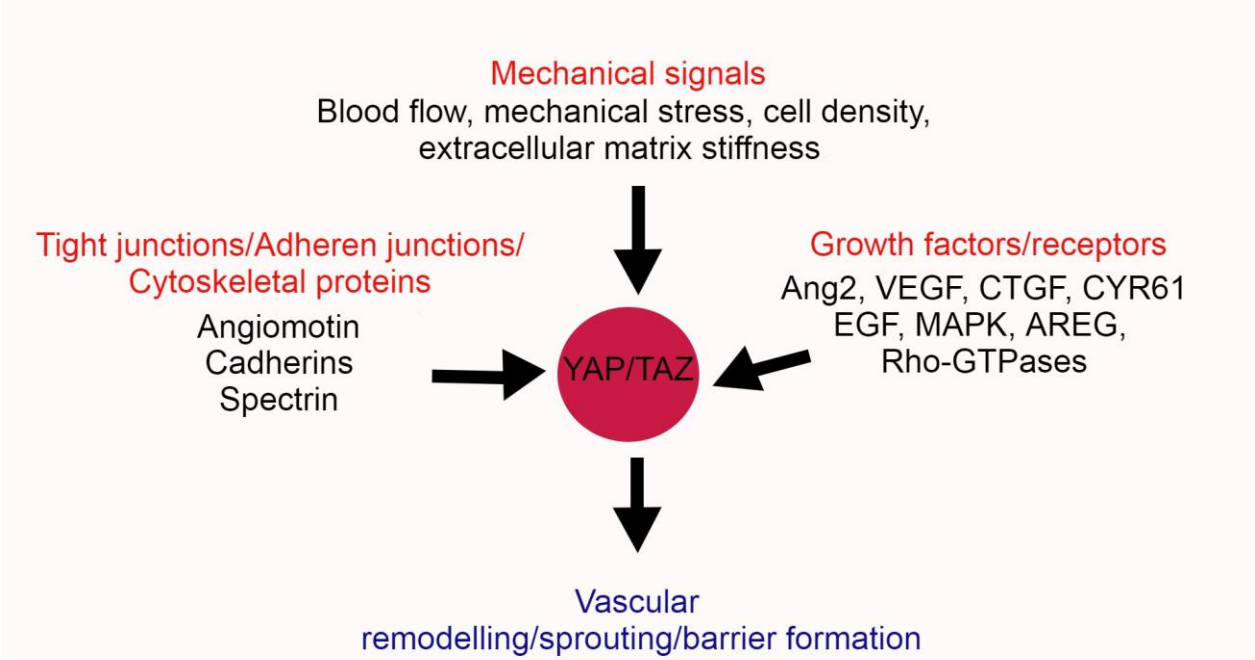


Fig. 5: Regulation of YAP/TAZ
Junction proteins, mechanical signals, and growth factors/receptors all regulate YAP/TAZ, either directly, or indirectly. This results, in turn, YAP/TAZ regulating vascular remodelling, angiogenesis, and vascular barrier formation.

## 2.7 YAP/TAZ role in cancer

YAP/TAZ not only have a role in EHE disease, they are oncogenic transcription factors in many solid tumours, levels of YAP/TAZ have been shown to be excessive in tumours, and it also increases the chance of tumour occurrence (Zanconato et al., 2016b, Yamaguchi and Taouk, 2020, Zanconato et al., 2016a). YAP/TAZ has been shown to be crucial for cancer initiation, progression, and metastasis (Zanconato et al., 2016b). It is involved in cell proliferation and upregulating genes involved in cell cycle control, such as *CCND1 (cyclin D1), CDC25 (cell division cycle 25), CDK1 (cyclin-dependent kinase 1)*, and *MCM*s (*minichromosome maintenance*) (Zanconato et al., 2015, Kapoor et al., 2014, Kim et al., 2019) (Yamaguchi and Taouk, 2020). However, with certain blood cancers, such as leukaemia, myeloma, and lymphoma, these show reduced levels of YAP/TAZ (Pearson et al., 2021, Cottini et al., 2014, Zheng et al., 2021). It has been shown that in acute myeloid leukaemia (AML)

and multiple myeloma, if YAP levels are restored, this causes cell death and reduces proliferation, indicating that under certain circumstances YAP is able to act as a tumour suppressor (Cottini et al., 2014, Piccolo et al., 2023). This tumour suppression activity is also seen in small cell lung cancer (SCLC), which is a neuroendocrine tumour (Pearson et al., 2021). Therefore, interestingly, it appears YAP acts differently, either as an oncogenic transcription factor or as a tumour suppressor, depending on the cell type (Barry et al., 2013, Cottini et al., 2014, Moroishi et al., 2015a).

In YAP/TAZ tumours with high expression, the leucine zipper transcription factor, Activator protein-1 (AP1) (Wagner, 2001), is involved with TEAD binding, but this does not happen with YAP/TAZ tumours with low expression (Pearson et al., 2021) (Piccolo et al., 2023). AP-1 is known to have a role in tumour transformation and growth (Zanconato et al., 2015). YAP/TAZ-TEAD is known to bind at enhancer sequences (and very rarely, at promoter sites) (Zanconato et al., 2015, Zanconato et al., 2018, Stein et al., 2015, Liu et al., 2016, Galli et al., 2015, Della Chiara et al., 2021). Once bound to an enhancer sequence, this complex can then bind to AP-1, which is thought to cause transcription of S-phase entry and mitosis target genes, in breast cancer cells (Zanconato et al., 2015). Enhancers are able to have contact with specific promoters via chromatin looping (Zanconato et al., 2015) (Battilana et al., 2021).It has been shown that YAP/TAZ cause *CDK9 (cyclin-dependent kinse 9), BRD4 (bromodomain-containing protein 4), and MED1 (mediator of RNA polymerase II transcription subunit 1)* transcriptional coactivators to bind to enhancers also (Piccolo et al., 2023). It is also thought that once BRD4 is bound at the same position, YAP/TAZ cause RNA polymerase II to bind to the YAP/TAZ target gene promoters (Piccolo et al., 2023).

YAP and TAZ activation can negatively affect patient prognosis. In many tumours, also those where YAP and TAZ are not primary drivers, studies have shown that high expression of YAP/TAZ (or nuclear localization) is related to poor prognosis, for instance in breast, colorectal, liver, lung, gastric, pancreatic, ovarian, endometrial, oesophageal, and bladder cancers (Zanconato et al., 2016b, Moroishi et al., 2015a, Lo Sardo et al., 2018, Yamaguchi and Taouk, 2020). This may be due to, for instance, YAP/TAZ also being involved in modulating immune checkpoint inhibitors and immune cell evasion (Pan et al., 2019): it has been shown to upregulate the chemokines *CXCL5 (C-X-C chemokine ligand 5)* and *CCL2 (C-C chemokine ligand 2),* which in turn causes the recruitment of immune suppressive myeloid-derived suppressor cells and M2 macrophages (Guo et al., 2017, Wang et al., 2016a). An immune checkpoint regulator, *PD-L1 (Programmed death ligand 1),* is also upregulated by YAP/TAZ (Janse van Rensburg et al., 2018, Kim et al., 2018).

In addition, Cordenonsi *et al*. showed that TAZ is crucial for maintenance of breast cancer stem cells, and it is possible to transform non-stem cancer cells to cancer stem cells (CSCs) via the upregulation of TAZ (Cordenonsi et al., 2011). YAP functions downstream of SOX2 to maintain CSCs (Basu-Roy et al., 2015). YAP also induces SOX9, which regulates CSC properties (Wang et al., 2019, Song et al., 2014) (Yamaguchi and Taouk, 2020). Furthermore, in the metastatic cascade, cancer cells migrate from primary tumours, to enter the lymphatic vessels and the bloodstream. This then allows tissues and organs to be invaded, creating secondary tumours (Chaffer and Weinberg, 2011, Valastyan and Weinberg, 2011). Nuclear localisation of YAP/TAZ has been shown to be upregulated in metastasis of lung, liver, pancreatic, breast, colorectal, and gastric cancer (Xie et al., 2012, Hu et al., 2014, Bartucci et al., 2015, Guo et al., 2015, Yang et al., 2015, Diaz-Martin et al., 2015) (Yamaguchi and Taouk, 2020).

A fourth reason may be the role of YAP/TAZ signalling in epithelial mesenchymal transition (EMT). EMT occurs when epithelial cells gain mesenchymal cell properties and lose cell polarity/cell-cell adhesion properties. It is also associated with cell motility (Shibue and Weinberg, 2017, Ye and Weinberg, 2015) and is thought to be the first step in metastasis (Shibue and Weinberg, 2017, Dongre and Weinberg, 2019). YAP/TAZ overexpression has been shown to cause EMT (Zhao et al., 2008, Zhang et al., 2009, Xiao et al., 2015, Overholtzer et al., 2006, Lei et al., 2008), and YAP/TAZ inhibition has been shown to reverse EMT in gastric, pancreatic and hepatocellular carcinoma (Xiao et al., 2015, Xie et al., 2015, Pan et al., 2017). Incomplete EMT is often seen in human tumours (Savagner, 2010), showing disrupted cell junctions and reduced epithelial cell polarity (Thiery et al., 2009). Scribble is vital for apicobasal polarity, organising the cell basolateral membrane (Macara, 2004). Cordenonsi *et al.* showed that EMT altered Scribble's localisation from the basolateral membrane to the cytoplasm, via Snail/Twist expression. They suggested that the upregulation of TAZ is caused in part by this Scribble inactivation, via EMT, to cause CSC characteristics (Cordenonsi et al., 2011). Scribble has also been shown to be regulated by Liver kinase B1 (LKB1) (Mohseni et al., 2014), which is a tumour suppressor (Mehenni et al., 1998, Jenne et al., 1998). Mohseni *et al*. showed that Scribble was delocalised in tumours with LKB1 mutation, there was a higher level of transcription via YAP, and lower activity of serine/threonine kinases from the Hippo pathway, in mice and human (Mohseni et al., 2014). It has also been shown that when LKB1 is deficient, YAP/TAZ is able to cause non-small cell lung cancer (Zhang et al., 2015). In epithelial cells, Scribble has been shown to be part of a Scribble/MST/LATS/TAZ complex, which causes MST phosphorylation of LATS, then LATS

phosphorylation of TAZ: hence Scribble was shown to cause activation of the Hippo pathway (Cordenonsi et al., 2011). Cordenonsi *et al*., showed that when Scribble was delocalised from the cell membrane, this caused TAZ to avoid inactivation (Cordenonsi et al., 2011). To further this concept, in breast cancer cells Scribble has also been found to be transported away from the cell membrane (Zhan et al., 2008), suggesting inactivation of the Hippo pathway (Cordenonsi et al., 2011).

Anoikis occurs when apoptotic cell death is induced by cell detachment. Inhibition of anoikis is crucial for metastasis (Paoli et al., 2013), and YAP/TAZ has been shown to inhibit this (Zhao et al., 2012). It has also been shown that fluid shear stress is thought to activate YAP/TAZ throughout circulation. This indicates that YAP/TAZ may promote tumour cell survival in the course of metastasis (Lee et al., 2017, Lee et al., 2018, Yamaguchi and Taouk, 2020). Therefore, as mentioned, YAP/TAZ are crucial for cancer initiation, progression, and metastasis (Zanconato et al., 2016b), and they may contribute in these ways in EHE disease also.

## 2.8 TAZ-CAMTA1 & YAP1-TFE3 role in cancer

In 2023, Neil *et al*. made an important discovery, which showed that TC expression caused hypertranscription in endothelial cells, which then led to DNA damage, resulting in cells entering S-phase of the cell cycle. They also found that there was diminished homologous repair, and cellular senescence (Neil et al., 2023). This is a response to cellular damage or stress, causing cell cycle arrest (Serrano et al., 1997, Campisi and d'Adda di Fagagna, 2007) (Krizhanovsky et al., 2008). Approximately half of all TC tumours have secondary mutations, of which CDKN2a are the most common (Seligson et al., 2019). When CDKN2a was knocked-out, this led to avoidance of senescence and uninhibited growth (Neil et al., 2023). Therefore, this may be a potential mechanism of action for TC.

As has been established, TC and YT both cause EHE disease (Tanas et al., 2011, Errani et al., 2011, Antonescu et al., 2013). Both TC and YT have also been shown to bind to the chromatin modifying protein, Ada2a-containing histone acetyltransferase (ATAC), which is a crucial oncogenic driver (Sardaro et al., 2014), and a possible therapeutic target for EHE (Merritt et al., 2021). TAZ/YAP bind to TEAD, whilst CAMTA1 and TFE3 are thought to be involved in chromatin remodelling (Merritt et al., 2018). Both transcriptomic and chromatin-binding profiles show that TC and YT partially express the same genes as full-length TAZ and YAP1, respectively, but also express a unique set of genes (Garcia et al., 2022, Merritt et al., 2021).

The importance of CAMTA1 and TFE3 was further supported by the fact that the ATAC complex subunits *YEATS2 (Yeats domain-containing 2*) and *ZZZ3 (Zinc-finger zz-type containing 3)* were the top hits from an RNAi screen (18 genes were examined which were hits in a previous BioID mass spectrometry experiment) with TAZ-CAMTA1 expressing SW872 cells, and *YEATS2* was also shown to be knocked-down in SW872 YT cells. (Merritt et al., 2021). *YEATS2* acts as a scaffolding subunit, binding the ATAC complex to acetylated H3, along with *ZZZ3* (Mi et al., 2017, Mi et al., 2018). They are also thought to bind GCN5 (Mi et al., 2017, Mi et al., 2018, Grant et al., 1997), which is a member of the histone acetyltransferase (HAT) family (Marcus et al., 1994, Candau et al., 1996), and cause H3K9 acetylation (Nagy and Tora, 2007, Mi et al., 2017). This then results in the chromatin unwinding and the DNA becoming accessible for transcription (Mi et al., 2017). The ATAC complex also has another subunit, *KAT14 (Lysine acetyltransferase 14)*, which has been shown to bind TC and YT (Merritt et al., 2021). In addition, *YEATS2* is known to be involved in several different cancers, such as ovarian, head and neck, and lung (Mi et al., 2017) (Merritt et al., 2021).

Extracellular matrix proteins which may be important for interaction with TC/YT, and hence tumour formation are FBLN5, ERBB3, and Fras1 (Merritt et al., 2021, Garcia et al., 2022). FBLN5 and ERBB3 have been shown to be significantly upregulated in TC expressing cell lines (qPCR to validate RNA-seq. in SW872/NIH3T3 cells), compared to control, and more than TAZ or CAMTA1 alone (Merritt et al., 2021). In addition, FRAS1 and FBLN5 are significantly upregulated in YT expressing cell lines (qPCR to validate RNA-seq. from SW872/NIH3T3 cells), compared to control, and more than in YAP expressing cell lines alone (Merritt et al., 2021). Therefore, it seems FBLN5, ERBB3 and FRAS1 are top candidates for further investigation.

FBLN5 is an extra-cellular matrix protein (ECM), and a member of the fibulin family (involved in the formation and maintenance of elastic fibres, loose connective tissue, and basement membranes) (Timpl et al., 2003, Argraves et al., 2003) (Albig and Schiemann, 2005). It is involved in cell motility, proliferation, angiogenesis, and tumorigenesis (Schiemann et al., 2002) (Albig and Schiemann, 2005), and has increased expression in fibrosarcoma (Schiemann et al., 2002), but decreased expression in prostate and lung cancer (Yue et al., 2009, Wlazlinski et al., 2007). FBLN5, activated by transforming growth factor (TGFβ), is thought to be involved in epithelial to mesenchymal transition (EMT), and has been shown to be involved in certain breast cancers (Lee et al., 2008). Also, integrinB1 binding has been shown to be a requirement for EMT via TGFβ (Bhowmick et al., 2001). VEGF has been shown to cause the downregulation of FBLN5, which indicates that FBLN5 may be an inhibitor of

angiogenesis (Albig and Schiemann, 2004, Albig et al., 2006) (Tang et al., 2014).

ERBB3 is a member of the EGR family of receptor tyrosine kinases, which are thought to be involved in cell migration, proliferation, and differentiation (Sithanandam and Anderson, 2008). It encodes HER3, which has been shown to be involved in cancer cell proliferation in several different types of cancer (Sithanandam and Anderson, 2008), such as head and neck, melanoma, lung, ovarian, breast, colorectal, and prostate (Ocana et al., 2013, Slesak et al., 1998, Friess et al., 1995, Yi et al., 1997, Leung et al., 1997) (Gandullo-Sanchez et al., 2022), even though it has very little protein kinase activity (Shi et al., 2010). Therefore, it is essential for HER3 function to bind HER2/EGFR, and form heterodimers (Collier et al., 2013, Littlefield et al., 2014) (Kiavue et al., 2020). Fraser syndrome protein 1 (FRAS1) is found in the basement membrane, in the sublamina densa (Pavlakis et al., 2011). The sublamina densa is located beneath the lamina densa; it is part of the dermis, and tethers the connective tissue to the basement membrane (Pavlakis et al., 2011). FRAS1, along with FREM1 and FREM2, are known to form a membrane complex (Pavlakis et al., 2011, Kiyozumi et al., 2012) (Wang et al., 2022). This is involved in cell adhesion and signalling (Gautier et al., 2008, McGregor et al., 2003) (Talbot et al., 2012).

## 2.9 RAS/MAPK & CTGF/Cyr61 in TC tumourigenesis

TC has been shown to signal through the MAPK (mitogen-activated protein kinase) pathway in tumourigenesis (Ma et al., 2022). The MAPK signalling pathway is involved in apoptosis, proliferation, differentiation, stress responses, angiogenesis and metastasis (Keshet and Seger, 2010, Sabio and Davis, 2014, Plotnikov et al., 2011, Guo et al., 2020). It is a protein kinase pathway, with between 3-5 sets of kinases (Guo et al., 2020), and is known to be activated via Ras, KC-mediated (Kupffer cells), Ca2+, or G protein-coupled receptor (Lawrence et al., 2008) (Guo et al., 2020). The MAP/ERK pathway is known to be involved in differentiation and proliferation in particular, and is part of the Ras Raf MEK ERK pathway (Chang and Karin, 2001, Yang and Liu, 2017, Yu et al., 2015c, Guo et al., 2020) (Guo et al., 2020).

Ma *et al.* found that the Ras/MAPK signalling pathway and *CTGF* are both vital for TC-mediated tumour growth (Ma et al., 2022). *CTGF* increases in a TC dependent and time dependent manner in TC expressing cells (NIH3T3). *Cyr61* also increased, but it was less reliable, as it also increased in the empty vector control cells (Ma, 2022). *CTGF* is a member of the CCN ligand family, which has been shown to have different integrins as receptors (Chu, 2008). Ma *et al.* also found that integrin αIIbβ3 is

involved in the TC pathway. They then looked at the Ras pathway, as Ras has been shown to be involved in different integrin-mediated signalling pathways (Kinbara, 2003, Clark, 1996). Ma *et al.* also found that when *CTGF* was silenced, this prevented anchorage-independent cell growth, which is conducive to tumour metastasis, but this did not happen with *Cyr61* silencing (Simpson et al., 2008, Ma et al., 2022). *CTGF* and *Cyr61* are ECM-associated proteins, but they are also cytokines which are involved in cell signalling (Lipson et al., 2012, Zhao et al., 2008, Kireeva et al., 1997). *CTGF* and *Cyr61* are also known to be involved with cancers such as prostate, colorectal, breast, oesophageal, glioma, and gastric (Lai et al., 2011, Huang et al., 2017, Dhar and Ray, 2010, Kleer, 2016, Ladwa et al., 2011, Zhou et al., 2009, Xie et al., 2004) (Ma et al., 2022).

## 2.10 CDKN2a in TC tumourigenesis

As previously mentioned, almost half of all TC tumours are thought to have secondary mutations: Seligson *et al.* showed that of all the clinical samples examined (49), the most common secondary mutation was CDKN2a, followed by CDKN2b, and the likelihood of any secondary mutation in patients with advanced disease was increased from 0% for EHE stage I/II to 80% for EHE stage III/IV (Seligson et al., 2019). To examine this in detail, CDKN2a knockout mice were crossed with EHE genetically engineered mouse models (GEMMs) to generate EHE CDKN2a knockout mice: these showed an increased susceptibility to tumour formation without altering the EHE phenotype (Seavey et al., 2023).

CDKN2a acts as a tumour suppressor, and is included in the tumour suppressor pathways, p53 and RB1 (Serrano, 1997, Komata et al., 2003, Hollstein et al., 1991, Weinberg, 1995) (Serra and Chetty, 2018). CDKN2a is cyclin-dependent kinase inhibitor 2a, which encodes cell cycle proteins, $p16^{INK4a}$, and $p19^{ARF}$ (Quelle et al., 1995). $P16^{INK4a}$ and $p19^{INK4d}$ (along with $p15^{INK4b}$ and $p18^{INK4c}$) inactivate cyclin-dependent kinase 4/6 by binding to it and thus inhibiting the binding of cyclin D (Sherr and Roberts, 1995, Hall et al., 1995, Pavletich, 1999) (Bockstaele et al., 2006). This in turn prevents phosphorylation of the Rb protein (Ewen, 1994), causing G1 phase arrest (Sherr and Roberts, 1995), and DNA synthesis inhibition (Dyson, 1998, Nevins, 1998) (Roussel, 1999). Although loss/inactivation of $P16^{INKa}$ is known to occur in approximately 50% of all human cancers, it's overexpression has also been linked to a worse outcome in cancers, such as ovarian, oral, prostate, cervical, and neuroblastoma (Lang et al., 2002, Ortega et al., 2002, Gonzalez and Serrano, 2006, Esteller et al., 2001, Ruas et al., 1999) (Li et al., 2011). $P19^{INK4d}$ is also known to be lost/inactivated in approximately 50% of all human cancers (Ruas and Peters, 1998) (Kelly-Spratt et al., 2004).

## 2.11 Genetically engineered mouse models (GEMM) of EHE

Until 2021, there was a lack of EHE cell lines/animal models, hence studying EHE proved problematic. In that year, a major breakthrough occurred when a mouse model of EHE was published (Seavey et al., 2021). A FLEx (flip-excision) system was used to create a conditional knock-in murine model of EHE, under the control of the endogenous promoter, TAZ (as in human). To create this model, the wild-type third exon of TAZ and an inverted section of the murine TC cDNA (TAZ exon 3 and CAMTA1exon 9 to exon24) construct was created, flanked by standard *loxP* and modified Lox2272 sites. *Cre* recombinase can then be used to control endothelial specificity ($CreER^{T2}$), replacing the endogenous TAZ locus with the TC fusion gene (Seavey et al., 2021). TAZ exon3 is switched for TAZ exon3 plus 3'CAMTA1 via *loxP* sites allowing *Cre* inversion (flip), then Lox2272 sites allowing *Cre* excision of the extra TAZ exon3 (Seavey et al., 2021). For tumorigenesis to occur in the mouse, two alleles of the TC locus are required (Seavey et al., 2021). TC mice were crossed with ubiquitously expressed, or endothelial-specific $CreER^{T2}$, then treated with Tamoxifen to activate *Cre*-mediated recombination. Both sets showed tumour growth, from 68.8-72.2% penetrance, in the liver, lungs, soft tissue, and peritoneal surface (Seavey et al., 2021). Similarly, human EHE tumours are also found in these areas (Sardaro et al., 2014). The TAZ-CAMTA1 mice tumours were histologically indistinguishable from human EHE tumours, and there was a marked overlap of tumour-specific genes between both, suggesting that murine and human EHE transcriptional profiles are akin (Seavey et al., 2021).

Driskill *et al*. produced a transgenic line from Cdh5-tTA (tetracycline-controlled transactivator) mouse x TRE (Tet response element)-TC, where TC inhibition occurs when doxycycline is administered to the mice, in a Tet-off system (Driskill et al., 2021). When the pregnant Mothers were not given doxycycline, no viable double transgenic progeny were found, which indicated that TC expression is embryonic-lethal. Hence, the mice were re-crossed, and pregnant Mothers were then kept on the doxycycline treatment until P0 (birth), when treatment was withdrawn to allow TC expression in the double-transgenic progeny. All these mice showed death before day 83. Tumours in the lungs showed an epithelioid phenotype, and stained positive for endothelial markers, such as CD31, Erg, and CD34, as well as CAMTA1, as would be expected (Driskill et al., 2021).

## 2.12 Zebrafish as a model organism

*Danio rerio*, or the zebrafish, is a freshwater teleost, and originates from the Himalayas (Mayden et al., 2007). Streisinger *et al*., first established the zebrafish as a genetic model organism (Streisinger et al.,

1981). Genetic homology between human genes and zebrafish is 71.4% (Howe et al., 2013), making them a strong candidate for translational research.
Although GEMMs are an excellent breakthrough, murine models have several limitations. Zebrafish are much more cost effective and are optically clear during development, making it possible to visualise blood vessel development live at (sub) cellular resolution.
High-throughput drug screening is also a major advantage of the zebrafish model eg. palmitoylation inhibitors (which block TEAD function) could be tested in high throughput (Chan et al., 2016). One potential issue is that zebrafish, like all other teleosts, have undergone an additional round of genome duplication compared to mammals (Meyer and Schartl, 1999). However, it has been shown that significant genes in pathways involved in human cancer are homologous with zebrafish genes, such as genes associated with haematopoiesis, neo-angiogenesis, immune cells, apoptosis, differentiation, migration, proliferation, and drug-resistance mechanisms (Payne and Look, 2009, Veinotte et al., 2014, Kirchberger et al., 2017) (Hason and Bartunek, 2019).

## 2.13 Genetic tools for generating zebrafish models

There are a number of genetic tools which can be used to generate zebrafish models. I decided to produce constructs and use Tol2 technology (Kwan et al., 2007) to incorporate the desired DNA into the zebrafish genome. As there were problems with using *fli1a* directly initially, I decided to use UAS/Gal4 (Scheer and Campos-Ortega, 1999) to enable expression of 'toxic' transgenes. When problems arose with using this system also, I decided to use the cre-lox system (Argos et al., 1986, Hoess et al., 1982, Hoess and Abremski, 1984). Finally, I also used the CRISPR system (Hruscha et al., 2013) to create CDKN2a/b mutations in the TC lines, as it had been shown to be the most common secondary mutation in human EHE tumours (Seligson et al., 2019).

### 2.13.1 Tol2

In this thesis I used Tol2 technology (Kwan et al., 2007) to incorporate DNA into the zebrafish genome. The Tol2 transposase originates from the Japanese medaka fish, *Oryzias latipes* (Koga et al., 1996). The Tol2 kit (Kwan et al., 2007) is used along with multi-site Gateway cloning (Hartley et al., 2000, Cheo et al., 2004) to produce a DNA construct.
An LR clonase enzyme mix is used to recombine attL (entry clone) and attR (destination vector) sites to attB (expression clone) and attP (by product) sites (Fig. 6) (Reece-Hoyes and Walhout, 2018). The expression clone is then co-injected alongside transposase mRNA (Kawakami et al., 2004) to ensure the DNA is efficiently incorporated into the genome. The construct produced contains specific DNA

sequences, named Tol2 elements, that are identified by the transposase to enable transposition (Abe et al., 2011). The use of transgenesis fluorescent markers makes selecting transgenics a simpler and quicker process.

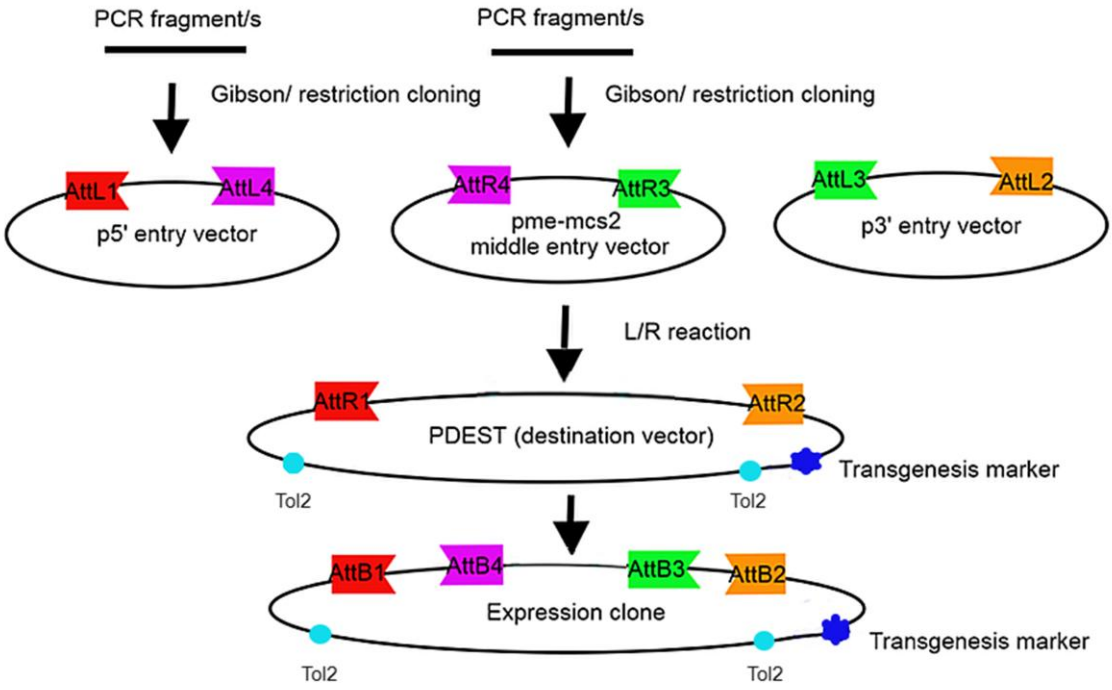


Fig. 6: Multi-site gateway cloning system, used with the iTol2 kit
PCR fragment/s/gene synthesised products were Gibson cloned/restriction digest cloned into p5E or pME-MSC2. These were then joined together by the Att sites, along with a p3E entry vector, via LR Clonase™ II Plus, into a PDEST vector.

### 2.13.2 CRISPR/cas9

The CRISPR/cas9 system is derived from bacteria, where the immune defence consists of Clustered Regularly Interspaced Short Palindromic Repeats (CRISPR) (Wiedenheft et al., 2012, Bhaya et al., 2011, Terns and Terns, 2011). In 2013, genome editing using the cas9/gRNA system occurred in eukaryotic cells (Mali et al., 2013b, Mali et al., 2013a, Cong et al., 2013).

The cas9 endonuclease is activated by binding to gRNA, which allows cas9 to identify the complementary PAM sequence (Gupta et al., 2019). The gRNA and complementary bases pair together, which results in a double-strand break from the cas9 endonuclease (Gupta et al., 2019). These can be repaired either by NHEJ (Non-homologous end joining) or HDR (Homology directed repair) (Gupta et al., 2019). NHEJ results in inserts/deletions (indels), which conclude with premature stop codons or frame shifts, and this is also an error-prone method of repair (Gupta et al., 2019). Whereas the HDR pathway repairs using a homologous sequence, and this is a more accurate method (Gupta et al., 2019).

I used CRISPR/cas9 technology (Hruscha et al., 2013) (Fig. 7) to create crispants (Burger et al., 2016, Wu et al., 2018). One or two copies of CDKN2a/b were knocked out in a *ubi: lox nls-mCherry lox TC t2a neon* background, as CDKN2a/b mutations are the most common secondary mutation seen in EHE patients (Seligson et al., 2019).

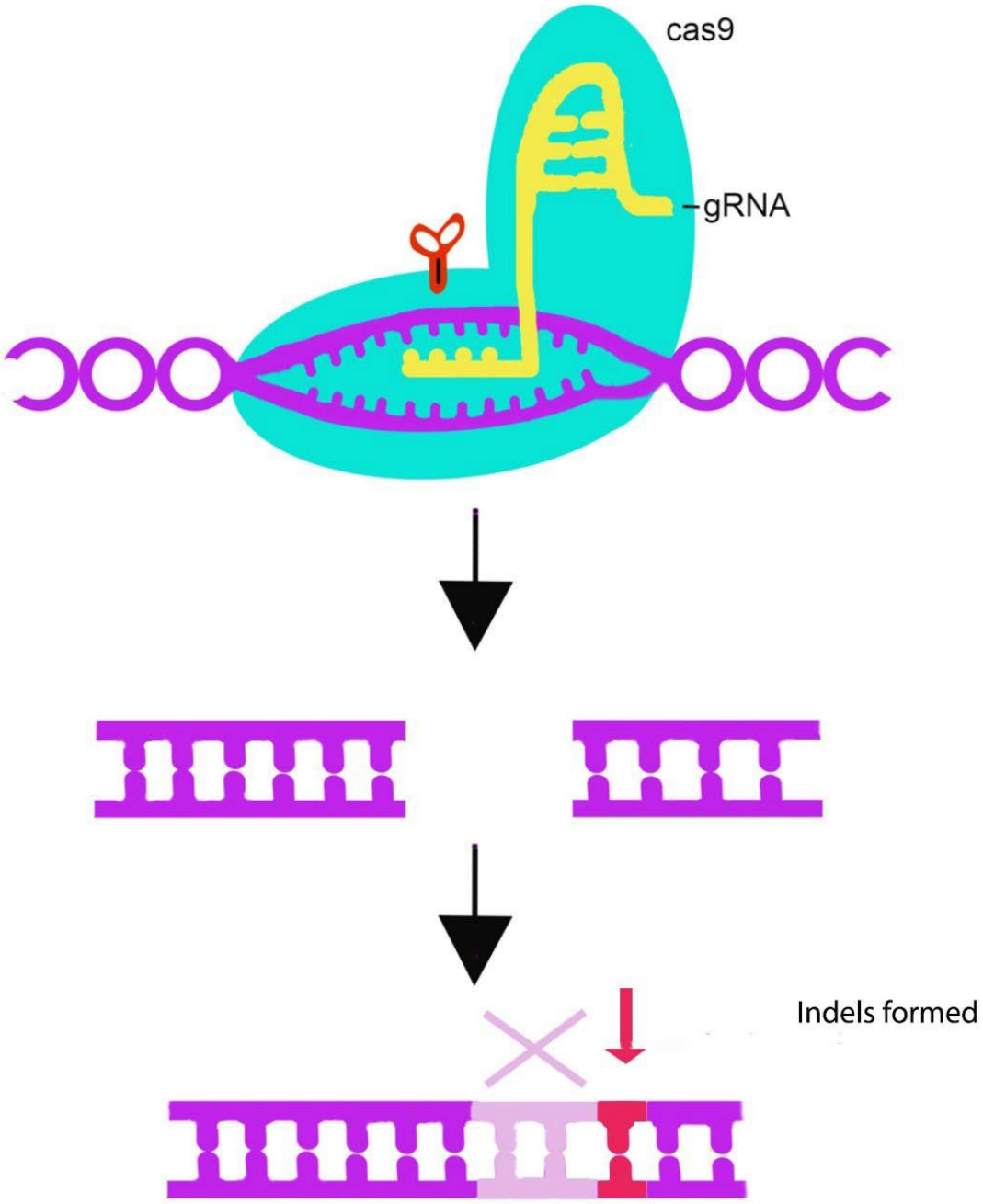


Fig. 7: Schematic representation of CRISPR cas9

The guide RNA (gRNA) binds to the DNA in the appropriate position, with cas9 cutting the DNA at this position. This can cause disruption to a gene/deletion of a gene. This was the case with CDKN2a/b guides used in this project. CRISPR/cas9 can also be used for insertions, etc.

### 2.13.3 Gal4/UAS system

Gal4 is a yeast transcriptional activator, which controls the expression of an Upstream Activating Sequence (UAS) promoter (Scheer and Campos-Ortega, 1999). A gene of interest (effector) can be fused to UAS, which will only be expressed when this line is crossed with the Gal4 line. Otherwise, the effector gene is silent (Scheer and Campos-Ortega, 1999) (Fig. 8), allowing establishment of lines that can express "toxic" transgenes.

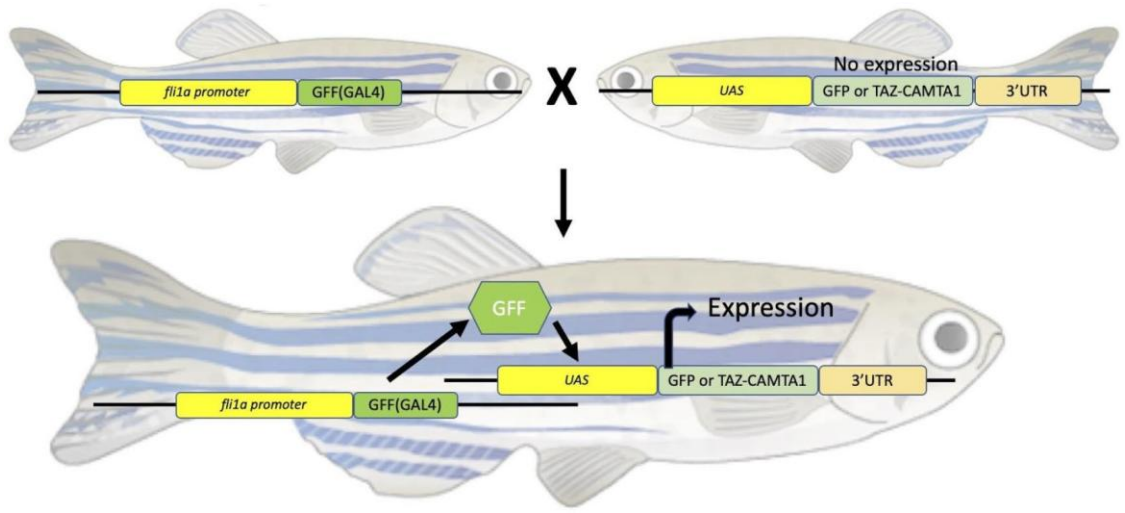


Fig. 8: Schematic representation of the Gal4/UAS system
This shows GFF activating expression of the gene in the endothelial cells, driven by *fli1a.*

### 2.13.4 Cre-lox system

The cre-lox system originates from the bacteriophage P1 cyclic recombinase *Cre* (Sternberg et al., 1986). *Cre* is a site-specific recombinase which causes DNA recombination at *loxP* sites (Argos et al., 1986, Hoess et al., 1982, Hoess and Abremski, 1984). In the example below, *ubi: lox nls-mCherry lox TAZ-CAMTA1 t2a neon* line is crossed with a *fli1*:*cre* line. The *mCherry* will be loxed out upon *Cre*

recombination, to allow temporal activation of the transgene. This will allow TC expression in the endothelial cells, as *Cre* will only be switched on in these cells (driven by *fli1*) (Fig. 9). Again, this allows the establishment of lines that can express "toxic" transgenes.

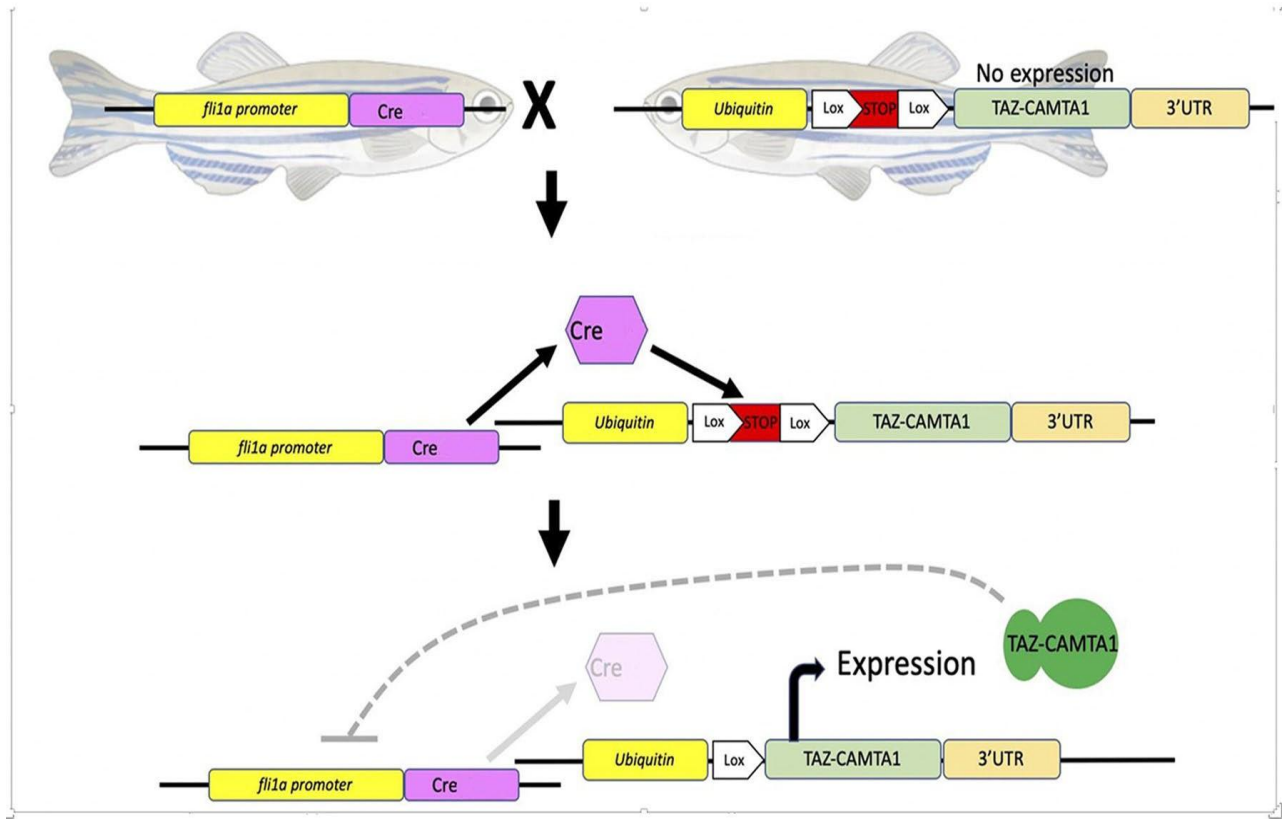


Fig. 9: The Cre lox-STOP-lox system

This shows how TAZ-CAMTA1 should be expressed in the progeny, when mCherry is loxed out using cre recombinase, for site-specific expression.

# 3 Aims and objectives

- To generate a transgenic zebrafish model of EHE with the TC gene fusion, and characterise this model using in situ hybridisation, qPCR, Antibody staining/RNA-seq.
- To generate a YT gene fusion EHE zebrafish model.
- Examine any TC/YT phenotypes and any tumours.
- Create mosaic knockouts with 1 or 2 CDKN2a/b copies lost in the TC background.
- To generate a dominant active TAZ line as a control.
- If a successful model is established, to perform a pilot screen to identify compounds which have the potential to modify the obtained phenotype.

# 4 Methods

## 4.1 Molecular Biology techniques

### 4.1.1 DNA transformation/cloning

A vial of NEB® 10B cells (C3019H) was thawed on ice for 10 mins, before transformation was performed according to the Manufacturer's instructions. 50µl was spread on to appropriate selective plates (carbenicillin/kanamycin), unless otherwise stated, with 50µg/ml antibiotic, and grown up-side down (to prevent condensation dripping on to the colonies) at 37ºC, overnight.

### 4.1.2 Bacterial culture/DNA extraction

Miniprep cultures were grown in 5ml LB broth in 5x volume culture tube for aeration, with the appropriate antibiotic (carbenicillin/kanamycin) at 50µg/ml, overnight, at 37ºC. Minipreps were performed according to the Manufacturer's instructions (27106, Qiagen).

Midiprep cultures were grown in 100ml LB broth (split into 2 x 50ml samples, then combined at the end for higher yield), with the appropriate antibiotic (as above) in 5x volume flask for aeration, overnight, at 37ºC. Midipreps (12643, Qiagen) were performed according to the Manufacturer's instructions.

### 4.1.3 Glycerol stocks

*E. coli* were mixed in 40% glycerol in 2:1 ratio, snap-frozen and stored long-term at -80ºC.

## 4.2 DNA plasmids/construct synthesis

| Plasmid | Source/Reference |
|---|---|
| pDESTTol2cg2 (395) | Dr. Rob Wilkinson (Kwan et al., 2007) |
| pDESTTol2pa2 (294) | Dr. Rob Wilkinson (Kwan et al., 2007) |
| p3E-sv40pA (302) | Dr. Rob Wilkinson (Kwan et al., 2007) |
| pME-EGFP (383) | Dr. Rob Wilkinson (Kwan et al., 2007) |
| pCS2 FA Tol2 TPase (396) | Dr. Rob Wilkinson (Kwan et al., 2007) |
| pDONRp2Rp3 (220) | Dr. Rob Wilkinson (Kwan et al., 2007) |
| p5E-MCS (228) | Dr. Rob Wilkinson (Kwan et al., 2007) |
| p5E fli1a:ep (478) | Dr. Rob Wilkinson (Villefranc et al., 2007) |
| pDESTTol2 cryaa:CFP | Dr. Nik Ogryzko |
| pToneTpase (Tol1) (1807) | Dr. Nathan Lawson |
| pCS2 Cre | Dr. A. Jacinto (Langenau et al., 2005) |
| pME-MCS2 | Dr. Rob Wilkinson |
| pUC57 dcas9 t2a neon (zbfish opt.) | Dr. Rob Wilkinson (Genewiz) |
| pBABE-Neo DF-TC (TAZ-CAMTA1) | Dr. Brian Rubin |
| pBABE-Neo DF-TC S51A | Dr. Brian Rubin |
| pLVX puro 3F TAZ 4sa | Dr. Bob Varelas (Hiemer et al., 2014) |
| p5 ubi: loxP EGFP loxP (27322) | Addgene (Mosimann and Zon, 2011) |
| pDONRp2R-p3 t2a neon | This thesis |
| p5 ubi: loxP nls-mCherry loxP | This thesis |
| p5 UAS | This thesis |
| pCS2 TAZ-CAMTA1 | This thesis |
| pCS2 TAZ-CAMTA1 S51A | This thesis |
| pCS2 Yap1-Tfe3 | This thesis |
| pCS2 Yap1-Tfe3 S94A | This thesis |
| pME-TAZ-CAMTA1 codon z | This thesis |
| pME-TAZ-CAMTA1 IDT | This thesis |
| pME-zbtaz-CAMTA1 | This thesis |
| pME-TAZ-CAMTA1 codon z (no STOP) | This thesis |
| pME-MCS2-EGFP TAZ | This thesis |
| pME-MCS2-EGFP-CAMTA1 | This thesis |
| pME-MCS2-EGFP STOP CAMTA1 | This thesis |
| pME-MCS2 Yap1-Tfe3 | This thesis |
| pME-MCS2 DA TAZ | This thesis |
| pME-MCS2 TAZ-CAMTA1 Ex15 | This thesis |
| pUC-GW mCherry (zbfish opt.) | Dr. Freek van Eeden (Genewiz) |

Table 1: Plasmids used in Tol transgenesis and Multi-site gateway cloning

| Plasmid | Source/Reference |
|---|---|
| pTol1-fli1ep: zf cre-2A-GFP | Dr. Nathan Lawson |
| fli1a:ERcreERcryAV (creER$^{t2}$) | Dr. Henry Roehl |
| fli1a: TAZ-CAMTA1 cg2 | This thesis |
| fli1a:TAZ-CAMTA1 codon z cryaa | This thesis |
| fli1a:TAZ-CAMTA1 IDT cryaa | This thesis |
| fli1a:zbtaz-CAMTA1 cryaa | This thesis |
| uas: TAZ-CAMTA1 codon z cryaa | This thesis |
| uas: EGFP cryaa | This thesis |
| fli1a: EGFP cryaa | This thesis |
| fli1a: EGFP-TAZ cryaa | This thesis |
| fli1a: EGFP CAMTA1 cryaa | This thesis |
| fli1a: EGFP STOP CAMTA1 cryaa | This thesis |
| ubi: loxP mCherry loxP TAZ-CAMTA1 codon z cryaa | This thesis |
| ubi: loxP mCherry loxP Yap1-Tfe3 codon z cryaa | This thesis |
| ubi: loxP mCherry loxP TAZ-CAMTA1 Ex15 codon z cryaa | This thesis |
| ubi: loxP mCherry loxP DA TAZ cryaa | This thesis |
| ubi: loxP nls-mcherry loxP EGFP cryaa | This thesis |

Table 2: Expression vectors used in zebrafish

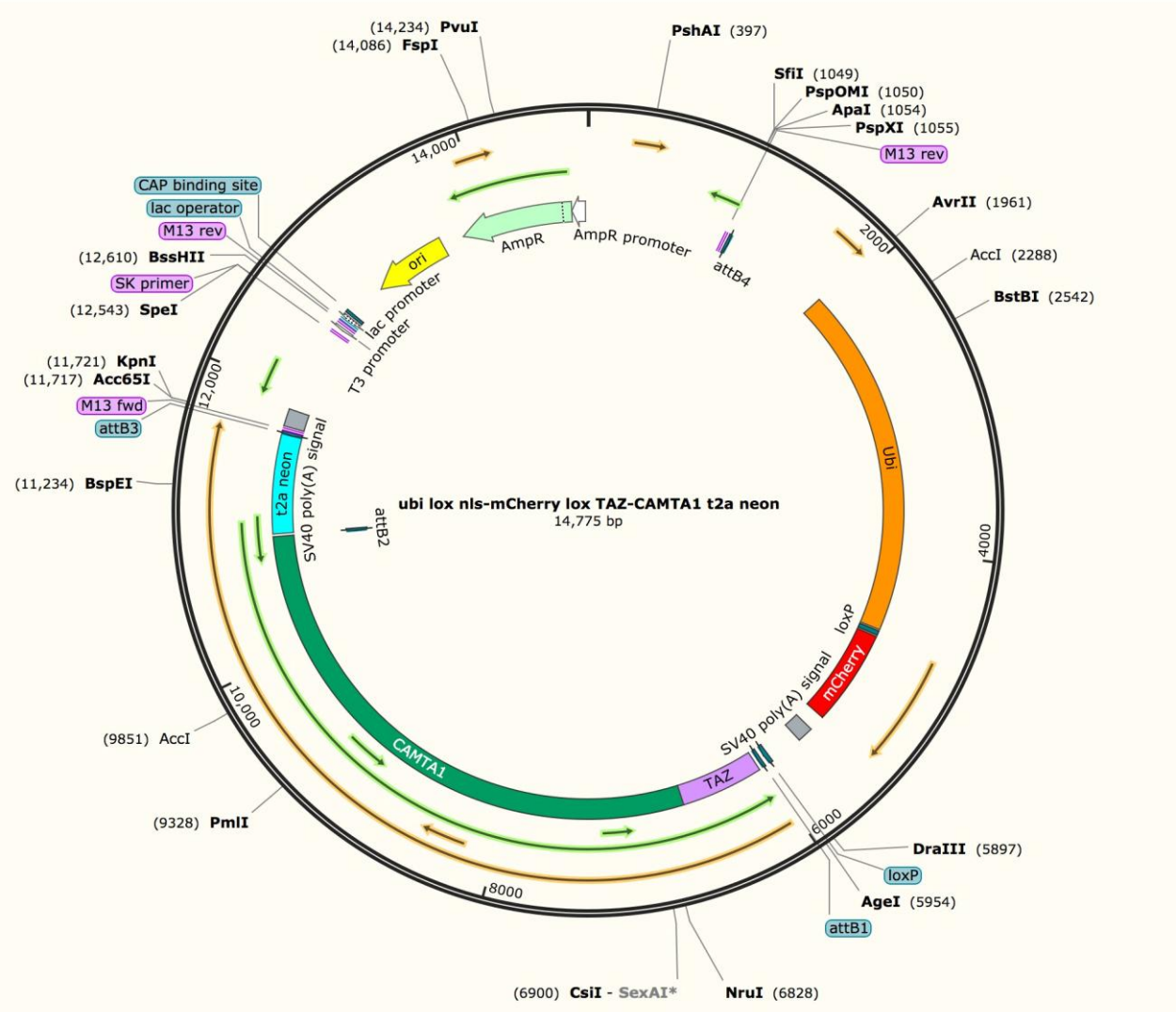


Fig. 10: Plasmid map for *ubi: lox nls-mCherry lox TAZ-CAMTA1 t2a neon*

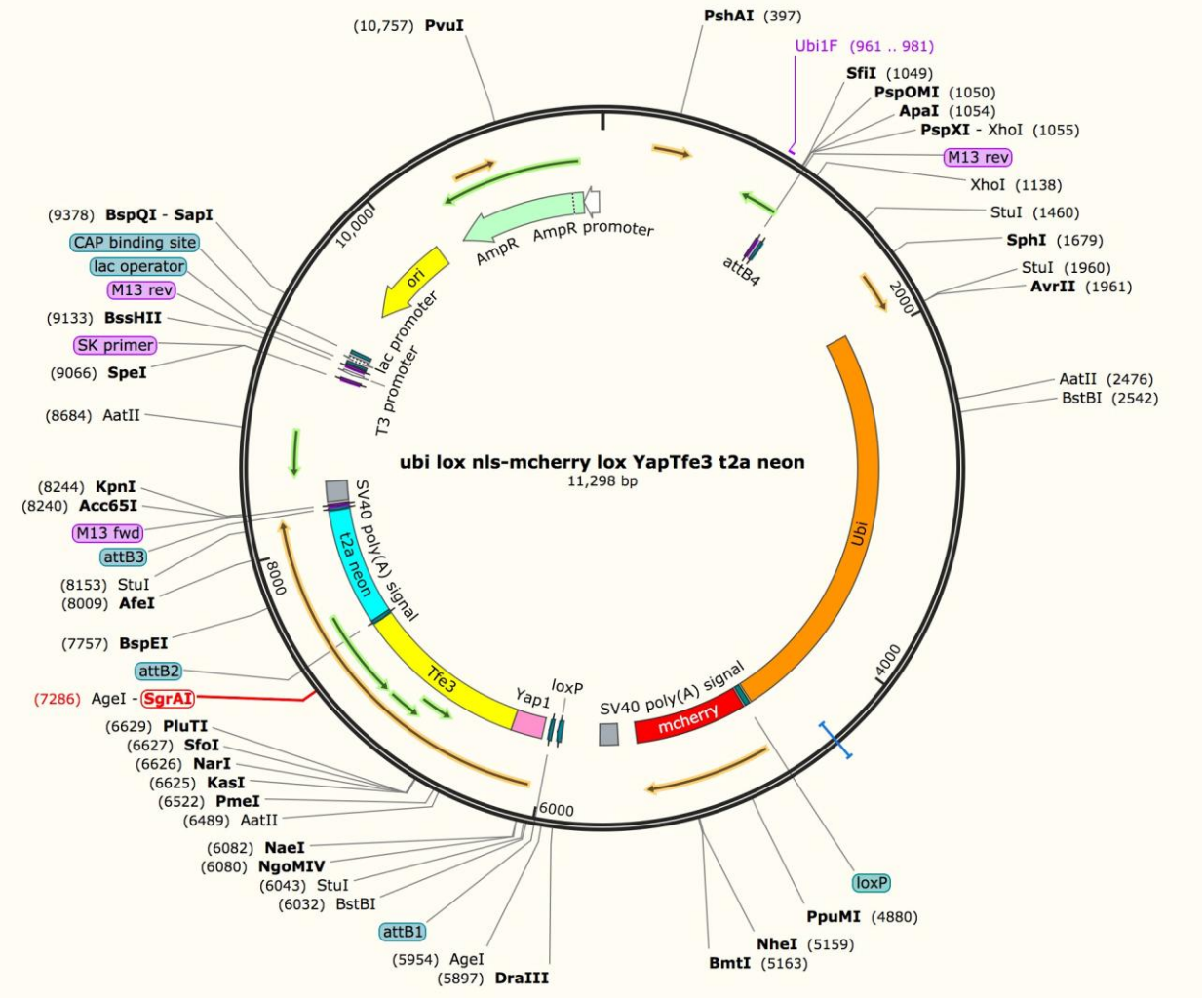


Fig. 11: Plasmid map for *ubi: lox mCherry lox Yap1-Tfe3 t2a neon*

All constructs were produced by restriction digest of DNA fragments (Genewiz, see Appendix) and backbone plasmids with the appropriate enzymes, then phenol purification, ligation, and cloning/Multi-site gateway cloning were performed, unless otherwise stated. The original human TAZ-CAMTA1 sequence used was a gift from Dr. Brian Rubin (table 1), cloned into pME-MCS2, then Gateway cloned into the appropriate destination vector. TAZ-CAMTA1 codon z was designed using codon z v3 program (Horstick et al., 2015). TAZ-CAMTA1 IDT was designed using codon optimization tool (IDT). The human TAZ sequence was switched for the equivalent zebrafish sequence, for the zebrafish TAZ-human CAMTA1 construct (Ensembl genome browser 113). The original Yap1-Tfe3 sequence used was designed using the zebrafish sequences (Ensembl genome browser 113): YAP1 (exon1) joined to

TFE3a (from exon 4), as with human (Antonescu et al., 2013), created by Genewiz (see Appendix), then cloned into pME-MCS2, and Gateway cloned into the appropriate destination vector. *mCherry* was a gift from Dr. Freek van Eeden, which was restriction digested, then ligated into p5 ubi: lox nls lox (with GFP removed via restriction digest), and Gateway cloned into the appropriate destination vector. All plasmid gifts were sequence verified before proceeding. T2a-neon was produced using Phusion® PCR. All purification from PCR was via QIAquick PCR purification kit (28106, Qiagen), unless multiple bands were present, then QIAquick gel extraction kit (28704, Qiagen) was performed on the whole sample, all according to Manufacturer's instructions. T2a-neon was then cloned into pDONRp2R-P3 (220 Tol2 kit) using BP Clonase™ II (11789020, Invitrogen), as described.

| Primer | Sequence | Product size (bp) |
|---|---|---|
| attB2-T2A-Neon-F | GGGGACAGCTTTCTTGTACAAAGTGG ccgagggcagaggcagtctgc | 832 |
| attB3 T2A-Neon-R | GGGGACAACTTTGTATAATAAAGTTGT TACTTGTACAGCTCGTCC | - |

Table 3: T2a neon primers to add attB sites for cloning into pDONRp2R-P3

Tol1, Tol2, pCS2 TAZ-CAMTA1/S51A/Yap1-Tfe3/ S94A mRNA was produced from in vitro transcription once plasmids had been created. pCS2 Yap-Tfe3 was produced by adding a restriction site (XhoI) via Phusion® PCR. This was then restriction digested, purified, ligated and cloned, as described.

| Primers | Sequence | Product size (bp) |
|---|---|---|
| YAP1-TFE3XhoIF | GCCACCATGGATCCGAACCAG | 1365 |
| YAP-TFE3 XhoIR | tgggatCTCGAGTCACAAGTCTTCCTC | - |

Table 4: Primers for Yap-Tfe3

### 4.2.1 Plasmid linearisation/purification

Plasmids (10µg) were linearised with the appropriate enzyme(s) at 37ºC for 3hrs, unless otherwise

stated. Digestion was confirmed on an agarose gel, and phenol purification was performed, as described. If multiple bands were present, gel extraction was performed using the QIAquick gel extraction kit (28704, Qiagen) on the whole sample, according to Manufacturer's instructions. Test digests (500ng) to confirm fragment insertion were performed with the appropriate enzyme(s) at 37ºC for 1hr, then run on a gel, as described.

### 4.2.2 Phenol/chloroform purification

Digest was made up to 300ul with milliq. 300µl Phenol/chloroform (P2069, Sigma) was added, mixed, and centrifuged at 13,000rpm at RT for 5mins. The top, clear supernatant was moved to a new tube and 300µl chloroform was added. This was mixed, then spun as previously. The top, clear layer was again moved to a new tube, then precipitated with 30µl (3M) NaAc pH 5.2, and 750µl EtOH, at -80ºC, for a minimum of 2hrs. The precipitate was centrifuged at 4ºC, maximum speed for 30mins, supernatant was removed, then 500ul EtOH was added. This was spun for 10mins at RT, then air-dried for 5 mins on the bench, taking care to remove all traces of EtOH. The pellet was then resuspended with 20µl milliq water.

### 4.2.3 Ligation/cloning

After restriction digest, plasmids were ligated using the Quick ligation™ kit (M2200S, NEB), in a 20µl reaction, according to Manufacturer's instructions, using 1:3 vector to insert molar ratio (calculated using https://tinyurl.com/yckdcr6x). 2µl was transformed using NEB 10β cells, according to Manufacturer's instructions, then 50µl was plated on the appropriate antibiotic selection plate and grown overnight at 37ºC. Colonies were picked and miniprep/midiprep was performed the next day, as described.

### 4.2.4 Ultramer annealing

To produce p5Euas, firstly uas BamHI ultramers (IDT) were annealed, then the fragment and p5E plasmid were restriction digested. The fragment was phosphorylated and the backbone was dephosphorylated, as described.

For the annealing, 20µl 10µM f and r primers were heated at 95ºC for 5mins, then cooled at room temperature (RT) for 1hr.

| Primer | Sequence | Product size (bp) |
|---|---|---|
| uasBAMHIF | GCAGCCCGGGGGATCGGAGTACTGTCCTCCGAGCG | 35 |
| uasBAMHIR | TAGAACTAGTGGATCCTCGGAGGACAGTACTCCGC | - |

Table 5: uas ultramers

### 4.2.5 Fragment phosphorylation

uas BamHI annealed ultramers were heated at 70ºC for 10mins, chilled on ice, then 5µl T4 ligase buffer, 1µl T4 ligase enzyme (M0202S, NEB), and 4µl milliq was added at 37ºC for 30mins. This was purified using the Minelute gel extraction kit (28604, Qiagen), according to Manufacturer's instructions.

### 4.2.6 Plasmid de-phosphorylation

0.5µl Shrimp alkaline phosphatase (SAP) was added to 10µl p5E-MCS plasmid, with 1µl Cutsmart buffer at 37ºC for 30mins, then heat inactivated at 65ºC for 5mins. This was then purified using the Minelute gel extraction kit (28604, Qiagen), according to Manufacturer's instructions.

p5E-MCS and uas BAMHI fragment were then ligated/cloned as described.

### 4.2.7 Gibson cloning

All Gibson cloning was planned *in silico* (Snapgene, 5.2.5). Gibson assembly® cloning kit (E5510, NEB) was used according to Manufacturer's instructions, with a 3:1 molar ratio insert to vector ratio. 100µl was then plated on the appropriate selection plate and grown at 37ºC overnight, colonies were picked, and miniprep/midiprep was performed, as described.

All primers were designed using Primer3 and purchased from IDT.

| Primer | Sequence | Product size (bp) |
|---|---|---|
| EGFP CAMTA1 fragF | TCTCGAGGGAGCTGGAGGATCTGTC | 4231 |
| EGFP CAMTA1 fragR | ATCTAGAGGGGTTCCCTGTCCCTTCTCAATTCT | - |
| EGFP CAMTA1 vecF | AGGGAACCCCTCTAGATTCTGCAGCCCTATAGC | 3343 |
| EGFP CAMTA1 vecR | CCAGCTCCCTCGAGAGGCCTTGAATTCCC | - |
| DA TAZfragF | TCCCATCGCCACCATGAATCCGGC | 1221 |
| DA TAZfragR | AACTCATCCAGCCAGGTTAGAAAGGGCT | - |
| DA TAZvecF | CCTGGCTGGATGAGTTTGGACAAACCAACCCA | 2599 |
| DA TAZvecR | ATGGTGGCGATGGGATCCTGCAAAAAGAAG | - |

Table 6: Gibson primers

### 4.2.8 Multi-site gateway cloning

All Gateway cloning was planned *in silico* (Snapgene, 5.2.5). Multi-site gateway cloning was used to create the final constructs I produced, using various plasmids from the Tol2 kit (Kwan et al., 2007). pME-EGFP (383) plasmid was used in a tandem construct as a positive control, in order to test construct pieces. LR Clonase™ II Plus (Invitrogen, 12538120) was used according to Manufacturer's instructions, except p5E, pME, p3E and pDEST vectors were used at 20fmol each, in TE buffer (10 mM Tris, 1mM EDTA, pH 8). The final mixture was then stored at -20ºC until use.

Where BP Clonase™ II (11789020, Invitrogen) was used, Manufacturer's instructions were followed.

2ul of either mixture was transformed into NEB® 10B cells (C3019H), then plated onto the appropriate antibiotic selection plate, as described. 3-6 colonies were then miniprepped, and restriction digest was performed to select the colonies with the correct insert (visualised on gel). Midiprep cultures were then grown as described, using the selected minipreps, as described.

### 4.2.9 In vitro transcription

mRNA was synthesized from linearised, purified DNA, using the SP6 mMessage mMachine™ kit (AM1340, Invitrogen), unless otherwise stated. This was according to Manufacturer's instructions, using 1µg DNA at 37ºC for 2hrs, then using 10M $NH_4Ac$ precipitation, as described. T7 mMessage mMachine™ kit (AM1344, Invitrogen) was used to make Tol1 mRNA (for co-injection with *fli1:zf cre-2A-GFP*), using 1µg DNA at 37ºC for 2hrs, according to Manufacturer's instructions, then 10M $NH_4Ac$ precipitation again was used.

### 4.2.10 RNA precipitation

33µl 10M $NH_4Ac$ and 350µl EtOH were added to the mixture, then left at -80ºC for 2hrs. The precipitate was then centrifuged at 14,000g for 30mins, and washed with 500ul EtOH. This was spun for 5mins at 14,000g, then air-dried for 5 mins on the bench, taking care to remove all traces of EtOH. The pellet was then resuspended in 20µl milliq water.

### 4.2.11 PCR

Polymerase chain reaction (PCR) was always performed from hotstart, with 40 cycles, unless Phusion PCR was used (15-20 cycles). PCRs were usually performed in 20ul, or 100ul where necessary. Touchdown PCR was used during Gibson cloning, at times, to improve primer binding specificity. All PCRs were performed using 5xFirepol® (04-12-00115, Solis Biodyne), except for cloning, where Phusion® (M0530L, NEB) was used for higher fidelity, according to Manufacturer's instructions. Biorad T100™ was used for all PCRs.

### 4.2.12 Recombination PCR test primer

| Primer | Sequence | Product size (bp) |
|---|---|---|
| TC out F1 | acatgggagaagtgcaaaaca | 358 |
| TC out R | TCCTGGGTCACATGGATCAC | - |
| TC in F | GGCCGCGACTCTAGATCATA | 662 |
| TC in R | TCCTTGTAGTCAGCTCCCTTG | - |
| YT out F | ttcgggtgaactatctcgttt | 429 |
| YT out R | TGAGTCTGGCAGCTTTCTCA | - |
| YT in R | GAGTCTCCCCGAACATGGAC | 689 (with TC in F) |
| DA TAZ out 2F | tgtttacagggatccAAGCTT | 221 |
| DA TAZ out 2R | CGAGGTCTGTGTCTAGGTCC | - |
| DA TAZ in R | acgcttacaatttacgccttaag | 260 (with TC in F) |

Table 7: Recombination test PCR primers

NB Primers used for TC Ex15 are the same as TC above.

### 4.2.13 PCR purification/Exosap

Exosap clean-up was performed prior to sequencing, using 1U Exonuclease I (M0293L, NEB), and 1U Shrimp alkaline phosphatase (783905000UN, Thermo Fisher), with 5ul PCR product, in 10ul reaction at 37ºC for 45mins, then 80ºC for 15mins.

### 4.2.14 Gel electrophoresis

Agarose (BIO-41025, Bioline; 16500-500, Invitrogen) gels were produced at 1%, or 3% if product size was less than 200bp, or when CRISPR products were run. 1 drop of 0.625mg/ml Ethidium bromide (diluted from 10mg/ml J62282, Alfar Aesar) was used per 50ml agarose. Gels were run in TAE buffer (40mM Tris Base, 20mM acetic acid, 1mM EDTA pH 8). 100-150ml gels were run at 120V for 30-40mins. CRISPR gels were run at 120V for 90 mins. 50ml gels were run at 80V for 30mins. DNA/RNA bands were visualised using the UVP Benchtop UV transilluminator, along with the BioDoc-It™ imaging system.

### 4.2.15 DNA synthesis

DNA was synthesized for numerous different constructs by Genewiz (Appendix).

### 4.2.16 DNA sequencing

DNA was sequenced commercially by Genewiz (100ng/µl DNA with 10µM primer).

### 4.2.17 Quantification of DNA/RNA

RNA/DNA was measured using the nanodrop (ND-1000) spectrophotometer: at 260/280, a minimum of 1.8 was used for qPCR. RNA was measured using 260/280 and 230/260 for RNA-seq. to determine purity: a minimum of 1.8 was used for both.

### 4.2.18 RNAseq preparation

*ubi:lox nls-mCherry lox TC t2a neon* x WT were injected with *Cre* mRNA. 10 embryos (5dpf) were tail-clipped, then the clips were amplified using PCR to identify embryos with the *ubi:lox nls-mCherry lox TC t2a neon* construct (via recombination PCR), for the injected embryos. The resulting embryos were stored in RNAlater$^{TM}$ (AM7020, Invitrogen), at -20$^{o}$C until needed, then pooled in triplicate samples for RNAseq analysis, using RFP uninjected fish as a control (these were sorted via RFP, then tail clipped and stored in RNAlater$^{TM}$ at -20$^{o}$C, and pooled as above).

Once RNA was synthesised as described below, 260/280 and 260/230 ratios were measured. Samples measured at >=1.8 for 260/280 and 260/230 were selected to ensure purity. These samples were then sent to Novogene for RNAseq, where they were polyA-enriched, primed with random hexamer for cDNA synthesis, and sequenced to a depth of 9GB, using Illumina paired-end 150 sequencing.

For RNAseq on *ubi: lox nls-mCherry lox Yap1-Tfe3 t2a neon* embryos, the process was repeated, except 1dpf embryos were used. Also, embryos were unsorted for fluorescence as it was too early to sort reliably at this stage: therefore, both sets of injected and uninjected fish were genotyped.

### 4.2.19 TRIzol$^{TM}$ RNA extraction for RNA-seq.

500µl TRIzol$^{TM}$ (15596018, Invitrogen) was added to 10 fish. Fish were passed through 20G needle, 20 times, for homogenisation. They were left at RT for 5 mins, then Direct-zol$^{TM}$ RNA microprep

(R2060, Zymo Research) kit was used for RNA seq. preparation, according to Manufacturer's instructions.

#### 4.2.20 TRIzol™ RNA extraction for qPCR

For primer-based qPCR, 500µl TRIzol™ was added to 10 embryos at 1dpf, (four groups of WT injected with YT construct, YT and *Cre* mRNA, TC construct and TC and *Cre* mRNA at 0.5nl, pre-sorted for RFP/GFP). Embryos were homogenised by pipetting up and down, then RNA extraction was performed according to Manufacturer's instructions.

For probe-based qPCR, 500µl TRIzol™ was added to 20 fish at 1, 2, 3, and 5dpf (TC, YT, and DA TAZ crosses (crossed to WT) were injected with 1nl *Cre* mRNA and uninjected fish were used as a control. All fish were unsorted for fluorescence). Fish were homogenised by pipetting up and down, then RNA extraction was performed according to Manufacturer's instructions.

## 4.3 Zebrafish techniques

### 4.3.1 Zebrafish husbandry/embryo maintenance

Zebrafish were kept at 28ºC according to Home Office regulations, on a 14:10hr light-dark cycle. Embryos were sorted for fertilization and kept in E3 (5mM NaCl, 0.17mM KCl, 0.33mM $CaCl_2$, 0.33mM $MgCl_2$, pH 7.2) with methylene blue at 0.0001% (Sigma) at 28ºC, except experiments where *Cre* mRNA was involved (31ºC). Fish were staged according to Kimmel (Kimmel et al., 1995).

Embryos were either raised, or discarded before 5.2dpf, according to Home Office Animals (Scientific Procedures) Act, 1986. All procedures were performed under Project licence PP4947590 (F. van Eeden), and Personal licence 40/9118 (E. Markham).

### 4.3.2 Zebrafish lines

Lines were generated from AB embryos, or rarely LWT. Transgenic lines were produced by injection with DNA and transposase, as described. Crispants were made by injection with CRISPR gRNAs and cas9 nuclease, as described.

Fish were screened by crossing with WT and examining the resulting embryos for particular fluorescence, depending on the marker. Founders were isolated and transgenic embryos were raised.

*fli1:GFF; uas:Gcamp7a* line (van Eeden lab.) was already established. This was used for crossing to various *uas* constructs from this thesis.

### 4.3.3 Zebrafish embryo collection and maintenance

Zebrafish were paired in mating boxes with dividers, overnight. Zebrafish females were stimulated by the light, to begin laying, but were prevented from doing so until the dividers were removed. The dividers were removed in a staggered manner, to ensure only a few fish laid embryos at a time, to allow enough time for injection.
After injection, embryos were sorted for unfertilised/dead embryos on the same day they were laid. They were placed into E3 medium and kept at 28ºC, unless otherwise stated.

### 4.3.4 Zebrafish anaesthesia

Embryos were anaesthetised with Tricaine (MS-222, Sigma), at a final concentration of 0.168%.

### 4.3.5 Micro-injection of embryos

Thin-walled borosilicate capillaries (TW120-4, WPI) were pulled on the micro-pipette puller (P-97 Sutter Instrument company, Novato), to form the micro-injection needles.
Needles were back-filled using micro-loader pipette tips (930001007, Eppendorf).
One cell stage embryos were injected into the yolk, using a Pneumatic Pico-pump injector (PV820, WPI), with 10% phenol red as a visual aid. Embryos were lined against a glass microscope slide (1238-3118, Fisher), inside a petri-dish (101R20, Thermo Fisher). Constructs were usually injected at 25ng/µl, except for CRISPR, which was injected at 20µM (final concentration). *Cre* mRNA was injected at 25ng/µl, TC mRNA (& control) was injected at 500ng/µl, and YT mRNA (& control) was injected at 100ng/µl. Injections were made with 1nl solution, except *Cre* mRNA injection was at 0.5nl for primer-based qPCR.

## 4.4 Zebrafish genomic DNA extraction

### 4.4.1 Prot K extraction

If the PCR product was expected to be >300bp, ProtK (P6556, Sigma) extraction was used. Embryos were placed into single wells in a 96 well plate, or single PCR tubes. TE extraction buffer (10mM Tris pH 8, 1mM EDTA pH 8, 0.1% Tween) was used (98ºC, 10mins) with 1.85mg/ml ProtK, at 55ºC overnight, then 98ºC for 10mins to denature ProtK. 1.5µl was added per PCR reaction.

#### 4.4.2 KOH extraction

If PCR products were expected to be < 300bp, KOH extraction was used (Sanger Institute protocol). 25ul 1x base solution (1.25M KOH, 10mM EDTA) was added to the embryos, then 95ºC for 30mins, then cooled for 5mins, vortexed and centrifuged for 2mins at 4200rpm, and 25µl of neutralization solution (2M Tris-HCl) was added. This was then vortexed as above, and 1.5µl was added per PCR reaction.

### 4.5 Zebrafish genome editing

#### 4.5.1 gRNA design

CDKN2a/b gRNA was designed using CHOPCHOP (https://chopchop.cbu.uib.no/) to generate CDKN2a/b crispants.

| gRNA | Sequence | PrimerF | PrimerR | Product size (bp) |
|---|---|---|---|---|
| CRISPR2 (ex2) | GAGGTGTGCTCCCT GTGTCG(GGG) | CCAGGTGATGAT GATGGGTAAC | TCGCAGTGATCTT TTGTATTGG | 186 |
| CRISPR5 (ex1) | GCGTCTAAACCTAC CTGTAT(AGG) | GCAGCCACCGGA AACATTT | cccatatagtcaaacaggtgt ga | 281 |
| CRISPR6 (ex2) | GATGATGGGTAACG CACCTT(TGG) | ATCATGACGTTA CTGGCGTTTA | GTGTCAATGAATC CGGTTCTG | 185 |

Table 8: CRISPRs gRNA and primer sequences

### 4.5.2 Co-injection of gRNA/cas9P

To produce crispants, one cell stage embryos, from *ubi*:*lox nls-mCherry lox TC t2a neon* x *fli1ep: zf cre-2A-GFP* were injected with CKND2a/b CRISPRs 2 and 6 (20µM each final concentration, IDT), with cas9 protein (2µM final concentration) (M0386T, NEB), and tracer (20µM final concentration, IDT) at 1nl. A second and third batch was also injected with CDKN2a/b CRISPRs 2,5, and 6 (20µM each final concentration, IDT), along with tracer (20µM final concentration, IDT), at 1nl.

### 4.5.3 CRISPR/cas9 guide efficiency

1-3dpf embryos were used to test CRISPR efficiency.
5/6 injected fish and 1/2 uninjected WT fish were used per guide.
'Smudging' of DNA bands suggested DNA mutations present, on 3% gel, run at 120V for 90mins.

## 4.6 Determination of injection efficiency

Constructs were selected for raising, according to GFP/RFP/CFP.

## 4.7 Selection of transgenic lines

*ubi*: *lox nls-mCherry lox TAZ-CAMTA1 t2a neon* founders with 50% RFP transmission were selected to ensure there was only 1 copy of the construct present. This was the same for all other founders.

## 4.8 Cre-lox recombination

*ubi*:*lox nls-mCherry lox TAZ-CAMTA1 t2a neon* x WT embryos were examined for RFP at 3dpf, as maternal contribution had lowered significantly by this point. *Cre* mRNA injected embryos were kept at 31ºC to aid *Cre* recombinase.

## 4.9 Zebrafish gene expression analysis

### 4.9.1 Fixing embryos

Embryos were fixed at various stages, for 2hrs at RT, or overnight at 4ºC, in 4% PFA, unless otherwise stated.

### 4.9.2 Dechorionation

Embryos were dechorionated using No.5 Dumont forceps (Agar Scientific).

### 4.9.3 Sample preparation

Fish were staged according to Kimmel *et al*., 1995. They were dechorionated if necessary, then fixed as previously described (4.9.1), and put into a MeOH series (30%, 60%, 100%) for 10mins each, then stored in 100% MeOH at least overnight, at -20ºC.

### 4.9.4 Whole mount *in situ* hybridization

#### *4.9.4.1 Plasmid probe synthesis*

| Plasmid | Restriction enzyme | Length (bp) |
|---|---|---|
| pME TAZ-CAMTA1 codon z | AccI | 1255 |
| pME TAZ-CAMTA1 IDT | FspI | 1886 |
| pME zbfish taz – CAMTA1 | Bsu36I | 974 |
| Fli1a: ERcreERcryAV | AgeI | 1087 |

Table 9: Plasmids used for probe synthesis

Probes were produced by appropriate restriction digest, then phenol purification and probe synthesis was performed, as described. A GFP probe used as a control was a gift from Dr. Stone Elworthy.

The second round of in situs were performed using TC probe, produced using PCR, then QIAquick PCR purification kit (28106, Qiagen), according to Manufacturer's instructions, and probe synthesis, as described. A nls-mCherry probe was produced via PCR, using the same method.

*In situ* probes were made by linearising 10µg DNA with the appropriate restriction enzyme, and checked on gel, then phenol/chloroform purified, as previously described, unless otherwise stated. 1µg of linearised, purified DNA was used in the probe synthesis reaction (unless PCR probe, where 100-200ng was used), along with DIG RNA labelling mix (11277073910, Roche), 20U of RNasin Ribonuclease inhibitor (N252B, Promega), 1x transcription buffer, 40U T7 RNA polymerase (P2078,Promega). 1µl was taken out to be run on gel later, with 1µl post-DNAse transcription mix. 2µl (4U) TURBO$^{TM}$ DNaseI (AM2238, Invitrogen) was added to the remainder for 30mins. The RNA was then precipitated using 10M $NH_4Ac$, as described.

| Probe | Sequence | Product size (bp) |
|---|---|---|
| TC cod z T3F | CATTAACCCTCACTAAAGGGAA TTTGCAGGATCCCATCGATG | 974 |
| TC cod z T7R | TAATACGACTCACTATAGGG GA GAGTCCACCATGTCAGGG | - |
| Nls-mcherryT3F | CATTAACCCTCACTAAAGGGAA GAAGTTATCCGGTCGCCAC | 781 |
| Nls-mCherryT7R | TAATACGACTCACTATAGGG TA TGATCTAGAGTCGCGGCC | - |

Table 10: Primers for in situ probes

#### 4.9.4.2 *In situ* hybridization

Whole mount *in situ* was performed according to Thisse (Thisse and Thisse, 2008), using DIG labelled anti-sense TAZ-CAMTA1, GFP, and nls-mCherry probes (500ng), at 2/3dpf, using 2% maleic acid block. Once samples were fixed, they were rinsed in PBS, and then bleached.

#### *4.9.4.3 Bleaching*

Embryos were submerged in a bleach solution (0.5xSSC, 5% formamide, 10% $H_20_2$) for 30mins at RT, then were washed in PBS, and put into a glycerol series, finally being imaged in 80% glycerol.

### 4.9.5 cDNA synthesis

cDNA was synthesised using 500ng RNA in 10µl reaction, using Protoscript® II First strand cDNA synthesis kit (E6560, NEB), according to Manufacturer's instructions for primer-based qPCR. cDNA was synthesised using 1000ng RNA in Lunascript® RT Supermix (E3010, NEB) in 20µl reaction, according to Manufacturer's instructions for probe-based qPCR. cDNA was diluted 1:10 before use in all reactions, except standard curve, as described.

### 4.9.6 Background DNA removal

RapidOut DNA removal kit (K2981, Thermo Fisher) was used to remove background DNA where necessary (qPCR), according to Manufacturer's instructions.

### 4.9.7 RT-qPCR

#### *4.9.7.1 Primer-based qPCR*

10 embryos at 1dpf were pooled from each group (four groups of WT injected with YT construct, YT and cre mRNA, TC construct and TC and cre mRNA, pre-sorted for RFP/GFP). These groups were homogenised in Trizol$^{TM}$ and RNA was extracted, and then cDNA was synthesised, as described.

qPCR primer optimisation was performed on primers I designed, using a standard curve, with cDNA concentrations at undiluted, 1:10, 1:100 and 1:1000, and primer efficiencies were then calculated. cDNA was initially primed using oligoDT but was then switched to random hexamer. This still gave poor primer efficiencies. Finally, plasmid DNA was used to test primer efficiencies. Primers with efficiency >90% were selected for use.

Cyr61 primer-based qPCR was performed using Hot FirePol® EvaGreen® qPCR Mix Plus (08-25-00001-5, Solis Biodyne), in 20µl reaction, on Biorad CFX96, C1000 Touch, Real Time PCR machine. Biological and technical repeats were used for all samples. The ddCT/fold change, relative to the control sample, was calculated using CFX/Excel software, and Rps29 was used as a reference gene.

| Primer | Sequence | Product size (bp) | Reference |
|---|---|---|---|
| Cyr61F | CCGTGTCCACATGTACATGGG | 238 | (Miesfeld et al., 2015) |
| Cyr61R | GGTGCATGAAAGAAGCTCGTC | - | - |
| Rps29F | TTTGCTCAAACCGTCACGGA | 110 | (Bower et al., 2017) |
| Rps29R | ACTCGTTTAATCCAGCTTGACG | - | - |

Table 11: qPCR primers

#### *4.9.7.2 Taqman™ qPCR*

*Cre* mRNA was injected into TC, YT, and DA TAZ crosses (with WT), and 20 fish (unsorted for fluorescence) were pooled from each group. There were also 20 fish from uninjected control groups used. These groups were homogenised in Trizol™ at day 1,2,3, and 5. RNA was extracted, and then cDNA was synthesised as described.

Taqman™ qPCR was performed using Taqman™ Universal PCR Mastermix (4304437, Thermofisher), according to Manufacturer's instructions, in 20µl reaction, on Biorad CFX96, C1000 Touch, Real Time PCR machine. Due to the large number of samples used, only technical repeats were used for all samples in this experiment. Cyr61 (CCN1, Dr03089097_m1, Thermofisher) probe was used. The ddCT/fold change, relative to the control sample, was calculated using CFX/Excel software, and Rps29 (Dr03152131_m1, Thermofisher) was used as a reference gene.

### 4.9.8 Zebrafish immunohistochemistry (IHC)

#### *4.9.8.1 Whole mount*

Embryos (60% epiboly)/tail pieces were rehydrated from MeOH storage, permeabilised with 10µg/ml proteinase K (P6556, Sigma) for 30sec. (24hr embryos were permeabilised with cold acetone for 7mins first, then ProtK for 15mins), and fixed in 4% PFA (28794.295, VWR) for 20mins. Embryos/tail pieces were blocked in 2% maleic acid (M0375, Sigma) buffer, then incubated overnight in primary Ab: rabbit anti-CAMTA1 (NBP1-93620, Novus Biologicals) 1:200 at 4ºC. Embryos/tail pieces were then incubated in secondary Ab: Alexa goat anti-rabbit 488 (A11034, Invitrogen) 1:500 overnight at 4ºC. Embryos/tail pieces were washed several times in PBS, then put into a glycerol series for imaging.

#### *4.9.8.2 Sections*

Sections were dewaxed with Histo-clear (NAT1334, SLS), rehydrated with EtOH, then boiled in 0.01M citrate buffer for antigen retrieval. Sections were blocked in 2% maleic acid buffer, then incubated in primary Ab: rabbit anti-CAMTA1 (NBP1-93620, Novus Biologicals) 1:200 overnight at 4ºC. Primary Ab: rabbit anti-L-plastin was also used as a positive control (GTX124420, Genetex) 1:200. Sections were then incubated in secondary Ab: Alexa goat anti-rabbit 488 (A11034, Invitrogen) 1:500 overnight at 4ºC. Secondary Ab alone was used as a negative control. Sections were washed several times in PBS, then put into a glycerol series for imaging.

## 4.10 Zebrafish histology

### 4.10.1 Immersion fixation/decalcification for sectioning

Selected fish were anaesthetised by immersion fixation to preserve cellular structure. Adult fish were immersed in concentrated tricaine until they were non-responsive (no tail response).
They were then fixed in 4% PFA, at 4ºC for 3-4days/RT for 2 days. The PFA was removed, and replaced with 2x PBS washes, then 0.25M EDTA pH 8 at RT for 2-4 days for decalcification. The EDTA was removed and replaced with 2x PBS washes, then stored in 70% EtOH at 4ºC until sectioning.

### 4.10.2 Sectioning

Fish were embedded only by Mrs. Maggie Glover (Technical Histology specialist, Oncology, University of Sheffield), using a Leica TP1020 tissue processor.

Fish were sectioned using a microtome (Leica RM2135), at 5µM, floated in a 47ºC waterbath, placed onto polysine® charged glass slides (631-1349, Menzel-Glazer, VWR), and left to dry overnight at 37ºC.

### 4.10.3 Hematoxylin & Eosin (H&E) staining

H&E staining was performed to standard protocols, using Xylene (X/0250/17, Fisher), Hematoxylin (GH5232, Sigma), Eosin (17372-8711, Acros Organics: 0.6% in Industrial methylated spirit (M/4450/17, IMS). Specimens were mounted in DPX (06522, Sigma), then dried overnight at RT.

## 4.11 Microscopy/Imaging

Live images were taken by using 3% methylcellulose (M0387, Sigma) to position the fish, where necessary.

In situ images were taken using the Leica M165FC stereo-microscope, using LASV4.3 software. GFP and RFP images, and immunohistochemistry (IHC) section images were taken on Leica M205FCA, using LAX software. IHC tail images were taken using Nikon W1 spinning disk confocal and analysed in Fiji 2.3.0.

## 4.12 Statistical analysis

### 4.12.1 Prism

Prism 9.3.1 was used for graphs and statistical analysis. Un-paired t-test was used to compare 2 groups with normalised distribution data. One-way ANOVA was used to compare 3 groups with non-parametric data, using the Kruskal-Wallis test. SEM was used in all cases.

## 4.13 Gene Set Enrichment Analysis (GSEA) and protein interaction analysis

Data from RNA-seq was analysed using Gene set enrichment analysis (GSEA) v4.3.2 from the Broad Institute/UC San Diego (Subramanian et al., 2005, Mootha et al., 2003), with Biomart (Ensembl release 109 (Martin et al., 2023)) for converting Cordenonsi YAP signature (Cordenonsi et al., 2011) and Seavey EHE (Seavey et al., 2021) gene sets from human to zebrafish.

Protein-protein interactions were examined using STRING database (https://string-db.org/), using the

top 50 enriched genes from RNAseq, for both TC and YT. This was performed using medium confidence (0.4), and experiment and coexpression interaction sources.

## 4.14 Aligning mapped RNAseq reads to the construct

### 4.14.1 In silico transgenic genome for mapping purposes

NCBI was used to select the zebrafish genome (GRCz11), both fna and gff (with annotations, provides locations of genes, exons, etc.) files were used. The transgenic fna file was created by copying the regular fna file into a text edit file, with the transgenic construct added to the end. This was done by duplicating the "mitochondrial genome" at the end of the zebrafish genome sequence file, still maintaining the correct formatting of the additional sequence, but removing all mitochondrial sequences. The gff file was created by copying the regular gff file into a text edit file and then adapting the required sequence and descriptors.

### 4.14.2 Galaxy

Galaxy Europe (https://usegalaxy.org/(Galaxy, 2022)), hisat2 program was used to align biological repeat reads. The BAM files produced were merged using Merge BAM files tool, then htseq-count was used to count the number of reads aligned with the gff file, and expression levels were calculated.

### 4.14.3 Alignment

Integrated genomics viewer (IGV) (Robinson et al., 2011), version 2.16.0, was used to align mapped reads to the transgenic genome (zebrafish genome containing the transgenic construct).

# 5 Results: Initial characterisation of TAZ-CAMTA1 in zebrafish and creation of *fli1a*:TAZ-CAMTA1 & Gal4/UAS models

*Epithelioid hemangioendothelioma* (EHE) is a rare, vascular sarcoma resulting from the TAZ-CAMTA1 (TC) fusion protein (Errani et al., 2011, Tanas et al., 2011) in 90% of EHE cases (Flucke et al., 2014), and YT in 10% of EHE cases (Antonescu et al., 2013). There were no animal models/cell lines at the beginning of this project. However, even though currently there are mouse models, zebrafish offer unique points. They are optically clear, produce many embryos, are cost-effective, and are amenable to high-throughput drug screens (MacRae and Peterson, 2015).

The aim was to create a zebrafish model of TC to further characterise EHE. In order to mimic human disease, endothelial expression of TC was required, as this is the tissue of origin in the human (Tanas et al., 2011). The *fli1a* promoter has been used extensively in the zebrafish field to drive endothelial cell expression, and is very well characterised, having been shown to drive robust expression of genes in endothelial cells (Lawson and Weinstein, 2002). Therefore, it was decided to use this promoter to drive TC directly and create transgenic animals that express this gene in the *fli1a* pattern.

## 5.1 Expression of TAZ-CAMTA1 and Yap1-Tfe3 by mRNA injection

Firstly, to test the effect of TC on the vasculature (and also to test whether human protein could be expressed in zebrafish), TC mRNA was produced by restriction digest of a human TC piece, which was a gift from Dr. B. Rubin. This was then ligated into the pcs2+ vector, as this contains an SP6 site to enable the production of mRNA. The plasmid was transformed in *E. coli*, then selected and purified, and used to generate RNA by *in vitro* transcription, using the SP6 mMessage mMachine$^{TM}$ kit (Fig. 12). TC mRNA was then injected into *fli1a:EGFP* embryos at 500pg, and scored/imaged at 1dpf. TC S51A was injected as a control. S51A is a serine to alanine change at position 51 in human. S51 is essential for binding to TEAD as the serine hydrogen bonds to tyrosine Y406 and glutamic acid E240 in TEAD (Li et al., 2010, Zhang et al., 2009, Zhao et al., 2008, Chen et al., 2010) (Kwon et al., 2022).

There was a substantial difference between the TC injected embryos and TC S51A injected embryos at 500pg ($P<0.001$, Chi-squared test). Some of the TC injected embryos showed a very abnormal morphological phenotype, with very few intersegmental vessels (ISVs) present (Fig. 13B, B'). Many of

these appeared to not have developed (Fig., 13, Table 12), whereas when the one amino acid change construct, TC S51A, was injected, this did not give the same phenotype. It gave a WT-like phenotype (Fig. 13A,A') or mildly abnormal (not shown) (Fig. 13). This shows that the TC effect was not just due to general toxicity.

Zebrafish Yap1-Tfe3 (YT) mRNA was created, as it was decided that YT may be easier to express. A YT piece was produced by Genewiz (originally designed for insertion into pME-MSC2), then a XhoI site was added via PCR, in order for restriction digest/ligation into pCS2 (Fig. 12). This was injected into *fli1a:EGFP* embryos in order to test the effect of overexpression of YT on the vasculature. This took an extended period of time to titrate, as I initially began at 500pg, as with TC, but finally used 100pg. This indicated that the "potency" of YT is much higher than TC. YT did appear to be quite toxic, with much embryo death/deformity. A control construct, YT S94A, was produced, with one amino acid change from serine to alanine at the equivalent of position 94 in human. It was shown that when YAP1 is mutated at serine 94 (S94), it is not able to bind/activate TEADs (Zhao et al., 2008). Surprisingly, S94A showed a high level of toxicity at 250pg. As I expected this to be non-functional, I concluded that there may be a contamination issue, so reproduced the RNA. However, this did not resolve the issue, as S94A still showed toxicity upon injection at 250pg.
Altogether, a range of concentrations were tried for YT (50, 100, 250, 500pg) and 100pg was the optimum. Below this most of the embryos gave a WT phenotype, and above this, there was a high death rate (28.6% death for YT and 24.1% for S94A at 250pg). Using the chi-squared test with 100pg YT vs YT S94A, P=ns. Overall, I concluded that it is possible S94A may have been dominant negative and interfered with endogenous YT.

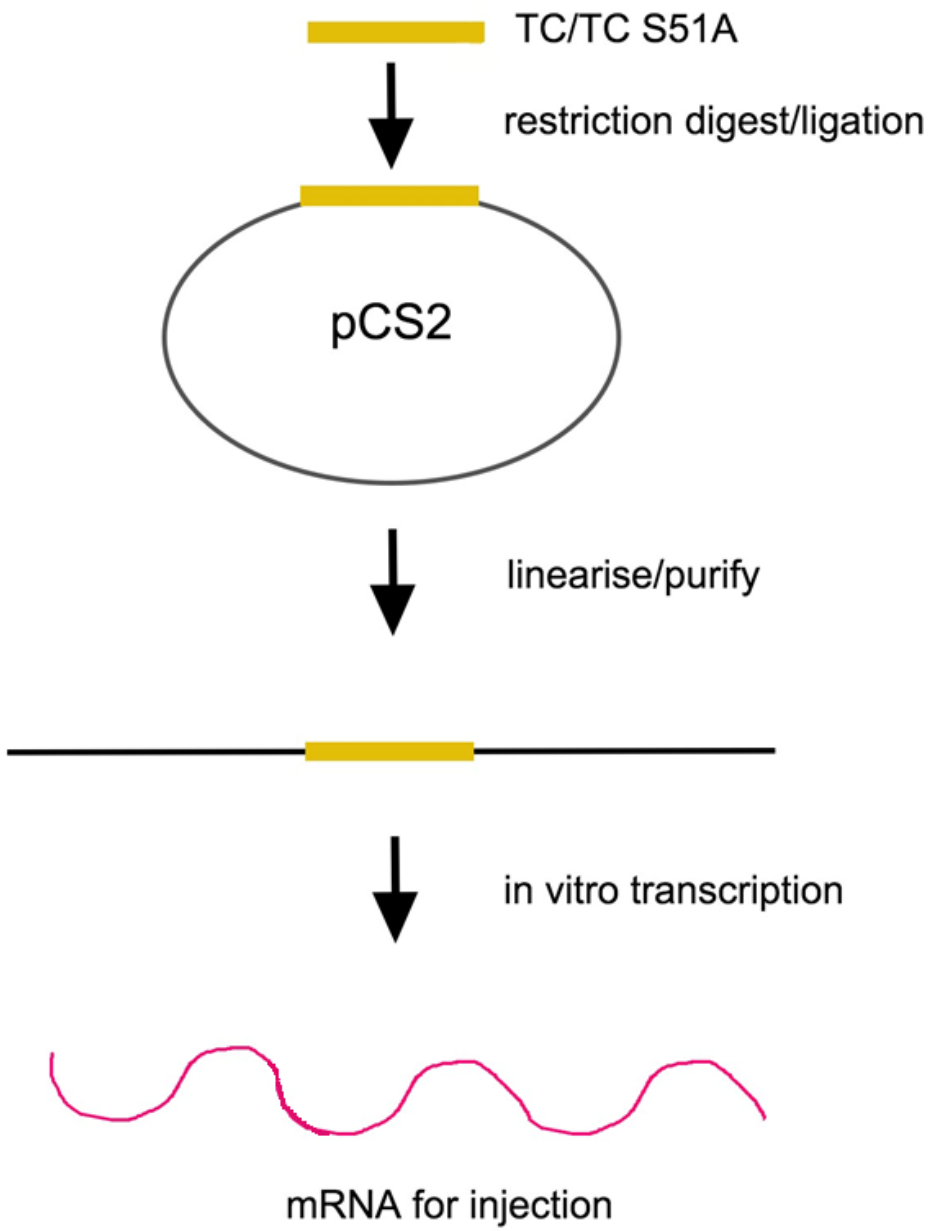


Fig 12: Schematic diagram to show production of TAZ-CAMTA1 mRNA
TC and TC S51A were both produced via restriction digest and ligation into pCS2, then in vitro transcription was performed from the linearized plasmid.
TC and TCS51A both originated from gifted plasmids.
YT and YTS94A were created via the same process, except a XhoI site was added via PCR (to a YT Genewiz fragment), before restriction digest/ ligation into pCS2.

| Phenotype | TAZ-CAMTA1 500pg | TAZ-CAMTA1 S51A 500pg | Yap1-Tfe3 **100**pg | Yap-Tfe3 S94A **100**pg |
|---|---|---|---|---|
| Class I (severely abnormal) | 9 | 0 | 8 | 13 |
| Class II (abnormal) | 6 | 20 | 4 | 0 |
| Class III (WT) | 10 | 9 | 31 | 34 |

Table 12: TAZ-CAMTA1/S51A and Yap1-Tfe3/S94A injected embryos, sorted into classes
There are more severely abnormal embryos in the TC injected embryos, compared to the control.
YT was injected at a much lower concentration than TC, as it appeared quite toxic at higher concentrations.
YT S94A also appears to have a considerable effect.
TAZ-CAMTA1(500pg) ***P<0.001
YAP1-TFE3 (100pg) P=ns, both Chi-squared test

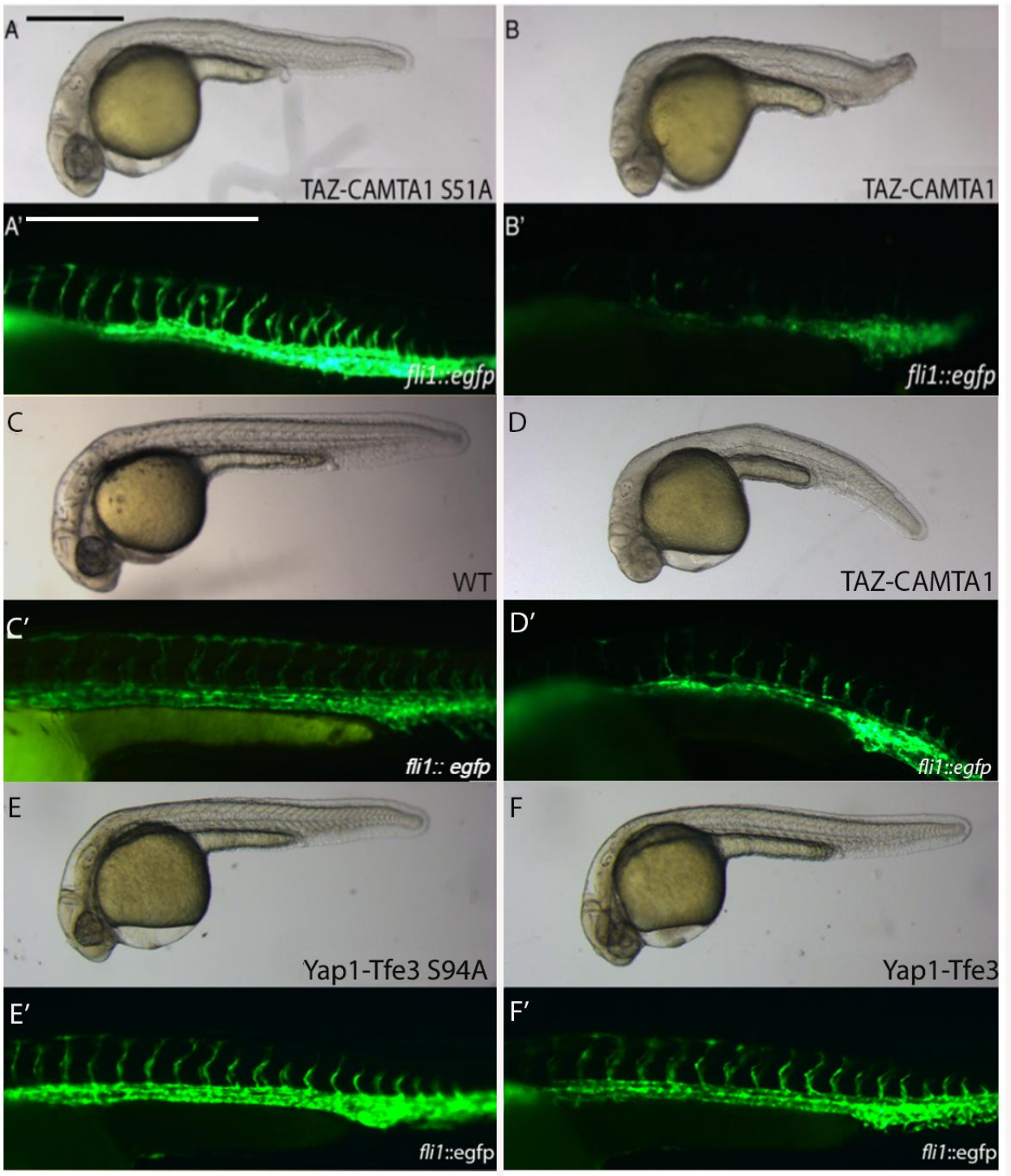


Fig. 13: TAZ-CAMTA1 mRNA and Yap1-Tfe3 mRNA injection into *fli1a*: *EGFP* at 1.5dpf
A, A': TAZ-CAMTA1 S51A amino acid change injected gives WT-like phenotype with visible ISVs (class III)
B,B': TAZ-CAMTA1 injected embryo and few ISVs visible (class I)
C, C': WT uninjected embryo and WT ISVs
D,D': TAZ-CAMTA1 injected embryo and some ISVs visible (class II)
E, E': Yap1-Tfe3 S94A amino acid change injected with some visible ISVs (class I)
F, F': Yap1-Tfe3 injected embryo with some visible ISVs (class I)
Scale: 0.5mm (Images compiled in Photoshop)

## 5.2 Testing CAMTA1 antibody on TAZ-CAMTA1 mRNA injected zebrafish

As mentioned previously, I planned to use an antibody (Ab) to detect TC in zebrafish later in the project, in order to distinguish TC induced tumours from spontaneous. WT zebrafish embryos were injected with TAZ-CAMTA1 mRNA at 500pg. Uninjected zebrafish served as a control. Embryos were then fixed at 24hrs and stored in MeOH until use. CAMTA1 Ab staining was performed, with all embryos showing no visible staining. It was thought this may be due to Ab penetration issues. Therefore, to circumnavigate this, I injected a new batch of embryos and fixed at 60% epiboly. Upon CAMTA1 Ab staining, the injected embryos showed green CAMTA1 nuclear staining, whereas the uninjected embryos did not show this (Fig. 14). This confirmed that the antibody was functional in zebrafish whole mount immunohistochemistry, and that RNA injection was indeed leading to the production of the fusion protein.

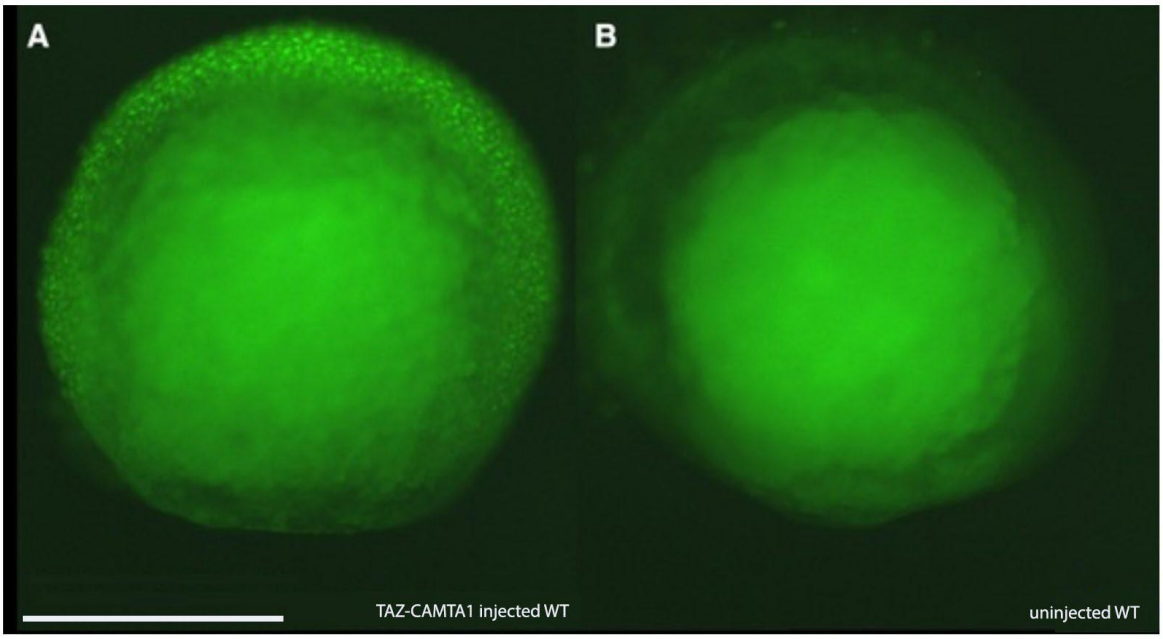


Fig. 14: CAMTA1 Ab staining at 60% epiboly
(A) TAZ-CAMTA1 mRNA injected embryo. Bright green spots representing (TAZ-)CAMTA1 positive nuclei can be observed.
(B) Uninjected embryo, with no CAMTA1 staining.
Both embryos are stained with anti-CAMTA1 (NBP1-93620, Novus Biologicals)
(N.B. both embryos show auto-fluorescence in the yolk).
Scale: 500μm

## 5.3 Generation and characterisation of *fli1a:TAZ-CAMTA1* zebrafish

As the mRNA injections and antibody staining showed that human TAZ-CAMTA1 was produced and active in zebrafish, *fli1a*:*TAZ-CAMTA1* constructs were produced, as EHE is known to originate in the endothelial cells of the blood vessels (Sardaro et al., 2014). These were injected to produce transgenics, initially using *cmlc2:egfp* as a transgenesis marker, then later using *cry:cfp*. This was due to the fact that there have been unpublished reports that the *cmlc2* promoter may interfere with other promoter function (R. Wilkinson, pers. comm.). Several independent lines were established which showed expression of the transgenesis marker. Transgenic fish showed normal development, and no abnormalities in blood vessel patterning were observed. In order to confirm that the *fli1a* promoter was working as expected, embryos from these lines were tested using whole mount *in situ* hybridisation. Highly surprisingly, these *in situs* did not show the expected *fli1a* expression pattern (Fig. 15). I hypothesised that the *fli1a* promoter may somehow have been altered in the 5' pENTRY plasmid that was used for making the constructs. Therefore, a *uas:EGFP* control line was produced and crossed with the *fli1a:GFF* line (using the same fli1a plasmid). The improved version of Gal4, Gal4FF (GFF) was used (Asakawa et al., 2008), under the control of the *fli1a* promoter. This line was previously established and known to be functional (R. Wilkinson, pers. comm.). However, this gave the expected *in situ* expression pattern (Fig.15E). Therefore, this showed that the results were not due to issues with the Gateway plasmids. Another reason for the unexpected difference may be that expression of TAZ-CAMTA1 is toxic, and only insertions that behave anomalously will survive through the germline of injected G0 fish. For this reason, it was decided to create models where TAZ-CAMTA1 would be switchable, based on the Gal4/UAS system.

## 5.4 Generation and characterisation of Gal4/UAS: TAZ-CAMTA1 model

Gal4 is a yeast transcriptional activator, which controls the expression of an Upstream Activating Sequence (UAS) promoter (Scheer and Campos-Ortega, 1999). A gene of interest (effector) can be fused to UAS, which will only be expressed when this line is crossed with the Gal4 line. Otherwise, the effector gene is silent (Scheer and Campos-Ortega, 1999) (Fig. 8), allowing establishment of lines that can express "toxic" transgenes. The improved version of Gal4, Gal4FF (GFF) was used (Asakawa et al., 2008), under the control of the *fli1a* promoter, once again.

At the time, the 5'Entry *uas* promoter plasmid in the Bateson Centre, Sheffield, had been shown to incorrectly function (F. van Eeden, pers. comm.). Therefore, a new *uas* promoter was created and tested to ensure functionality. It was produced by annealing ultramers, then restriction digest of both

this and the p5E plasmid, before phosphorylating the fragment, and dephosphorylating the plasmid, then ligation, cloning, and purification. A *uas:EGFP* construct was produced in tandem to ensure the promoter was working, and this was shown to be the case.

Several different versions of *uas*: *TAZ-CAMTA1* transgenics were created using *cry:cfp* as a transgenesis marker, some with a t2a-NEON tag (a bright version of GFP), and others without. Transmitters were identified by *cry:cfp* expression, then crossed to the *fli1a*:*GFF* line. Embryos were then fixed at 2dpf and stored in MeOH until *in situ* was performed, using the TC probe. However, this still did not give the expected *fli1a* expression pattern from *in situ* (Fig. 15). 50% embryos had a darker staining in the head, which were expected to be the embryos with the GFF, and hence the active form of TC. I also used GFP neon to visualise TAZ-CAMTA1, with a t2a linker (self-cleaving), but did not see any GFP at this point. To check that the issue was not due to the *fli1a*:*GFF* line, the *uas*:*EGFP* line was crossed with this, in parallel to the above cross. In contrast to the *uas*:*TAZ-CAMTA1* line, this did express GFP in the expected *fli1a* pattern (Fig. 15, E) in 50% of the embryos (with GFF, using the GFP probe). This led to the conclusion that the problem was likely to lay with human TAZ-CAMTA1.

One possibility was that human sequences may not express well in zebrafish. As I wanted to maintain the human amino acid sequence (as this would be possible to detect using human antibodies, which would be important for future experiments), I designed two zebrafish optimised TAZ-CAMTA1 constructs. These were designed using 2 different optimisation algorithms (Genewiz and IDT). This would also change the primary sequence considerably, thus if there were DNA sequences in our construct that for some unknown reason interfered with expression, the codon optimisation process may have altered these. These optimised sequences were cloned into middle entry vectors and were used to assemble new Gateway constructs for transgenesis. Constructs were sequence verified, and again injected into embryos in order to generate new transgenic lines, which contained these optimised TAZ-CAMTA1 sequences. These would be under the control of the *fli1a* or *uas* promoter. Several independent transgenic lines were generated. However, these also did not give the expected expression in the blood vessels, both under direct *fli1a* and indirect *fli1a* control *(fli1a:GFF x uas)* (Fig. 15).

Finally, in an attempt to further adapt sequences towards zebrafish, I replaced the n-terminal human TAZ (from TAZ-CAMTA1) with the equivalent zebrafish sequence, creating a "zebrafish Taz-human CAMTA1" chimera. Human CAMTA1 was retained to allow detection of the fusion by a commercially available human antibody. I had zebrafish TAZ-human CAMTA1 synthesised (Genewiz), and this was again cloned into a middle entry vector, assembled into a destination vector,

and transgenics were produced. However, all these approaches failed to produce a transgenic which expressed TAZ-CAMTA1 in an endothelial pattern (Fig. 15).

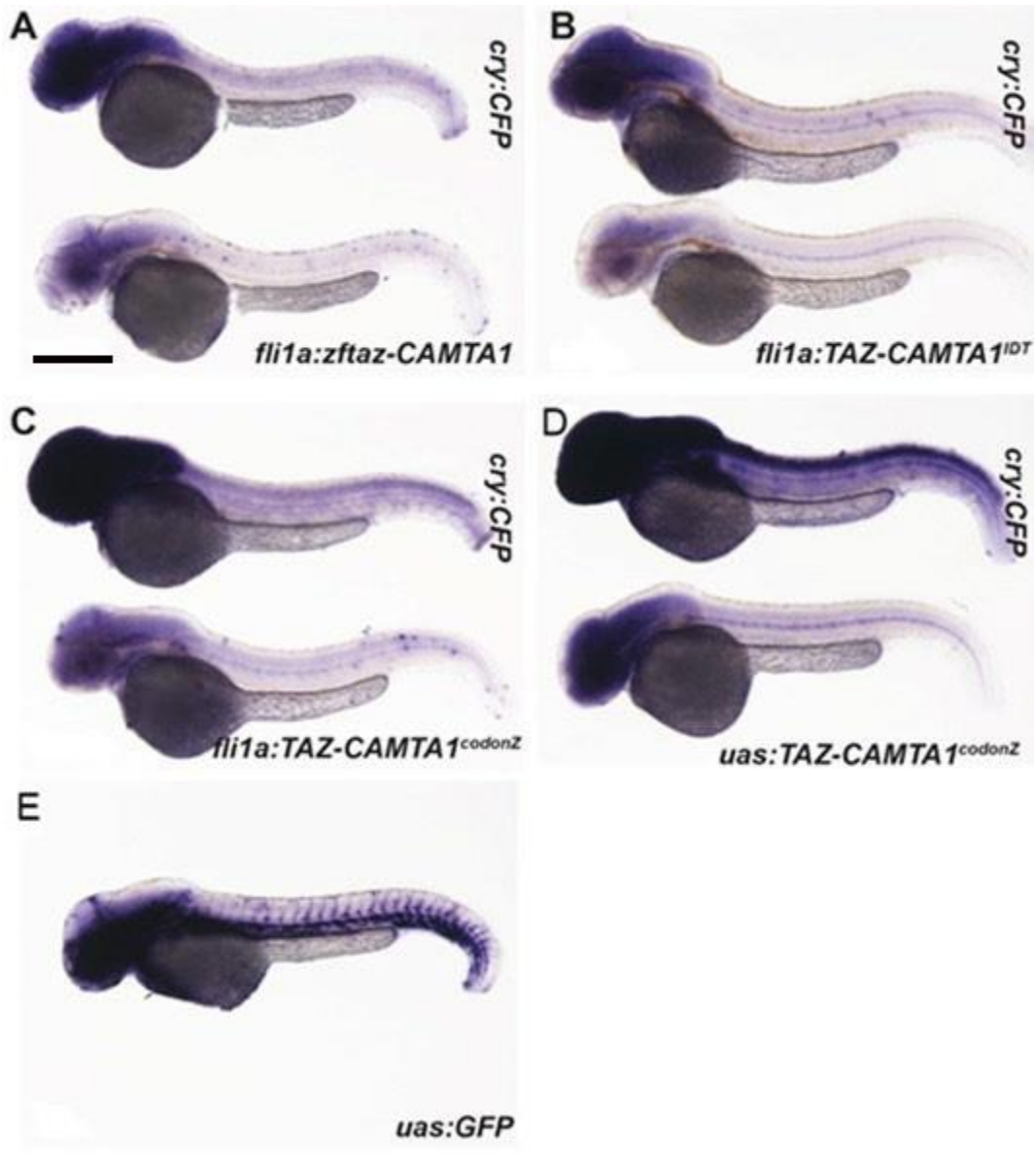


Fig. 15: *In situ* on a variety of lines with *TAZ-CAMTA1* plasmid probes at 2dpf
A-E: The top fish is CRY positive, the bottom fish is CRY negative in each section. There is higher expression in the CRY positive fish, but not the expected *fli1a* expression pattern, as in the control (E). A-D: TC probe, E: GFP probe.
Scale bar: 0.5mm

## 5.5 CAMTA1 appears to be the source of expression-interfering sequence elements

From my previous experiments, it appeared that the TAZ-CAMTA1 gene sequence behaved differently from the GFP sequence, when driven by the same promoter. We speculated that there may be sequence elements in the construct that somehow influenced expression. Therefore, I examined the source of the expression-interfering sequence elements by cloning TAZ and CAMTA1 as EGFP fusion proteins, behind a *fli1a* promoter. Restriction digest was used to isolate these fragments, then these were ligated into *fli1a*:*EGFP*, and cloned in *E. coli*, then purified.

These constructs were injected, along with *fli1a:EGFP* as a positive control (Fig. 16C). GFP ISVs were noted in *fli1a*: *EGFP-TAZ* (Fig. 16A), and the positive control, and analysed as G0 mosaics. No ISVs were labelled in *fli1a:EGFP-CAMTA1* (Fig. 16B). Therefore, it seemed that CAMTA1 may have been the source of expression-interfering elements.

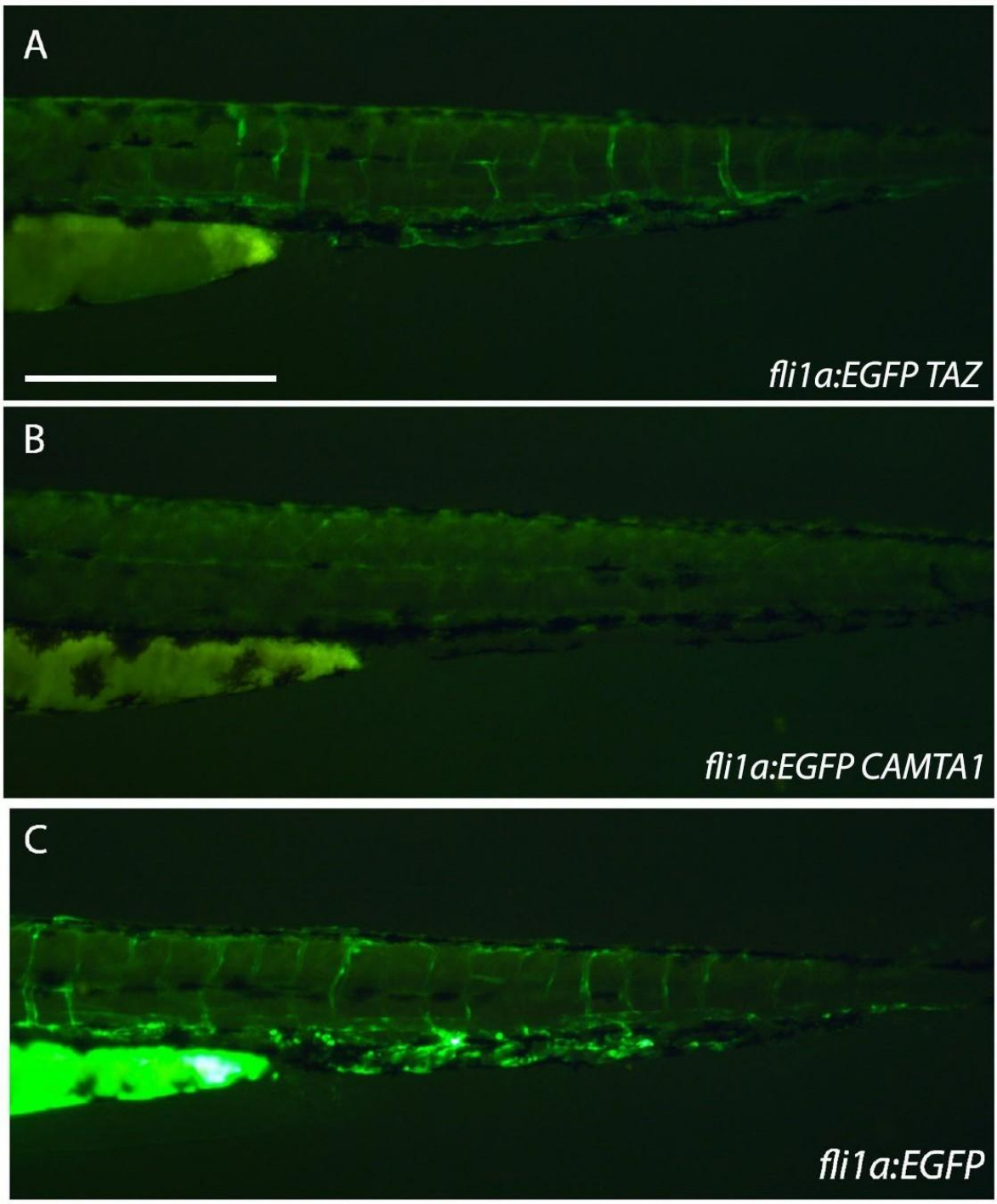


Fig.16: ISV EGFP expression in embryos injected with a variety of *fli1a* constructs at 3dpf A) *fli1a*:*EGFP-TAZ*, B) *fli1a*:*EGFP-CAMTA1*, and C) *fli1a*:*EGFP*.

There is expression of EGFP in *fli1a*:*EGFP-TAZ*, but almost no expression in *fli1a*:*EGFP-CAMTA1*.

Scale bar: 0.5mm

### 5.5.1 Further analysis of TAZ-CAMTA1 expression issues

Based on results with the previous transgenics, I hypothesised that the problem with TC expression was possibly due to DNA element(s) or protein feedback on the *fli1a* promoter, or both issues may have been involved. Evidence for the protein feedback (Fig. 17) came from our collaborator, V. Kouskoff's lab.: they found that expression of TC in mouse stem cells led to downregulation of *fli1* expression in RNAseq experiments (Neil et al., 2023).

With respect to DNA elements, a *fli1a:EGFP-CAMTA1* was constructed, with and without a STOP sequence post-EGFP, to show whether a DNA element/stem loop was present. If a DNA element/stem loop was present, there would have been an expected premature transcriptional end, with no EGFP expression (Fig. 18A). Conversely, if there was no stem loop, the polyA tail would be transcribed and there would be expected EGFP expression (Fig. 18B). An issue with this approach is that it would lead to a very long 3' UTR, which might lead to reduced expression also. *fli1a*:*EGFP-STOP-CAMTA1* was constructed. The *fli1a*:*EGFP-CAMTA1* without the STOP sequence and *fli1a: EGFP* (positive control) had already been constructed (Chapter 5.5). The *fli1a:EGFP-STOP-CAMTA1* was constructed by restriction digest of a *fli1a:EGFP-STOP-CAMTA1* DNA piece (Genewiz), ligation into linearised *fli1a:EGFP-CAMTA1*, cloning in *E. coli,* and purification.

There was no apparent GFP expression with the STOP sequence (Fig. 19A), which suggested that the issue was a DNA element(s), as opposed to promoter feedback. Data was shown to be significant, both between *fli1a:EGFP-STOP-CAMTA1* and *fli1a:EGFP,* and *fli1a*:*EGFP-CAMTA1* and *fli1a:EGFP* (Kruskal-Wallis, *P< 0.05) (Fig. 20). However, this experiment was not fully conclusive, as the construct with a STOP would have an unnaturally long UTR, which could also interfere with expression.

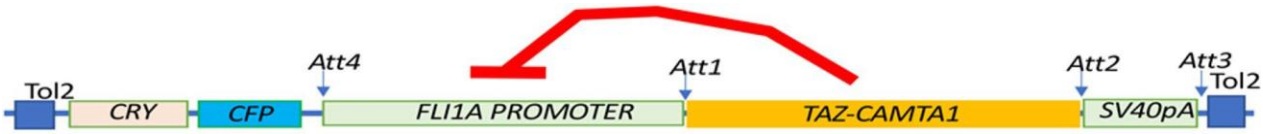


Fig. 17: Schematic representation of negative feedback on the *fli1a* promoter
TAZ-CAMTA1 is thought to cause negative feedback onto the fli1a promoter.

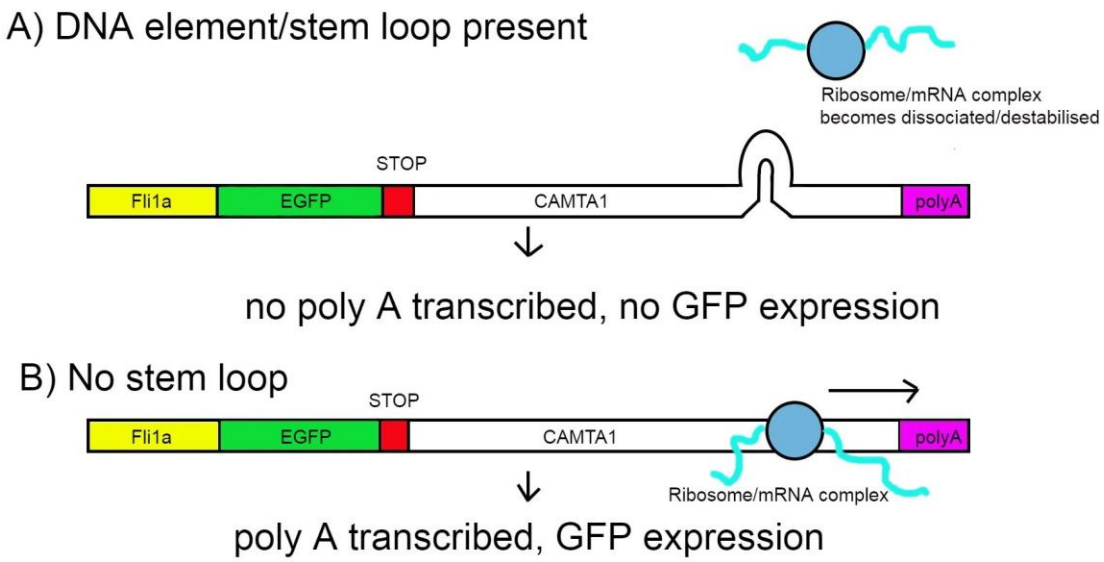


Fig. 18: Schematic representation of transcription of EGFP when a STOP sequence is added before CAMTA1, with and without stem loop
A) If a DNA element/stem loop is present, the ribosome will not continue and there will be a premature transcriptional end, hence no EGFP expression.
B) If there is no stem loop present, the polyA tail will be transcribed, and there would be expected EGFP expression.

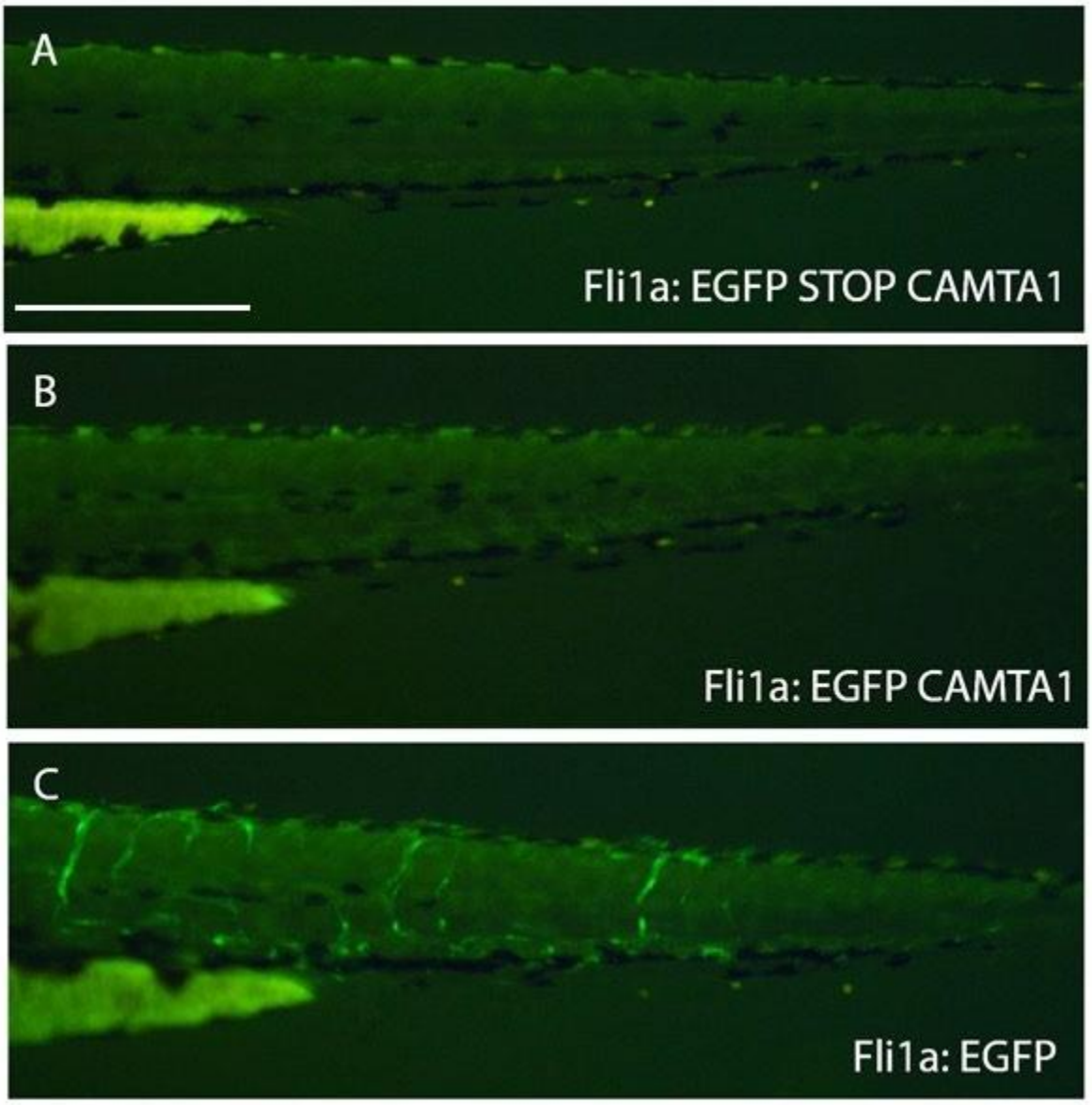


Fig. 19: No. of ISVs when embryos were injected with different *fli1a* constructs at 3dpf, to identify whether there is a stem loop/DNA interfering element(s) in CAMTA1
A) *fli1a:EGFP-STOP-CAMTA1* – no visible ISVs.
B) *fli1a:EGFP-CAMTA1* – no visible ISVs.
C) *fli1a:EGFP* - ISVs were only visible in the positive control.
Scale bar: 0.5mm

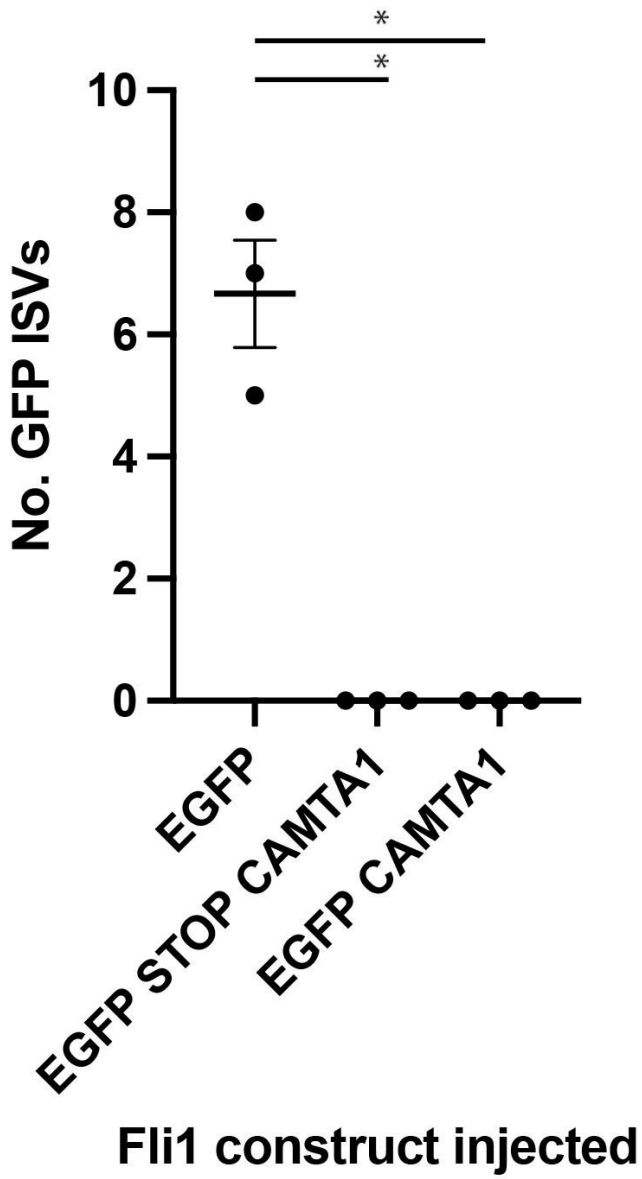


Fig. 20: No. of ISVs in different *fli1a* construct injected WT at 3dpf, to identify whether there is a stem loop/DNA interfering element(s) in CAMTA1
*fli1a:EGFP (positive control), fli1a:EGFP STOP CAMTA1, fli1a:EGFP-CAMTA1* constructs were used. There was no visible EGFP in any injected constructs, except the positive control. Kruskal-Wallis, *P< 0.05.

GFP experiments showed that CAMTA1 appeared to be the source of the expression-interfering sequence elements. Further experiments suggested that the issue was a DNA element(s), as opposed to promoter feedback. However, this experiment uses CAMTA1 as a very long 3' UTR at 4.2kb (average length of human 3' UTRs is ~1kb (Hong and Jeong, 2023)). Long UTRs are associated with lower levels of gene expression due to less stability (Sandberg et al., 2008) (Schwerk and Savan, 2015). Therefore, depending on GFP for this experiment may not have been reliable.

To conclude, TC had a significant effect when TC mRNA was injected into fli1a:GFP, vs TC S51A control. YT was not significant when compared to the YT S94A control, with injection into fli1a:GFP embryos. When in situ hybridisation was performed on transgenic TC embryos with a TC probe, this did not show the expected fli1a vessel pattern, even though controls did show this. Finally, CAMTA1 appeared to be the section causing expression issues, rather than TAZ. The cre-lox system was chosen next, as a different, inducible model.

# 6 Results: TAZ-CAMTA1 - cre-lox system

In the previous chapter, I established that the *fli1a* promoter showed a surprising sensitivity to TAZ-CAMTA1 (TC). It failed to drive expression either directly, or also indirectly, using Gal4 as an intermediate transcription factor. This was difficult to explain, but as both systems relied on continued activity of *fli1a* as the driver of expression, and it was established by a collaborator that TAZ-CAMTA1 protein was able to downregulate endothelial cell promoter expression (Neil et al., 2023), I decided to try a system that would be independent of an endothelial promoter. Instead, I would use a generic promoter that can drive expression, independent of cell type. The *ubiquitin* (*ubi*) promoter has been reported to be such a promoter and has been used extensively by the zebrafish community (Mosimann and Zon, 2011).

In addition, it was necessary to use an inducible system for spatial and temporal control. Therefore, I decided to use the *cre-lox* system. Cre is a site-specific recombinase which causes DNA recombination at loxP sites (Argos et al., 1986, Hoess et al., 1982, Hoess and Abremski, 1984). An *ubi:lox nls-mCherry lox TAZ-CAMTA1 t2a neon* line was planned to be crossed with a *fli1a*:*creER*$^{T2}$ line. This was expected to allow *mCherry* to be loxed out upon *Cre* recombination (fli1a: creERt2 lines did not show correct expression, therefore a fli1:cre GFP line was used (see 6.1) Fig. 21). There should be TAZ- CAMTA1 expression in the endothelial cells, as *Cre* would only be switched on in these cells (driven by *fli1a*), upon tamoxifen treatment. It would also allow the testing of activity of the *ubi* promoter at the transgenic insertions site, through visualisation of *mCherry*.

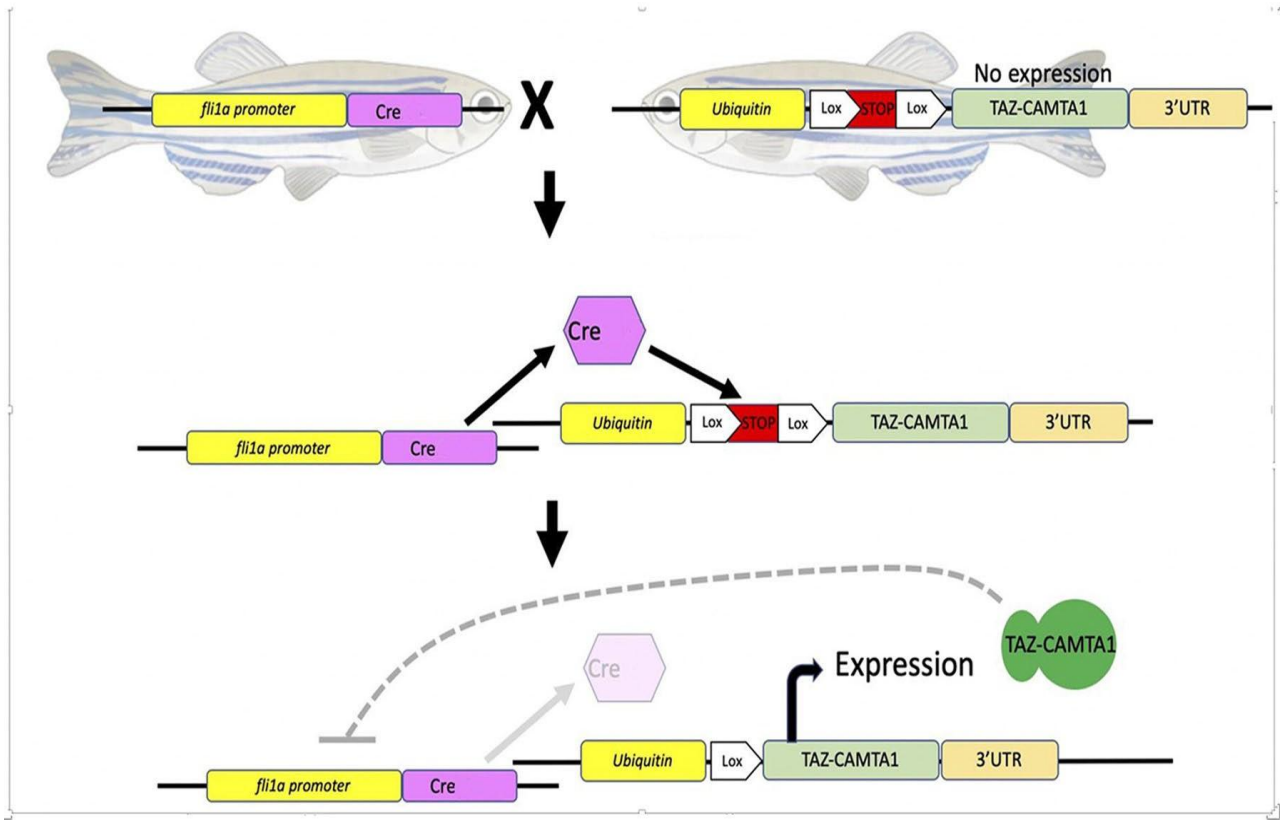


Fig.21: The Cre lox-STOP-lox system

This shows how TAZ-CAMTA1 should be expressed in the progeny, when mCherry is loxed out using cre recombinase, for site-specific expression.

## 6.1 Generation and characterisation of *fli1a* driven Cre line

A *fli1a*:*creER*$^{T2}$ line was created by injecting the construct (gifted by Dr. H. Roehl) in WT embryos. *fli1a*:*creER*$^{t2}$ fish were screened for founders using *cry:venus* as a transgenesis marker, and *in situ hybridisation* was performed on the resulting embryos to check for correct endothelial expression of *Cre*. Four lines were tested: all showed unexpected, generalised staining, with no *fli1a* expression pattern (data not shown). The construct was sequenced for *fli1a* and was found to be correct. Nevertheless, I was concerned that the *fli1a* promoter (that was being used by various groups in the

Bateson Centre, Sheffield), was somehow suboptimal, and that this may also have led to the expression (Chapter 5). Therefore, a construct was obtained from Dr N. Lawson, who initially isolated the *fli1a* promoter (Lawson and Weinstein, 2002). This construct drives a *cre-EGFP* fusion gene and has the advantage that the expression can be visualised, thus ensuring that *fli1a* is working correctly as a promoter, in injected G0 founders. This was found to be the case, and AA8 (Fig. 22) and AF22 lines were established, which showed the correct endothelial expression of *Cre-EGFP*.

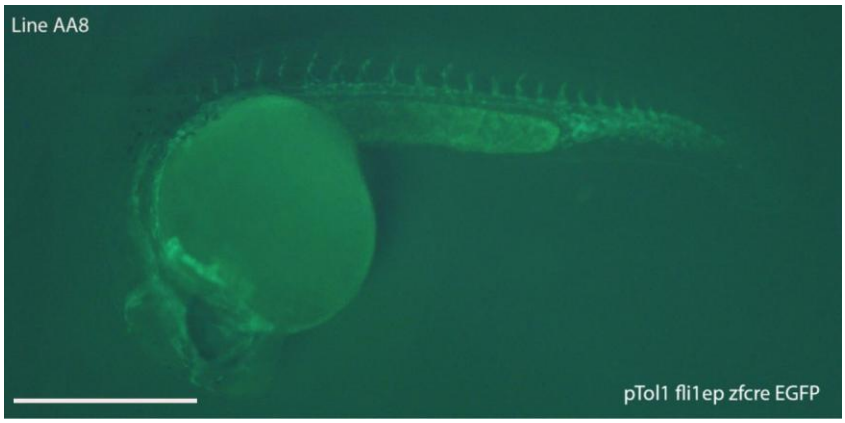


Fig. 22: *pTol1 fli1a:ep zfcre* EGFP at 1dpf
Image showing the GFP blood vessels of line AA8.
Scale bar: 0.5mm
Image is compiled using Photoshop.

## 6.2 Generation and characterisation of *ubi:lox nls-mCherry lox TAZ-CAMTA1 t2a neon*

### 6.2.1 *ubi:lox nls-mCherry lox TAZ-CAMTA1 t2a neon* fish show recombination upon *Cre* activation

The *ubi* promoter has been reported to be suitable to drive high level generic expression of proteins in zebrafish, as mentioned above (Mosimann and Zon, 2011). This promoter was made "switchable" by inserting a *lox nls-Cherry STOP lox* cassette behind it, followed by TAZ-CAMTA1-t2a-neon. t2a Neon is a self-cleaving element that should lead to production of both TAZ-CAMTA1 and Neon (a bright version of GFP) (Shaner et al., 2013). When inserted in the genome, the *ubi* promoter will drive *nls-mCherry*. This will allow direct visualisation to check the correct expression and activity level (from the brightness of the *mCherry* fluorescence) of the *ubi* promoter in G0 founders, and F1 transgenics.

An *ubi*:*lox nls-mCherry lox TAZ-CAMTA1 t2a neon* construct was created by firstly producing a *p5E ubi:lox nls-Mcherry lox* construct, using the p5 *ubi:lox GFP lox* (Addgene, 27322, (Mosimann et al., 2011)) backbone (the line it was going to be crossed to already had *venusCRY*, a green eye marker). A HindIII MfeI nls-*mCherry* DNA piece was produced (Genewiz, Appendix), then restriction digested and ligated into linearised p5 *ubi*:*lox GFP lox* (27322, Addgene) (GFP was removed via restriction digest). This was then cloned into *E. coli* and purified. Multi-site Gateway cloning was then used to produce the final *ubi*:*lox nls-mCherry lox TAZ-CAMTA1(codon z optimised) t2a Neon* construct, using the destination vector, pDestTol2pA2 (Fig. 23). In order to test immediately that the lox cassette could be removed, and TAZ-CAMTA1-t2a-neon could be activated, *ubi*:*lox nls-mCherry lox TAZ-CAMTA1 t2a neon* construct was injected into wild-type (WT) embryos, along with *Cre* mRNA, and the control without *Cre*. This showed mosaic *mCherry* expression, with a clear change from RFP in the uninjected embryos, to GFP in the injected embryos (Fig. 24).

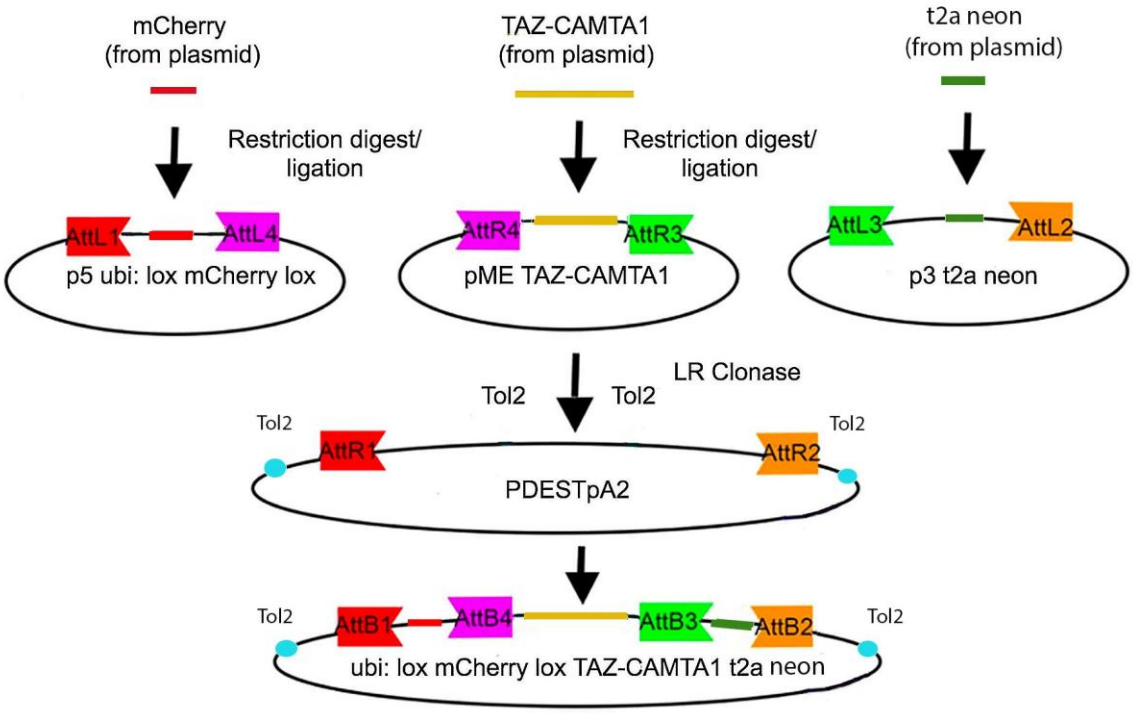


Fig. 23 Multi-site gateway cloning diagram
P5, pME-MCS2 and p3 plasmids were cloned together in the desination vector, in order to produce the final expression clone.
mCherry plasmid was produced by Genewiz. TC plasmid was gifted (B. Rubin), and t2a neon was also produced via Genewiz, and further cloned into pDONRp2R-P3.

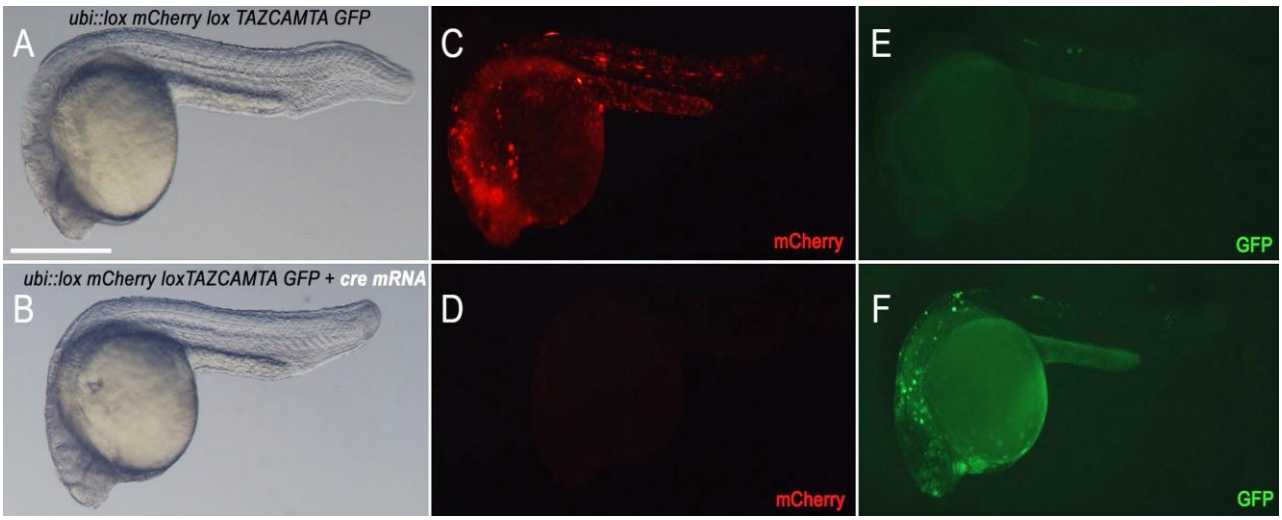


Fig. 24: Recombination test: Injection of *ubi:lox nls-mCherry lox TAZ-CAMTA1 t2a neon* into WT embryos, with and without *Cre* mRNA at 1dpf
A, C, E) an embryo injected with the construct only, and no *Cre* mRNA. C) nuclear RFP, and E) no GFP, as expected. B, D, F) an embryo injected with the construct, plus *Cre* mRNA. D) no RFP, and F) GFP spots, which indicated that the lox system was working.
Scale bar: 0.5mm

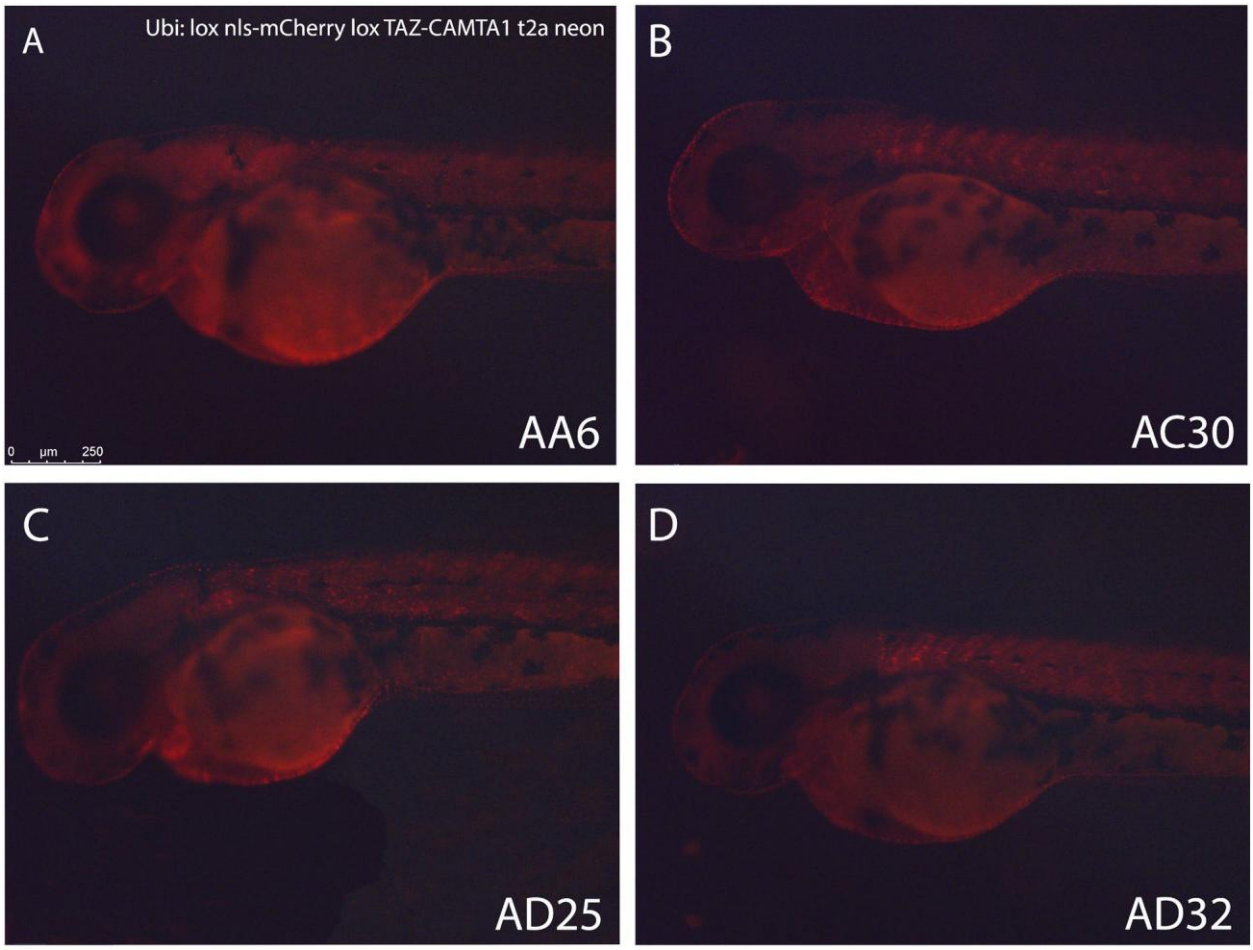


Fig. 25: RFP levels in *ubi: lox nls-mCherry TAZ-CAMTA1 t2a neon* lines at 3dpf
A,B,C,D) All separate founders

### 6.2.2 TC shows recombination via PCR

*ubi*:*lox nls-mCherry lox TAZ-CAMTA1 t2a neon* fish were screened, and founders were obtained (Fig. 25). Lines were tested by crossing to WT, and injecting embryos with *Cre* mRNA, to test the *lox* sites. Unfortunately, although no RFP was seen in the injected embryos, indicating recombination had taken place, no GFP could be visualised either. There did not appear to be a problem with accessibility of the *lox* sites, as this occurred in all founders tested to date. Nevertheless, to visualise the effect of *Cre* mRNA injection molecularly, primers for a PCR recombination test were designed. 'Outside' primers were designed to only show a band if *mCherry* (RFP) had been 'loxed out' upon *Cre* mRNA injection (Fig. 26, A, green arrows). 'Inside' primers were designed to show a band for the presence of the *lox*

*mCherry lox* cassette, as an unrecombined control (Fig. 26 A, red arrows). The PCR with the outside primers showed the correct size bands (358bp) upon co-injection with *Cre* mRNA and the transgene DNA (Tg *Cre*), and these were not seen in transgene DNA injected embryos – bands will only be present if transgene is present and *Cre* mRNA is injected (Fig. 26, B). This indicated that the STOP cassette could be removed, and recombination occurred correctly in transgenic line, AA6. A non-recombined PCR showed bands where RFP was present (662bp), in the transgene DNA injected mCherry positive embryos (Tg), but when *Cre* mRNA was injected only a weak amplification was observed (Tg *Cre*). This indicated that little *mCherry* was present, and that the STOP cassette had been efficiently 'loxed' out (Fig. 26, C). I hypothesized that Neon was not visible in the embryos as the expression levels may have been very low.

*ubi: lox nls-mCherry lox TAZ-CAMTA1 t2a neon* x *fli1a:cre EGFP* were also crossed to check that there was recombination in the lines. Embryos were sorted for the transgene (RFP) and *Cre* (GFP). The PCR from these fish showed a band of the correct size (358bp) with both the transgene and *Cre* (Tg cre), but not in the fish with the transgene only (Tg) (Fig. 27, B). This indicated that the STOP cassette can be removed and recombination can occur in transgenic line AA6 (bottom bands are primer-dimer). The non-recombined pcr showed bands where *mCherry* is present (662bp), in the embryos with the transgene and Cre (Tg cre), and transgene (Tg) alone, as *mCherry* is expressed ubiquitously (Fig. 27, C).

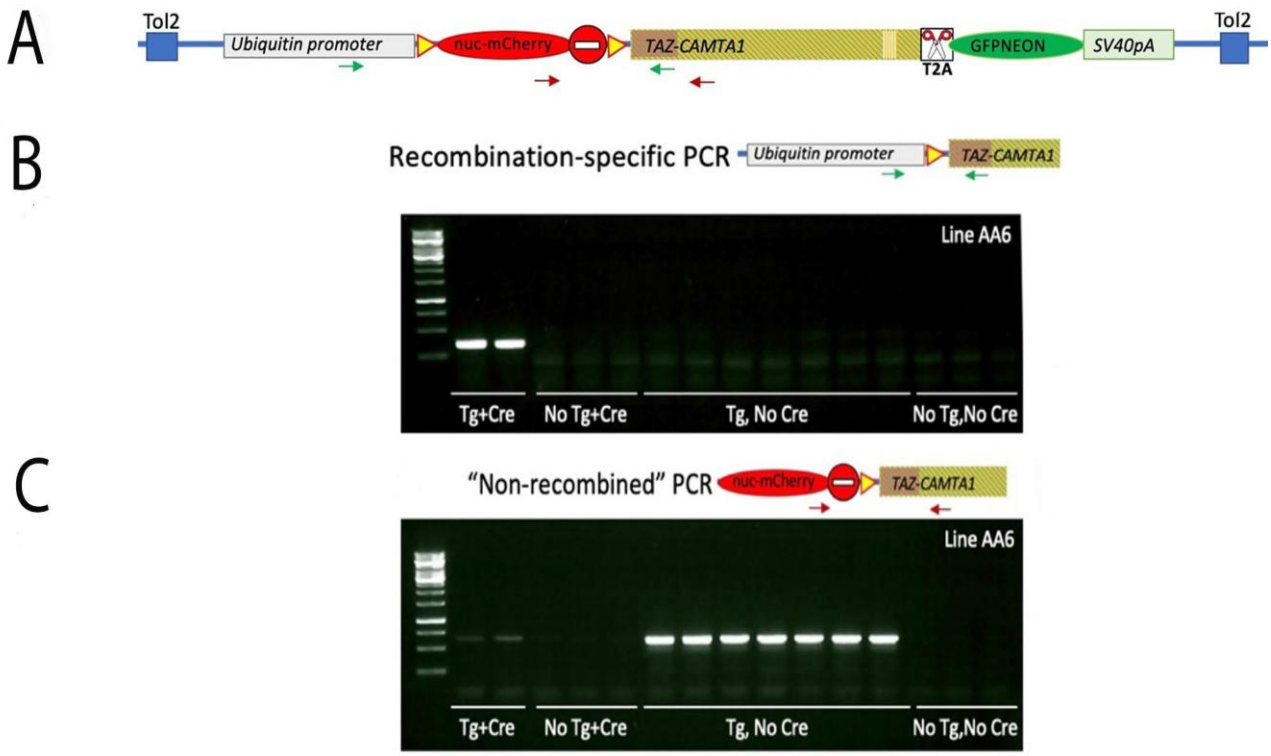


Fig. 26: Recombination-specific PCR test (with *Cre* mRNA coinjection) for TAZ-CAMTA1
A) Schematic representation of *ubi: lox nls-mCherry lox TAZ-CAMTA1 t2a neon*.
B) A PCR showing bands upon injection with TAZ-CAMTA1 DNA & *Cre* mRNA (Tg cre) – bands will only be present if transgene is present and *Cre* mRNA is injected (358bp). This indicates the STOP cassette can be removed and recombination can occur in transgenic line AA6.
C) A non-recombined PCR, showing bands where *mCherry* is present (662bp), in the TAZ-CAMTA1 DNA injected *mCherry* embryos (Tg no *Cre*), but a poorly working PCR when *Cre* mRNA is coinjected, indicating that little *mCherry* is present (Tg *Cre*), and has been 'loxed' out.

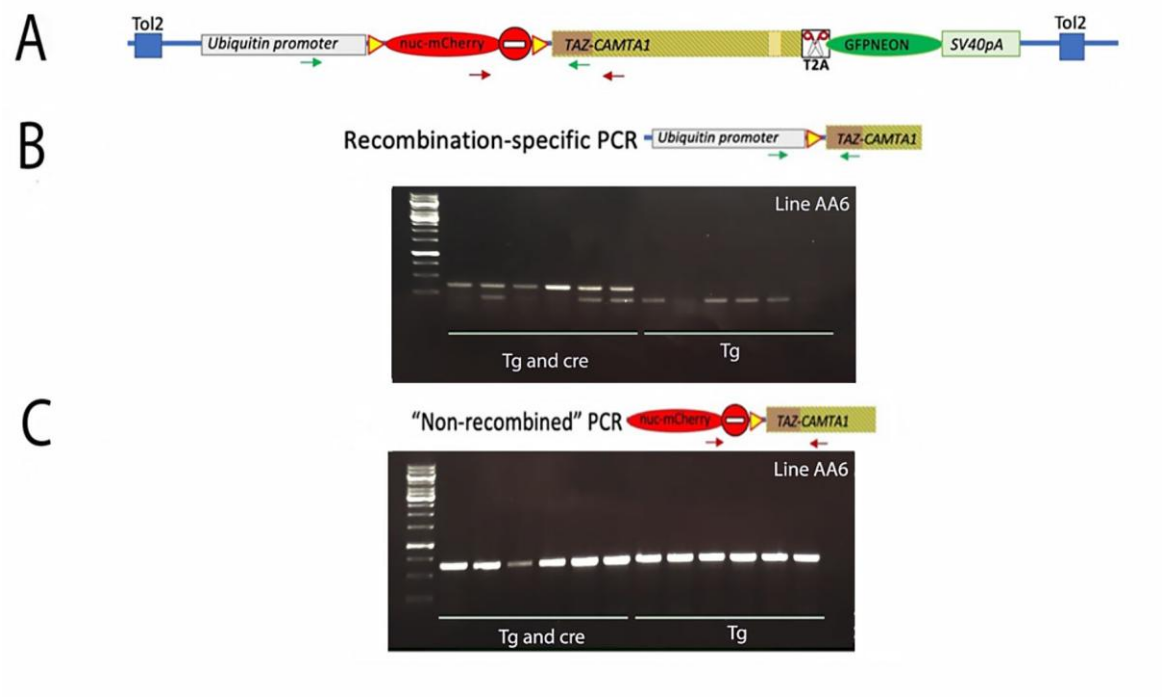


Fig. 27: Recombination-specific PCR test (with transgenic lines) for TAZ-CAMTA1
A) Schematic representation of *ubi: lox nls-mCherry lox TAZ-CAMTA1 t2a neon*.
B) A PCR showing bands of *ubi: lox nls-mCherry lox TAZ-CAMTA1 t2a neon* x *fli1a:cre EGFP* (Tg cre) – bands will only be present if transgene and *Cre* are present (358bp). This indicates that the STOP cassette can be removed and recombination can occur in transgenic line AA6 (bottom bands are primer-dimer).
C) A non-recombined PCR, showing bands where *mCherry* is present (662bp), in the *ubi: lox nls-mCherry lox TAZ-CAMTA1 t2a neon* x *fli1a:cre EGFP* embryos (Tg and *Cre*), and Tg alone. *mCherry* is expressed ubiquitously (ie. also outside the vessels, where *Cre* is expressed).

### 6.2.3 *In situ hybridisation* on the cre-lox lines does not show the *flia* pattern

As preliminary tests showed that the *lox* cassette was functional, next expression of TC in the *cre-lox* lines was performed, via *in situ*. A TC plasmid probe was produced, along with a control *mCherry* probe, which were used to stain *ubi*: *lox nls-mCherry lox TAZ-CAMTA1 t2a neon* embryos (crossed with WT), at 3dpf. These were injected with *Cre* mRNA, alongside uninjected controls. I was interested in showing changes in expression, when comparing transgenic animals with and without the *lox-STOP-lox* cassette. The expectation was that transgenic embryos that have not been switched would express mRNA for *mCherry,* and no mRNA for TC. Whereas embryos that have *Cre* mRNA injected and have lost the loxed *mCherry* sequence, would lose *mCherry* expression and gain TC

expression. A TC probe (1255bp) was produced from the pME-MCS2 TAZ-CAMTA1 construct. This was created by restriction digest and purification, then a RNA probe with a DIG label was produced via *in vitro* transcription. The *mCherry* probe (781bp) was produced via PCR.

From *in situ* data, in line AA6/7, fish 2, outcrossed to WT, and *cre* mRNA injected, 50% had TC stain as expected (data not shown). However, very surprisingly, in pre-sorted, RFP positive and *Cre* uninjected fish, 50% embryos had darker stain for TC also. It was highly unexpected to see TC stain in the pre-sorted RFP uninjected embryos, as *mCherry* was present, therefore TC should not have been expressed. It was possible that the AA6/7 line that was tested was anomalous. Therefore, I tested several different founder lines, again comparing *Cre* mRNA injected embryos and uninjected embryos with TC probe and saw the same result. I thought this unexpected result may be due to some background staining from the plasmid probe used. If the plasmid is not completely linearised, this can lead to background staining due to the possibility that other plasmid sequences are also present in the probe being transcribed. Hence a TC PCR probe was made to test this possibility, as a probe made from an amplified PCR product should be free of contaminating plasmid sequences.

To produce the new TC PCR probe (974bp), primers were designed with a T7 sequence, in order to amplify gDNA. Bulk PCR was performed, then purification and transcription, again using a DIG label. The new TAZ-CAMTA1 probe was used to stain *ubi*: *lox nls-mCherry lox TAZ-CAMTA1 t2a neon* embryos, injected with *Cre* mRNA (embryos from B2 and B4 fish shown, AD25 line - Fig. 28). From *Cre* injected fish (Fig. 28, A and B), this appeared to show that there was a difference in embryos with and without the transgene, using the TC probe. However, from these 2 images I could not deduce for certain which fish had the transgene, although levels of RFP in *Cre* mRNA injected embryos had decreased dramatically (seen when examined under the microscope prior to *in situ*). This suggested that recombination did indeed take place, and that the embryo with the darker stain had the activated transgene. The uninjected fish were then examined: Fig. 28, C shows uninjected embryos from the B2 fish, stained with the control, *mCherry* probe. This was as expected, as the pre-sorted RFP fish had much darker stain than the RFP negative fish. However, in Fig. 28, D, this showed darker stain for the TC probe in the pre-sorted RFP, uninjected fish. I would expect no TC expression in the uninjected RFP fish, as *mCherry* would still be present, as it had not been loxed out. Hence, I decided to use qPCR as a different method to examine TC expression, as *in situ* gave unexpected results with 2 separate TC probes.

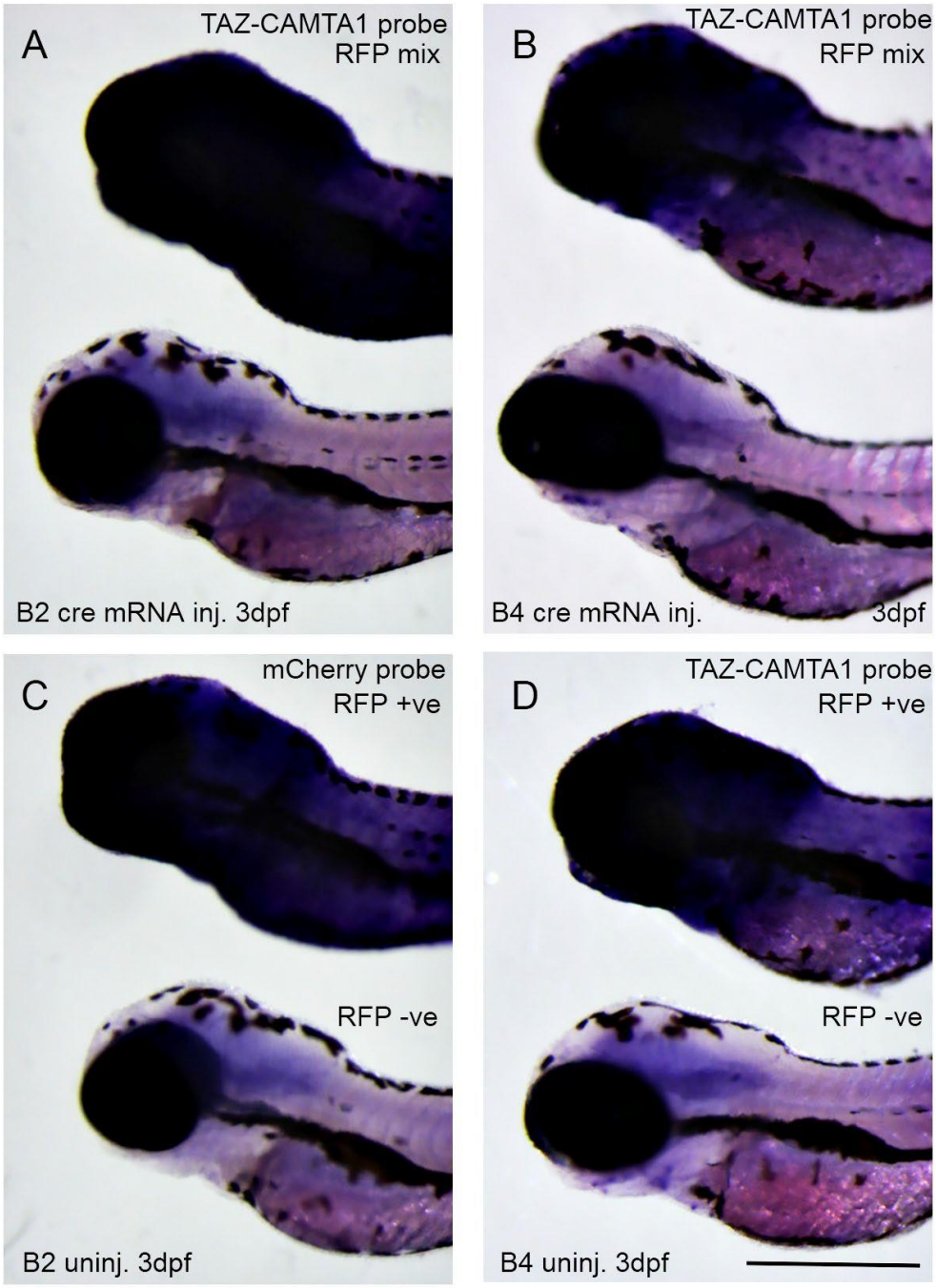


Fig. 28: *In situ* images to show TAZ-CAMTA1/mCherry expression at 3dpf
A) TAZ-CAMTA1 probe staining in *ubi*: *lox nls-mCherry lox TAZ-CAMTA1 t2a neon* injected with *Cre* mRNA, in embryos from fish B2 and C) uninjected embryos with the control *mCherry* probe.
B) TAZ-CAMTA1 staining in embryos from a different fish, B4, with *Cre* mRNA injection, and D) TAZ-CAMTA1 probe with uninjected embryos.
Scale bar: 0.5mm.

## 6.3 Preliminary qPCR optimisation for TAZ-CAMTA1

qPCR for TC (and *mCherry* as control) was performed, to show expression levels for the TC lines. Firstly, qPCR primers were designed, standard curves were performed, and primer efficiencies were calculated. Unexpectedly, all primer sets gave poor primer efficiencies. When qPCR primers were designed, it was not initially realised that there was an intron in *ubi*; therefore, primers were not designed around this, and there was a need to use the DNA removal kit. Otherwise, contaminating gDNA may have been amplified, leading to unreliable levels of RNA expression.

cDNA was initially primed using oligoDT but was then switched to random hexamer to ensure the full-length of TC was reverse-transcribed, as it is a large construct (TC is 5628bp, 4857bp without neon). This still gave poor primer efficiencies. I hypothesised that this may be due to weak expression of TC. Therefore, plasmid DNA was used to test primer efficiencies, and primer sets were then found to have good primer efficiencies, confirming that expression levels were likely to be low. This contrasted with the aforementioned *in situ* hybridisation (ISH) results. At this time, the results were returned from RNA-seq, and it was decided that this would deliver a more reliable and detailed picture of TC expression (Chapter 7). Therefore, further qPCR experiments for TC were not pursued.

To conclude, when WT lines were coinjected with the transgenic TC construct and Cre mRNA, this showed a reduction in RFP and expression of GFP, as expected if the transgene was expressed, and mCherry was loxed out. However, when Cre was injected into a transgenic TC line, there was a reduction in RFP, but no expression of GFP. Therefore, a PCR was designed to detect recombination in the lines. The PCR showed recombination did indeed occur in several different transgenic zebrafish lines (images above for AA6 line only). When in situ was performed on transgenic TC lines, this appeared to show that there was high TC expression in the mCherry selected embryos, which would not be expected, as TC expression is expected once mCherry has been loxed out. Further examination was warranted via RNAseq.

# 7 Results: RNAseq using TAZ-CAMTA1 transgenics

Due to problems with *in situ* and optimisation of qPCR primers, it was decided to use RNA sequencing (RNAseq) to examine TAZ-CAMTA1 (TC) expression levels in detail in the *ubi:lox nls-mCherry lox TAZ- CAMTA1 t2a neon* line. High-throughput DNA sequencing has become extremely advanced so that it is possible to use it to sequence RNA at a very high scale (Wang et al., 2009). As RNAseq provides information on the entire transcriptome, it will therefore also allow the determination of whether there is an impact of TC on the transcriptome, in addition to providing information on TC expression itself. It will also allow the comparison of this data to previous RNAseq experiments, using activated forms of YAP1/TAZ in other organisms. More importantly, it will also allow precise mapping of RNAseq reads to the TC gene, and may therefore provide information to identify regions where there may be a RNA transcriptional block in the TC coding sequence.

From RNAseq, I attempted to address the following questions that relate to the confusing results from Chapter 6 (Fig 29):

- Q1 Does the number of reads mapped to the transgenic construct drop after the transcriptional STOP sequence in *mCherry*, when injection of *Cre* was not performed (Fig. 24A)?

- Q2 Does the number of reads mapped to TC increase after *lox-mCherry STOP-lox* removal (Fig. 24B)?

- Q3 Are there 'suspicious' drop-offs in coverage of TC?

- Q4 In the expression of zebrafish genes, is there an increase in expression of well-known TAZ targets?

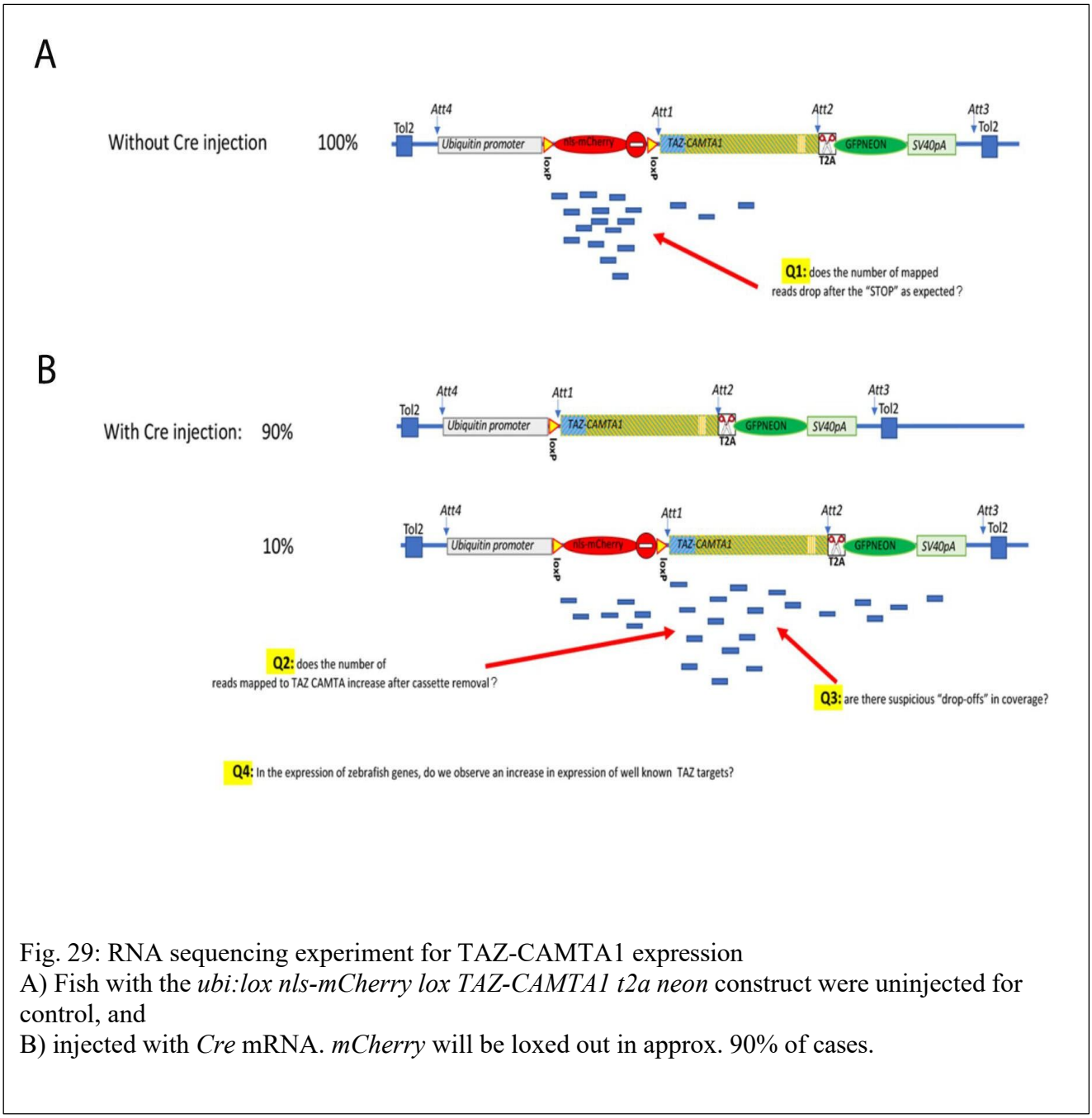


Fig. 29: RNA sequencing experiment for TAZ-CAMTA1 expression
A) Fish with the *ubi:lox nls-mCherry lox TAZ-CAMTA1 t2a neon* construct were uninjected for control, and
B) injected with *Cre* mRNA. *mCherry* will be loxed out in approx. 90% of cases.

To generate RNA samples, *ubi:lox nls-mCherry lox TAZ-CAMTA1 t2a neon* carrier (line AA6) was paired with WT. Approximately 50% of the embryos were injected with *Cre* mRNA to remove the STOP cassette and induce TC expression. Embryos were pooled in triplicate samples for RNAseq analysis at 5dpf. Uninjected fish which contained the transgene, and therefore expressed *mCherry*, were used as a control, and were easily sorted for *mCherry* fluorescence. *Cre* injected fish were examined under the microscope, and loss of *mCherry* expression was confirmed, showing that *Cre* was functional. However, this posed a problem in that it was no longer possible to identify embryos with

the transgene from embryos which were non-transgenic. Therefore, injected larvae were tail-clipped, with the anterior region being stored in RNAlater$^{TM}$, and the tail section being used for genotyping. After genotyping, transgenic larvae were selected and pooled for RNA isolation (10 embryos per sample, in triplicate). Initial tests failed to generate RNA of adequate purity (A260/A230 >= 1.8 was required). After numerous tests, it was determined that this was due to use of an RNA Qiagen purification kit, and the use of an alternative Zymo kit delivered RNA of satisfactory quality. Once RNA was purified, a cDNA library was synthesised (Wang et al., 2009). Adapters were bound to the cDNA to enable identification, then these were sequenced from both ends (paired-end sequencing) (Wang et al., 2009).

## 7.1 RNA-seq. quality control

Illumina paired-end 150 sequencing (150bp reads from either end) was used for this RNA-seq. The quality control was performed by Novogene. The number of clean reads used in the analysis for each sample is noted below (Table 13).

| Sample | No. of reads |
|---|---|
| Injected1 | 84989232 |
| Injected2 | 70744658 |
| Injected3 | 59612840 |
| Uninjected1 | 93616332 |
| Uninjected2 | 76796416 |
| Uninjected3 | 78682394 |

Table 13: Number of reads used for each sample in RNAseq for TC

### 7.1.1 Principal Component Analysis (PCA)

PCA is a statistical method to reduce several sets of data down to two dimensions. It examines how the data is grouped and was performed on the gene expression value (FPKM). The first principal component gives a ‘line of best fit’ in the direction of the largest variability in the data. The second

principal component gives the direction with the second largest variability in the data (https://tinyurl.com/5bfxt4kz).

Injected samples are more dispersed than uninjected samples, hence the injected samples show more variance, as may be expected. Nevertheless, injected and uninjected samples overall appear to cluster in separate areas, with PC2 being the most differentiated (Fig. 30).

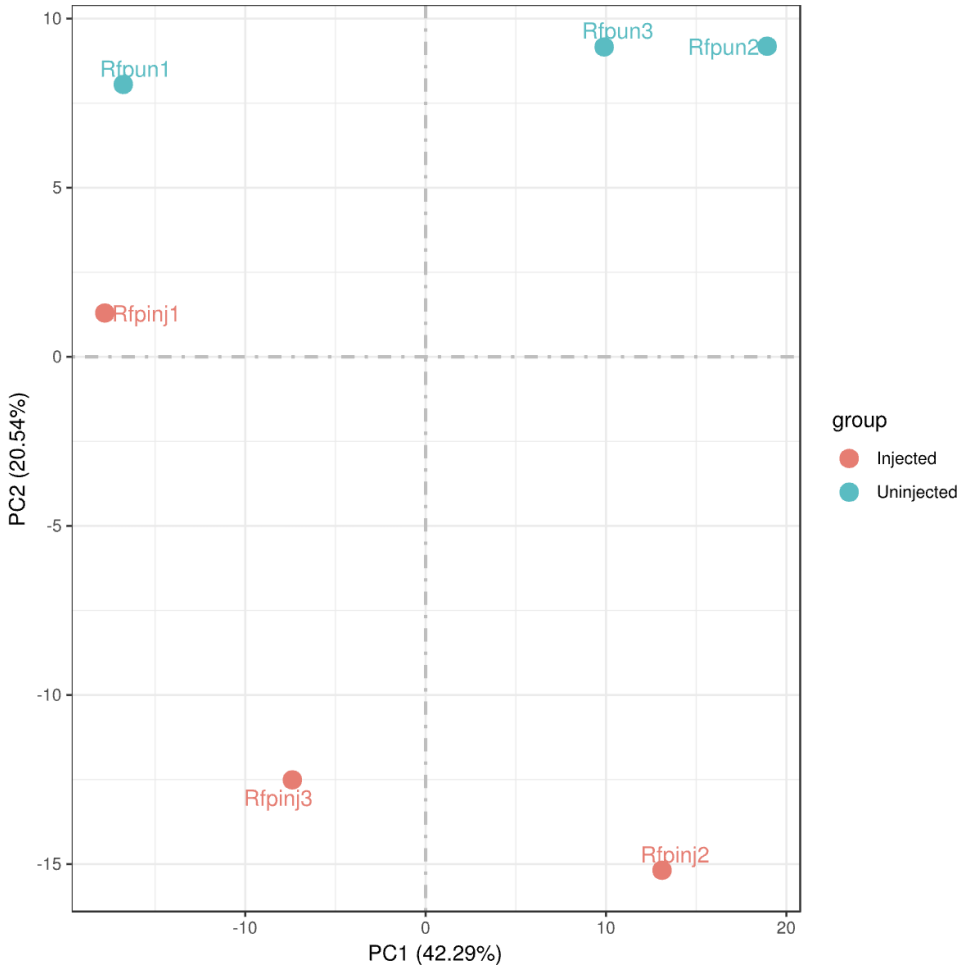


Fig. 30: Principal component analysis (PCA) for TAZ-CAMTA1
This shows the intergroup and intragroup differences.
PCA was performed on the gene expression value (FPKM) of all samples.
Injected samples are more widely dispersed than uninjected samples.

From the other QC data, all the samples had average error rate of less than 0.03%. Generally, a single base error rate should be lower than 1% (Novogene report). Also, the GC content appeared unremarkable. Overall, the quality and amount appeared to be satisfactory, and I continued with expression analysis.

## 7.2 Differential expression analysis

After sequencing and basic quality controls were finished, differential expression analysis was performed to identify the number of genes that have expression levels which are significantly different within each group. The differential gene histogram shows the total number of genes (1888); the number of upregulated genes (936), and the number of downregulated genes (952), when comparing injected to uninjected samples (DeSeq pvalue<=0.05, log2FoldChange>=0.0) (Fig. 31).

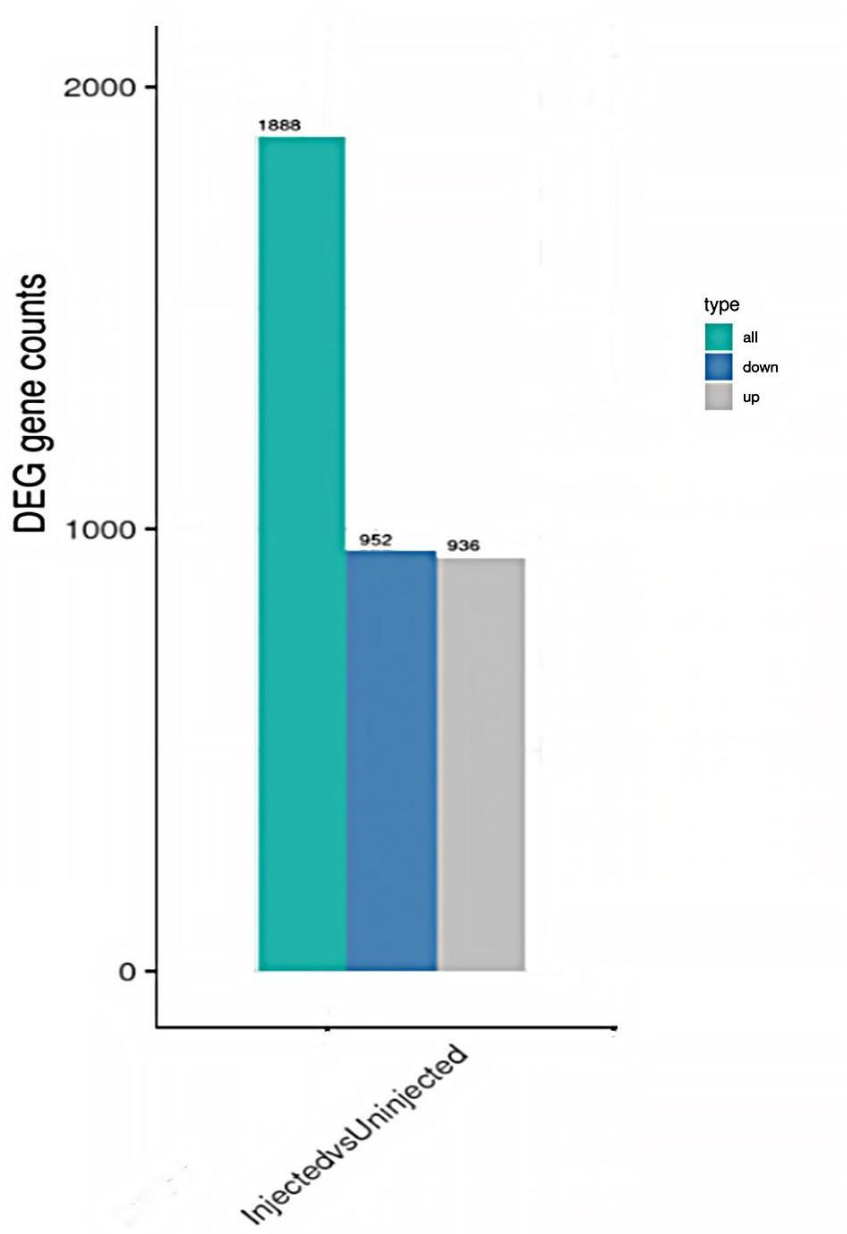


Fig. 31: Differential gene histogram for TAZ-CAMTA1
Differential gene histogram: number of upregulated and downregulated genes are shown for injected vs uninjected samples
DeSeq pvalue<=0.05, log2FoldChange>=0.0

### 7.2.1 Volcano plot of differentially expressed genes

Volcano plots can be used to infer the overall distribution of differentially expressed genes. In the figure, the x-axis shows the fold change in gene expression between different samples, and the y-axis shows the statistical significance of the differences. Red dots represent up-regulated genes and green dots represent down-regulated genes (Novogene report). The threshold for -log10(p value) is 1.301 (significance is taken as <0.05, -log10 of 1.301 = 0.05). For upregulated genes, there were 195 genes above 2 fold increase, and 99 genes above 3 fold increase.

From the top 15 DE upregulated genes, of note is Cyr61 (11$^{th}$ most upregulated) (Table 14, Fig. 32). As previously mentioned, Cyr61 is a well-known YAP/TAZ target (Zhang et al., 2011, Lai et al., 2011). Also upregulated are *jund, junba, junbb, and fosl1a*: the jun and fos families are all associated with the AP-1 transcription factor complex (Curran and Franza, 1988). AP-1 is known to have a role in tumour transformation and growth (Zanconato et al., 2015). YAP/TAZ-TEAD is known to bind at enhancer sequences (and very rarely, at promoter sites) (Zanconato et al., 2015, Zanconato et al., 2018, Stein et al., 2015, Liu et al., 2016, Galli et al., 2015, Della Chiara et al., 2021). Once bound at an enhancer sequence, this complex can then bind to AP-1, which is thought to cause transcription of S-phase entry and mitosis target genes, in breast cancer cells (Zanconato et al., 2015), as previously described.

Although the DE data gives information with respect to individual genes regarding expression changes, it is still difficult to distil larger patterns from this. Therefore, I decided to examine TC expression in further detail.

| Top downregulated DE genes | Top upregulated DE genes |
|---|---|
| si_dkey-251i10.2 (REELD1 orthologue) | sik1 |
| CABZ01021592.1 | nfil3-6 |
| dpm2 | btg2 |
| gch2 | guca1ab.2 |
| and3 | novel1201 |
| rhcgl1 | dio3b |
| Novel4350 | elnb |
| bco1l | bicdl2 |
| hmox1a | jund |
| tmem106a | junba |
| scarb1 | **cyr61** |
| rhcgb | junbb |
| rps3a | fosl1a |
| and2 | obscnb |
| cyp2k6 | ier2a |

Table 14: Top 15 downregulated and upregulated DE genes for TC
Most noteworthy is cyr61 in the upregulated set.

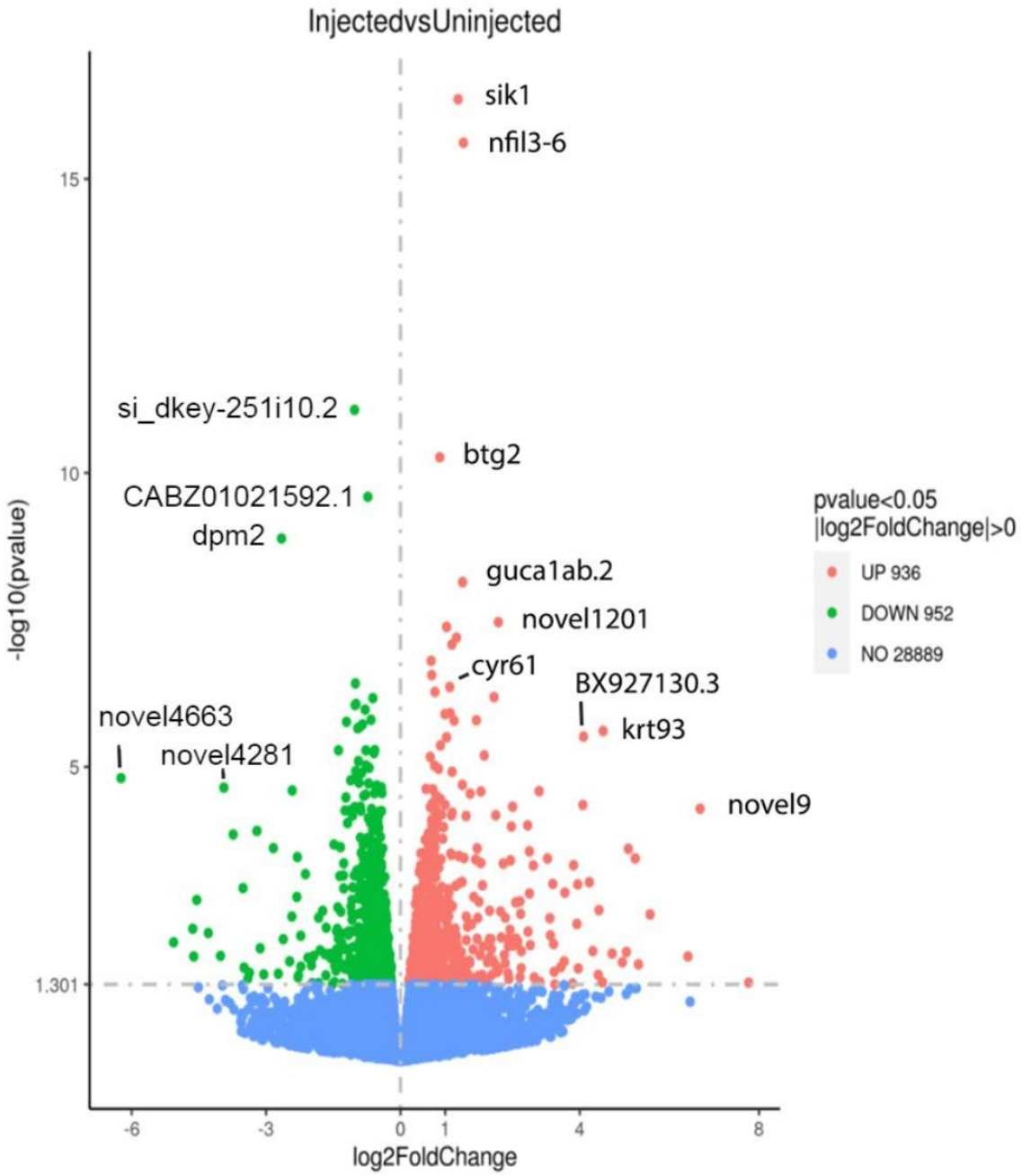


Fig. 32: Volcano plot for TAZ-CAMTA1
The x-axis shows the fold change in gene expression between different samples.
The y-axis shows the statistical significance of the differences.
Red dots represent up-regulated genes and green dots represent down-regulated genes.
The dashed lines indicate the threshold lines for differential gene screening criteria.
The DE genes with the most significant/highest change are labelled.
N.B. BX927130.3 is a pseudogene, novel are uncharacterised genes.
Si_dkey-251i10.2 is REELD1 orthologue.

## 7.3 Detailed analysis of TAZ-CAMTA1 expression from the RNAseq data, by remapping reads to the transgenic genome & using Gene Set Enrichment Analysis (GSEA)

### 7.3.1 Detailed expression analysis of *mCherry* and TAZ-CAMTA1 in the RNAseq dataset

The original RNAseq analysis did not have information on RFP or TC expression, as RNAseq reads are mapped to a standard zebrafish genome that does not contain those sequences. Unfortunately, the genome sequence of the transgenic line itself is unknown. Therefore, it was necessary to create a manually "adapted" zebrafish genome sequence that would allow the analysis of expression levels of the transgenic construct. A new reference genome was produced by adding the transgene information to two 'genome files' that are used for mapping reads. This was done by duplicating the "mitochondrial genome" at the end of the zebrafish genome sequence file, still maintaining the correct formatting of the additional sequence, but removing all mitochondrial sequences. Also, adding the required sequence and descriptors, and then adapting sequence descriptions in the second GFF file that accompanies the raw sequence file. The GFF file provides locations of genes, exons, and other functional annotations. These adapted files were then loaded into Galaxy (https://usegalaxy.org/ (Galaxy, 2022)) and analysed to create BAM files of injected and uninjected samples. Then Galaxy was used to count reads from RNAseq, and expression levels were calculated. The Integrative Genomics Viewer (IGV) (Robinson et al., 2011) was used to visualise the mapped reads against the adapted reference genome, for both *Cre* injected and uninjected embryos with the *ubi*:*lox nls-mCherry lox TAZ-CAMTA1 t2a neon* construct.

### 7.3.2 Expression level of TAZ-CAMTA1 and *mCherry*

To recapitulate, *ubi*:*lox nls-mCherry lox TC t2a neon* x WT embryos were injected with *Cre* mRNA. They were used for RNAseq analysis at 5dpf, using RFP uninjected fish as a control. Data from RNAseq for uninjected fish, showed that *mCherry* had an FPKM (fragments per kilobase per million) of 14.463, whereas TC had 0.025, showing a 579-fold 'drop-off.' This showed that there was indeed a strong 'drop-off' in coverage after the STOP sequence, as expected. This appeared to show that the STOP sequence was efficiently preventing read-through into the TC coding sequence. *mCherry* showed a 12.5x decrease for *Cre* injected embryos, compared to control expression (Fig. 33). As recombination is induced by injection of *Cre* mRNA, and this is not always evenly distributed throughout the embryo, injections may not always lead to 100% recombination in all injected embryos.

Based on these values, it can be estimated that 92% of the chromosomes in the injected embryos were recombined successfully. In comparison, there was an unexpected result with TC, as the expression level for this only increased to 0.085 FPKM upon injection, which is 170-fold lower than what was observed with *mCherry* prior to injection. TC showed a 3.4x increase in expression for *Cre* injected embryos, compared to uninjected control (Fig. 33). However, I would expect the levels of *mCherry* and TC to be similar, as they are both under the same promoter, in the same construct. Therefore, TC expression, although increased upon *Cre* injection, is still much lower than expected.

These results are conflicting with the *in situ* experiments described in the previous chapter, which showed unexpectedly strong TC expression in *Cre* uninjected embryos, whereas the RNAseq data showed that only a very low number of reads were mapped to the TC gene. *In situ* data would predict that there would be a reduction in the expression level after *Cre* injection, but this was not seen from the RNAseq data.

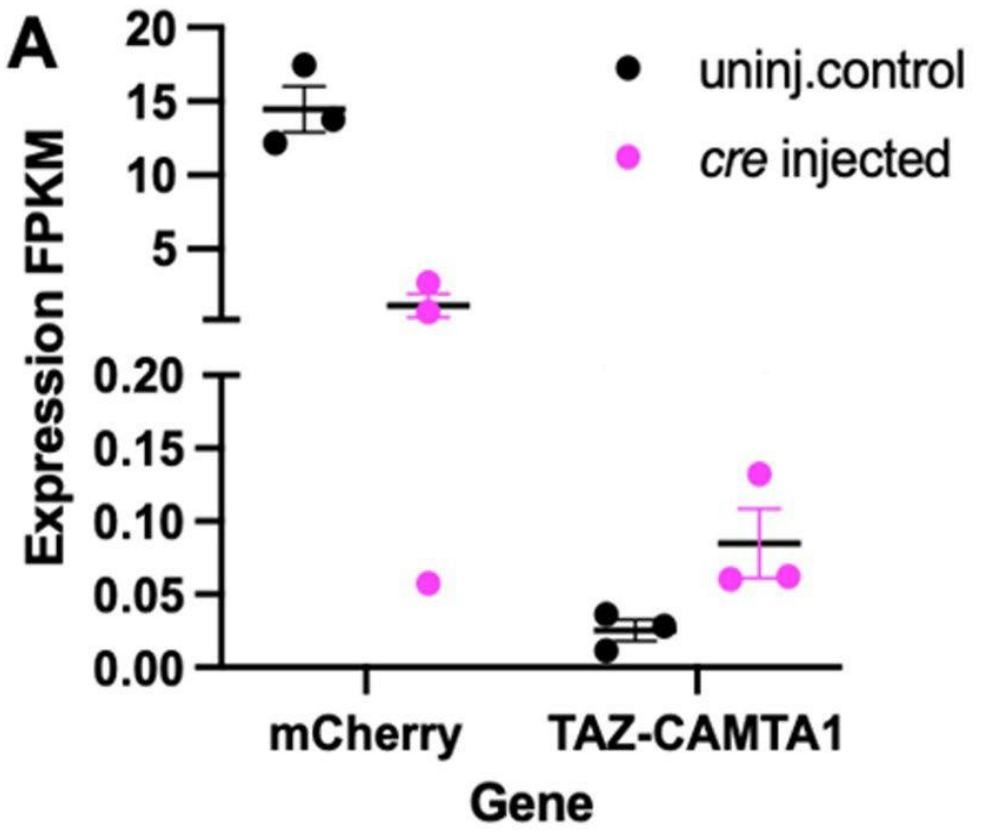


Fig. 33: Expression level of TAZ-CAMTA1 vs *mCherry*, from RNA seq data
Expression of *mCherry* is shown for uninjected samples vs *Cre* injected, and the same for TAZ-CAMTA1 expression. *mCherry* shows a 12.5x decrease for *Cre* injected embryos, vs a 3.4x increase for TC in *Cre* injected embryos.
FPKM = fragments per kilobase per million.

Finally, I wanted to investigate whether there was any drop-off in the number of reads mapped to TC, which may have indicated that the RNA-polymerase had difficulty in transcribing the full-length of the sequence. Although the number of mapped reads was low, nevertheless, it was observed that unexpectedly, transcription of the construct stopped prematurely. It stopped at approx. 8.3kb, 2.4kb

prior to the end of the construct (Fig. 34). This occurred in CAMTA1, exon 15, in the ankyrin domain (ankyrin repeats are known to effectuate the interaction of different proteins (Li et al., 2006)), before the IQ domain and the NLS.

The IGV (Robinson et al., 2011) data also showed that for the injected reads (Fig. 34, A), TC is expressed, but there is also expression of *mCherry*. Even though the 'loxing' of mCherry is efficient, it is not 100%, hence there will still be some mCherry expression, as previously described. In Fig. 34, B, for the uninjected reads, this showed that *mCherry* is expressed, as expected, but there is also a small amount of TC expression (Chapter 11.2).

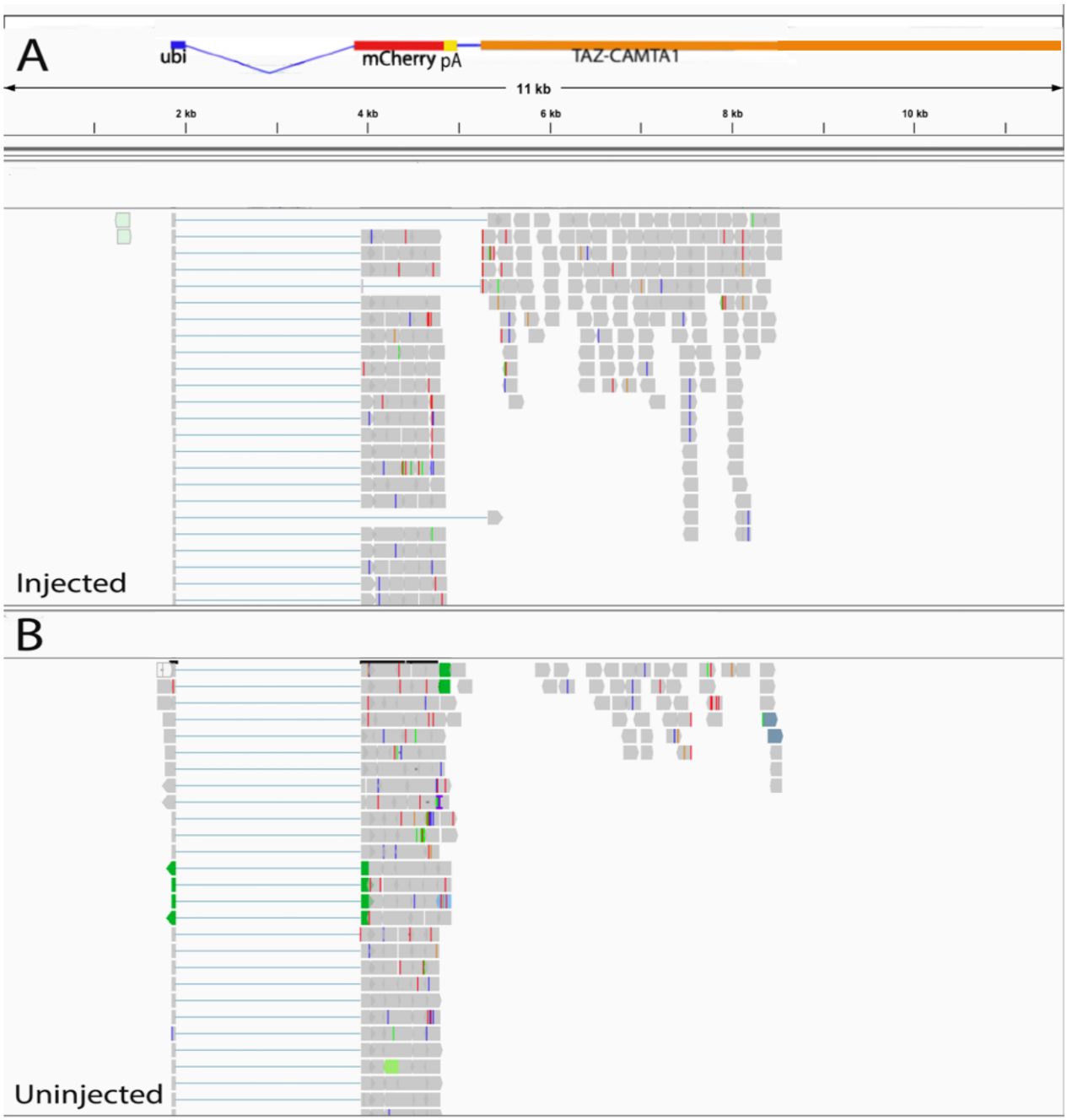


Fig. 34: Reads mapped to align with the TAZ-CAMTA1 transgenic genome
A) Injected reads – TC is expressed, but *mCherry* is also expressed, as 'loxing' *mCherry* out is not 100% efficient.
B) Uninjected reads – *mCherry* is expressed, but there is also a small amount of TC expression.
Both show unexpected halt of transcription at approx. 8.3kb (full construct approx. 10.7kb).
Snapshot of expression (all reads not shown).
pA = polyA
Thin, coloured lines indicate base mismatches
(A=green, C=blue, T=red, G=orange)

### 7.3.3 Gene set enrichment analysis showed that YAP/TAZ target genes were upregulated

As a sizeable number of DE genes were found after deletion of the STOP cassette, it was difficult to determine overall patterns from lists of DE genes. Therefore, I decided to use the transcriptome data to check if there was a "functional" effect of removal of the STOP cassette. Despite difficulty in detection of TC expression, there was still an increase in expression post-*Cre* injection. Therefore, it was possible that the functional effects could be seen in expression of target genes that are known from mammalian studies. DE analysis data from RNAseq was used in Gene set enrichment analysis (GSEA) (Broad Institute, (Subramanian et al., 2005, Mootha et al., 2003)), to compare my data to the Seavey (EHE, (Seavey et al., 2021)) and Cordenonsi (YAP, (Cordenonsi et al., 2011)) overrepresented gene sets.

An enrichment score (ES) is a cumulative score determined by moving from zero down each ranked list, adding a number when there is a gene present from my gene set, and subtracting when there is not (Subramanian et al., 2005). The level of increase/decrease is based on the Kolmogorov-Smirnov test (Subramanian et al., 2005). Hence the higher the score, the higher probability that the gene set is towards the upregulated end of the ranked list (negative number for downregulation) (Broad Institute, https://tinyurl.com/2tkverhf). The normalised enrichment score (NES) is when the data is normalised to consider the size of each set (Subramanian et al., 2005). In order to do this comparison, it was necessary to convert the EHE and YAP1 sets from human into zebrafish ie. discover whether there were individual orthologues of the human genes in zebrafish and create a 'zebrafish gene set.' A narrow set were defined for both EHE (56 genes) and YAP1 (38 genes), which only included 1-1 orthologues. Biomart (Ensembl release 109 (Martin et al., 2023)) was used to create this 'zebrafish gene set' then this data was used in GSEA (Broad Institute, (Subramanian et al., 2005, Mootha et al., 2003) ) to plot graphs for the top 20 genes. An Estrogen data set (104 genes) was used as a completely unrelated control.

The data showed that there was an increase in YAP/TAZ targets genes, with significance of $P<0.001$, when my data was compared to both gene sets. The leading edge is the slope at the beginning showing a subset of genes which contribute most to the enrichment score. These were steep when my data was compared to both EHE and YAP1 data sets, with a cluster of lines at the beginning of the enrichment plots (Fig. 35, A and B). This did not happen when my data was compared to a totally unrelated data set (Estrogen), as expected (Fig. 35, C).

I also checked the individual top scoring genes from the list. Although not significant, it was of note that *Serpine1* and *TGFβ* were present when my data was compared to both YAP1 and EHE data sets. *Serpine1* controls ECM remodelling (Simone et al., 2014) (Simone and Higgins, 2015) and is linked to a worse prognosis in a number of cancers (Andreasen et al., 1997, McMahon and Kwaan, 2015) (Pavon et al., 2016). *TGFβ* is a known tumour suppressor, which usually prevents cell proliferation, halting the cell cycle in G1 phase, and activating apoptosis (Reddy et al., 1994, Rotello et al., 1991, Derynck et al., 2001). However, it also controls tumour advancement via paracrine and autocrine signalling (Oft et al., 1998, Roberts and Sporn, 1987). *Cyr61* was also present in both lists and was the top hit when compared to each data set (Fig. 35, D). This is a well-known YAP/TAZ target, associated with the ECM (Zhang et al., 2011, Lai et al., 2011, Kireeva et al., 1997). From differential expression data, this showed that the log2fold change for *Cyr61* was 1.10 (2.14 fold change), and the P(adj.)< 0.001, which was the only significant gene from both lists.

Also, from the STRING database, using the top 50 upregulated genes, there appears to be protein-protein interactions between the fos and jun families (Fig. 36). These families are associated with the AP-1 transcription factor complex (Curran and Franza, 1988). YAP/TAZ-TEAD is known to bind at enhancer sequences (and very rarely, at promoter sites) (Zanconato et al., 2015, Zanconato et al., 2018, Stein et al., 2015, Liu et al., 2016, Galli et al., 2015, Della Chiara et al., 2021). Once bound at an enhancer sequence, this complex can then bind to AP-1, which is thought to cause transcription of S-phase entry and mitosis target genes, in breast cancer cells (Zanconato et al., 2015), as previously described. Data from the STRING database also showed that the reactome pathway that is significantly enriched is muscle contraction. It is unknown how this is related to TC.

In conclusion, TC RNAseq data showed that expression levels of TC were low, but did increase upon Cre mRNA injection, as expected. When the data was examined, this showed that Cyr61 was significantly upregulated for TC. The RNAseq data also showed that TC was not fully expressed, prematurely ending at approximately 8.5kb, prior to the NLS. GSEA showed that when my data was compared to YAP1 and EHE specific datasets, *Cyr61* was the only significant gene in both cases.

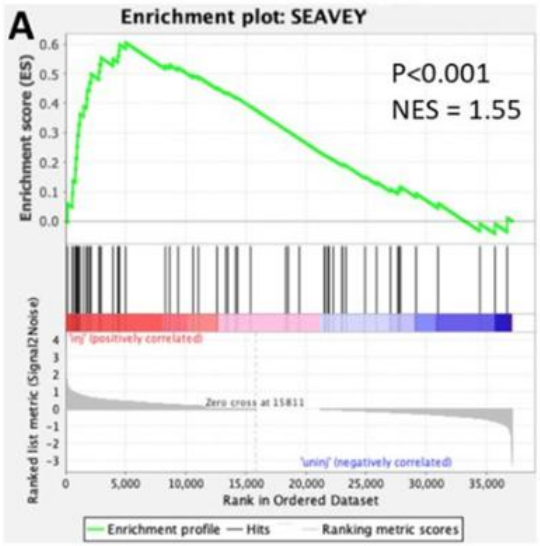


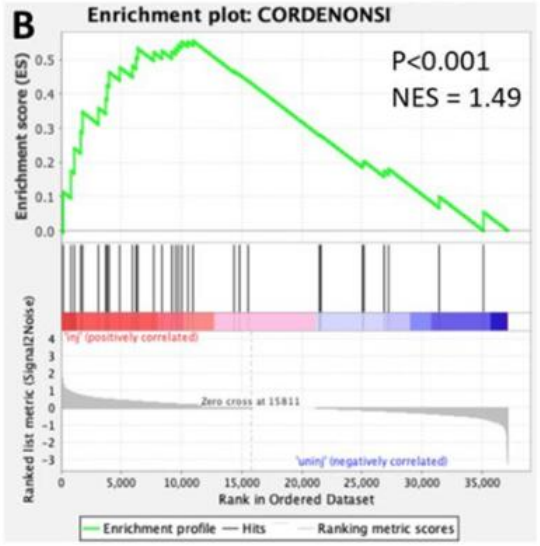


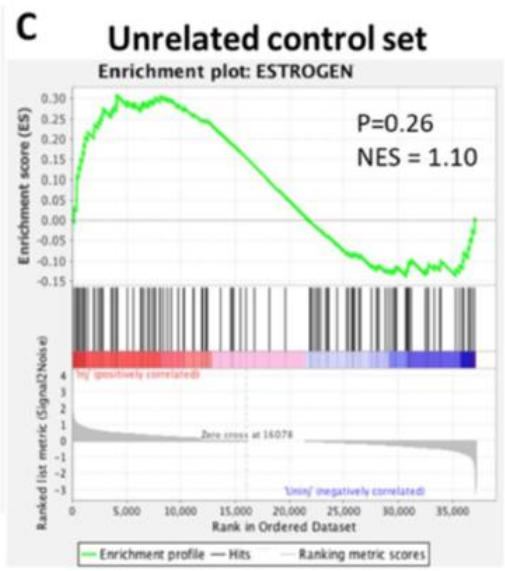


D

| Seavey top 15 (EHE) | Cordenonsi top 15 (YAP1) |
|---|---|
| cyr61 | cyr61 |
| angpt2a | ccn2a |
| SRPX2 | serpine1 |
| FBLN7 | AXL |
| SCARF2 | tgfb2 |
| wtip | dusp1 |
| ANKRD2 | FLNA |
| serpine1 | agfg2 |
| CIQTNF2 | mdfic |
| npas1 | TNS1 |
| tgfb2 | crim1 |
| PLAT | tk1 |
| KIF26B | DLC1 |
| mylk3 | gas6 |
| osgin2 | DAB2 |

Fig. 35: Gene set enrichment analysis (GSEA)
My TAZ-CAMTA1 gene set compared to:
A) Seavey EHE set
B) Cordenonsi YAP1 signature set
C) Estrogen (unrelated control set)
D) The top 15 genes for Seavey (EHE) and Cordenonsi (YAP1)

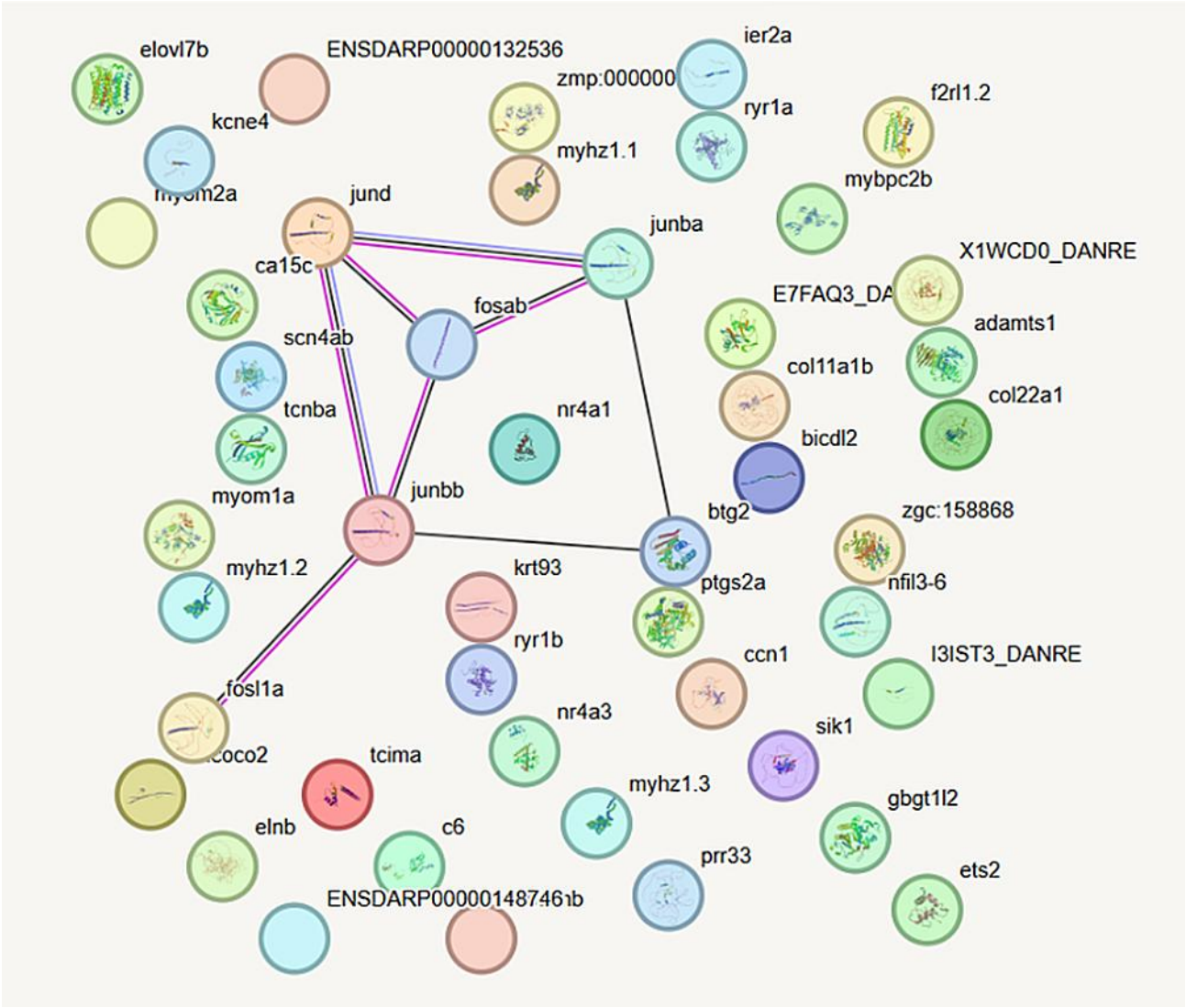


Fig. 36: Protein-protein interaction for TC
There appears to be interaction between the fos and jun families, using the top 50 upregulated genes. Medium confidence (0.4)

# 8 Results: Analysis of adult *ubi: lox nls-mCherry lox TAZ-CAMTA1 t2a neon* zebrafish

Although expression levels of TAZ-CAMTA1 (TC) were low after induction, there were functional effects of the gene detected in the RNAseq data. Therefore, several fish lines were raised and were kept under observation for potential tumour growth. *ubi: lox nls-mCherry lox TAZ-CAMTA1 t2a neon (AD25)* x *fli1a: cre EGFP (AF22)* and *ubi: lox nls-mCherry lox TAZ-CAMTA1 t2a neon (AA6/7)* x *fli1a: cre EGFP (AA8)*, either with CDKN2a/b CRISP mutations, or without, were raised. CDKN2a/b was injected in some batches, as this has been shown to be the most common secondary mutation in human EHE tumours (Seligson et al., 2019), as previously noted. Tumours were seen in some of the TC 'activated' fish, but not in controls, as noted below. However, the one tumour tested did not appear to be of TC origin.

## 8.1 Survival rates

Fish were raised from *ubi: lox nls-mCherry lox TAZ-CAMTA1 t2a neon (AD25)* x *fli1a:cre EGFP (AF22)* (RFP and GFP) 'activated' TC (19 raised), and RFP only controls (30 raised). At 2 months old, one of the 'activated' group had what appeared to be a small head tumour (Fig.39), so this and a control were taken for fixing and sectioning. At 6 months of age, 5 from each group were taken out to be fixed and sectioned to examine for any tumours. Two of the 'activated' fish had tail tumours at 1yr 7 months. These were fixed and imaged, along with a control (Fig. 40). Notably, the survival rate for the activated group was 37% vs 80% for the control group (Table 15). Survival rates assume fish removed without tumours would have survived if they were left to be raised for longer. Therefore, the survival rate for the activated group is less than half of the control group, which may be of importance. Hence, it appears that TC did have an effect in this group of fish, but this experiment would need to be repeated.

*ubi: lox nls-mCherry lox TAZ-CAMTA1 t2a neon (AA6/7)* x *fli1a:cre EGFP (AA8)* lines and controls were raised - fish were raised for both, but none of these showed any tumours (41 fish for 'activated,' 40 for control). 5 of the 'activated' and control fish were removed at 6 months of age for fixing and sectioning, but no tumours were found. A batch of these fish were also injected with CDKN2a/b (CRISPR 2 and 6) and were raised. One of these was found to have a gill tumour (Fig. 41) (35 fish were raised for 'activated' and control, resulting in 30 'activated' and 23 control surviving (86-69%

survival rates) at 1yr 10 months (until the end of the project) (Table 15). The gill tumour was discovered at 9 months in the 'activated' group. This was fixed and sectioned, along with a control (Fig. 41). Therefore, there were slightly lower survival rates for CDKN2a/b injected fish when this group is compared to the same line, but with no CDKN2a/b injection. However, these rates are still well within usual survival rates (the University of Manchester reported that their average zebrafish survival rate was 65% in 2017 (Mortell et al., 2017).

Further fish were raised from *ubi: lox nls-mCherry lox TAZ-CAMTA1 t2a neon (AD25)* x *fli1a: cre EGFP (AF22)*, but with different controls: TC 'activated' with CDKN2a/b injection or TC 'activated' without injection (controls). This was due to the *fli1a:cre EGFP* line being F1 generation, therefore it was possible for fish to have 2 copies of the transgene, and it was difficult to obtain RFP fish alone, if all of the embryos had GFP. No tumours were seen for either group. 46 from activated and 40 from control group were raised, and 35 survived at 10 months of age for both groups (76-88% survival rate) until culled (Table 16). Another batch from this line were also injected with CDKN2a/b guides 2,5, and 6, but no tumours were seen. 27 'activated' and 21 control were raised, and 16 'activated' and 20 control survived at 10 months (59-95% survival rates), until culled (Table 16). Although no tumours were seen in these groups, unfortunately they were only 10 months when the experiment ended. The same line without CRISPR injection had a 37% survival rate at 1yr 10 months (Table 15), so it is possible these fish may have developed tumours at a later time point, or this may have been a spurious event, but further work would need to be undertaken to be conclusive.

| Lines | No. of fish raised | No. of fish removed for analysis | No. of visible 'tumours' | No. of fish at end of experiment | Age of fish at end of experiment | Survival rate (%) |
|---|---|---|---|---|---|---|
| AD25 x AF22 activated | 19 | 8 (3 with tumours, 5 without) | 3 | 2 | 1yr 10months | 37++ |
| AD25 x AF22 control | 30 | 22 (8&14)+ | 0 | 2 | 1yr 10 months | 80++ |
| AA8 x AA6/7 activated | 41 | 5 | 0 | 35 | 1yr 4 months | 98 |
| AA8 x AA6/7 control | 40 | 5 | 0 | 34 | 1yr 4 months | 98 |
| AA8 x AA6/7 Activated CDKN2a/b 2+6 guides | 35 | 1 (gill tumour) | 1 | 30 | 1yr 10 months | 86 |
| AA8 x AA6/7 Control CDKN2a/b 2+6 guides | 35 | 1 | 0 | 23 | 1yr 10 months | 69+++ |
| AA8 x AA6/7 Activated CDKN2a/b 2+5+6 guides | 30 | 0 | 0 | 24 | 1yr 1 month | 80 |
| AA8 x AA6/7 Control CDKN2a/b 2+5+6 guides | 33 | 0 | 0 | 26 | 1yr 1 month | 79 |

Table 15: Survival rates and 'tumours' (phenotype) in different TC lines
+ 14 culled to even batch numbers
Survival rates assume fish removed without tumours would have survived if left to be raised for longer.
++ 2 remaining at the end of the experiment + 5 (activated) or 22 (control) for removed fish with no tumours, used for survival rates.
+++ 23+1 (no tumour) removed, used for survival rates.

| Lines | No. of fish raised | No. of fish removed for analysis | No. of visible 'tumours' | No. of fish at end of experiment | Age of fish at end of experiment | Survival rate (%) |
|---|---|---|---|---|---|---|
| AD25 x AF22 Activated CDKN2a/b 2+5+6 guides | 46 | 0 | 0 | 35 | 10 months | 76 |
| AD25 x AF22 Activated No guides | 40 | 0 | 0 | 35 | 10 months | 88 |
| AD25 x AF22 Activated CDKN2a/b 2+5+6 guides | 27 | 0 | 0 | 16 | 10 months | 59 |
| AD25 x AF22 Activated No guides | 21 | 0 | 0 | 20 | 10 months | 95 |

Table 16: Survival rates and 'tumours' (phenotype) in different TC lines with different controls

## 8.2 Generation and characterisation of CDKN2a/b mutants

CDKN2a/b was chosen as a gene to knockout in TC lines, as it has been shown to be the most common secondary mutation in human EHE tumours, and therefore may enhance tumorigenesis (Seligson et al., 2019), as mentioned. CDKN2a is cyclin-dependent kinase 2a, which encodes cell cycle proteins, $p16^{INK4a}$, and $p19^{ARF}$ (Quelle et al., 1995). One set of embryos were injected with 2 CRISPRS (2 and 6, both situated on exon 2) and one set were injected with 3 CRISPRS (2,5, and 6, all situated on exon 2, except CRISPR 5 is on exon 1) (Fig. 37 & 38).

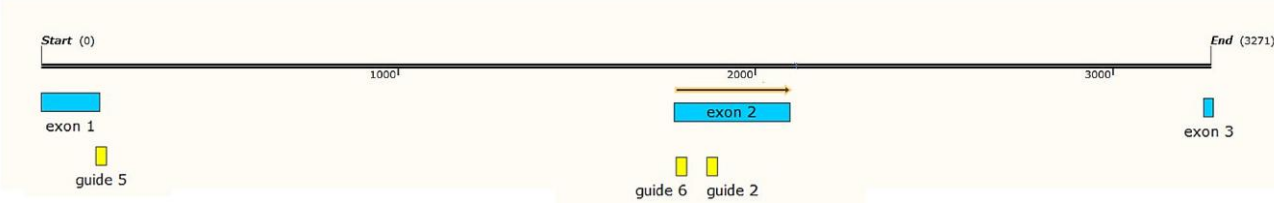


Fig.37: CRISPR2a/b CRISPR guide position
Guide 5 is positioned on exon 1, and guide 2 and 6 are positioned on exon 2.

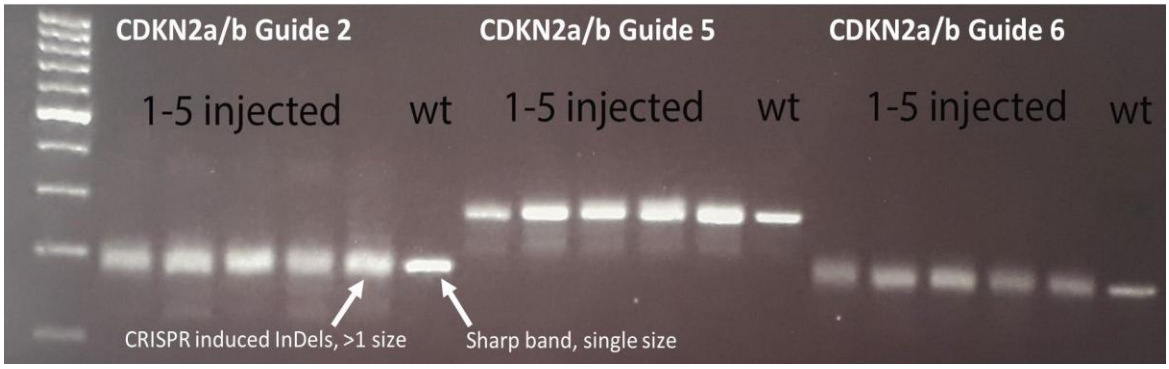


Fig. 38: CDKN2a/b CRISPR guide injection
CDKN2a/b guides 2,5,and 6 were injected into *ubi: lox nls-mCherry lox TAZ-CAMTA1 t2a neon* lines. The 6th band in every set is a WT, uninjected control.

## 8.3 Tumour histology and H&E/CAMTA1 staining

Five fish from *ubi: lox nls-mCherry lox TAZ-CAMTA1 t2a neon* x *fli1a:cre EGFP* (RFP & GFP selected) ie. TC 'active' fish were fixed and sectioned at 6-7 months of age, along with 5 control fish *ubi*: *lox nls-mCherry lox TAZ-CAMTA1 t2a neon* (RFP selected only). This was done for 2 different TC lines: TC AA6/7 x *fli1a:cre EGFP* AA8 and TC AD25x *fli1a:cre EGFP* AF22. 1 'tumour' was seen in the AD25 x AF22 small tumour fish (Fig. 39A,A'). However, upon sectioning this fish, the tumour was not apparent. I hypothesised that it may have been something other than a tumour eg. an accumulation of fluid which collapsed under sectioning. There were 3 other fish seen with tumours. One was AA6/7 x AA8 line, which was also co-injected with CDKN2a/b, CRISPR 2 and 6. This had a gill tumour (Fig. 41). This tumour was H&E stained, which clearly showed tumour morphology (Fig. 42A). This fish was also stained with CAMTA1 antibody to test whether the tumour arose from TC.

The results showed that no CAMTA1 staining was apparent (Fig. 43A), suggesting that the tumour may have been sporadic and not originated from TC. TC mRNA injected embryos were used to check the CAMTA1 antibody was functional prior to this staining, and this was shown to be the case (data not shown). There were 2 other tail tumours seen in AD25 x AF22 (Fig. 40), and these were CAMTA1 stained. They showed that there was unexpected staining of CAMTA1 in the blood cells, but not in the nuclei, as would be expected (Fig. 44A). DAPI appeared to show background staining for these tails also (44B). The AA6/7 x AA8 line, which was co-injected with CDKN2a/b, CRISPR 2 and 6, was raised until the end of the project and no further tumours were seen (at 1 year, 10 months).

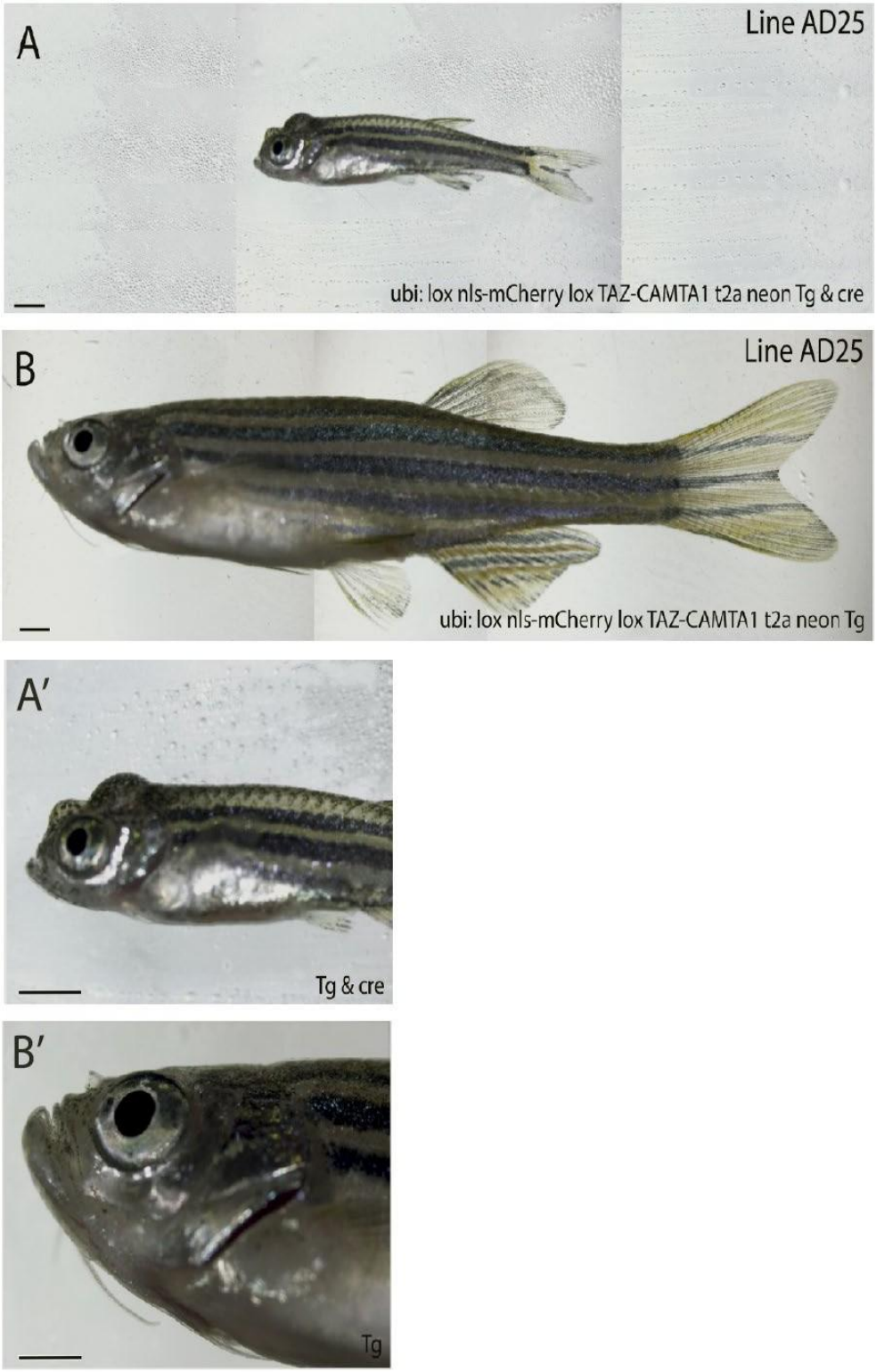


Fig. 39: *ubi: lox nls-mCherry lox TAZ-CAMTA1 t2a neon (AD25)* x *fli1a: cre EGFP (AF22)* head images at 2 months
A: TAZ-CAMTA1 (Tg) and cre selected
B: TAZ-CAMTA1 (Tg) only selected
A': Close-up of A, showing apparent head tumour; B': Close-up of control
Scale: 1mm Images compiled in Photoshop.

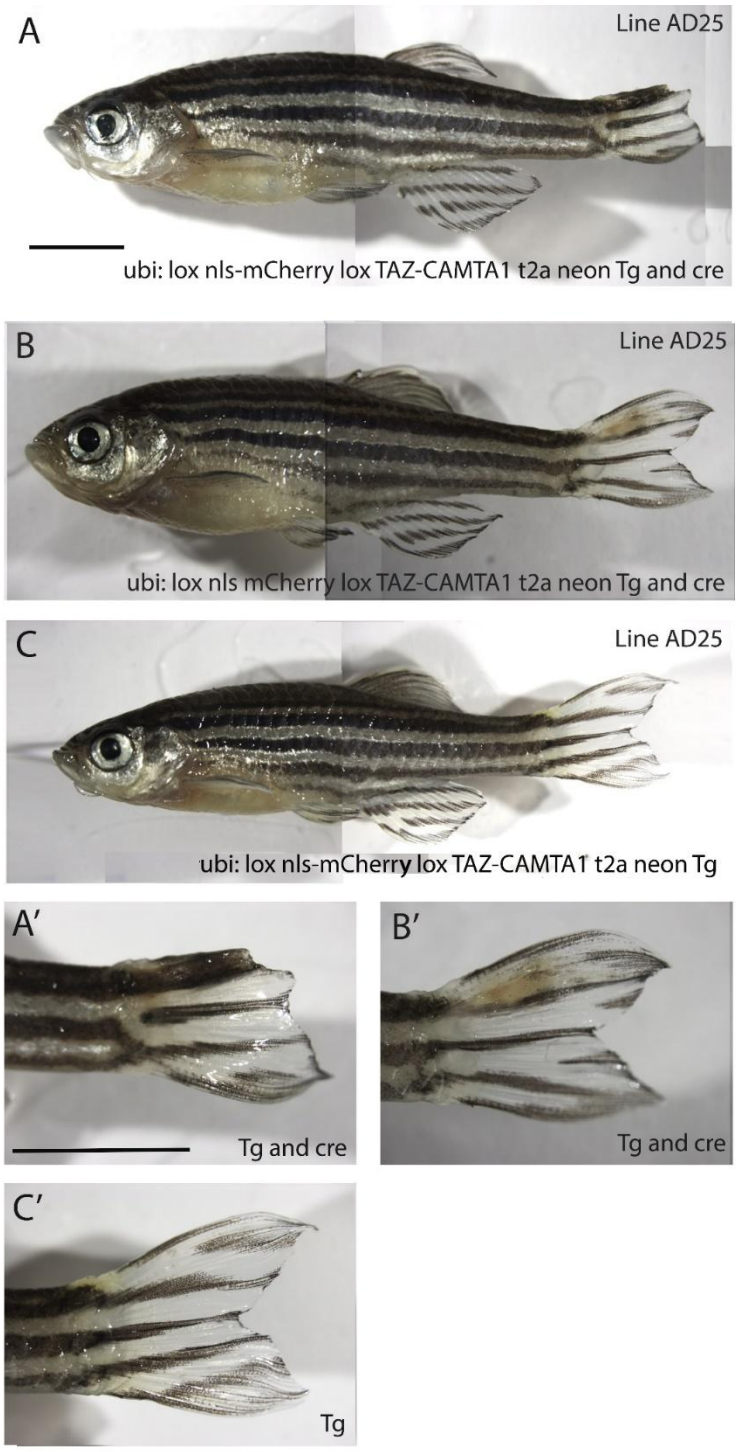


Fig. 40: *ubi: lox nls-mCherry lox TAZ-CAMTA1 t2a neon (AD25)* x *fli1a: cre EGFP (AF22)* tail tumours at 1 yr, 7 months
A: TAZ-CAMTA1 (Tg) and cre selected
B: TAZ-CAMTA1 (Tg) and cre selected
C: TAZ-CAMTA1 (Tg) only selected
A': close-up of A, showing apparent tail tumour
B': close-up of B, also showing apparent tail tumour
C': close-up of C, showing regular tail. Scale: 5mm. Images compiled in Photoshop.

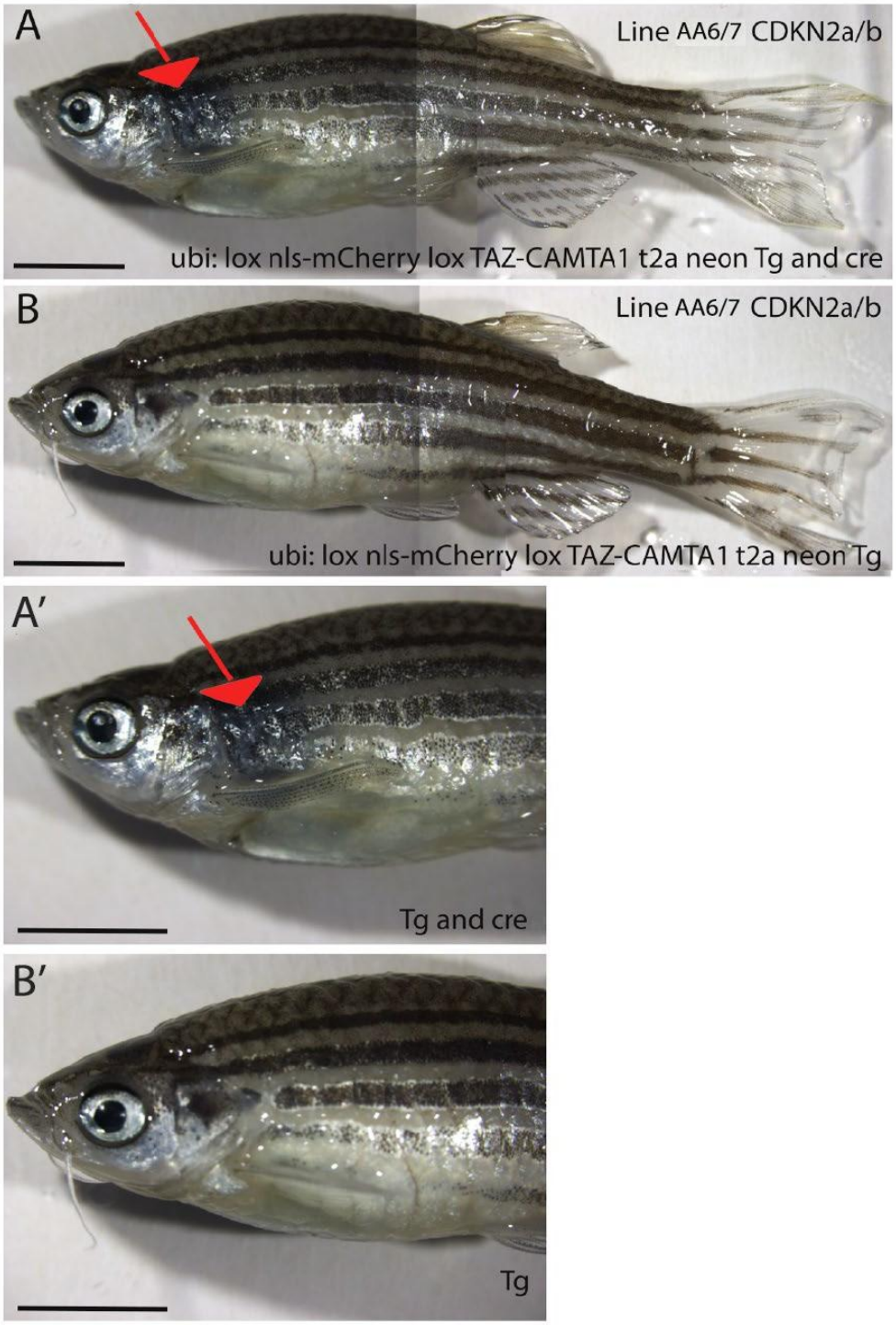


Fig. 41: *ubi: lox nls-mCherry lox TAZ-CAMTA1 t2a neon (AA6/7)* x *fli1a: cre EGFP (AA8*) *neon injected CDKN2a/b (CRISPR 2 and 6*) tumour at 9 months
A: TAZ-CAMTA1 (Tg) and cre selected
B: TAZ-CAMTA1 (Tg) only selected
A': close-up of A, showing gill tumour
B': close-up of B with no tumour. Scale: 5mm.
Images compiled in Photoshop.

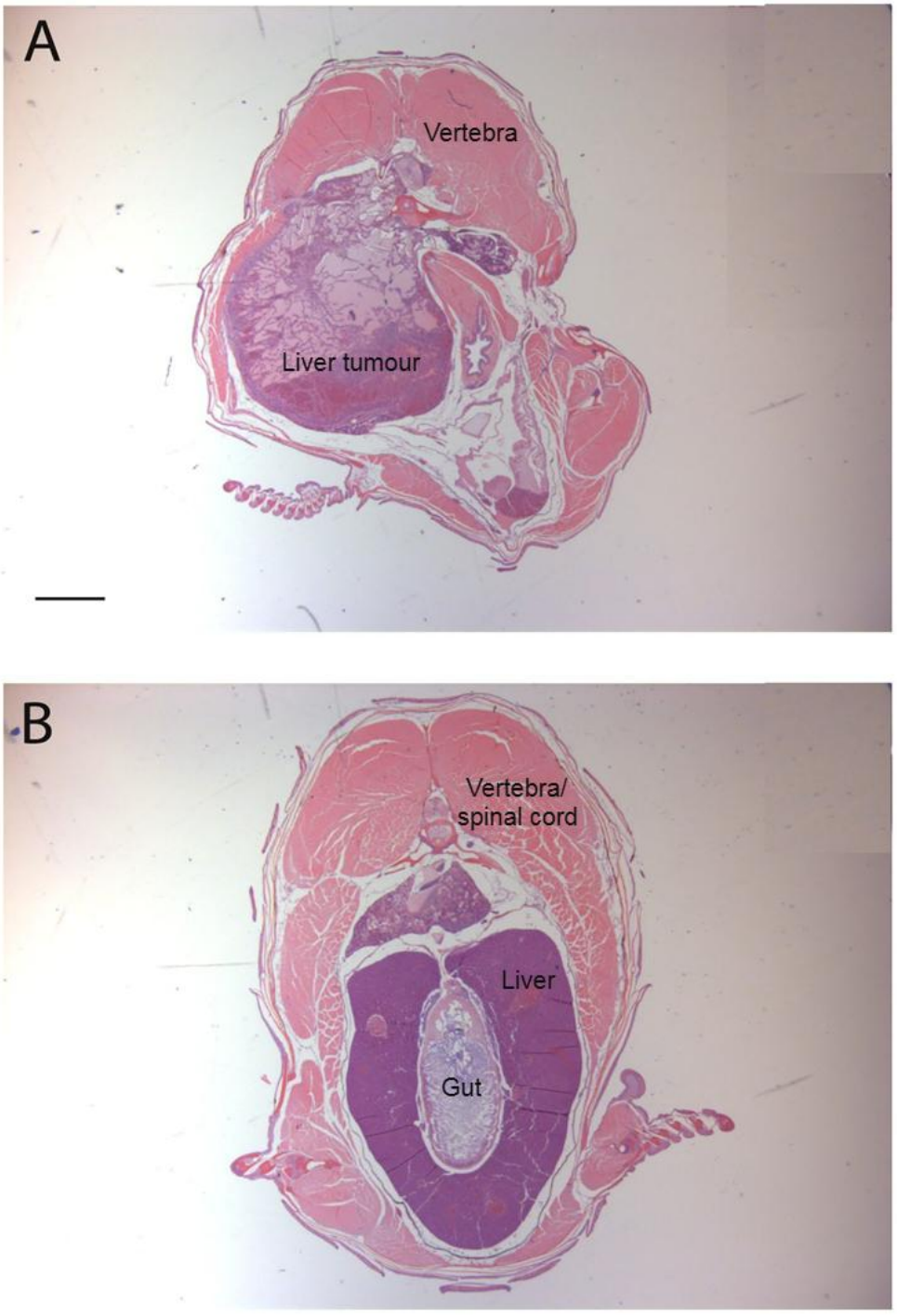


Fig. 42: *ubi: lox nls-mCherry lox TAZ-CAMTA1 t2a neon (AA6/7)* x *fli1a: cre EGFP (AA8) injected CDKN2a/b (CRISPR 2 and 6)* (gill tumour) histology
A: TAZ-CAMTA1 (Tg) and cre selected with visible tumour.
B: TAZ-CAMTA1 (Tg) only selected with regular histological features.
Scale: 1mm
Images compiled in Photoshop.

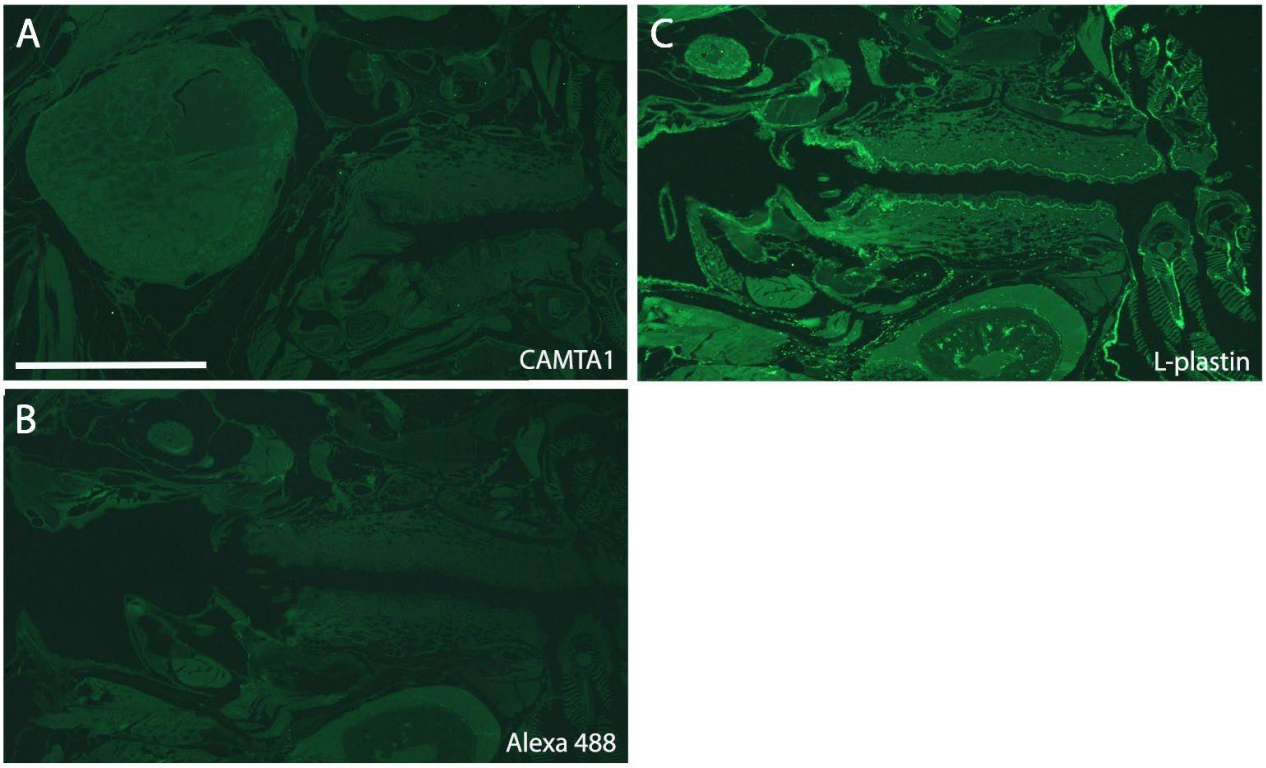


Fig. 43: CAMTA1 antibody staining of *ubi: lox nls-mCherry lox TAZ-CAMTA1 t2a (AA6/7) t2a neon* x *fli1a:cre EGFP (AA8) injected CDKN2a/b (CRISPR 2 and 6)*
A: TC GFP & RFP with CAMTA1 Ab, which shows no nuclear CAMTA1 staining in the tumour.
B: TC GFP & RFP with Alexa 488 alone, which shows background staining (negative control).
C: TC GFP & RFP with L-plastin Ab control, which shows L-plastin staining (positive control).
Scale: 1mm

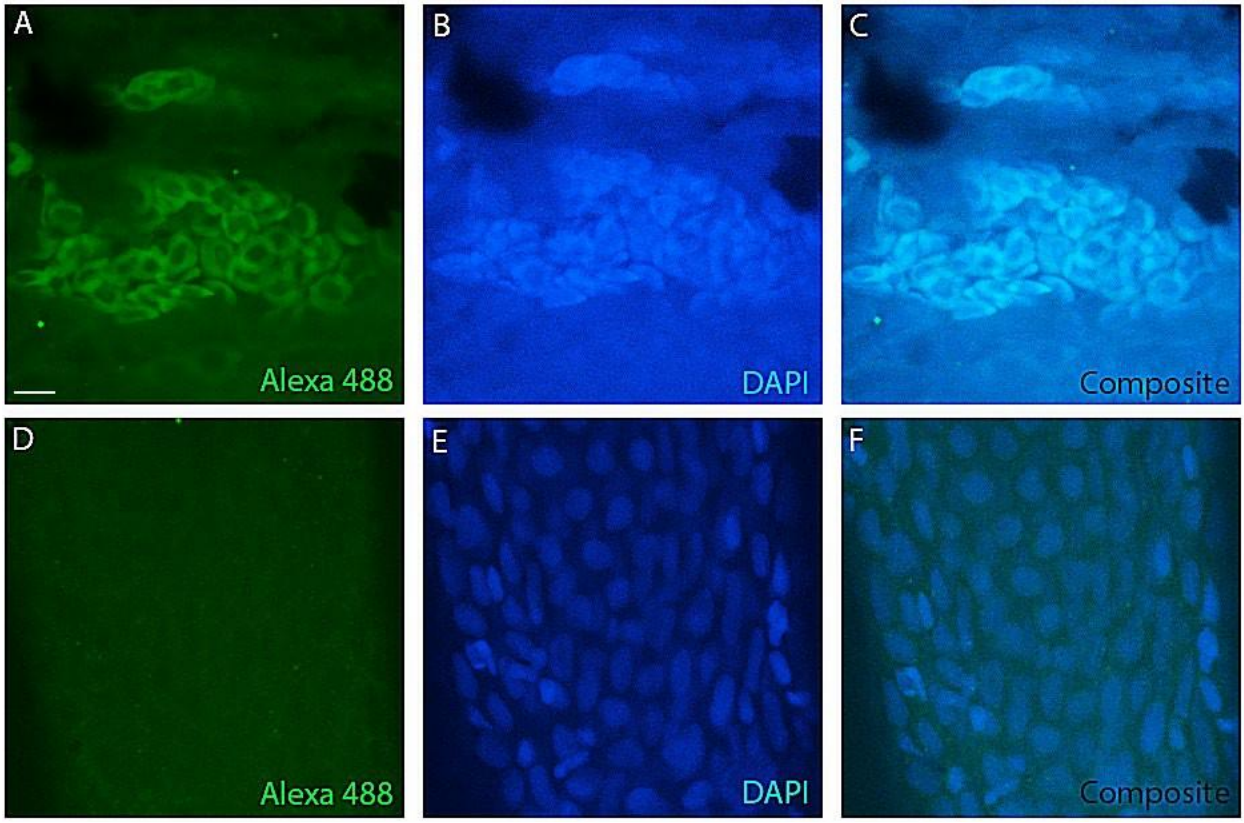


Fig. 44: CAMTA1 antibody staining of *ubi: lox nls-mCherry lox TAZ-CAMTA1 t2a (AD25) t2a neon* x *fli1a:cre EGFP (AF22*) tails
A: TC GFP & RFP with CAMTA1 Ab, which shows blood cell, but not nuclear CAMTA1 staining in the tumour.
B: TC GFP & RFP with DAPI, which shows background staining in the tumour.
C: TC GFP & RFP tumour composite.
D: TC RFP with CAMTA1 Ab, which shows no CAMTA1 staining in the control fish.
E: TC RFP with DAPI, which shows nuclear staining in the control.
F: TC RFP control fish composite.
Scale: 10µm
Image compiled in Photoshop

In conclusion, there were a few tumours seen, but only one group had a survival rate which was notable at 37% (AD25 x AF22, activated). However, it would be expected to see tumours in all activated lines if TC was the cause. CAMTA1 staining was negative, which suggested that TC was not the origin of the tested tumour. In addition, this line has been used in further experiments where this reduced survival rate was not observed, but this was only until 10 months of age. Therefore, the reduced survival rate could have been a spurious event, but further testing would be necessary.

# 9 Results: Generation and characterisation of further *Epithelioid hemangioendothelioma* transgenic constructs

As Yap1-Tfe3 (YT) mRNA had previously been injected and shown to cause high levels of 'toxicity,' (Chapter 5 and below) and YT is a much shorter construct than TAZ-CAMTA1 (TC), it was decided to produce a YT cre-lox model. YT is 2142bp (1371bp without neon), whereas TC is 5628bp (4857bp without neon), hence I hypothesised that YT may be easier to transcribe. Gene length is known to control levels of transcription: longer genes tend to be expressed at a lower level than shorter genes (Castillo-Davis et al., 2002, Urrutia and Hurst, 2003, Chiaromonte et al., 2003) (Brown, 2021). As there were previous issues with TC expression, dominant active (DA) TAZ was also produced for use as a positive control. In addition, it was hypothesised that a new TC construct with introns surrounding CAMTA1, exon15, may aid expression. Previously, CAMTA1, Exon 15, showed an unexpected, premature stop of transcription from RNAseq data (Chapter 7). Introns are well-known to increase expression when present in the transcribed sequence: this is known as 'intron-mediated enhancement' (IME), and results in an increase in translational efficiency (Mascarenhas et al., 1990), and in cytosolic, mature mRNA (Callis et al., 1987) (Shaul, 2017). Therefore, a new TC Ex15 construct was also produced.

## 9.1 YAP1-TFE3 mRNA injection generally shows death or WT phenotype

To test the effect of YT on the vasculature, I produced YT mRNA: firstly, by restriction digest of a YAP1-TFE3A DNA piece (Genewiz), then ligation into the linearised pcs2+ vector (this contains an SP6 site to enable the production of mRNA). This was then cloned in *E. coli* and purified. It was then linearised, and the SP6 mMessage mMachine$^{TM}$ kit was used to transcribe YT mRNA. Then this was injected into *fli1a:EGFP* embryos to visualise and analyse the effect of overexpression of YT on the vasculature. As mentioned, Zebrafish YT mRNA was injected into *fli1a*: GFP embryos, with S94A as a control (Chapter 5.1). Using the chi-squared test with 100pg, YT vs YT S94A, P=ns. Overall, mRNA injections were consistent with YT being more effective than TC.

## 9.2 Generation and characterisation of *ubi*: *lox nls-mCherry lox YAP1-TFE3 t2a neon* zebrafish

As TC expression levels were seen to be low from RNAseq data, and YT mRNA appeared to be more active in embryos, I decided to produce a YT zebrafish model, using the same ubi cre-lox model as TC. 10% of EHE cases are due to YT translocation (Antonescu et al., 2013). Also, YT is much shorter than TC, as described previously. The end of YAP1 exon 1 (SHSRQ), and TFE3A from exon 4 (VQTH) (where the fusion proteins join in human), were checked and found to be the same in human and zebrafish (Antonescu et al., 2013). Therefore, it was possible to use the zebrafish version to make a construct, in order to attempt to simulate human disease in zebrafish. This fusion gene was designed *in silico* (Appendix), ordered from Genewiz, then used for further cloning experiments. A *ubi*:*lox nls-mCherry lox YAP1-TFE3 t2a neon* construct was created using the YAP1-TFE3 piece (Genewiz) for the middle-entry clone: YAP1-TFE3 was restriction digested and ligated into pME-MCS2, then cloned in *E. coli* and purified. Multi-site Gateway cloning was then used to produce the final *ubi*:*lox nls-mCherry lox TAZ-CAMTA1 t2a neon* construct.

### 9.2.1 YAP1-TFE3 fish show recombination upon *Cre* activation

Firstly, as a test for functionality, *Cre* mRNA was coinjected with YAP1-TFE3 construct DNA, in order to discover if the lox sites were able to recombine. This efficiently reduced *mCherry* expression, as with TC, and showed mosaic GFP expression, as expected (Fig. 45). Embryos were raised, and once the lines were mature*, ubi*:*lox nls-mCherry lox Yap1-Tfe3 t2a neon* lines were screened, and founders were obtained (3A & 5A). *Cre* mRNA was then injected into embryos from these lines, and this also efficiently reduced *mCherry* expression, indicating recombination had taken place. However, no GFP could be visualised once again. Therefore, primers for a PCR recombination test were designed.

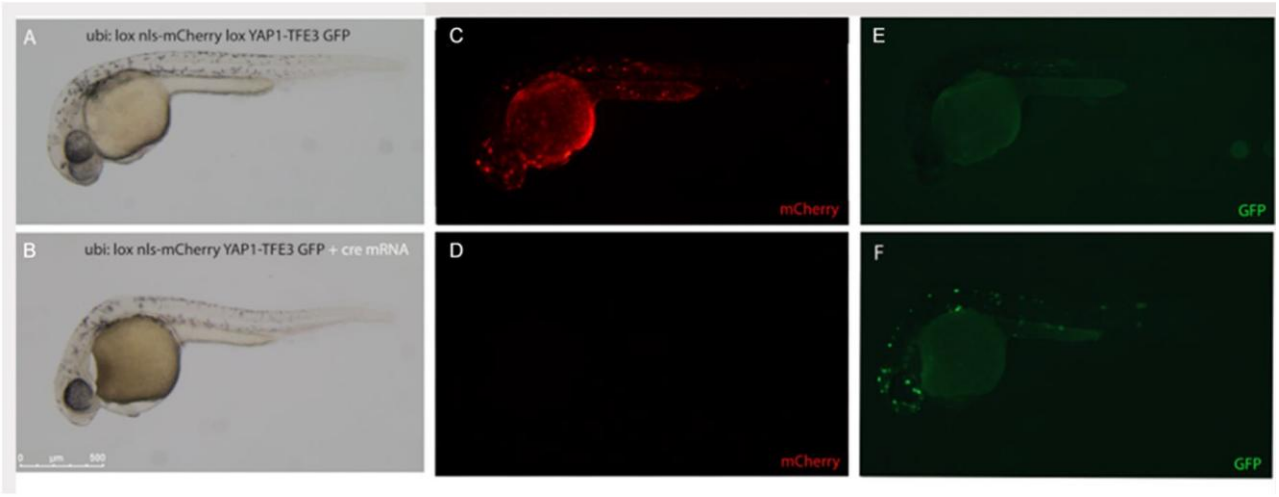


Fig. 45: Recombination test: Injection of *ubi*:*lox nls-mCherry lox YAP1-TFE3 t2a neon* into WT embryos, with and without *Cre* mRNA, at 1dpf
A, C, E) an embryo injected with the construct only, and no *Cre* mRNA. C) nuclear RFP, and E) no GFP, as expected.
B, D, F) an embryo injected with the construct, plus *Cre* mRNA. D) no RFP, and F) GFP spots, which indicates that the lox system is working.

### 9.2.2 YT shows recombination using PCR

'Outside' primers were designed to only show a band if *mCherry* had been 'loxed out' upon crossing with *fli1:cre EGFP*. 'Inside' primers were designed to show a band for *mCherry* as a control, as with TC. As the final aim was to activate YT specifically in the endothelial cells only, I crossed *ubi: lox nls-mCherry lox Yap1-Tfe3 t2a neon* to *fli1a:cre EGFP* to check if recombination can be detected in the relevant embryos of selected line, 3A. Resulting embryos were sorted for the transgene (*mCherry*) and *Cre* (GFP). The PCR from these fish showed a band of the correct size (429bp), with both the transgene and *Cre* (Tg *Cre*), but not in the fish with the transgene only (Tg) (Fig. 46, B). This indicated that the STOP cassette could be removed, and recombination could occur in transgenic line 3A (faint bottom bands are primer-dimer).
The non-recombined PCR showed a band (689bp) where *mCherry* is present. This band is seen both in the embryos with the transgene and Cre (Tg *Cre*), and transgene (Tg) alone, which is to be expected as *Cre* should only be expressed in a subset of (*fli1a*-expressing) cells (Fig. 46, C).

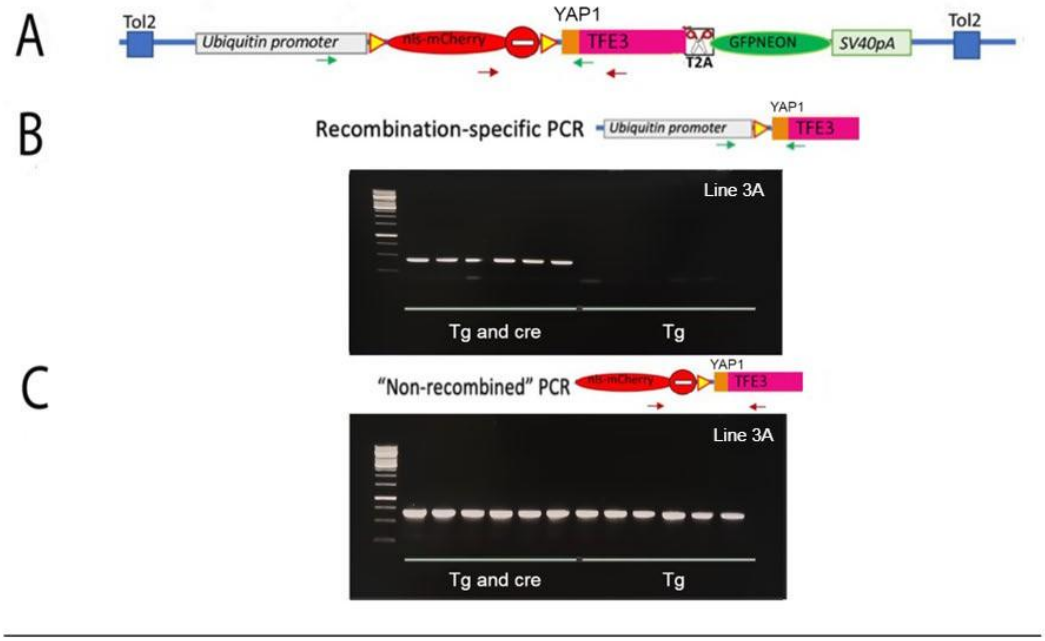


Fig. 46: Recombination-specific PCR test (with transgenic line) for Yap1-Tfe3
A) Schematic representation of *ubi: lox nls-mCherry lox Yap1-Tfe3 t2a neon*
B) A PCR showing bands of *ubi: lox nls-mCherry lox Yap1-Tfe3 t2a neon* x *fli1a:cre EGFP* (Tg *Cre*) – bands will only be present if transgene and *Cre* are present (429bp). This indicates that the STOP cassette can be removed and recombination can occur in transgenic line, 3A.
C) A non-recombined PCR, showing bands where *mCherry* is present (689bp), in the *ubi: lox nls-mCherry lox Yap1-Tfe3 t2a neon* x *fli1a:cre EGFP* embryos (Tg *Cre*), and Tg alone. *mCherry* is expressed ubiquitously.

## 9.3 Generation and characterisation of *ubi*: *lox nls-mCherry lox dominant active (DA) TAZ t2a neon* zebrafish

As there were issues with TC expression, it was decided to use a dominant active (DA) TAZ construct alongside, as a positive control. A TAZ 4SA construct was used, where 4 serines from the conserved HXRXXS motif were mutated to alanine, to prevent TAZ phosphorylation, hence making it constitutively active (Lei et al., 2008). To produce the *ubi*:*lox nls-mCherry lox DA TAZ t2a neon* construct, firstly the middle entry vector was created via Gibson cloning. Primers were designed and used to PCR the Plvx puro 3F TAZ 4sa construct, then this was cloned in *E. coli* and purified. The final plasmid was constructed using Multi-site Gateway cloning.

### 9.3.1 DA TAZ fish show recombination upon *Cre* activation

*ubi*:*lox nls-mCherry lox DA TAZ t2a neon* construct was injected into WT embryos, along with *Cre* mRNA, to test the lox sites. This worked work well, with a clear change from RFP to GFP (Fig. 47). Embryos were raised, and once the DA TAZ lines were mature, they were screened for the transgene, and were injected with *Cre* mRNA to test recombination in the lines. As with TC, RFP was lost upon *Cre* injection, but neon was not visible. Again, recombination primers were designed to test this.

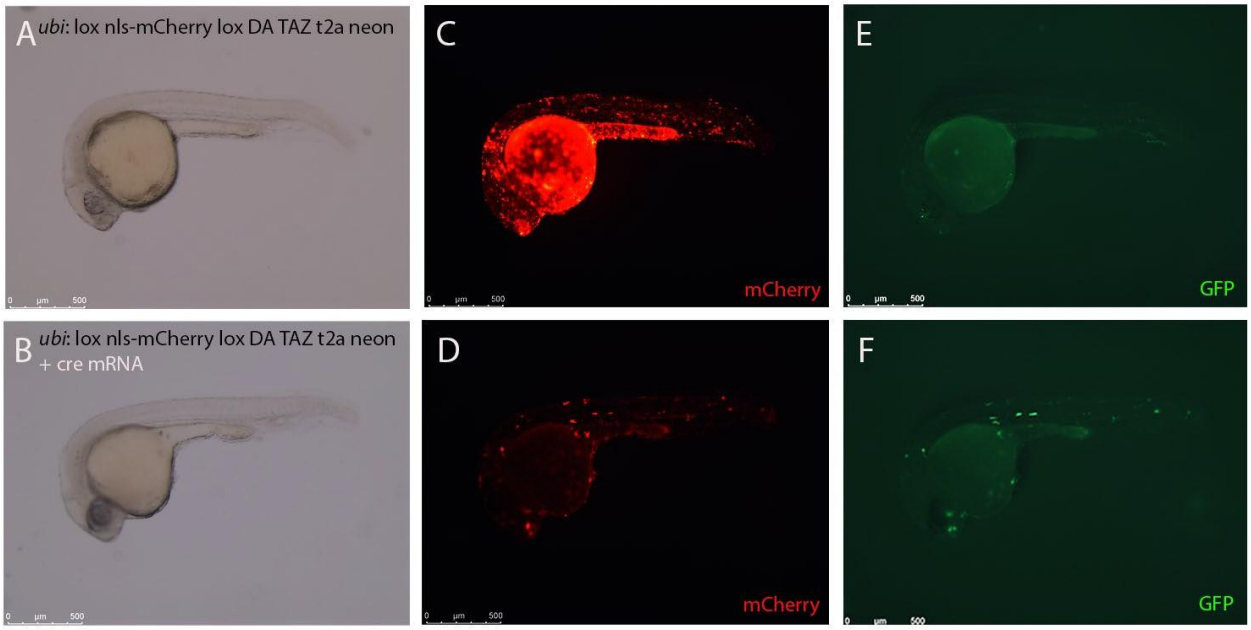


Fig. 47: Recombination test: Injection of *ubi*:*lox nls-mCherry lox DA TAZ t2a neon* into WT embryos, with and without
*Cre* mRNA, at 1dpf
A, C, E) an embryo injected with the construct only, and no *Cre* mRNA. C) nuclear RFP, and E) no GFP. B, D, F) an embryo injected with the construct, plus *Cre* mRNA.
D) few RFP spots, and F) GFP spots, which indicated that the lox system was working.

### 9.3.2 DA TAZ shows recombination via PCR

Once the new DA TAZ line (3B) was mature, fish were screened for the transgene and were crossed, *ubi: lox nls-mCherry lox TAZ-CAMTA1 DA TAZ t2a neon* x *fli1a:cre EGFP,* to check that there was recombination in the lines. Embryos were sorted for the transgene (RFP) and *Cre* (GFP). The PCR from these fish showed a band of the correct size (233bp) with both the transgene and *Cre* (Tg *Cre*),

but not in the fish with the transgene only (Tg) (Fig. 48, B). This indicates the STOP cassette can be removed and recombination can occur in transgenic line 3B. The non-recombined PCR showed bands (260bp) where *mCherry* is present, in the embryos with the transgene and Cre (Tg *Cre*), and transgene (Tg) alone, as *mCherry* is expressed ubiquitously (Fig. 48, C).

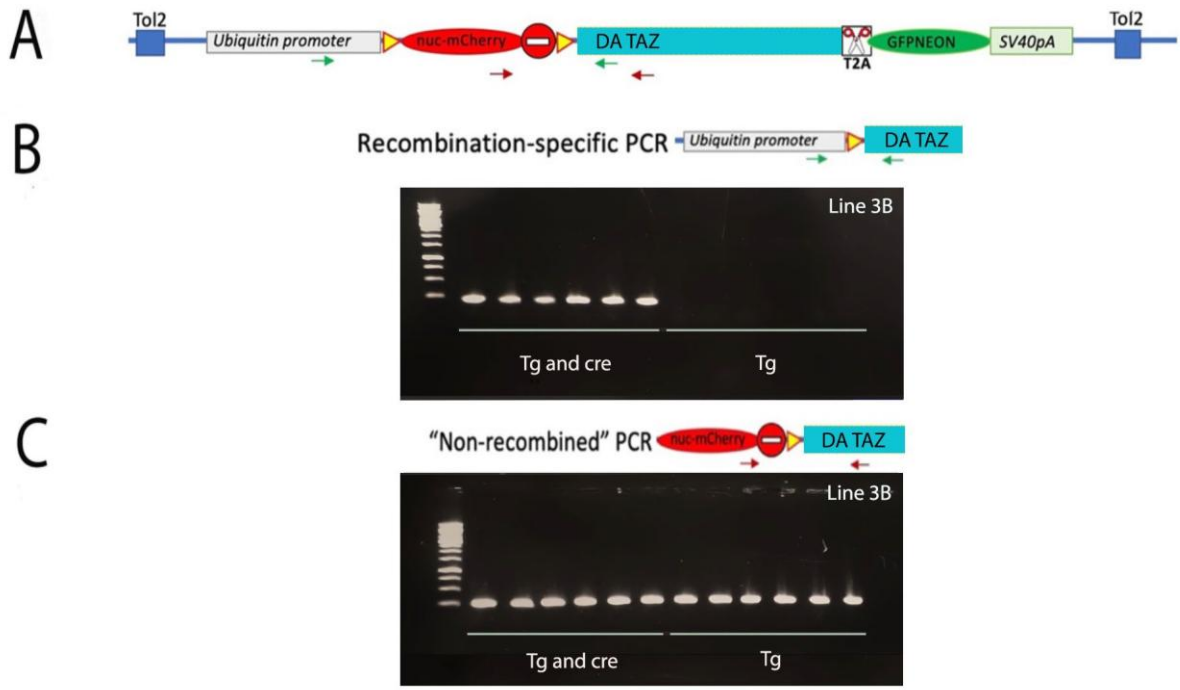


Fig. 48: Recombination-specific PCR test (with transgenic lines) for DA TAZ
A) Schematic representation of *ubi: lox nls-mCherry lox DA TAZ t2a neon*.
B) A PCR showing bands of *ubi: lox nls-mCherry lox DA TAZ t2a neon* x *fli1a:cre EGFP* (Tg cre) – bands will only be present if transgene and *Cre* are present (233bp). This indicates that the STOP cassette can be removed and recombination can occur in transgenic line, 3B.
C) A non-recombined PCR, showing bands where *mCherry* is present (260bp), in the *ubi: lox nls-mCherry lox DA TAZ t2a neon* x *fli1a:cre EGFP* embryos (Tg *Cre*), and Tg alone. *mCherry* is expressed ubiquitously.

## 9.4 Generation and characterisation of new *ubi: lox nls-mCherry lox TAZ-CAMTA1 Ex15 t2a neon* zebrafish

A further alternative was to create an improved version of the TC zebrafish model. It was decided this could be done via adding introns either side of CAMTA1, exon 15, as the RNAseq data previously showed a drop in expression at this point (Chapter 7). This would split the construct into smaller exons of 3.1, 0.3, and 2.2kb, as opposed to a long exon of 5.6kb. It was hoped that these introns may 'break-up' potential signals in the DNA sequence that caused transcription to stop. An additional reason for adding introns either side of CAMTA1, exon 15, was that transgenes with introns are known to express at a higher level than transgenes without (Brinster et al., 1988). It is also known that introns which are positioned close to the promoter are able to enhance transcription (Brinster et al., 1988, Furger et al., 2002, Samadder et al., 2008), but it was discovered that in the previous TC construct, there was an intron in the 5' UTR already present. Therefore, I did not need to add any further introns near the promoter.

This new construct was produced in two stages, as an extra ATG in the 5'UTR was discovered and required removal. This was in order to prevent the ribosome competing with this and the start ATG, and the flanking introns to CAMTA1, exon 15, also were required. Two DNA pieces were synthesised by Genewiz, cut via appropriate restriction digests, phenol purified, then ligated into linearised pME-MCS2 in two steps (one piece at a time). Multi-site gateway cloning was used to produce the final construct.

### 9.4.1 New TAZ-CAMTA1 fish show recombination upon *Cre* activation

The new construct, *ubi:lox nls-mCherry lox TAZ-CAMTA1 Ex15 t2a neon* was injected into WT embryos, along with *Cre* mRNA, in order to test the lox sites. This worked work well, with a clear change from RFP to GFP (Fig. 49). As with all other constructs tested, RFP was lost upon *Cre* injection when embryos from the lines were used, but neon was not visible. Again, recombination primers were designed to test this.

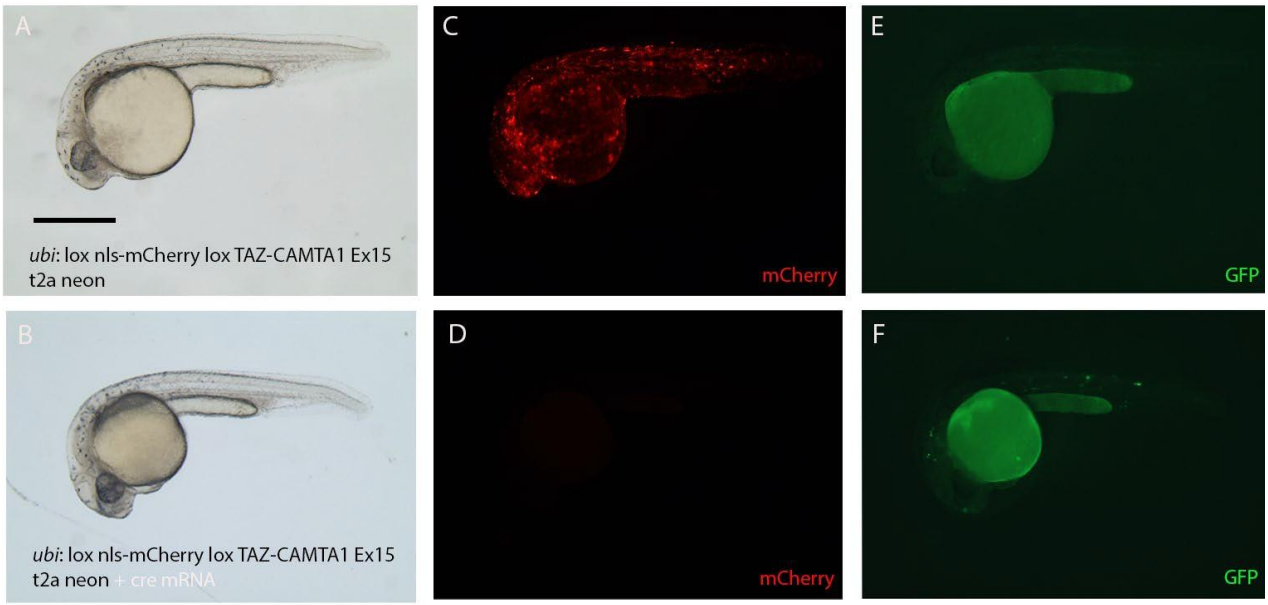


Fig. 49: Recombination test: Injection of *ubi*:*lox nls-mCherry lox TAZ-CAMTA1 Ex15 t2a neon* into WT embryos, with and without *Cre* mRNA, at 1dpf
A, C, E) an embryo injected with the construct only, and no *Cre* mRNA. C) nuclear RFP, and E) no GFP, as expected. B, D, F) an embryo injected with the construct, plus *Cre* mRNA. D) no RFP, and F) GFP spots, which indicate the lox system is working.
Scale: 0.5mm

### 9.4.2 TC Ex15 shows recombination via PCR

I crossed *ubi: lox nls-mCherry lox TAZ-CAMTA1 Ex15 t2a neon (AM1)* x *fli1a:cre EGFP* to check that there was recombination in the lines. Embryos were sorted for the transgene (RFP) and *Cre* (GFP). The PCR from these fish showed a band of the correct size (358bp), with both the transgene and *Cre* (Tg *Cre*), but not in the fish with the transgene only (Tg) (Fig. 50, B). This indicates the STOP cassette can be removed and recombination can occur in transgenic line AM1 (bottom bands are primer-dimer). The non-recombined PCR showed bands (662bp) where *mCherry* is present, in the embryos with the transgene and Cre (Tg *Cre*), and transgene (Tg) alone, as *mCherry* is expressed ubiquitously (Fig. 50, C).

A higher level of lethality in one batch of TC Ex15 was observed, therefore a further batch of TC Ex15 were raised to see if this level of lethality was reproducible. This showed that there were no high levels of lethality in the second batch. Hence, the first set appeared to be an anomalous result.

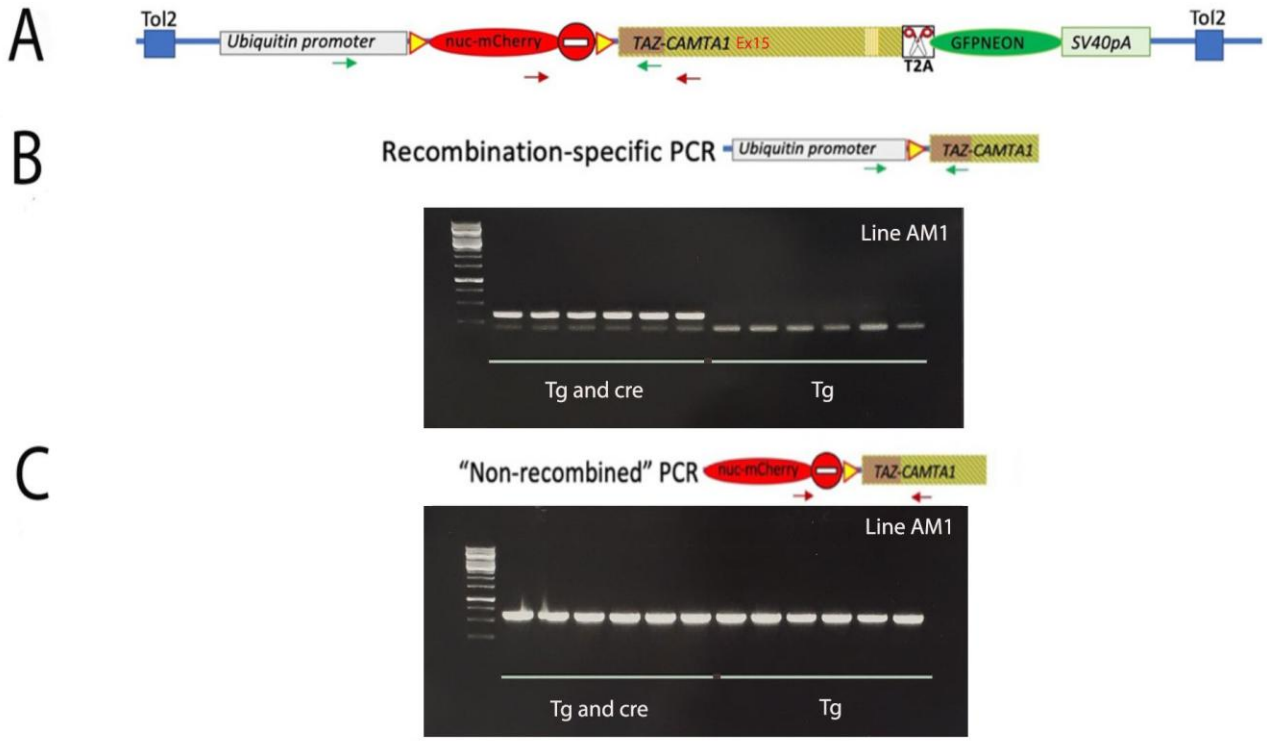


Fig. 50: Recombination-specific PCR test (with transgenic lines) for TAZ-CAMTA1 Ex15
A) Schematic representation of *ubi: lox nls-mCherry lox TAZ-CAMTA1 Ex15 t2a neon*.
B) A PCR showing bands of *ubi: lox nls-mCherry lox TAZ-CAMTA1 Ex15 t2a neon* x *fli1a:cre EGFP* (Tg *Cre*) – bands will only be present if transgene and *Cre* are present (358bp). This indicates the STOP cassette can be removed and recombination can occur in transgenic line AM1 (bottom bands are primer-dimer).
C) A non-recombined PCR, showing bands where *mCherry* is present (662bp), in the *ubi: lox nls-mCherry lox TAZ-CAMTA1 Ex15 t2a neon* x *fli1a:cre EGFP* embryos (Tg *Cre*), and Tg alone. *mCherry* is expressed ubiquitously.

### 9.4.3 Activated TC and YT show an effect on the vasculature at 1dpf, but DA TAZ does not

Although initial analysis of transgenic lines did not reveal major morphological defects, more subtle defects may have been present. In order to further quantify and compare the effect of TC, YT, and DA TAZ on the vasculature, where the effect of these transgenes was most likely to occur, *ubi: lox nls-mCherry TC/YT/DA TAZ t2a neon* lines were crossed with *fli1:cre EGFP* fish. Unfortunately, TC Ex15 lines were not available at this point, therefore the original TC was used for this experiment. Once crossed, the embryos were sorted for active TC/YT/DA TAZ (RFP and GFP) and control (GFP only). The tail vasculature was then imaged at 1dpf, using the *Cre-EGFP* as an endothelial reporter. ISVs were identified by labelling -1 to -9 pre-anal vessel, and 1 to 9 post-anal vessel. Subsequently, each ISV was given a score 0-4, where 0 was invisible, 1 was a quarter growth, 2 was half-way growth, 3 was three-quarter growth and 4 was when the vessel was fully extended to the dorsal side of the tail. These values were added to create a score and were then plotted (Fig. 51). This scoring was performed blinded and showed that there was a significant difference between active TC and sibling (sib.) control, and between active YT and sib. control. However, surprisingly, there was no significant difference between length/number of ISVs for active DA TAZ and sib. control (this was designed as a positive control) (Fig. 51). Note, as each set (eg. TC active and TC sib. control) was imaged on a different day, the embryos may have been a slightly different age, and therefore sets cannot be compared accurately. However, active and sib. controls in a set were precisely the same age and are therefore directly comparable. As these results showed significant difference for active YT vs YT sibs, it was decided to perform RNAseq to examine expression levels of YT.

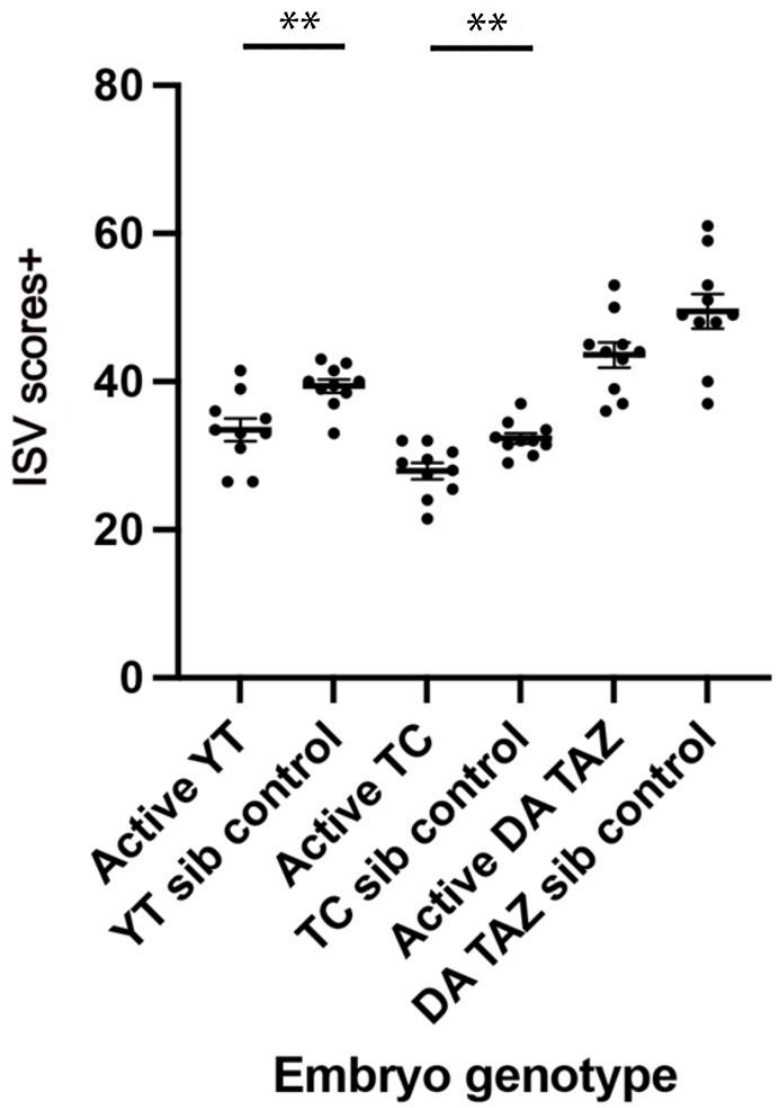


Fig. 51: ISV scores for active lines vs controls at 1dpf
*ubi:lox nls-mCherry lox TC/YT/DA TAZ t2a neon x fli1:cre EGFP* were sorted and ISVs were scored.
+Each ISV length was scored 1-4, then summed to give a total for each embryo.
**P<0.01, unpaired t-test

## 9.5 *Cyr61* as a reporter for activity of EHE oncogenes

As it was unclear which was the best time-point to use for RNAseq, as over time gene expression may have been down-regulated, it was thought beneficial to use *Cyr61* as a read-out for YT/TC/DA TAZ

activity, at a set of distinct time points. In the RNAseq analysis performed in Chapter 7, *Cyr61* was a top hit, and is a known target gene for both EHE and YAP/TAZ signalling (Cordenonsi et al., 2011, Seavey et al., 2021, Zhang et al., 2011, Lai et al., 2011). Therefore, it was deemed a top candidate for qPCR as a read-out for TC/YT activation. This would allow quicker tests to evaluate and compare different constructs for their potential to express active EHE oncogenes.

### 9.5.1 YT appears to upregulate *Cyr61* more than TC

For qPCR, I used published primers for *Cyr61* (Miesfeld et al., 2015), and *Rps29* (Bower et al., 2017) as a housekeeping gene. qPCR was performed on WT embryos co-injected with *ubi*: *lox nls-mCherry lox YAP1-TFE3 t2a neon* DNA and *Cre* mRNA, and YT construct alone (1dpf). This was also done with co-injection of *ubi: lox nls-mCherry lox TAZ-CAMTA1 t2a neon* DNA and *Cre* mRNA, and the TC construct alone. The average fold change was plotted for these groups (Fig. 52). There was a higher fold change with YT and *Cre* injection compared to YT alone (average 1.53), than with TC and *Cre* injection compared to TC alone (average 1.22). Therefore, there was a 53% increase when YT was 'switched on,' compared to a 22% increase when TC was 'switched on.' ddCT was used for the statistics: there was a statistical difference between YT and *Cre* and YT injection alone (P=0.002), using an unpaired t-test. Overall, this appeared to show that *Cyr61* was able to be used as a read-out for TC and YT activity, using these specific primers. However, it was then discovered that the *Cyr61* published primers were in Exon 5 (3' UTR), as opposed to spanning an intron-exon boundary. Even though a RapidOut DNA removal kit was used, it was still possible that this could have led to amplification of background genomic DNA, therefore, a *Cyr61* Taqman$^{TM}$ probe was used from hereon (this is target specific, so unable to amplify background gDNA).

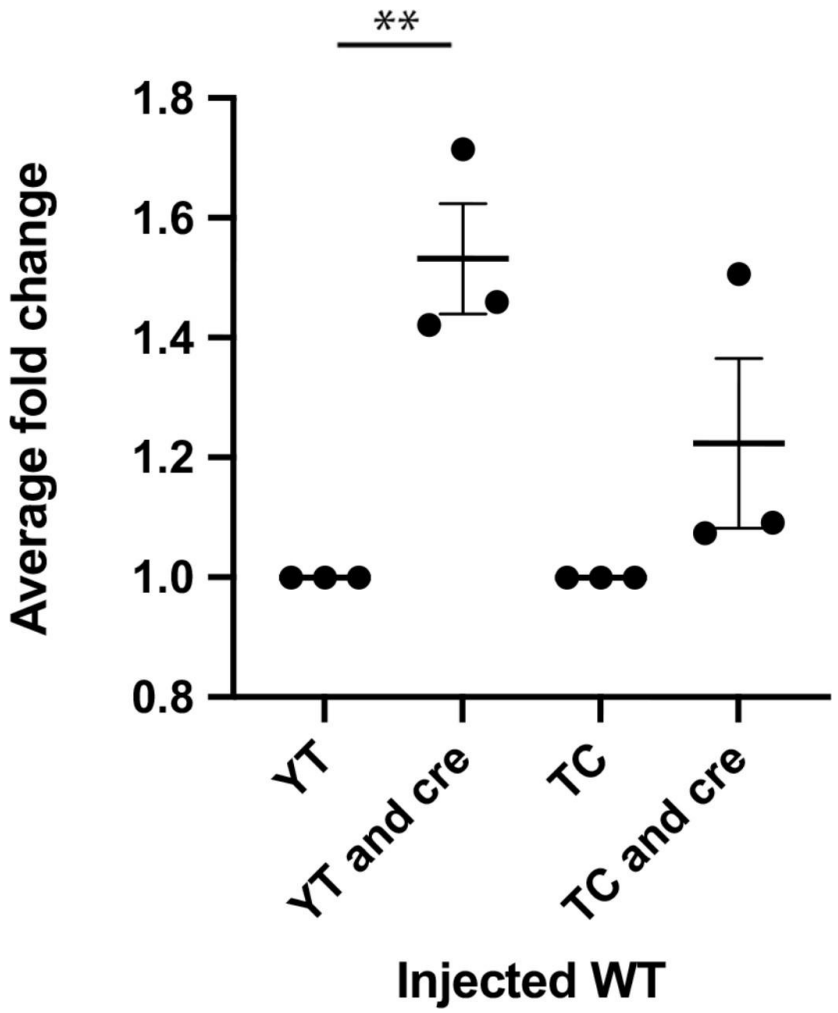


Fig. 52: Average fold change for *Cyr61* with injection of different constructs, at 1dpf
YAP1-TFE3 construct, with and without *Cre* mRNA, was injected into WT embryos.
TAZ-CAMTA1, with and without *Cre* mRNA, was injected into WT.
ddCT was used for statistical analysis, however average fold change is shown in the graph to aid understanding. **P<0.01, unpaired t-test

#### *9.5.1.1 YT lines show an increased response for Cyr61 target gene at 1dpf*

It was deemed that RNAseq on *Cre* injected YT lines (Chapter 10) would be beneficial, in order to compare expression levels of YT vs TC, whether target genes eg. *Cyr61* were induced, and to check whether the whole constructs were translated. In addition, the previous RNAseq on TC was performed

at 5dpf, but at the time it was unclear if this was the optimal time point, due to a lack of knowledge on suitable target genes. In order to decide the best time point to use, TC, YT, and dominant active (DA) TAZ crosses (crossed to WT) were injected with *Cre* mRNA, and mock (phenol red) injected fish were used as a control. Embryos were collected at 1, 2, 3, and 5dpf, and all were unsorted for fluorescence, as this was not visible in the *Cre* mRNA injected fish. As there were issues with TC expression, it was decided to use a DA TAZ construct, alongside, in this experiment. Transmission rates were 50% for TC as the F2 generation was used. Transmission rates were checked for YT and DA TAZ, and 50% transmission rates were used for this experiment (this was checked as only F1 generations were available and it was necessary to ensure only one copy of the transgene was present for comparison). RNA was extracted, cDNA was synthesised and Taqman$^{TM}$ qPCR was performed. As only 50% of the samples expressed the transgene, the fold change was doubled. The data showed that the largest fold change was for both TC and YT *Cre* injected fish at 1dpf, at 2.6 fold change, whereas DA TAZ with *Cre* injection had 2.3 fold change at 1dpf (Fig. 53). Activated TC/YT were >= 1.5 fold change for all days tested, however DA TAZ decreased over time, and dipped below control levels at 0.75, at 5dpf. Therefore, from the available data, the fusion genes generally appeared more active than dominant active TAZ, especially at 5dpf (Fig. 53). As *Cyr61* expression appeared to trend downwards over time, 1dpf was chosen for further RNAseq analysis.

Notably, later, when the TC Ex15 lines were available, the same experiment was performed as above, using TC and TC Ex15 at 1dpf and 5dpf. This showed that when Cre was injected, TC Ex15 showed a higher fold change (3.1x) than TC (2.2x) at 1dpf, but at 5dpf, TC Ex15 (1.9x) was lower than TC (3.4x) (Fig. 54). Therefore, there was not a high difference in fold change between both TC and TC Ex15.

In conclusion, *ubi: lox mCherry lox Yap1-Tfe3 t2a neon, ubi: lox mCherry DA Taz t2a neon*, and *ubi: lox mCherry lox TC Ex15 t2a neon* constructs were created and coinjected into zebrafish with Cre. All constructs showed recombination upon coinjection, via reduction in RFP and increase in GFP, as expected. Recombination PCR primers were designed for all 3 new constructs, and the PCR tests showed that there was recombination for Yap1-Tfe3, DA TAZ, and TC Ex15 lines. The original TC line and Yap1-Tfe3, and DA TAZ lines were crossed to *fli1:cre EGFP*, and IGVs were scored. This showed a significant difference for TC and YT vs controls, but not for DA TAZ. Cyr61 Taqman qPCRs were also performed at different time points, and showed that when TC, YT, and DA TAZ were coinjected with *Cre*, Cyr61 was highest at 1dpf. Therefore, 1dpf was the time point chosen for further RNAseq analysis.

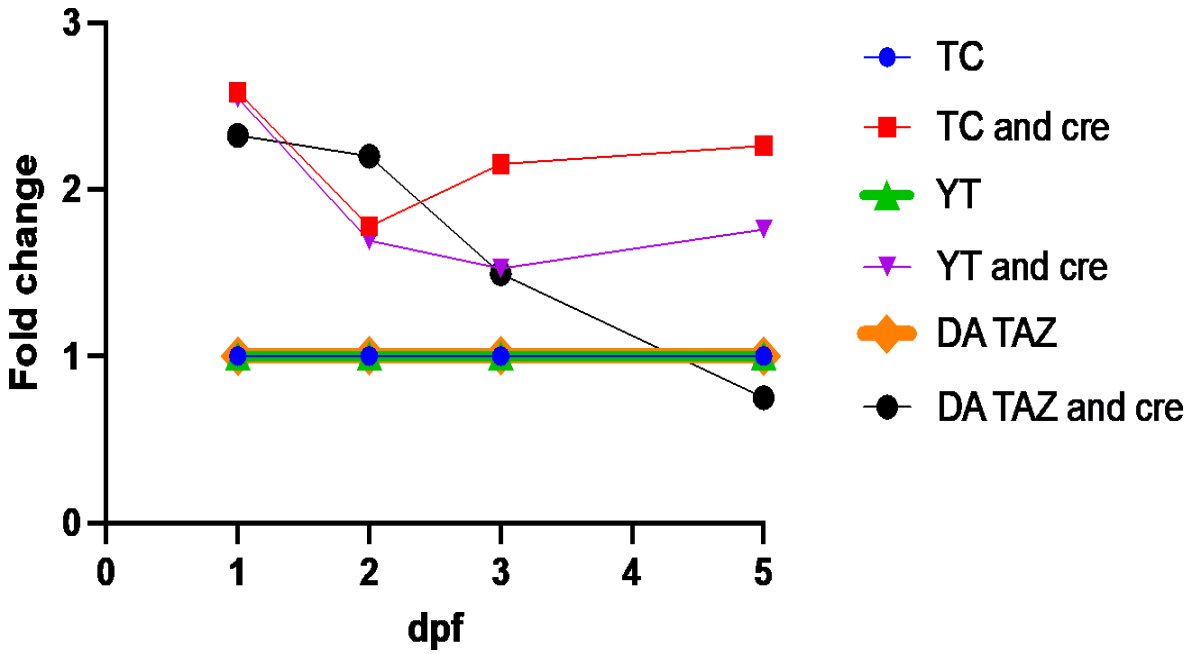


Fig. 53: Fold change for Cyr61 at 1, 2, 3 & 5dpf (Taqman) with injection of transgenic lines TC, YT & DA TAZ lines were used, with *Cre* injection or mock injection (phenol red).

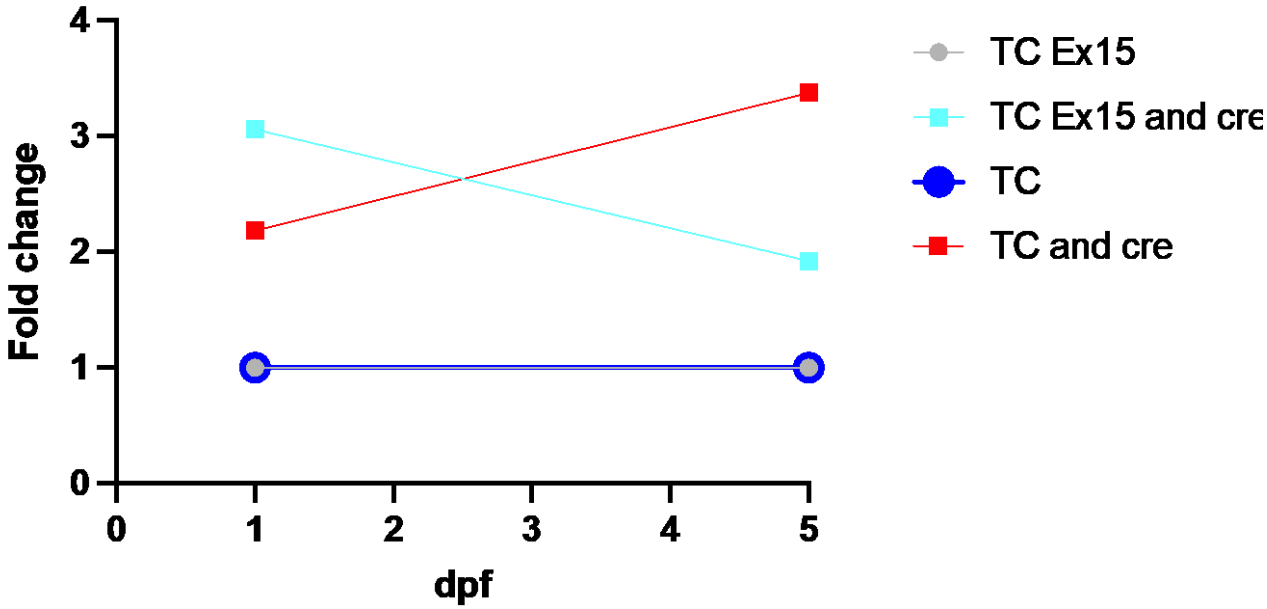


Fig. 54: Fold change for Cyr61 at 1 & 5dpf (Taqman) with injection of transgenic lines TC Ex15 and TC lines were used, with *Cre* injection or mock injection (phenol red).

# 10 Results: RNAseq: Yap1-Tfe3 transgenics

RNAseq on TAZ-CAMTA1 (TC) provided valuable information on expression of both the transgene and its effects on the transcriptome. As there was limited time available and no tumours had yet appeared in the Yap1-Tfe3 (YT) fish, it was decided to look at YT expression levels in detail in the *ubi: lox nls-mCherry lox Yap1-Tfe3 t2a neon* line, using RNAseq. It will also allow comparison of my data to previous RNAseq experiments, using activated forms of YAP1/TAZ in other organisms. Again, importantly, it will also allow precise mapping of RNAseq reads to the YT gene.

To generate RNA samples, *ubi:lox nls-mCherry lox Yap1-Tfe3 t2a neon* carrier (line 3A) was paired with WT. Approximately 50% of the embryos were injected with *Cre* mRNA to remove the STOP cassette, and induce YT expression. Embryos were pooled in triplicate samples for RNAseq analysis at 1dpf. Uninjected fish which contained the transgene, and therefore expressed *mCherry*, were used as a control. It was not possible to identify transgenic embryos from non-transgenic embryos reliably at this stage. Therefore, larvae were tail-clipped, with the anterior region being stored in RNAlater$^{TM}$, and the tail section being used for genotyping. After genotyping, transgenic larvae were selected and pooled for RNA isolation (10 embryos per sample). Once RNA was purified, a cDNA library was synthesised (Wang et al., 2009). Adapters were bound to the cDNA to enable identification, then these were sequenced from both ends (paired-end sequencing) (Wang et al., 2009).

## 10.1 RNAseq quality control

Illumina paired-end 150 sequencing (150bp reads from either end) was used for this RNAseq. The quality control was performed by Novogene. The number of clean reads used in the analysis for each sample is noted below (Table 17).

| Sample | No. of reads |
|---|---|
| Injected1 | 97824180 |
| Injected2 | 72853126 |
| Injected3 | 95060968 |
| Uninjected1 | 100552926 |
| Uninjected2 | 101082646 |
| Uninjected3 | 113426610 |

Table 17: The number of reads used for each sample in RNAseq, for YT

### 10.1.1 Principal Component Analysis (PCA)

PCA is a statistical method to reduce several sets of data down to two dimensions. It examines how the data is grouped and was performed on the gene expression value (FPKM). The first principal component gives a 'line of best fit' in the direction of the largest variability in the data. The second principal component gives the direction with the second largest variability in the data (https://tinyurl.com/5bfxt4kz).

Uninjected samples were more dispersed than injected samples, hence the uninjected samples show more variance. Overall, injected and uninjected samples appear to cluster in separate areas, with PC1 having the most variance (although YTuninj3 is less clustered than the other uninjected samples) (Fig. 55).

From the other QC data, all my samples had an average error rate of less than 0.02%. Generally, a single base error rate should be lower than 1% (Novogene report). Also, the GC content appeared unremarkable. Overall, the quality and amount appeared to be satisfactory, and I continued with expression analysis.

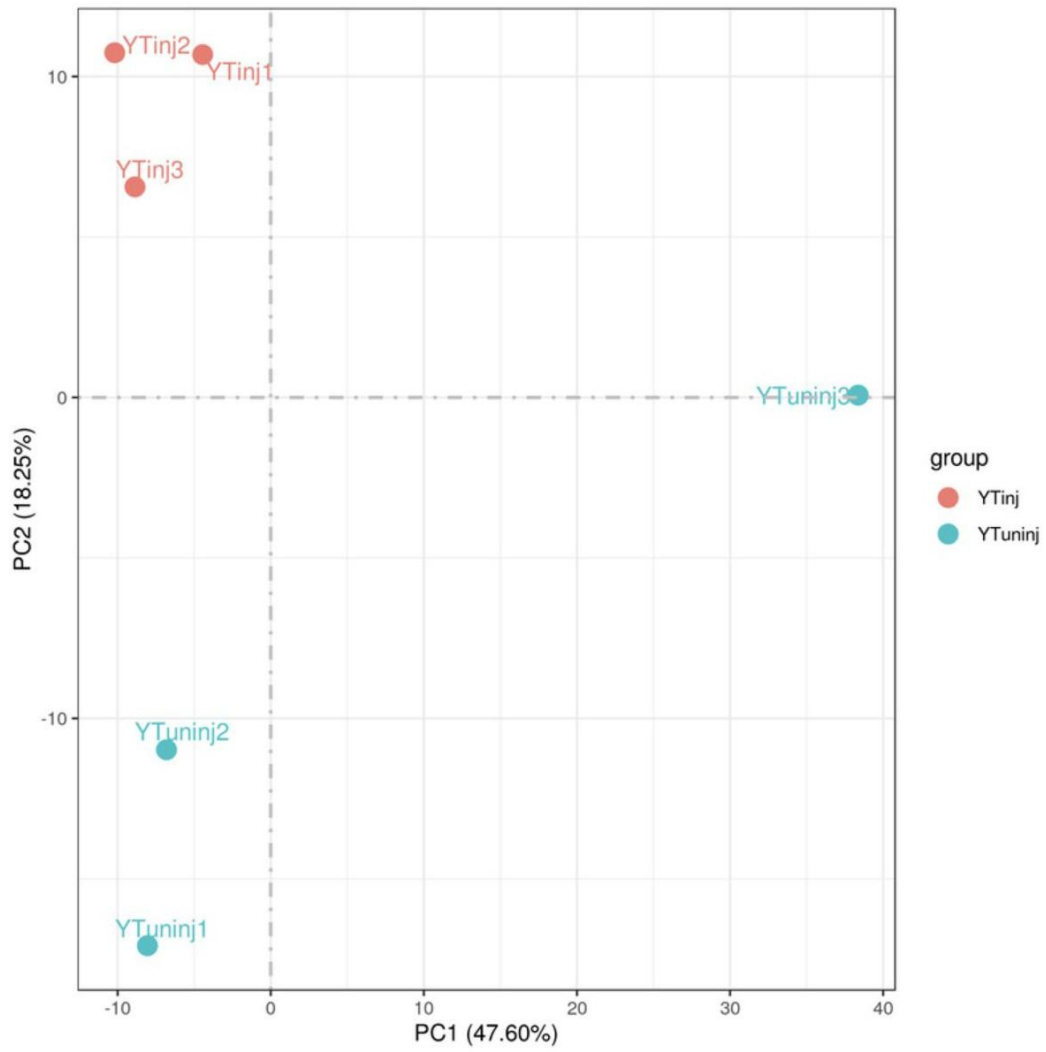


Fig. 55: Principal component analysis (PCA) for Yap1-Tfe3
This shows the intergroup and intragroup differences.
PCA was performed on the gene expression value (FPKM) of all samples.
Uninjected samples and injected samples mainly cluster separately (but YTuninj3 is less clustered).

## 10.2 Differential expression analysis

After sequencing and basic quality controls were finished, differential expression analysis was performed to identify the number of genes that have expression levels which are significantly different

within each group. The differential gene histogram shows the total number of genes (156); the number of upregulated genes (114), and the number of downregulated genes (42), when comparing injected to uninjected samples (DESeq2 padj <=0.05 , log2FoldChange >=1.0) (Fig. 56). Therefore, the results were significant, with a fold change of >=2.

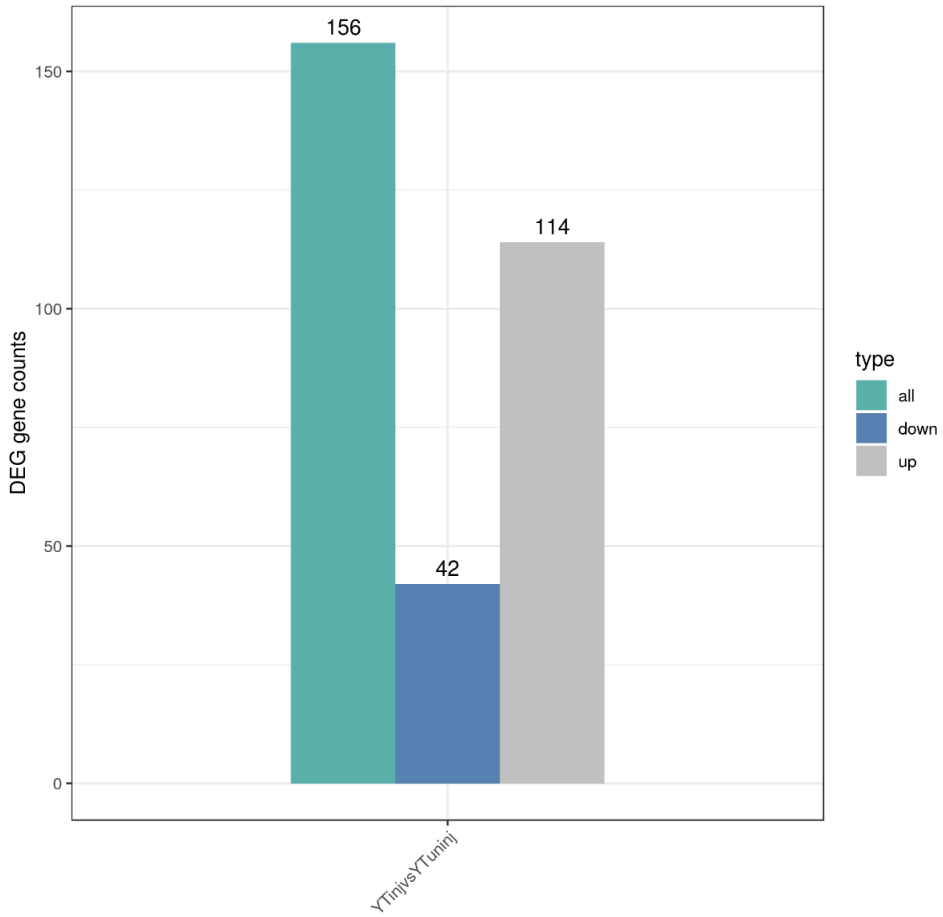


Fig: 56: Differential gene histogram for Yap-Tfe3
Number of upregulated and downregulated genes are shown for injected vs uninjected samples
DESeq2 padj <=0.05, log2FoldChange >=1.0

### 10.2.1 Volcano plot

Volcano plots can be used to infer the overall distribution of differentially expressed genes. In the figure, the x-axis shows the fold change in gene expression between different samples, and the y-axis shows the statistical significance of the differences. Red dots represent up-regulated genes and green dots represent down-regulated genes (novogene report) (Fig. 57). For upregulated genes, there were 112 genes above 2 fold increase, and 53 genes above 3 fold increase. Unfortunately, there did not appear to be any genes of interest in the top 15 down/upregulated genes (Table 18).

| Top downregulated DE genes | Top upregulated DE genes |
|---|---|
| Novel452 | RARRES3 |
| Atoh | rgra |
| Mipb | apodb |
| fut9d | mhc2dgb |
| krt1-19d | Si:ch73-236c18.3 |
| novel2754 | he1.3 |
| f7i | zgc:113314 |
| novel4904 | epdl1 |
| Crygmx | si:ch211-120k19.1 |
| CU634008.1 | slc37a2 |
| wfikkn2a | pah |
| s100a11 | pkhd1l1 |
| novel131 | phospho1 |
| bhlhe22 | rab38c |
| BX465834.1 | kcnj1a.3 |

Table 18: Top 15 downregulated and upregulated DE genes for YT

Although the differential expression data gives information with respect to individual genes on expression changes, it is difficult to differentiate larger patterns from the changes in gene expression, therefore I decided to use Gene set enrichment analysis (GSEA) (Subramanian et al., 2005, Mootha et

al., 2003).

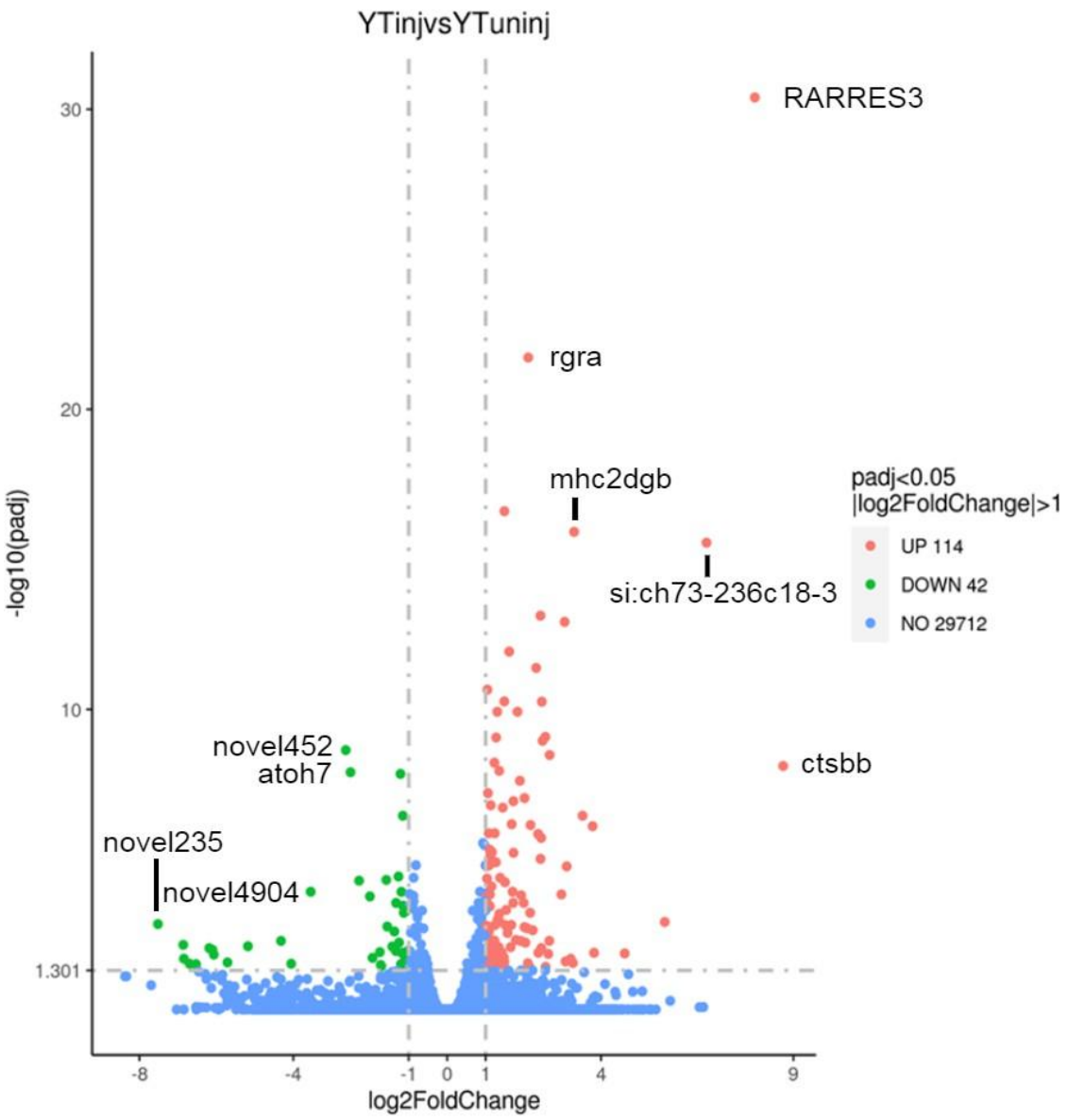


Fig. 57: Volcano plot for Yap1-Tfe3
The x-axis shows the fold change in gene expression between different samples.
The y-axis shows the statistical significance of the differences.
Red dots represent up-regulated genes and green dots represent down-regulated genes.
The dashed lines indicate the threshold lines for differential gene screening criteria.
NB Cyr61 is not significant for YT.

## 10.3 Detailed analysis of Yap1-Tfe3 expression from the RNAseq data, by mapping reads to the transgenic genome & using Gene Set Enrichment Analysis (GSEA)

### 10.3.1 Detailed expression analysis of *mCherry* and Yap1-Tfe3 in the RNAseq dataset

Once again, it was necessary to create a manually "adapted" zebrafish genome sequence that would allow the analysis of expression levels of the transgenic construct. A new reference genome was made by adding the transgene information to two 'genome files' that are used for mapping reads, as previously described (Chapter 7). The adapted files could then be loaded into Galaxy (https://usegalaxy.org/ (Galaxy, 2022)), and analysed to create BAM files of injected and uninjected samples. Then Galaxy tools were used to count reads from RNAseq, and expression levels were calculated. The Integrative Genomics Viewer (IGV) (Robinson et al., 2011) was used to visualise the mapped reads against the adapted reference genome, for both *Cre* injected and uninjected embryos with the *ubi*:*lox nls-mCherry lox Yap1-Tfe3 t2a neon* construct.

### 10.3.2 Expression level of Yap1-Tfe3 and *mCherry*

To recapitulate, *ubi*:*lox nls-mCherry lox YT t2a neon* x WT embryos were injected with *Cre* mRNA. They were used for RNAseq analysis at 1dpf, using RFP uninjected fish as a control. Data from RNAseq showed that for uninjected fish, *mCherry* had an FPKM of 91.234, which fell to 1.38 upon *Cre* injection. Therefore, *mCherry* showed a 66.1x decrease for *Cre* injected embryos, compared to control expression (Fig. 58). As recombination is induced by injection of *Cre* mRNA, and this is not always evenly distributed throughout the embryo, injections may not always lead to 100% recombination in all of the injected embryos. Based on these values, it can be estimated that 98% of the chromosomes in the injected embryos were recombined successfully.

In comparison, there was an unexpected result with YT, as the expression level for this also decreased from 15.748 to 6.546 FPKM. This is a 2.4x decrease in expression for *Cre* injected embryos, compared to control (Fig. 58). As YT levels are expected to increase upon *Cre* injection, as the *mCherry* STOP cassette is 'loxed out,' this is highly surprising. Also, notably, the expression level for YT when *Cre* is injected is 6.546, which is much lower at a 13.9-fold drop, compared to the *mCherry* uninjected level at 91.234. The IGV (Robinson et al., 2011) data also showed that for the injected reads, YT appears to be fully transcribed (unlike TC), and *mCherry* is loxed out when *Cre* injection occurs (Fig. 59A).

However, in Fig. 59B, for the uninjected reads, this showed that *mCherry* is expressed, as expected, but there is also YT expression. This is likely to be due to read-through the *mCherry* STOP sequence.

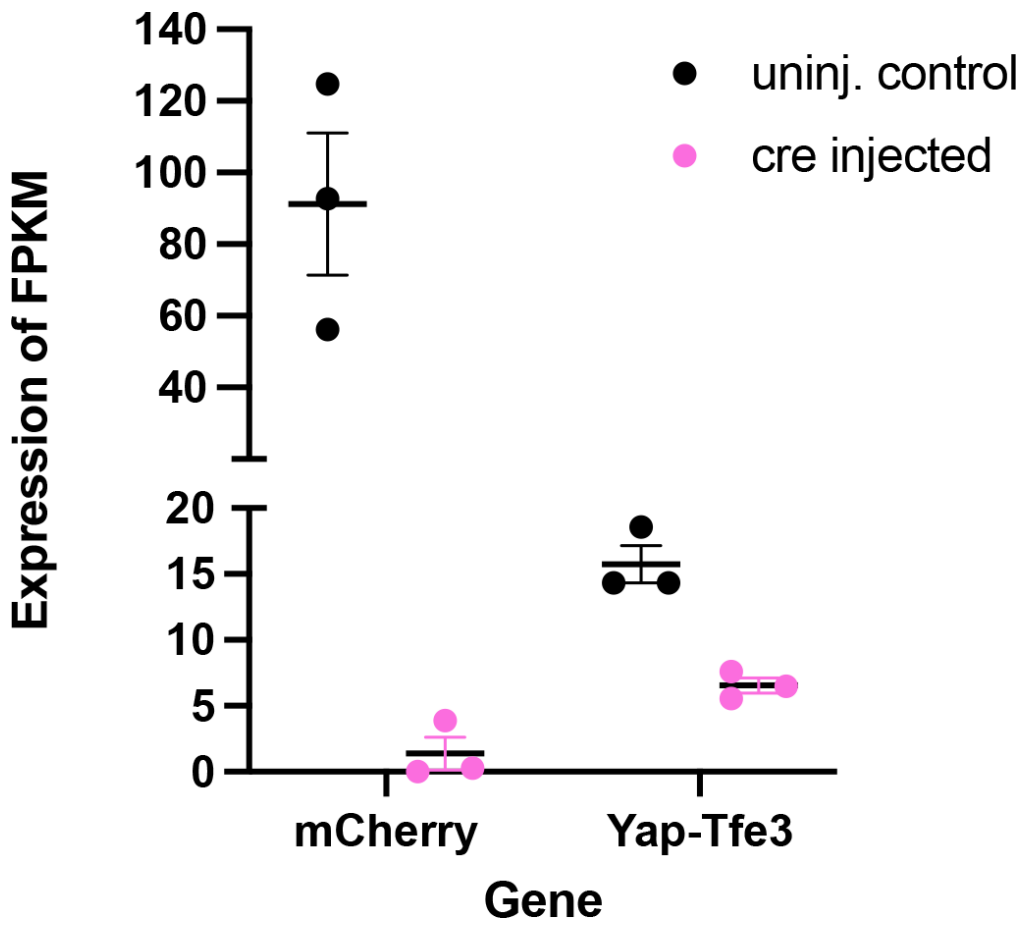


Fig. 58: Expression level of Yap1-Tfe3 vs *mCherry*, from RNAseq data
Expression of *mCherry* is shown for uninjected samples vs *Cre* injected, and the same for YT expression. *mCherry* shows a 66.1x decrease for *Cre* injected embryos, vs a 2.4x decrease for YT in *Cre* injected embryos.
FPKM = fragments per kilobase per million.

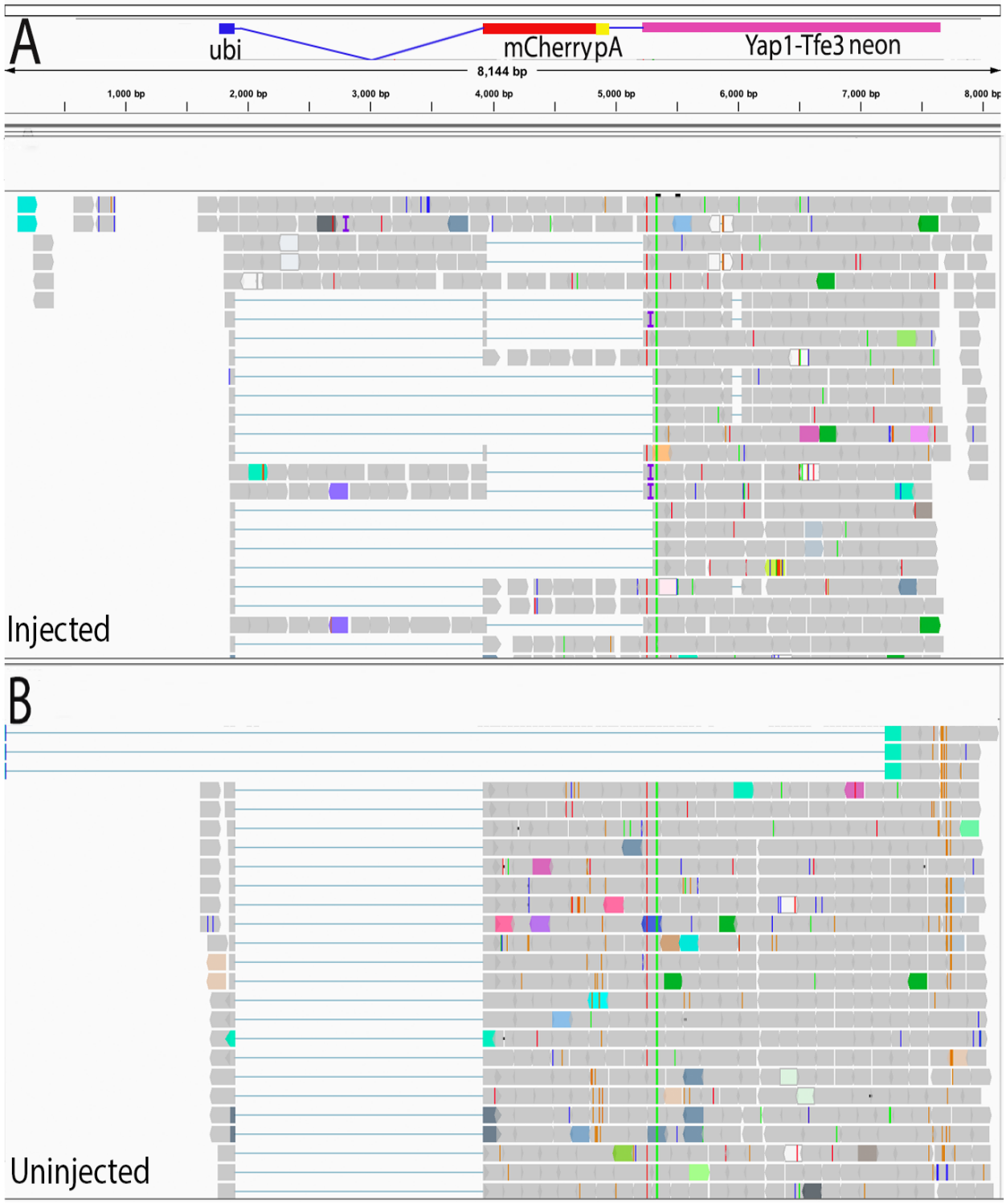


Fig. 59: Reads mapped to align with the transgenic Yap1-Tfe3 genome
A) Injected reads show *mCherry* is mainly loxed out upon *Cre* injection and Yap-Tfe3 is expressed.
B) Uninjected reads show a higher expression of *mCherry*, also with Yap1-Tfe3 expression. Snapshot of expression (all reads not shown).
pA = polyA
Thin, coloured lines indicate base mismatches
(A=green, C=blue, T=red, G=orange)

### 10.3.3 Gene set enrichment analysis (GSEA) showed that YAP/TAZ target genes were upregulated, but changes were not significant

When the STOP cassette was deleted in the transgenic lines, this did not lead to expression of detectable levels of GFP (neon). Therefore, I decided to use the transcriptome data to check if there was a "functional" effect of removal of the STOP cassette. It was possible that the functional effects of YT could be seen in expression of target genes that are known from mammalian studies, as with TC. Data from RNAseq was used in Gene set enrichment analysis (GSEA) (Broad Institute, (Subramanian et al., 2005, Mootha et al., 2003)), to compare my data to the Seavey (EHE, (Seavey et al., 2021)) and Cordenonsi (YAP, (Cordenonsi et al., 2011)) overrepresented gene sets. These mammalian sets had already been converted into zebrafish sets for the previous RNAseq (Chapter 7). Estrogen was again used as a completely unrelated control set. The results showed that there was an increase in YAP/TAZ targets genes when my data was compared to both gene sets. The leading edge is the slope at the beginning showing a subset of genes which contribute most to the enrichment score. This is steep when my data is compared to both EHE and YAP1 data sets, with a cluster of lines at the beginning of the enrichment plots (Fig. 60A/B). This does not happen when my data is compared to a seemingly unrelated data set (Estrogen) (Fig. 60C), which was as expected. However, the data is significant and normal enrichment score (NES) is higher when YT is compared to the Estrogen control set, but not the YAP1 and EHE data sets, which is highly unexpected. Although not significant, it was of note that *Serpine1*, *TGFβ*, and *Cyr61* were present again when my data was compared to both YAP1 and EHE data sets, as with TC. However, the only significant gene was hexb, which gave a log2fold change of 0.51 (1.42 fold change), P(adj)<0.001. *Hexb* has recently been discovered to control glycolysis in glioblastoma through YAP1 activation (Zhu et al., 2024).

Using the STRING database for the top 50 upregulated genes, this showed that there were no protein-protein interactions (Fig. 61). It also showed that there are no enriched reactome pathways for YT.

In conclusion, YT RNAseq data showed that expression levels of YT did not increase upon Cre mRNA injection, but actually decreased, which was highly unexpected. The RNAseq data also showed that YT was fully expressed, unlike TC. The IGV data showed that YT was expressed in the uninjected fish, which was also very unexpected. GSEA showed that *hexb* was the only significant gene when my data was compared to the YAP1 dataset.

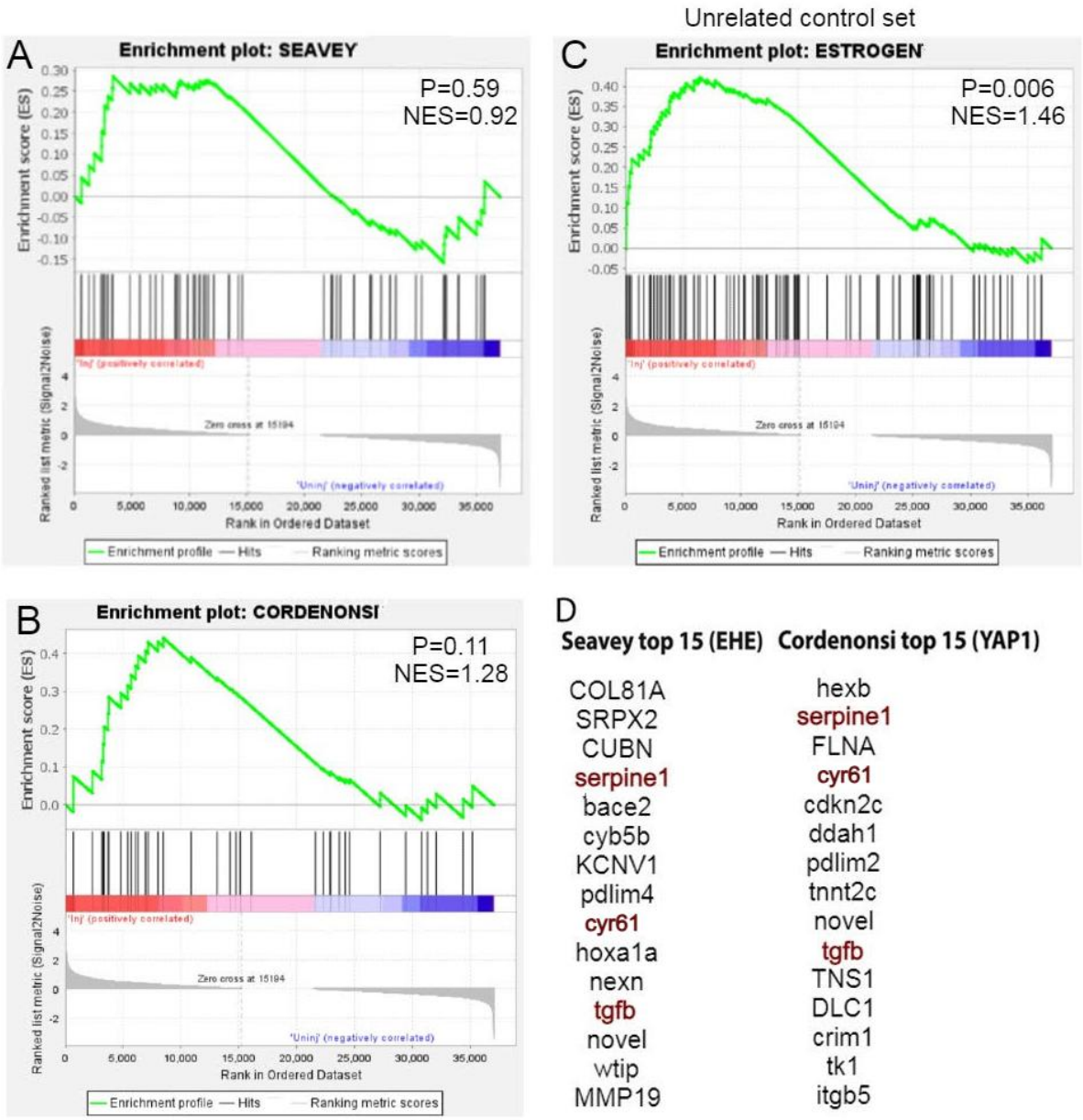


Fig. 60: Gene set enrichment analysis for Yap-Tfe3
Yap1-Tfe3 gene set compared to:
A) Seavey EHE set
B) Cordenonsi YAP1 signature set
C) Estrogen (unrelated control set)
D) The top 15 genes for Seavey (EHE) and Cordenonsi (YAP1)

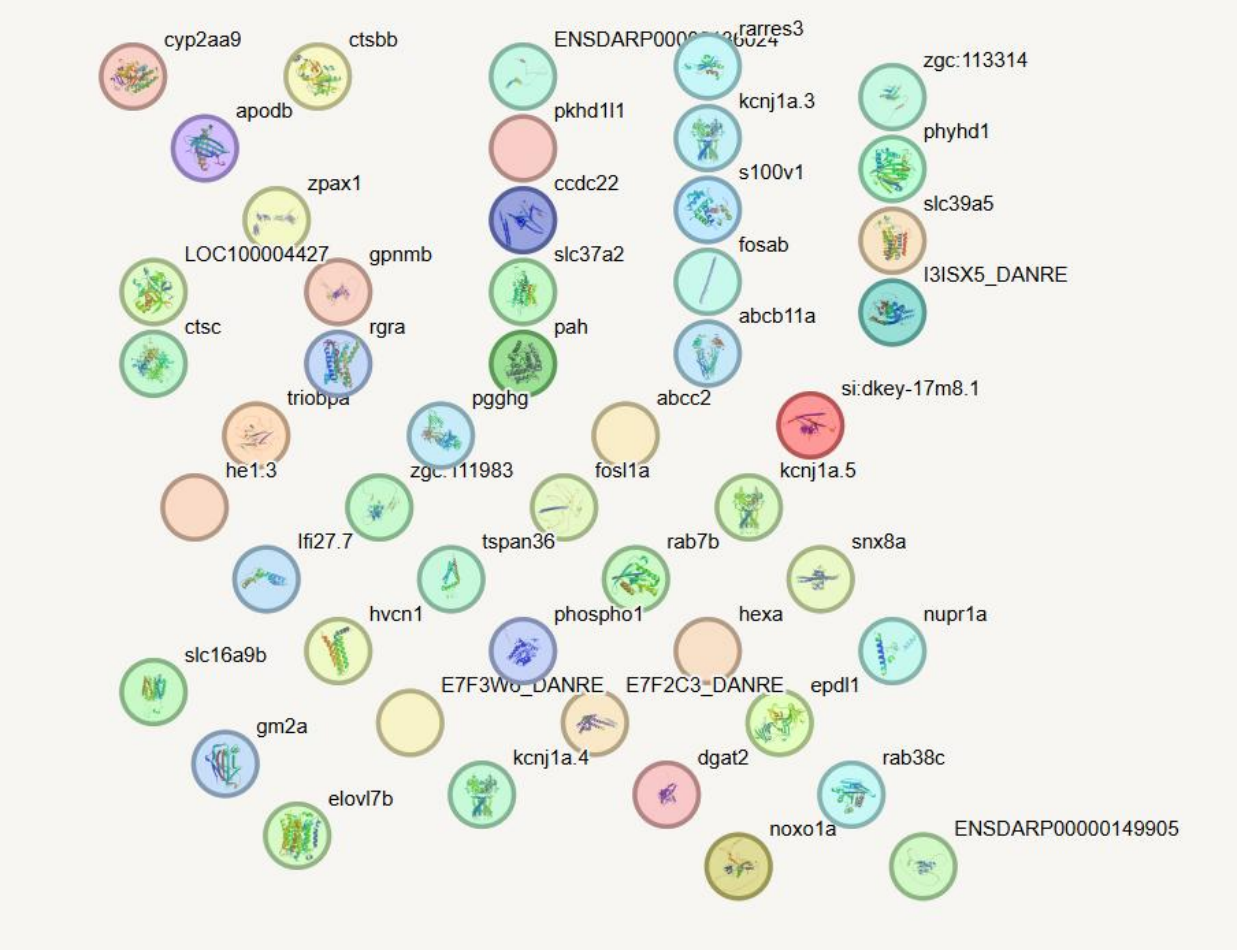


Fig. 61: Protein-protein interaction for Yap1-Tfe3
There does not appear to be any interactions for YT (no lines visible), using the top 50 upregulated genes.
Medium confidence (0.4)

# 11 Discussion

In this thesis, I described how I used several different systems aimed at producing a transgenic zebrafish model of *Epithelioid hemangioendothelioma* (EHE). In order to mimic human disease, endothelial expression of TAZ-CAMTA1 (TC) was required (Tanas et al., 2011). I first attempted to directly control TC expression using the *fli1a* promoter. I then used a Gal4/UAS system, and a cre-lox system. Initially, I used TC which causes 90% of EHE cases (Flucke et al., 2014), then I tried YT, which causes 10% of EHE cases (Antonescu et al., 2013). If a working EHE transgenic zebrafish model had been produced, this could have potentially offered a high-throughput model for drug screening, which may have eventually led to much-needed therapeutic treatments. Although, some experiments are not conclusive, it is clear that such a model is much more difficult to produce than initially anticipated.

## 11.1 Creating a zebrafish TAZ-CAMTA1 model

Initially, I tested TC mRNA on the zebrafish vasculature via injection into *fli1a EGFP* embryos. There appeared to be an effect of TC on vasculature development at 500pg, whereas the TC control, TC S51A, which is rendered unable to bind TEAD (Zhang et al., 2009), had much less of an effect at the same concentration (Chapter 5). This showed that the effect of TC was not just due to generalised toxicity caused by injection of mRNA, as the control only had a 1 amino acid change. I also tested Yap1-Tfe3 (YT) mRNA on the zebrafish vasculature at 100pg. Below this, most of the embryos gave a WT phenotype and above this, there was a high death rate. The data for 100pg YT vs YT S94A was not statistically significant. Hence, it is possible S94A may act dominant negative and interfere with endogenous YT. Li et al., showed that YAP S94A did not activate TEADs, but still maintained the ability to activate RUNX2 and ErbB4, however, which suggests that even if YAP is unable to bind/activate TEAD, it is still able to maintain transcriptional ability (Li et al., 2010). After titrations, I used 500pg TC and 100pg YT to attempt to visualise the effect of these fusion proteins on the vasculature, which indicated that YT has a stronger effect than TC. Once I had shown that TC did have an effect, I attempted to create the first TC zebrafish transgenic model.

Firstly, I attempted to directly control human TC expression using the *fli1a* promoter (Chapter 5), as EHE is known to originate in the endothelial cells of the blood vessels (Sardaro et al., 2014). This was not successful, showing non-specific *in situ* staining. This may have been due to expression of the

transgene being 'toxic,' and only insertions that behaved anomalously with respect to TC expression making it through the germline of injected G0 fish. fli1a drives ubiquitous, transient expression before and during early gastrulation, so the transgene may have affected early endothelial specification, and endothelial cells may not be able to withstand the transgene at later stages (personal comm., Nathan Lawson). Alternatively, it was hypothesised that when unoptimized human TC was used, ie. not zebrafish codon optimised, this may have caused zebrafish DNA methylation, and hence silencing (Jahner et al., 1982, Stewart et al., 1982, Li and Zhang, 2014, Keshet et al., 1986). Therefore, this experiment was repeated using zebrafish-optimised TC (using 2 different optimisation algorithms), but still, non-specific *in situ* staining was seen. I next used a temporally controlled model to circumvent potential toxicity of the TC transgene.

The first temporally controlled system I created was a Gal4/UAS system. Gal4 is a yeast transcriptional activator, which controls the expression of an Upstream Activating Sequence (UAS) promoter (Scheer and Campos-Ortega, 1999). A gene of interest, which is the effector (TC), can be fused to *uas*, which will only be expressed when this line is crossed with the Gal4 line. Otherwise, the effector gene (TC) is silent (Scheer and Campos-Ortega, 1999). This allows the establishment of lines that can express "toxic" transgenes. *uas*:*TAZ-CAMTA1* was crossed with *fli1a:GFF* (an improved version of Gal4) (Asakawa et al., 2008), but this model was also unsuccessful, with non-specific *in situ* staining. As a control, the *uas*:*EGFP* line was crossed with the same *fli1a:GFF* line. In contrast to the *uas:TAZ-CAMTA1* line, this did express GFP in the expected *fli1a* pattern (Fig.15). This led to the conclusion that the problem was likely to lay with human TC. It is possible human sequences may not express well in zebrafish. Therefore, I used zebrafish-optimised TC (using 2 different optimisation algorithms) here also, but still saw non-specific *in situ* staining. It is possible that the coding optimisation was insufficient in 'disguising' the human coding sequence. Also, endothelial cells are known to be sensitive to highly active transactivation domains e.g. Gal4, but we used GFF, which should have helped with this (personal comms, Nathan Lawson). I then tried zebrafish TAZ bound to human CAMTA1 (human CAMTA1 was retained as there was an antibody available). This was also unsuccessful and showed non-specific staining from *in situ* (Fig. 15). I next attempted to examine whether TAZ or CAMTA1 contained sequence-interfering element(s).

In order to identify the source of expression-interfering sequence elements, TAZ and CAMTA1 were cloned behind *fli1a:EGFP*. GFP ISVs were noted in *fli1a:EGFP-TAZ*, but not in *fli1a*:*EGFP-CAMTA1* (Fig. 16). This indicated that CAMTA1 may have been the source of expression-interfering element(s). However, it was then reported that there was negative feedback of the *fli1a* promoter on TC (Neil et

al., 2023), thus I attempted to discover whether the problem was negative feedback or sequence-interfering element(s).

To discover whether TC expression issues were with negative feedback or sequence-interfering element(s), I produced a *fli1a:EGFP-STOP-CAMTA1* construct (*fli1a:EGFP-CAMTA1* construct was used as a control). The hypothesis was that if a DNA element/stem loop was present, the ribosome would not continue and there would be a premature transcriptional end, hence no EGFP expression. However, if there was no stem loop present, the polyA tail would be transcribed, and there would be expected EGFP expression (Fig. 18). The results showed that there was no apparent GFP expression with the STOP construct (Fig. 19), which suggested that the issue was a DNA element(s) as opposed to promoter feedback, although it could have possibly been both. ISVs were also counted and plotted in a graph (Fig. 20). This showed a significant difference between *fli1a:EGFP* control, and both *fli1a:EGFP-STOP-CAMTA1* and *fli1a:EGFP-CAMTA1*. An important caveat of this approach is that it would lead to an unnaturally long 3' UTR at 4.2kb (average length of human 3' UTRs is ~1kb (Hong and Jeong, 2023)). Long UTRs are associated with lower levels of gene expression due to less stability (Sandberg et al., 2008) (Schwerk and Savan, 2015). Therefore, depending on GFP for this experiment may not have been reliable, and hence these experiments were not conclusive. As the previous temporally controlled system (Gal4/UAS) had not given the desired endothelial expression, it was decided to use another temporally controlled system that would avoid the effects of negative feedback of TC on the *fli1a* promoter, by employing a different, more generic promoter to drive TC expression.

Cre-lox was the next temporally controlled system used to avoid 'toxicity.' This system uses the well-established promoter, *ubi*, which should drive generic expression in the embryo. Cre is a site-specific recombinase which causes DNA recombination at loxP sites (Argos et al., 1986, Hoess et al., 1982, Hoess and Abremski, 1984). *ubi:lox nls- mCherry lox TAZ-CAMTA1 t2a neon* lines were crossed with a *fli1a*:*cre* line. This was expected to allow *mCherry* to be loxed out upon *Cre* recombination, and hence show TAZ- CAMTA1 expression in the endothelial cells, as *Cre* would only be switched on in these cells (driven by *fli1a*). It also allowed the testing of activity of the *ubi* promoter at the transgenic insertions site, through visualisation of *mCherry*.

*ubi*:*lox nls-mCherry lox TC t2a neon* was tested for recombination and was deemed to be working appropriately. Neon was visible upon DNA construct and *Cre* mRNA co-injection. However, upon the establishment of transgenic lines, injection with *Cre* mRNA for TC, YT, and DA TAZ showed no

visible GFP (unfortunately there was not enough time to test this in the TC Ex15 lines). I hypothesised that neon may not be visible either due to low expression or silencing, which can occur by methylation (Keshet et al., 1986). DNA short tandem repeats, and transgenes that fall into or beside transposon sites are more likely to be silenced (Akitake et al., 2011, Feng et al., 2010). Single copies are much less likely to be silenced than multiple copies of a transgene (Akitake et al., 2011). It has been shown that even if a transgene expresses well in the 1$^{st}$ generation, it can become silenced upon further generations in a heritable manner (Goll et al., 2009). However, it has been shown that Tol2 primarily integrates adjacent to the transcription start site (TSS), where there is open chromatin (in human cells) (Grabundzija et al., 2010).

In order to properly characterise TC expression, *ubi*:*lox nls-mCherry lox TC t2a neon* embryos were used in *in situ* and showed, surprisingly, that in pre-sorted, RFP positive and *Cre* uninjected fish, 50% embryos had darker stain for TC, as with *Cre* mRNA injected embryos. It was highly unexpected to see TC stain in the pre-sorted, RFP uninjected embryos, as *mCherry* was present, which contains a STOP sequence and polyadenylation site. This should lead to transcriptional termination, and therefore, TC should not have been expressed. This was also seen in several different founder lines. I hypothesised that this unexpected result may have been due to some background staining from the plasmid probe used, hence a TC PCR probe was made to test this possibility. I used the new TC probe to stain *ubi*: *lox nls-mCherry lox TAZ-CAMTA1 t2a neon* embryos injected with *Cre* mRNA (Fig. 28). However, in Fig. 28D, this also showed darker stain for the TC PCR probe in the pre-sorted RFP, uninjected fish. This TC staining may have been due to read-through the mCherry STOP sequence. Therefore, due to the unusual behaviour of the various transgenes, it was decided to use RNAseq to provide a more detailed view on expression of the transgene, and its potential effect on the zebrafish transcriptome.

## 11.2 RNAseq on TAZ-CAMTA1 embryos

To generate RNA samples, *ubi:lox nls-mCherry lox TAZ-CAMTA1 t2a neon* carrier (line AA6) was paired with WT. Approximately 50% of the embryos were injected with *Cre* mRNA to remove the STOP cassette, and induce TC expression at 5dpf. Samples were sent to Novogene for analysis. Differential expression (DE) analysis was performed and showed the total number of DE genes (1888); the number of upregulated genes (936), and the number of downregulated genes (952), when comparing injected to uninjected samples (Fig. 31).

After *Cre* injection, expression of TC increased, but was much lower than expected at 3.4x the original FPKM. *mCherry* had a 12.5x FPKM decrease for *Cre* injected embryos (*mCherry* is loxed out hence the decrease) (Fig. 33). Although TC had an increase upon *Cre* injection as expected, the difference in levels of FPKM for *mCherry* were much higher than for TC (12.5-fold change). I would expect the FPKM levels of TC in the *Cre* injected embryos to be similar to *mCherry* in uninjected embryos, as they are both in the same construct, under the same promoter (*ubi*). However, this was not seen. The lower levels of expression could have been due to the size of the construct: TC is 5628bp (4857bp without neon). It may also have been due to the fact that RNAseq used an oligodT primer for poly A enrichment. If there are few polyA tails available due to premature ending, then the RNA could also be poorly reverse transcribed, when cDNA template is produced for sequencing. Therefore, non-polyadenylated transcripts were selected against in the RNAseq experiment and TC expression levels may not be reliable due to this. Low expression may also be caused by gene regulation via post-transcriptional modifications, such as DNA methylation, histone modifications, and alternative splicing/polyadenylation (Zhang et al., 2020), or by non-coding RNAs (Mattick and Makunin, 2006).

In order to analyse TC expression more closely, RNAseq reads were mapped to the transgenic genome, using IGV (Robinson et al., 2011). In Fig. 34B, for the uninjected reads, this showed that *mCherry* is expressed, as expected, but there is also a small amount of TC expression. This may be due to possibly an internal promoter, or *ubi* could be mis-spliced to cause this. Further, deeper sequencing would be required to answer this question. For the injected reads, (Fig. 34A), this showed that *mCherry* was also expressed, as 'loxing' *mCherry* out was not 100% efficient. Importantly, this also showed that TC transcription seemed to end prematurely, in exon 15, in the ankyrin repeat section of CAMTA1. Therefore, the NLS would not have been transcribed in these embryos, and this may lead to poor/no polyadenylation, thereby affecting detection by RNAseq. Notably, although low, there was still an increase in TC expression in *Cre* injected embryos.

Importantly, even though expression of TC was low, and an unusual distribution of reads mapped to the construct were observed, there was also an increase in EHE target genes from GSEA data (Subramanian et al., 2005, Mootha et al., 2003). This included the well-established target gene, *Cyr61* (Lai et al., 2011, Zhang et al., 2011, Seavey et al., 2021), which suggests that TC may have still entered the nucleus by an unknown method, or that full-length TC is still produced, despite the surprising RNAseq results. MASK1 (ANKHD1) has an NLS and has been shown to bind to YAP/TAZ to support nuclear transport (Sidor et al., 2019) (Manning et al., 2020). However, it is unknown if this is able to occur with YT/TC, as only a portion of Yap1/TAZ is present (Fig. 1A) (Tanas et al., 2016,

Antonescu et al., 2013). Also, MAML1 has been shown to increase nuclear localisation, and tumourigenesis, by binding YAP/TAZ WW domains (Kim et al., 2020). This could have an effect on TC, as the TAZ WW domain is present in the fusion protein (Tanas et al., 2016).
Interestingly, for YT, the YAP1 section does not appear to have a WW domain (Antonescu et al., 2013). In addition, the results are from using TC embryos at 5dpf. It is possible that full-length TC is produced at 1dpf, for example. Therefore, further characterisation of the TC construct may be warranted.

Premature ending of transcription could be due to the fact that the coding sequence for TC is very large at 5628bp (4857bp without neon), with only one intron in 5' UTR (at 2.6 - 4.6kB, with TC neon polyA ending at 11.8kb). The average exon length for zebrafish is 219bp (Suetsugu et al., 2013), which shows TC was unnaturally long. Gene length is known to control levels of transcription: longer genes tend to be expressed at a lower level than shorter genes (Castillo-Davis et al., 2002, Urrutia and Hurst, 2003, Chiaromonte et al., 2003) (Brown, 2021). Low expression could also be due to the fact that the RNA was polyA-enriched prior to cDNA being produced for RNAseq, which means that non-poly adenylated transcripts were selected against. RNA secondary structure could also be a factor (Kozak, 2005), although the fact that there appeared to be expression issues with both usual and codon optimised versions of TC make this somewhat less likely.

It has been found that translational efficiency and mRNA stability are affected by 5' and 3' untranslated regions (UTR)s, which are vital to these processes (van der Velden and Thomas, 1999, Bashirullah et al., 2001). In the TC/YT constructs, a 5' *ubi* UTR and a 3' sv40pA UTR was used. 3' UTRs of α-globin, β-globin, and albumin have been thoroughly examined, as these proteins have a lengthy half-life, and generate high levels of protein (Volloch and Housman, 1981, Ross and Sullivan, 1985). Therefore, β-globin 3' UTR could be inserted into the TC/YT constructs to improve translation efficiency/mRNA stability (Zarghampoor et al., 2019). The 5' UTR provides pre-initiation translation complex binding sites and secondary structures (Sonenberg and Hinnebusch, 2009). It is thought that altering the 5' UTR has the most effect on translation efficiency (Asrani et al., 2018). Hence, the 5' UTR of β-globin could be inserted into the TC/YT constructs for improved efficiency.

The kozak sequence is also known to be involved in translation efficiency (Zarghampoor et al., 2019). The optimal vertebrate kozak sequence is GCCRCCAUGG (R is A/G), with R and the final G having the most impact on translation (Kozak, 1986, Babendure et al., 2006) (Zarghampoor et al., 2019). The first TC construct used had a different kozak: GCAACAAUGG, which represented a good kozak, but

not fully optimal. It was thought that this may have been a reason why GFP was not visible when Cre mRNA was injected into the TC lines. However, this kozak was optimised in the next set of constructs, in order to exclude the fact that this was causing poor expression, and GFP was still not seen in the YT/DA TAZ, and TC Ex15 lines. As the YT, DA TAZ, and new TC (Ex15) constructs all had an optimal kozak sequence: GCCACCAUGG, this should have led to optimal translational efficiency.

Despite difficulty in detection of TC expression, it was possible that it's functional effects could be seen in expression of target genes that are known from mammalian studies. Therefore, data from RNAseq was used in Gene set enrichment analysis (GSEA) (Broad Institute - (Subramanian et al., 2005, Mootha et al., 2003). The results showed that there were 3 genes which came up in the top 15 hits, when my data was compared to both EHE (Seavey et al., 2021) and YAP1 (Cordenonsi et al., 2011). These were *Cyr61 (CCN1), serpine1, and tgfβ2*. However, only *Cyr61* was significant (*Cyr61* was the top hit for both gene sets) (Fig. 35). This is a well-known YAP/TAZ target, associated with the ECM (Lai et al., 2011, Zhang et al., 2011, Kireeva et al., 1997). Although there has been an inability to detect high levels of TC from RNAseq data, nevertheless, the expected target genes were still expressed. Therefore, low levels of TC expression could have a large impact on transcription. However, it is also possible that after deletion of the *mCherry* STOP cassette, TC is induced but is in some way able to downregulate its own expression, leading to low TC expression by 5dpf, despite the protein still being active and functional.

## 11.3 Analysis of adult ubi: lox nls-mCherry lox TAZ-CAMTA1 t2a neon zebrafish

Fish were raised and kept under observation for potential tumour growth. Notably, the survival rate for the AD25 x AF22 line, without CDKN2a/b injection, was 37% vs 80% for control, at 1yr 10 months. This was also a line which produced 2 tumours, which were CAMTA1 Ab stained. This showed that there was CAMTA1 staining in the blood cells (Fig. 44A), and not the nuclei, where CAMTA1 is expected to be seen. Also, DAPI appeared to show background staining (Fig. 44B), compared to the control, which showed nuclear DAPI staining (Fig. 44E) (nuclear DAPI is expected). It is possible the CAMTA1 Ab and DAPI are staining, for example, porphyrin in the blood cells. Therefore, the CAMTA1 Ab staining suggested that these tumours were not of TC origin. The same line was used again, but with CDKN2a/b CRISPR injected. This showed that there were no tumours up to 10 months of age, when the experiment ended. It would have been informative if these fish could have been grown to the same age, in order to see whether the low survival rate was reproducible. All the other lines had 59-98% survival rates. The University of Manchester reported that their average zebrafish

survival rate was 65% in 2017 (Mortell et al., 2017). Therefore, 59% is close to the average survival rate.

The other tumour was seen with the AA6/7 x AA8 line, which was also co-injected with CDKN2a/b, CRISPR 2 and 6. This had a gill tumour (Fig. 41), which was H&E stained, and clearly showed tumour morphology (Fig. 42A). This fish was stained with CAMTA1 antibody to test whether the tumour arose from TC. The results showed that no CAMTA1 staining was apparent (Fig. 43A), suggesting that the tumour may have been sporadic and not originated from TC. Also, the frequency of tumours was very low and occurred in adult fish, which reduces the benefits of using a zebrafish model, especially in the light of the development of mouse models.

## 11.4 Further zebrafish EHE models

Three further models were also created based on the previous results: Yap1-Tfe3, DA TAZ, and TAZ-CAMTA1 Ex15. Firstly, as TC expression levels were seen to be low from RNAseq data, and YT mRNA appeared to be highly active in embryos, it was decided to produce a YT zebrafish model, using the same *ubi* cre-lox model as TC. 10% of EHE cases are due to YT translocation (Antonescu et al., 2013). Also, YT is much shorter than TC, as described previously, which may allow for greater expression. In addition, it was decided to use a dominant active (DA) TAZ construct alongside, as a positive control. Finally, a further alternative was to create an improved version of the TC zebrafish model. It was decided that this may be best done via adding introns either side of CAMTA1, exon 15, as the RNAseq data previously showed a drop in expression at this point (Chapter 7). In addition to promoting expression of the gene by 'breaking-up' the large exon, introns may disrupt potential secondary structures in the sequence, in that region. An extra ATG in the 5' UTR was removed (for TC and YT), to prevent the ribosome competing with this and the start ATG, and flanking introns were added to CAMTA1, exon 15.

All lines were successfully created. As a test for functionality, *Cre* mRNA was injected to discover if the *lox* sites were able to recombine in the new lines. This efficiently reduced *mCherry* expression, as with TC, indicating recombination had taken place. However, no GFP could be visualised once again in all lines tested. Therefore, primers for a PCR recombination test were designed. The PCRs showed that recombination did indeed take place for YT, DA TAZ, and TC Ex15.

In order to further quantify and compare the effect of TC, YT, and DA TAZ on the vasculature, where the effect of these transgenes was most likely to occur, *ubi: lox nls-mCherry TC/YT/DA TAZ t2a neon* lines were crossed with *fli1:cre EGFP* fish (unfortunately, TC Ex15 lines were not available at this point, therefore the original TC was used for this experiment). The embryos were sorted, then the tail vasculature was imaged and scored at 1dpf, using the *Cre-EGFP* as an endothelial reporter, as previously described. This showed that there was a significant difference between active TC and sibling control, and between active YT and sibling control (Fig. 51). However, surprisingly, there was no significant difference between length/number of ISVs for active DA TAZ and sibling control (this was designed as a positive control). It appeared TC and YT had a stronger effect on vasculature/ISV growth at 1dpf. Therefore, it is possible that CAMTA1 could elevate levels of transcription of genes associated with blood vessel/ISV growth.

## 11.5 RNAseq on Yap1-Tfe3 embryos

As it was unclear which was the preferable time point to use for RNAseq, due to the fact that over time gene expression may have been down-regulated, it was thought beneficial to use *Cyr61* as a read-out for YT/TC/DA TAZ activity, at a set of distinct time points. In the RNAseq analysis performed in Chapter 7, *Cyr61* was a top hit and is a known target gene for both EHE and YAP/TAZ signalling (Cordenonsi et al., 2011, Seavey et al., 2021, Zhang et al., 2011, Lai et al., 2011). TC, YT and DA TAZ crosses (crossed to WT) were injected with *Cre* mRNA, and mock injected (phenol red) fish were used as a control, at several different time points. The Taqman$^{TM}$ qPCR data showed that the largest fold change was for both TC and YT *Cre* injected fish at 1dpf, at 2.6 fold change, whereas DA TAZ with *Cre* injection had 2.3 fold change at 1dpf (Fig. 53). Activated TC/YT were >= 1.5 fold change for all days tested, however DA TAZ decreased over time, and dipped below control levels at 0.75, at 5dpf. Therefore, the fusion genes generally appeared more active than dominant active TAZ, especially at 5dpf (Fig. 53). As *Cyr61* expression appeared to trend downwards over time, 1dpf was chosen for further RNAseq analysis on the YT line.

Notably, later, when the TC Ex15 lines were available, the same experiment was performed as above, using TC and TC Ex15 at 1dpf and 5dpf. This showed that there was not a high difference in fold change for *Cyr61* between TC and TC Ex15 at both time points (Fig. 54). Therefore, overall, TC Ex15 did not appear to improve *Cyr61* expression much. It is possible that more introns were needed, etc. This could be further investigated by performing RNAseq on TC Ex15 embryos, as with TC and

YT.

To generate RNA samples for RNAseq, *ubi:lox nls-mCherry lox Yap-Tfe3 t2a neon* carrier (line 3A) was paired with WT. Approximately 50% of the embryos were injected with *Cre* mRNA to remove the STOP cassette and induce YT expression at 1dpf. Differential expression (DE) analysis was performed and showed the total number of DE genes (156); the number of upregulated genes (114), and the number of downregulated genes (42), when comparing injected to uninjected samples (Fig. 56).

Detailed read-mapping from RNAseq showed that for uninjected fish, there was a 5.8-fold FPKM 'drop-off,' moving from *mCherry* to YT. This showed that there was indeed a 'drop-off' in coverage after the STOP sequence, as expected, but this was far from TC, which was a 579-fold FPKM 'drop-off.' This showed that the STOP sequence may not have been efficient at preventing read-through into the YT coding sequence. *mCherry* showed a 66.1x FPKM decrease for *Cre* injected embryos, compared to control expression. In comparison, YT showed a 2.4x FPKM decrease in expression for *Cre* injected embryos, compared to control (Fig. 58). Although, notably, there was still much expression of YT, even when the STOP cassette was present (15.748 FPKM). As YT levels are expected to increase upon *Cre* injection, as the *mCherry* STOP cassette is 'loxed out,' this is highly surprising. Thus, the following model could be proposed: in uninjected embryos, the *mCherry* sequence could be efficiently transcribed by the *ubi* promoter, and many of the mRNAs could not terminate at the expected *mCherry* polyA sequence, but rather extend into the YT sequence (read-through), which would then be part of the 3'UTR. Hence, the 2.4 fold FPKM drop would be the result of comparing expression of "YT-as-UTR" (uninjected) to "YT-as-coding sequence" (injected) (Fig. 62). When *mCherry* is removed, YT is under the *ubi* promoter and the YT sequence itself could be somehow less conducive to transcription. Although YT expression decreased (2.4x) upon *Cre* activation, there was still a reasonable level at 6.546 FPKM, as opposed to TC, which increased to only 0.085 FPKM (3.4x increase). Therefore, I would have expected to have seen some upregulation of YAP1 target genes, as with TC, but this was not seen from the GSEA (Subramanian et al., 2005) data. This may have been due to a too low threshold to trigger YAP1 target gene expression, or the time point (1dpf) may have been too early for an increase in these target genes (TC RNAseq was at 5dpf). Overall, it was concluded from the RNAseq data that the transcriptional termination site of *mCherry* may not be functioning correctly, and this warranted a detailed examination of the precise sequence.

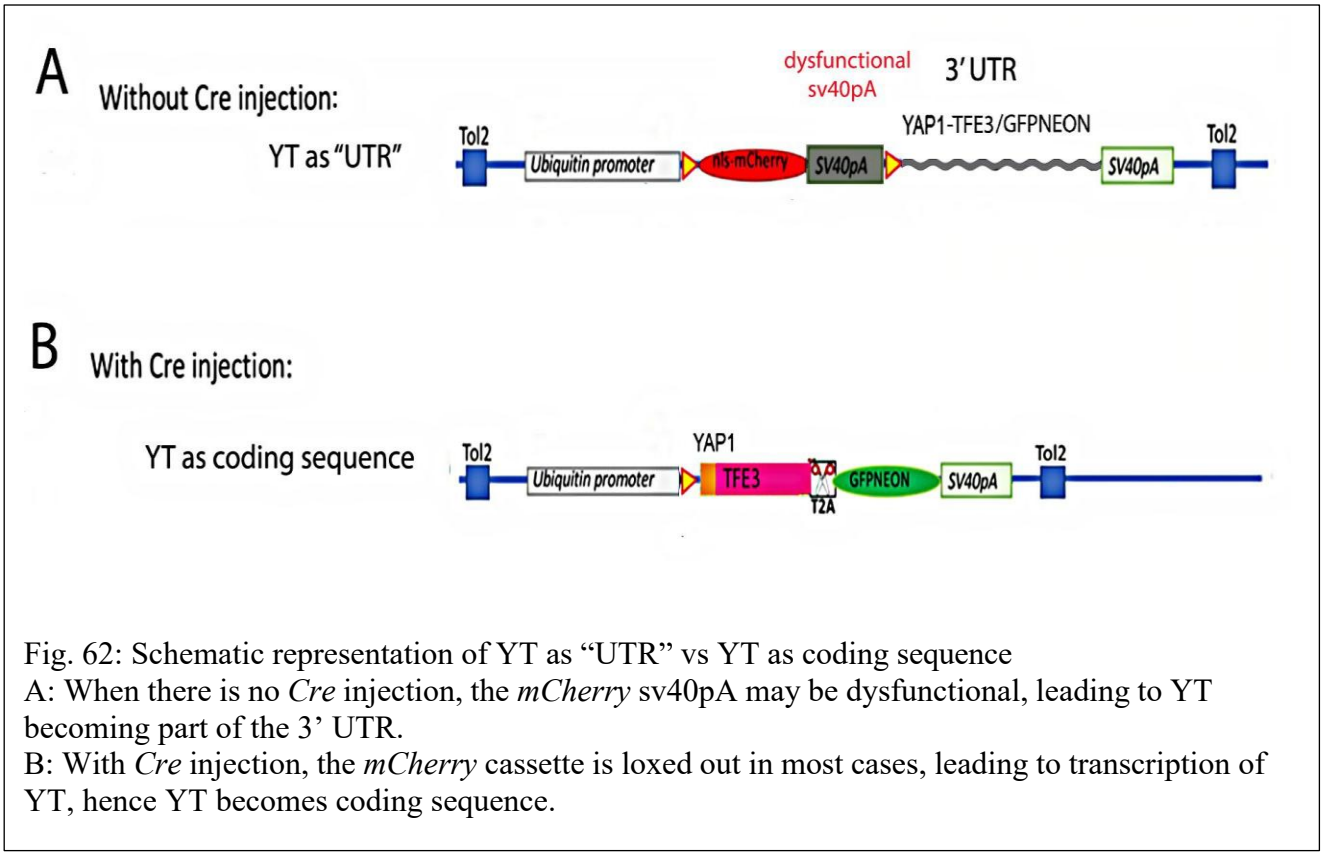


Fig. 62: Schematic representation of YT as "UTR" vs YT as coding sequence
A: When there is no *Cre* injection, the *mCherry* sv40pA may be dysfunctional, leading to YT becoming part of the 3' UTR.
B: With *Cre* injection, the *mCherry* cassette is loxed out in most cases, leading to transcription of YT, hence YT becomes coding sequence.

In addition to the well-known AAUAAA, both an upstream U-rich sequence, and a downstream GU- rich sequence has been shown to improve efficiency of 3'end processing/generation (Gil and Proudfoot, 1984, McLauchlan et al., 1985, Gil and Proudfoot, 1987, Carswell and Alwine, 1989, DeZazzo et al., 1991, Valsamakis et al., 1991, Moreira et al., 1995, Brackenridge and Proudfoot, 2000, Venkataraman et al., 2005, Danckwardt et al., 2007, Proudfoot, 2011). Also, an additional factor which has been shown to affect processing efficiency is the specific 3' cleavage site nucleotide sequence (Chen et al., 1995) (Proudfoot, 2011). It is thought that the polyadenylation site (PAS) is situated 10- 30 nucleotides prior to the cleavage site (Tian and Graber, 2012). In addition, noncanonical sequences have been shown to be less efficiently identified, and therefore this may also affect 3' processing (Boreikaite and Passmore, 2023).

Cleavage and polyadenylation occur via the Cleavage and polyadenylation factor (CPSF) binding to the PAS (Sheets et al., 1990), and the Cleavage stimulation factor (Cstf) binds the GU/U-rich DSE (Beyer et al., 1997, Takagaki and Manley, 1997). It was previously predicted that there are 3 optimal downstream element (DSE) motifs which aid 3'-end processing (motifs predicted using Gibbs

Recursive Sampler (Thompson et al., 2003) /MEME (Bailey and Elkan, 1994)/Improbizer (Ao et al., 2004) programs) (Salisbury et al., 2006). For both TC and YT, there was a H. sapiens UUUUUU 2nd DSE present, and a D. rerio CAAAAT (CAAACA is optimal) 3rd DSE present (Salisbury et al., 2006). Although there are GU sequences present post-sv40pA, there does not appear to be a predicted GU-rich sequence for either species present (1st DSE - most common are CUGUGG or CUGUGU for H. sapiens or D. rerio, respectively) (Salisbury et al., 2006). It is possible that if optimal DSE sequences were present (especially 1st DSE), that the TC/YT RNA would be transcribed and hence expressed appropriately, as these sequences are predicted to aid in 3'-end processing (Salisbury et al., 2006).

The IGV (Robinson et al., 2011) data also showed that for the injected reads (Fig., 59A), *mCherry* was loxed out when *Cre* injection occurred, and YT was fully expressed, unlike for TC, where transcription ended prematurely. However, in Fig. 59B, for the uninjected reads, this showed that *mCherry* was expressed, as expected, but there was also YT expression. This was likely to be due to read-through the *mCherry* STOP sequence, as mentioned previously. As YT transcription ended as expected, with full transcription taking place (Fig.59A), it may be expected that a proportion of the transgenic fish would get the disease. However, due to time limits, these fish were only able to be grown to 6-9 months in any case, with 2 potential tumours seen up to date, out of 19 fish in the 'activated' group (survival rate of 58% in YT 'activated' fish vs 88% survival rate in control fish). Also, in the RNAseq experiment, only a single 'snap-shot' of the transcriptome was produced: 5dpf and 1dpf were used for TC and YT, respectively. Therefore, it is possible that there is another preferable time point which could be used. This would need further investigation, possibly by performing further qPCR on other target genes, or RNAseq could be performed for YT at 5dpf, for a direct comparison to be made. The GSEA data for YT showed that there were 3 genes which came up in the top 15 hits, when my data was compared to both EHE (Seavey et al., 2021) and YAP1 (Cordenonsi et al., 2011). These were *Cyr61 (CCN1), serpine1, and tgfβ*, as with TC. However, none of these were significant. The only gene which was significant was *hexb* (from comparison to the YAP1 data set (Cordenonsi et al., 2011)). *Hexb* has recently been discovered to control glycolysis in glioblastoma through YAP1 activation. *Hexb* stabilizes tumour-integrin β1 (*ITGB1)/*integrin-linked kinase *(ILK)* complex, which causes YAP1/Hif1α to be activated. *Hif1α* then supports further *hexb* transcription and various genes that control glycolysis (Zhu et al., 2024).

## 11.6 Other zebrafish cancer models and future work

There have been many cancers modelled in zebrafish, such as melanoma, peripheral nerve sheath

tumour (PNST), angiosarcoma, germ cell tumour, rhabdomyosarcoma (RMS), thyroid cancer, pancreatic cancer, hepatocellular cancer (HCC), intestinal tumour, testicular tumour, T-cell acute lymphoid leukaemia (T-ALL), acute lymphoid leukaemia (ALL), chronic myeloid leukaemia (CML), and myelodysplastic syndrome (MDS) (Hason and Bartunek, 2019). One of the first transgenic zebrafish cancer models was *zRag2: EGFP cMyc*, which drove the over-expression of human c-myc in T-cells (Langenau et al., 2003). This resulted in the onset of T-cell acute lymphoblastic leukaemia (Langenau et al., 2003). However, this model was modified by using the *Cre-lox* system, as the zebrafish died at approximately 3 months in the original system (Langenau et al., 2005).

There are a number of transgenic zebrafish cancer models using fusion genes, such as AML-ETO (hsp70 promoter), NUP98-HOXA9 (spi1promoter/lox system), MYST3-NCOA2 (spi1 promoter), RUNX1-CBF2T1 (cmv promoter) (all cause acute myeloid leukaemia – AML) (Yeh et al., 2008, Forrester et al., 2011, Zhuravleva et al., 2008, Kalev-Zylinska et al., 2002), TEL-AML1 (xef promoter, causes acute lymphoid leukaemia - ALL) (Sabaawy et al., 2006), BCR-ABL1 (hsp70 promoter, causes chronic myeloid leukaemia - CML) (Xu et al., 2020), PAX3-FOX01 (β-actin, cmv, ubi promoters, causes Rhabdomyosarcoma) (Kendall et al., 2018), and EWS-FLI1 (hsp70, β-actin, causes Ewing's sarcoma) (Leacock et al., 2012) (McConnell at el., 2021). This shows that the heat-shock promoter (hsp70) has been quite widely used in the production of transgenic zebrafish models. The heat-shock promoter (hsp70) is used for temporal control of expression in zebrafish (Krone et al., 1997, Santacruz et al., 1997), and is a promoter which could be used if further models of EHE were to be produced. However, this would need to be used in conjunction with another system to ensure tissue specificity. A cre-lox system could be used in this instance, but the sv40pA would need to be improved. Additionally, Tetracycline-induced transcriptional activation (Tet-on/off) can also be used for reversible temporal control of gene expression (Gossen et al., 1995) once a well-functioning model is established (as was used in the other EHE mouse model (Driskill et al., 2021)). Although *ubi* has been shown to result in ubiquitous high expression when used in conjunction with the Tol2 system in zebrafish, both in embryos and adults (Mosimann and Zon, 2011), my results and other experiments from the F. van Eeden lab., at the Bateson Centre, Sheffield, suggest that *ubi* may not properly drive gene expression in some cases. Other promoters I could have tried are murine fetal liver kinase (*flk1*), c-type lectin domain family 14A (*Clec14A*), and *Cdh5* (cadherin 5, VE-cadherin), which all drive expression in/on endothelial cells (Ronicke et al., 1996, Mura et al., 2012, Carmeliet et al., 1999). However, there is a risk that this may lead to downregulation of the endothelial promoters via negative feedback from the transgene (Neil et al., 2023).

Another possibility would be to use Bacterial artificial chromosome (BAC) recombineering, which could be used to place the TC gene under the endogenous *taz* promoter, as is the case in human patients (Tanas et al., 2011, Errani et al., 2011). Messerle *et al*. were the first group to describe how BACs could be used to express a (herpes) virus genome in a murine model (Messerle et al., 1997). BAC vectors are similar to the fertility factor (F-factor) plasmid in *E. coli*, which is a circular, supercoiled plasmid, and can hold DNA fragments of up to 300kb (O'Connor et al., 1989, Shizuya et al., 1992, Monaco and Larin, 1994) (Hall et al., 2012). BACs containing the desired gene can be grown in specialised *E.coli*, and are integrated by bacteriophage-mediated homologous recombination (Suster et al., 2011). These can then be purified and injected, along with Tol2 transposase, for integration into the zebrafish genome (Suster et al., 2011).

CRISPR knock-in could also be used into an endothelial gene eg. using Geneweld. This is where homology-mediated end joining (HMEJ) repair is used at a target site, for integration of DNA, via short homology arms. This can be done using up to 48kb deletion/replacement, with a donor comprising homology arms, either side of two CRISPR/Cas9 sites (Wierson et al., 2020).

In addition to changing the UTR, chromatin insulators could be used to prevent read-through at the *mCherry* STOP sequence position. These are sequences which are involved in chromatin assembly and transcriptional control (Le Gall et al., 2015). They are <1kb in length (Savitsky et al., 2016) and have been shown to obstruct enhancer effect on promoters (Geyer and Corces, 1992, Kellum and Schedl, 1991), and/or block heterochromatin progression, which would lead to silencing (Sun and Elgin, 1999). These occur via chromatin loops and/or nucleosome alterations (West et al., 2002, Gaszner and Felsenfeld, 2006). Another possibility would have been to use endogenous TAZ as a promoter, similarly to a genetically engineered mouse model (Seavey et al., 2021). Although the mouse model used a FLEx system to replace endogenous TAZ with TC when activated via *Cre*, and used embryonic stem cells (ESCs), which are not available for zebrafish (Seavey et al., 2021). However, I produced a *TAZ: lox-nls- mCherry lox TAZ-CAMTA1 t2a neon* construct, but *mCherry* expression was not visible upon construct injection. Therefore, this line was not produced, as it would have been difficult to use with no visible fluorescent marker. This construct had a 2kb (2069bp) promoter, but the precise promoter/enhancer elements driving TAZ expression are unknown, and it is highly likely that this sequence could have been incomplete. Therefore, BAC recombineering may be a preferable option, as it would allow the inclusion of a large amount of surrounding sequence, as BACs are able to hold inserts of >300kb (Shizuya et al., 1992).

DA TAZ and TC Ex15 could have been use for RNAseq to discover what was happening at a molecular level, but in the end, the aim of the project was to create a zebrafish model of EHE, and DA TAZ was a side project. There had also been observed a higher level of lethality in one batch of TC Ex15, therefore, it was decided to wait for YT RNAseq results before doing any further RNAseq, and a further batch of TC Ex15 were raised to see if this level of lethality was reproducible. This showed that there were no high levels of lethality in the second batch. Therefore, the first set appeared to be an anomalous result, but only 2 batches were grown to 3-6 months, with no visible tumours up to date, and a detailed analysis was unable to be performed due to time constraints.

As the mouse models have been produced, and do emulate EHE disease well, it is possible that an adult zebrafish model may not be as useful. An advantage of a zebrafish model was in studying embryos, where detailed examination of endothelial cells is possible. In the experiment where *ubi:lox nls-mCherry lox TC/YT/DA TAZ t2a neon x fli1:cre EGFP* embryos were sorted and length/number of ISVs were scored (Fig. 51), there were significant differences between activated and control embryos. Nevertheless, it was a still a weak phenotype, and did not provide much information on the functional effects of YT and TC. If strong embryonic phenotypes had occurred in the larvae, these could have been helpful to understand the function of TC. Therefore, a more promising avenue may be in using zebrafish as a xenograft model, as an EHE-21 cell line is now available (unpublished, Pasquali lab.). Patient-derived xenograft models can be used as a tool to examine metastasis and for screening therapeutic drugs (Suhail et al., 2019). Zebrafish also do not have a mature adaptive immune system until 3 weeks post-fertilization, making them an ideal candidate for this (Willett et al., 1999). Zebrafish xenograft models have previously been used to study cancers such as leukaemia, lymphoma, melanoma, neuroblastoma, sarcoma, germ cell, liver, lung, ovary, breast, colon, pancreas, GI tract and prostate (Haldi et al., 2006, Marques et al., 2009, Weiss et al., 2009, Zhao et al., 2009, Corkery et al., 2011, Chapman et al., 2014, Lin et al., 2019, Ghotra et al., 2012, Vaughan et al., 2015, Latifi et al., 2011, Wong et al., 2019, Smith et al., 2013, Gaudenzi et al., 2017, He et al., 2012) (Chen et al., 2021).

Recent research has produced GEMMs of EHE, which will improve our knowledge and understanding of this rare sarcoma. However, there is still room for a more cost-effective model for high-throughput drug screening. There are many questions which are still unanswered, eg. What specifically causes the gene translocations to occur? Is it possible to block the gene fusion proteins? How do two different gene fusions cause the same disease?

## 11.7 Conclusion

The work in this thesis shows that TAZ-CAMTA1 and Yap1-Tfe3 zebrafish models were created. Although both were shown to cause recombination upon *Cre* activation, which indicated that the transgenes would be expressed, in the TC model, transcription ended early, causing a truncated transcript and omitting the NLS, at 5dpf. It was shown that CAMTA1 was the problematic piece regarding transcription, specifically exon 15. Although TC expression was low, it still increased upon activation via *Cre* injection. Four tumours were seen in the TC model: the one which was tested appeared to be negative for CAMTA1 stain, and therefore was not likely to be EHE. A top hit from TC RNaseq, when the data for activated TC were compared to the EHE (Seavey et al., 2021) and YAP1 (Cordenonsi et al., 2011) data sets, using GSEA (Subramanian et al., 2005, Mootha et al., 2003), was *Cyr61. Cyr61* is a well-known Yap1/TAZ target (Zhang et al., 2011, Lai et al., 2011). RNAseq on YT transgenics showed that full expression of YT did occur at 1dpf, although there appeared to still be YT expression in uninjected embryos. This may have been due to read-through the *mCherry* polyA sequence, and the YT sequence could then be seen as part of the 3'UTR.

When this project began, there were no EHE models, hence a robust zebrafish model would have provided the opportunity for high-throughput drug screens, thus potentially offering drug treatments to patients. This would offer hope for patients, as they often live for years aware of the dormant disease, not knowing when it will become aggressive, with no standard treatments available (Sardaro et al., 2014). Creating a zebrafish model would have been extremely beneficial to the EHE community, as although a GEMM has now been created, zebrafish are cost-efficient, transparent as embryos (to examine blood vessel development), and a great tool for high-throughput drug screening.

Although EHE is rare (Sardaro et al., 2014), it is driven by constitutively activated YAP/TAZ signalling. This is a vital pathway, involved in many cancers (Zanconato et al., 2016b), hence any breakthroughs with EHE may also have had significant implications for other cancers. Although expression of the transgenes has shown to be surprisingly difficult in zebrafish, the use of zebrafish xenotransplants may be the way forward to create a preclinical model to test potential disease-modifying drugs, for treatment of EHE.

# 12 Appendix

TAZ-CAMTA1 codon z ClaI SalI

AACCAATGCATTGGATGCATATCGATGGATCAGCAACAATGGACTATAAAGACGACGACGACAAGGGAGCT
GACTACAAGGATGATGATGACAAGAACCCTGCTTCTGCTCCTCCTCCTCTGCCTCCTCCTGGACAGCAGGTGA
TCCATGTGACCCAGGACCTGGACACTGACCTGGAGGCTCTGTTCAACTCTGTGATGAACCCAAAGCCTTCTTC
TTGGAGAAAGAAGATCCTGCCTGAGTCTTTCTTCAAGGAGCCTGACTCTGGATCTCACAGCAGACAGTCTTCT
ACTGACTCTTCTGGAGGACACCCTGGCCCAAGACTGGCTGGAGGCGCTCAGCATGTGCGCTCTCACTCTTCTC
CTGCTTCTCTCCAGCTGGGAACTGGAGCTGGAGCCGCTGGATCTCCTGCTCAGCAGCATGCTCATCTGAGACA
GCAATCTTATGATGTCACTGATGAGCTGCCTCTGCCTCCTGGATGGGAAATGACCTTTACCGCTACTGGACAG
AGATACTTTCTGAACCACATTGAGAAGATCACCACCTGGCAGGACCCAAGAAAGGCCATGAATCAGCCTCTG
AACCACATGAACCTCCACCCAGCTGTGTCTAGCACCCCTGTCCCTCAGAGAAGCATGGCTGTGTCTCAGCCA
AACCTGGGAGCTGGAGGATCTGTCCACCACAAGTGCAACTCTGCCAAACACAGAATTATCTCTCCAAAGGTG
GAGCCAAGAACTGGAGGATATGGATCTCACTCTGAGGTGCAACACAATGATGTGTCTGAGGGAAAGCATGA
GCACTCTCACAGCAAGGGATCTTCTCGCGAGAAGAGAAATGGAAAGGTGGCCAAGCCTGTCCTCCTCCACCA
GTCTTCTACTGAGGTGTCTAGCACCAACCAGGTGGAGGTGCCTGACACCACCCAGTCTTCTCCTGTGAGCATC
TCTTCTGGCCTGAACTCTGACCCTGACATGGTGGACTCTCCTGTGGTGACTGGAGTGTCTGGAATGGCTGTGG
CTTCTGTGATGGGATCTCTGTCTCAGTCTGCTACTGTGTTCATGTCTGAGGTGACCAACGAGGCTGTGTACAC
CATGTCTCCAACTGCTGGCCCAAACCACCATCTGCTGTCTCCTGATGCTAGCCAGGGACTCGTGCTGGCTGTG
TCTTCTGATGGACACAAGTTTGCTTTCCCTACTACTGGATCTTCTGAGTCTCTGAGCATGCTCCCAACCAATGT
GTCTGAGGAGCTCGTGCTGAGCACCACCCTGGATGGAGGAAGAAAGATCCCAGAGACCACCATGAACTTTG
ACCCTGACTGCTTTCTGAACAACCCAAAGCAGGGACAGACCTATGGAGGAGGAGGCCTGAAGGCTGAGATG
GTGTCTAGCAACATCAGACACTCTCCTCCTGGAGAGCGCTCTTTCTCTTTCACTACTGTGCTGACCAAGGAGA
TCAAGACTGAGGACACCTCTTTTGAGCAGCAGATGGCCAAGGAGGCTTACTCTTCTTCTGCTGCTGCTGTGGC
TGCTTCTTCTCTGACCCTGACCGCTGGATCTTCTCTGCTGCCTTCTGGAGGAGGACTGTCTCCTAGCACCACCC
TGGAGCAGATGGACTTCTCTGCCATTGACAGCAACAAGGACTACACCTCTTCTTTCTCTCAGACTGGACACTC
TCCTCACATCCACCAGACCCCTTCTCCTTCTTTCTTCCTCCAGGATGCTAGCAAGCCTCTGCCTGTGGAGCAG
AACACCCACTCTTCTCTGTCTGACTCTGGAGGAACCTTTGTGATGCCAACCGTGAAGACTGAGGCTTCTTCTC
AGACCTCTTCTTGCTCTGGACATGTGGAGACCAGAATTGAGAGCACCTCTTCTCTCCACCTGATGCAATTCCA
GGCCAACTTCCAGGCCATGACCGCTGAGGGAGAGGTGACTATGGAGACCTCTCAGGCCGCTGAGGGATCTG
AGGTGCTCCTGAAGTCTGGAGAACTCCAGGCTTGCTCTTCTGAACATTACCTGCAGCCAGAGACCAATGGAG
TGATCCGCAGCGCTGGAGGAGTGCCAATCCTGCCTGGAAATGTGGTGCAGGGACTGTACCCTGTGGCTCAGC
CTTCTCTGGGAAATGCTAGCAACATGGAGCTGTCTCTGGACCACTTTGACATCTCTTTCAGCAACCAATTCTC
TGACCTGATCAATGACTTTATCTCTGTGGAGGGAGGATCTAGCACCATCTATGGACATCAGCTGGTGTCTGGA
GACAGCACTGCTCTGTCTCAGTCTGAGGATGGAGCCCGCGCTCCTTTCACCCAGGCTGAGATGTGCCTGCCTT
GTTGCTCTCCTCAGCAGGGATCTCTCCAGCTGTCTTCTTCTGAGGGAGGAGCTAGCACTATGGCTTACATGCA
TGTGGCTGAGGTGGTGTCTGCTGCTTCTGCCCAGGGAACCCTGGGAATGCTCCAGCAGTCTGGAAGAGTGTT
CATGGTCACTGACTACTCTCCTGAGTGGTCTTACCCTGAGGGAGGAGTGAAGGTGCTGATTACCGGACCTTG
GCAGGAGGCTAGCAACAACTACTCTTGCCTGTTTGATCAAATCTCTGTGCCTGCTTCTCTGATTCAGCCTGGA
GTGCTGAGATGCTACTGCCCTGCTCATGATACTGGACTGGTGACCCTCCAGGTGGCTTTCAACAACCAGATCA
TCAGCAACTCTGTGGTGTTTGAGTACAAGGCCCGCGCTCTGCCAACCCTGCCTTCTTCTCAGCATGACTGGCT
GTCTCTGGATGACAACCAGTTCAGAATGAGCATCCTGGAGAGACTGGAGCAGATGGAGAGAAGAATGGCTG
AGATGACTGGATCTCAGCAACATAAGCAGGCTTCTGGAGGAGGATCTTCTGGAGGAGGATCTGGATCTGGAA
ATGGAGGATCTCAGGCTCAGTGTGCTTCTGGAACTGGCGCTCTGGGCTCTTGTTTTGAGAGCAGAGTGGTGGT
GGTGTGTGAGAAGATGATGAGCAGAGCTTGCTGGGCCAAGAGCAAGCACCTGATCCACAGCAAGACCTTCA
GAGGAATGACCCTCCTCCACCTGGCTGCTGCCCAGGGATATGCCACCCTGATCCAGACCCTGATCAAGTGGA
GAACCAAGCATGCTGACAGCATTGACCTGGAGCTGGAGGTGGACCCTCTCAATGTGGACCACTTCTCTTGCA
CCCCTCTGATGTGGGCTTGTGCTCTGGGACACCTGGAGGCTGCTGTCGTGCTGTACAAGTGGGACAGAAGAG
CCATCAGCATCCCTGACTCTCTGGGACGCCTGCCTCTGGGAATTGCCAGAAGCAGAGGACACGTGAAGCTGG
CTGAGTGCCTGGAGCACCTCCAAAGAGATGAGCAGGCTCAGCTGGGACAGAACCCAAGAATCCATTGCCCT
GCTTCTGAGGAGCCTAGCACTGAGTCTTGGATGGCTCAGTGGCACTCTGAGGCCATCTCTTCTCCAGAGATCC
CTAAGGGAGTGACCGTGATTGCTAGCACCAACCCTGAGCTCAGAAGACCACGCAGCGAGCCTAGCAACTACT
ACTCTTCTGAGTCTCACAAGGACTACCCTGCTCCTAAGAAACACAAGCTGAACCCTGAGTACTTCCAGACCA
GACAGGAGAAGCTGCTGCCAACTGCTCTGTCTCTGGAGGAGCCAAACATCAGAAAGCAGTCTCCTTCTAGCA
AGCAGTCTGTGCCAGAGACCCTGTCTCCTTCTGAGGGAGTGAGAGACTTCTCTAGAGAGCTGTCTCCTCCAAC
CCCAGAGACTGCTGCTTTCCAGGCTTCTGGATCTCAGCCTGTGGGAAAGTGGAACAGCAAGGACCTGTACAT

TGGAGTGTCTACTGTGCAGGTGACCGGAAACCCTAAAGGAACCTCTGTGGGAAAGGAGGCTGCTCCTTCTCA
GGTGAGACCAAGAGAGCCAATGTCTGTGCTGATGATGGCCAATAGAGAGGTGGTGAACACTGAGCTGGGAT
CTTACAGAGACAGCGCCGAGAACGAGGAGTGTGGACAGCCAATGGATGACATCCAGGTGAACATGATGACC
CTGGCTGAGCACATCATTGAGGCCACCCCTGACCGCATCAAGCAGGAGAACTTTGTCCCAATGGAGTCTTCT
GGACTGGAGCGCACTGACCCTGCCACCATCTCTAGCACCATGTCTTGGCTGGCTTCTTACCTGGCTGATGCTG
ATTGCCTGCCTTCTGCTGCTCAGATCCGCTCTGCTTACAATGAGCCTCTGACCCCTTCTAGCAACACCTCTCTG
TCTCCTGTGGGATCTCCTGTGAGCGAGATTGCTTTTGAGAAGCCAAACCTGCCTTCTGCCGCTGACTGGTCTG
AGTTCCTGTCTGCTAGCACCAGCGAGAAGGTGGAGAATGAGTTTGCTCAGCTGACCCTGTCTGACCATGAGC
AAAGAGAGCTGTATGAGGCTGCCAGACTGGTGCAGACTGCTTTCAGAAAGTACAAAGGAAGACCTCTGAGA
GAGCAGCAGGAGGTGGCTGCTGCTGTGATCCAGAGATGCTACAGAAAGTATAAGCAGTATGCTCTGTACAA
GAAGATGACCCAGGCTGCCATCCTGATCCAGAGCAAGTTCCGCTCTTACTATGAGCAGAAGAAGTTCCAGCA
GAGCAGAAGAGCTGCTGTGCTGATCCAGAAGTACTACCGCTCTTACAAGAAGTGTGGAAAGAGAAGACAGG
CCAGAAGAACTGCTGTGATTGTGCAGCAGAAGCTGCGCTCTTCTCTCCTGACCAAGAAGCAGGACCAGGCTG
CCAGAAAGATCATGCGCTTTCTGAGACGCTGCAGACACTCTCCTCTGGTGGACCACAGACTGTACAAGCGCT
CTGAGAGAATTGAGAAGGGACAGGGAACCTAAGTGGACGTCGACGTCGGCCATAGCGGCCGCGGAA

ClaI SalI IDT zebrafish opt. TAZ-CAMTA1

ATCGATGGATCCGCAACCATGGATTATAAGGACGACGATGATAAGGGCGCAGACTATAAAGATGATGACGA
CAAAAACCCAGCCTCCGCTCCCCCTCCACTTCCTCCGCCTGGGCAACAGGTCATACATGTGACTCAGGATTTG
GATACGGATTTGGAAGCTCTTTTTAACTCCGTAATGAACCCTAAACCCTCATCTTGGCGGAAAAAGATCCTTC
CTGAGTCATTCTTCAAAGAACCAGACTCTGGCTCCCACAGTCGCCAGAGCTCTACCGACAGTTCCGGCGGAC
ACCCGGGCCCTCGGCTGGCTGGTGGTGCTCAACACGTTAGGTCTCACTCATCCCCTGCGAGTTTGCAGTTGGG
GACAGGGGCCGGAGCGGCGGGTAGTCCCGCTCAACAACATGCACACCTCCGACAGCAGAGCTACGACGTAA
CAGATGAACTCCCTCTTCCTCCTGGTTGGGAGATGACATTTACCGCAACAGGACAGAGATACTTTTTGAATCA
TATCGAAAAGATAACGACGTGGCAAGACCCAAGAAAGGCAATGAACCAGCCGTTGAACCATATGAACCTTC
ACCCAGCTGTATCATCTACTCCTGTGCCGCAGAGGAGCATGGCCGTATCACAGCCGAACCTCGGCGCAGGTG
GGAGTGTTCACCACAAATGTAACAGTGCGAAACATCGTATAATCTCCCCAAAGGTGGAGCCTAGAACCGGTG
GTTATGGCTCTCATAGTGAGGTGCAACATAATGATGTATCTGAGGGCAAACACGAGCACAGCCATTCTAAAG
GATCCTCAAGGGAGAAACGTAATGGTAAGGTAGCTAAGCCTGTGCTGTTGCATCAAAGCAGTACCGAAGTG
AGTAGTACTAATCAAGTCGAGGTACCAGATACAACTCAGAGTAGTCCTGTAAGCATCTCATCCGGATTGAAT
AGCGACCCTGACATGGTCGATTCACCGGTTGTCACCGGGGTTAGTGGAATGGCGGTTGCAAGTGTTATGGGG
AGCTTGAGCCAATCTGCGACTGTATTTATGAGTGAAGTGACAAATGAGGCGGTTTATACCATGTCCCCTACC
GCTGGACCTAATCACCACCTTCTCAGTCCTGACGCTTCTCAAGGCTTGGTGCTCGCCGTGTCATCTGACGGCC
ACAAGTTTGCCTTTCCCACCACTGGTTCATCAGAGTCACTGTCCATGCTGCCAACTAATGTGTCAGAAGAGCT
GGTACTCAGCACGACATTGGATGGAGGGCGCAAAATACCAGAAACCACGATGAACTTTGACCCTGACTGTTT
TTTGAATAACCCCAAGCAGGGCCAAACTTACGGGGGCGGCGGTCTTAAAGCAGAGATGGTTTCAAGTAATAT
ACGCCACTCCCCACCAGGGGAGCGTTCTTTCAGCTTCACTACCGTACTCACAAAGGAGATTAAAACGGAGGA
TACGTCATTTGAACAGCAGATGGCTAAGGAAGCTTATAGTAGCAGCGCGGCGGCCGTGGCCGCATCTTCTCT
CACCCTCACTGCTGGTTCCAGCCTCCTTCCCTCTGGTGGAGGCCTCAGTCCGAGTACCACACTGGAACAAATG
GACTTCTCCGCCATAGACTCTAATAAGGACTATACGTCAAGCTTCTCCCAGACTGGCCACTCACCACATATTC
ACCAGACCCCCAGTCCATCTTTCTTTCTTCAGGACGCTTCAAAGCCCCTCCCCGTCGAGCAAAACACACATTC
ATCACTTTCCGATTCTGGAGGGACTTTTGTCATGCCCACTGTTAAAACGGAGGCTAGCAGCCAAACTAGTAG
CTGCAGTGGACACGTTGAAACTCGGATAGAGTCTACGTCATCACTCCATCTGATGCAGTTCCAAGCGAATTTT
CAGGCTATGACCGCTGAAGGTGAGGTTACCATGGAGACGAGTCAGGCGGCGGAGGGGTCCGAGGTGCTCCT
CAAATCCGGGGAGCTCCAGGCATGCAGCTCTGAACATTACCTGCAACCTGAGACAAACGGCGTAATACGTTC
TGCAGGAGGTGTTCCGATTCTTCCTGGGAACGTTGTTCAAGGTCTTTACCCCGTAGCCCAACCTTCCCTTGGT
AACGCGAGCAACATGGAACTTTCATTGGATCATTTCGATATCAGCTTTTCAAACCAATTCTCCGACCTCATAA
ACGATTTTATATCCGTAGAGGGAGGCAGCTCTACAATCTACGGGCATCAGTTGGTTAGCGGAGATTCTACTG
CGCTTAGCCAAAGTGAGGATGGAGCCAGGGCGCCATTCACGCAGGCGGAGATGTGCTTGCCGTGCTGTTCCC
CACAACAAGGTTCCCTCCAATTGTCCAGCAGTGAAGGGGGCGCTAGTACAATGGCGTATATGCATGTAGCAG
AAGTTGTTTCAGCAGCCTCAGCGCAGGGTACCCTGGGTATGCTTCAACAAAGCGGGCGGGTATTCATGGTGA
CCGATTATAGTCCTGAGTGGAGTTATCCTGAAGGTGGTGTGAAGGTACTCATCACTGGCCCTTGGCAGGAAG
CCAGTAACAACTATAGTTGCCTCTTTGATCAGATATCAGTACCGGCGTCTCTCATCCAACCAGGAGTCCTTCG
GTGCTATTGCCCGGCACATGACACCGGGCTTGTCACATTGCAGGTAGCCTTTAACAATCAAATCATCTCAAAC
TCAGTAGTTTTTGAATACAAGGCACGAGCCCTTCCAACACTTCCGTCAAGTCAACATGACTGGTTGTCCCTCG
ACGACAATCAATTCCGAATGTCAATACTTGAGCGACTCGAACAAATGGAGCGAAGGATGGCAGAAATGACG
GGATCTCAACAACACAAGCAAGCGTCCGGCGGCGGTTCCTCTGGAGGAGGTAGTGGCTCCGGTAACGGCGG
AAGTCAGGCGCAATGTGCTTCAGGTACAGGGGCGCTGGGGAGCTGTTTCGAAAGCCGCGTGGTCGTGGTATG
TGAAAAGATGATGAGCCGTGCCTGTTGGGCGAAAAGTAAGCACCTCATCCATTCAAAAACTTTTAGAGGCAT

GACCCTGTTGCATTTGGCCGCAGCACAGGGGTACGCCACTCTGATTCAGACTCTTATCAAGTGGCGCACGAA
ACATGCTGACTCAATTGACCTTGAATTGGAAGTGGACCCGTTGAACGTTGACCACTTCTCATGTACACCCCTC
ATGTGGGCGTGCGCACTCGGCCATCTGGAGGCTGCAGTAGTACTGTACAAGTGGGACCGTCGGGCCATTAGT
ATTCCCGATAGCCTGGGCCGTCTCCCCCTGGGTATTGCCCGTAGTCGTGGTCACGTGAAACTTGCAGAATGTC
TGGAGCACCTTCAAAGAGATGAACAAGCGCAACTGGGCCAGAATCCCCGAATACACTGCCCAGCATCAGAA
GAGCCGAGCACGGAGAGCTGGATGGCGCAATGGCATAGCGAAGCAATTTCCAGTCCGGAGATCCCGAAGGG
AGTGACCGTAATCGCAAGTACTAACCCCGAACTCAGAAGACCCCGTTCCGAACCGAGCAACTACTACTCAAG
TGAGTCACACAAAGATTACCCCGCACCAAAAAAACATAAGCTGAACCCGGAGTACTTTCAGACCCGTCAGG
AAAAGCTCCTTCCAACGGCGTTGAGTTTGGAAGAACCGAATATCCGAAAACAGTCACCCTCTAGCAAACAGT
CAGTACCTGAGACGCTCAGCCCCTCCGAGGGCGTCAGGGACTTCTCACGCGAGCTTAGTCCACCTACACCAG
AGACTGCCGCCTTTCAAGCTTCAGGTAGCCAGCCCGTAGGGAAATGGAATTCTAAGGATCTGTATATTGGAG
TAAGCACAGTGCAAGTTACGGGCAATCCGAAGGGCACGTCAGTAGGTAAGGAAGCAGCTCCATCACAAGTT
AGGCCGAGGGAACCGATGAGCGTCCTGATGATGGCAAATCGGGAAGTAGTGAATACGGAGCTTGGTTCATA
TCGTGATTCAGCCGAGAACGAAGAGTGTGGCCAGCCGATGGATGATATCCAAGTTAACATGATGACCTTGGC
TGAACATATAATAGAAGCGACGCCCGACCGCATTAAGCAAGAAAACTTTGTCCCAATGGAGAGTTCTGGCCT
GGAACGTACCGACCCAGCTACTATCAGTTCCACTATGTCTTGGCTCGCCTCCTACCTTGCGGATGCAGATTGT
CTCCCAAGCGCGGCTCAGATCCGTTCTGCGTACAACGAACCGCTGACGCCGTCTAGCAACACAAGCCTCTCA
CCTGTAGGGTCCCCCGTTTCAGAGATAGCTTTTGAGAAACCGAACCTTCCTAGTGCGGCAGATTGGAGTGAA
TTCCTTTCTGCCTCCACCAGTGAGAAAGTTGAAAACGAGTTTGCTCAACTGACGCTCTCTGACCATGAGCAAA
GAGAACTGTACGAGGCGGCGCGGTTGGTCCAGACGGCCTTCCGAAAATACAAGGGCCGCCCTTTGAGAGAG
CAACAGGAAGTGGCGGCAGCCGTCATTCAGAGGTGTTACCGAAAGTACAAACAATACGCTTTGTACAAAAA
AATGACTCAGGCAGCAATATTGATCCAGTCAAAATTTAGGTCATATTACGAACAAAAGAAATTCCAACAGTC
CAGGAGGGCAGCTGTTCTGATTCAGAAATATTATAGATCCTATAAAAAATGTGGCAAACGTAGGCAGGCAA
GAAGAACAGCTGTCATCGTTCAACAGAAACTTCGTTCTAGCTTGCTCACCAAGAAGCAGGATCAAGCGGCGA
GGAAAATCATGCGGTTCCTTAGGCGGTGTCGTCATTCCCCTCTGGTGGACCACCGTCTTTATAAGCGTTCAGA
ACGGATTGAGAAAGGGCAGGGCACATGAGTCGAC

AccI PvuI PME TAZ-CAMTA1 codon z (to remove STOP)

GTCTACTGTGCAGGTGACCGGAAACCCTAAAGGAACCTCTGTGGGAAAGGAGGCTGCTCCTTCTCAGGTGAG
ACCAAGAGAGCCAATGTCTGTGCTGATGATGGCCAATAGAGAGGTGGTGAACACTGAGCTGGGATCTTACA
GAGACAGCGCCGAGAACGAGGAGTGTGGACAGCCAATGGATGACATCCAGGTGAACATGATGACCCTGGCT
GAGCACATCATTGAGGCCACCCCTGACCGCATCAAGCAGGAGAACTTTGTCCCAATGGAGTCTTCTGGACTG
GAGCGCACTGACCCTGCCACCATCTCTAGCACCATGTCTTGGCTGGCTTCTTACCTGGCTGATGCTGATTGCC
TGCCTTCTGCTGCTCAGATCCGCTCTGCTTACAATGAGCCTCTGACCCCTTCTAGCAACACCTCTCTGTCTCCT
GTGGGATCTCCTGTGAGCGAGATTGCTTTTGAGAAGCCAAACCTGCCTTCTGCCGCTGACTGGTCTGAGTTCC
TGTCTGCTAGCACCAGCGAGAAGGTGGAGAATGAGTTTGCTCAGCTGACCCTGTCTGACCATGAGCAAAGAG
AGCTGTATGAGGCTGCCAGACTGGTGCAGACTGCTTTCAGAAAGTACAAAGGAAGACCTCTGAGAGAGCAG
CAGGAGGTGGCTGCTGCTGTGATCCAGAGATGCTACAGAAAGTATAAGCAGTATGCTCTGTACAAGAAGATG
ACCCAGGCTGCCATCCTGATCCAGAGCAAGTTCCGCTCTTACTATGAGCAGAAGAAGTTCCAGCAGAGCAGA
AGAGCTGCTGTGCTGATCCAGAAGTACTACCGCTCTTACAAGAAGTGTGGAAAGAGAAGACAGGCCAGAAG
AACTGCTGTGATTGTGCAGCAGAAGCTGCGCTCTTCTCTCCTGACCAAGAAGCAGGACCAGGCTGCCAGAAA
GATCATGCGCTTTCTGAGACGCTGCAGACACTCTCCTCTGGTGGACCACAGACTGTACAAGCGCTCTGAGAG
AATTGAGAAGGGACAGGGAACCGCTTTCTTGTACAAAGTTGGCATTATAAGAAAGCATTGCTTATCAATTTG
TTGCAACGAACAGGTCACTATCAGTCAAAATAAAATCATTATTTGCCATCCAGCTGATATCCCCTATAGTGAG
TCGTATTACATGGTCATAGCTGTTTCCTGGCAGCTCTGGCCCGTGTCTCAAAATCTCTGATGTTACATTGCAC
AAGATAAAATAATATCATCATGAACAATAAAACTGTCTGCTTACATAAACAGTAATACAAGGGGTGTTATGA
GCCATATTCAACGGGAAACGTCGAGGCCGCGATTAAATTCCAACATGGATGCTGATTTATATGGGTATAAAT
GGGCTCGCGATAATGTCGGGCAATCAGGTGCGACAATCTATCGCTTGTATGGGAAGCCCGATGCGCCAGAGT
TGTTTCTGAAACATGGCAAAGGTAGCGTTGCCAATGATGTTACAGATGAGATGGTCAGACTAAACTGGCTGA
CGGAATTTATGCCTCTTCCGACCATCAAGCATTTTATCCGTACTCCTGATGATGCATGGTTACTCACCACTGC
GATCCCCGGAAAAACAGCATTCCAGGTATTAGAAGAATATCCTGATTCAGGTGAAAATATTGTTGATGCGCT
GGCAGTGTTCCTGCGCCGGTTGCATTCGATTCCTGTTTGTAATTGTCCTTTTAACAGCGATCG

Zbfish WWTR1-human CAMTA1 ClaI SalI

ATCGATGGAGCCGCTCAGACTGAGAGAGAGAGAGAGAGAGAGAGAGAGAGAGAGGCTTGAGTTTACAAAC
TTTCAGAAACTCCGCGATCGGACGCAGGAGGAACAAAAAACTCTCCAAACTCCACGCGGGACAACATGACA
AACGCCTTTCTAGCTTTATGACAACTTTTCGACGACTTACAAACACTTTTCAACTCGGCTGAAACTACTTAAG
GACGAAAAACAGGAAAAGTTCCTACAGGAATTTTTTTTTCCATCGGCCATTTTAATCGAAGTTTGTTTTGACC

ATGAGCGGTAATCCTCTCCAGCCGATACCGGGCCACCAGGTGATCCATGTCGCCAAAGACCTGGACACGGAT
CTGGAGGCTCTTTTTAACTCGGTCATGAACCCGAAACCGAGCTCCTGGAGGAACAAGGATATGCCGCAGTCT
TTCTTCCAGGAGCCGGACTCGGGCTCCCACTCCCGGCAGTCCAGCGCGGACTCCGGTTCTCTCCCGCCGAGG
GTCCACTTTCGCTCGCGCTCATCTCCGGCGTCCCTACAGCTGCCGGCGGGCTCCGTGAGCGGCCCGAGCCCCG
GGAGACTCCACTCCCACACCCGGCACCAGTCCTGCGATGTGGCCGAGGAGCTGCCGCTGCCCCCTGGGTGGG
AGATGGCCTTCACCCCCAACGGCCAGAAGTACTTTCTCAATCACATTGAGAAGATCACCACATGGCACGACC
CCAGGAAGAGCATGACGCCCTCGGTGGCCCAGCTGAGCCTCCATAATCAGGTCTCCAACACCGCCAGCATCC
AGCAGCGCTCCATGGCCCTCTCTCAGCCCAACCTGATGGTGGACAGCCCGGTGGTCACAGGTGTGTCCGGTA
TGGCGGTGGCCTCTGTGATGGGGAGCTTGTCCCAGAGCGCCACGGTGTTCATGTCAGAGGTCACCAATGAGG
CCGTGTACACCATGTCCCCCACCGCTGGCCCCAACCACCACCTCCTCTCACCTGACGCCTCTCAGGGCCTCGT
CCTGGCCGTGAGCTCTGATGGCCACAAGTTCGCCTTTCCCACCACGGGCAGCTCAGAGAGCCTGTCCATGCT
GCCCACCAACGTGTCCGAAGAGCTGGTCCTCTCCACCACCCTCGACGGTGGCCGGAAGATTCCAGAAACCAC
CATGAACTTTGACCCCGACTGTTTCCTTAATAACCCAAAGCAGGGCCAGACGTACGGGGGTGGAGGCCTGAA
AGCCGAGATGGTCAGCTCCAACATCCGGCACTCGCCACCCGGGGAGCGGAGCTTCAGCTTTACCACCGTCCT
CACCAAGGAGATCAAGACCGAGGACACCTCCTTCGAGCAGCAGATGGCCAAAGAAGCGTACTCCTCCTCCG
CGGCGGCTGTGGCAGCCAGCTCCCTCACCCTGACCGCCGGCTCCAGCCTCCTGCCGTCGGGCGGCGGCCTGA
GTCCCAGCACCACCCTGGAGCAGATGGACTTCAGCGCCATCGACTCCAACAAGGACTACACGTCCAGCTTCA
GCCAGACGGGCCACAGCCCCCACATCCACCAGACCCCCTCCCCGAGCTTCTTCCTGCAGGACGCCAGCAAAC
CCCTCCCCGTCGAGCAGAACACCCACAGCAGCCTGAGTGACTCTGGGGGCACCTTCGTGATGCCCACGGTGA
AAACGGAGGCCTCGTCCCAAACCAGCTCCTGCAGCGGTCACGTGGAGACGCGGATCGAGTCCACTTCCTCCC
TCCACCTCATGCAGTTCCAGGCCAACTTCCAGGCCATGACGGCAGAAGGGGAGGTCACCATGGAGACCTCGC
AGGCGGCGGAAGGGAGCGAGGTCCTGCTCAAGTCTGGGGAGCTGCAGGCTTGCAGCTCTGAGCACTACCTG
CAGCCGGAGACCAACGGGGTAATCCGAAGCGCCGGCGGCGTCCCCATCCTCCCGGGCAACGTGGTGCAGGG
ACTCTACCCCGTGGCCCAGCCCAGCCTCGGCAACGCCTCCAACATGGAGCTCAGCCTGGACCACTTTGACAT
CTCCTTCAGCAACCAGTTCTCCGACCTGATCAACGACTTCATCTCCGTGGAGGGGGGCAGCAGCACCATCTAT
GGGCACCAGCTGGTGTCGGGGGACAGCACGGCGCTCTCACAGTCAGAGGACGGGGCGCGGGCCCCCTTCAC
CCAGGCAGAGATGTGCCTCCCCTGCTGTAGCCCCCAGCAGGGTAGCCTGCAGCTGAGCAGCTCGGAGGGCGG
GGCCAGCACCATGGCCTACATGCACGTCGCCGAGGTGGTCTCGGCCGCCTCGGCCCAGGGCACCCTAGGCAT
GCTGCAGCAGAGCGGACGGGTGTTCATGGTGACCGACTACTCCCCAGAGTGGTCTTACCCAGAGGGAGGAGT
GAAGGTCCTCATCACAGGCCCGTGGCAAGAAGCCAGCAATAACTACAGCTGCCTGTTTGACCAGATCTCAGT
GCCTGCATCCCTGATTCAGCCTGGGGTGCTGCGCTGCTACTGCCCAGCCCATGACACTGGTCTTGTGACCCTA
CAAGTTGCCTTCAACAACCAGATCATCTCCAACTCGGTGGTGTTTGAGTACAAAGCCCGGGCTCTGCCCACG
CTCCCTTCCTCCCAGCACGACTGGCTGTCGTTGGACGATAACCAGTTCAGGATGTCCATCCTGGAACGACTGG
AGCAGATGGAGAGGAGGATGGCCGAGATGACGGGGTCCCAGCAGCACAAACAGGCGAGCGGAGGCGGCAG
CAGTGGAGGCGGCAGCGGGAGCGGGAATGGAGGGAGCCAGGCACAGTGTGCTTCTGGGACTGGGGCCTTGG
GGAGCTGCTTTGAGAGCCGTGTGGTCGTGGTATGCGAGAAGATGATGAGCCGAGCCTGCTGGGCGAAGTCCA
AGCACTTGATCCACTCAAAGACTTTCCGCGGAATGACCCTACTCCACCTGGCCGCTGCCCAGGGCTATGCCA
CCCTAATCCAGACCCTCATCAAATGGCGTACAAAGCACGCGGATAGCATTGACCTGGAACTGGAAGTTGACC
CCTTGAATGTGGACCACTTCTCCTGTACTCCTCTGATGTGGGCGTGTGCCCTAGGGCACTTGGAAGCTGCCGT
CGTGCTGTACAAGTGGGACCGTCGGGCCATCTCGATTCCCGACTCTCTAGGAAGGCTGCCTTTGGGAATTGCC
AGGTCACGGGGTCATGTGAAATTAGCAGAGTGTCTGGAGCACCTGCAGAGAGATGAGCAGGCTCAGCTGGG
ACAGAACCCCAGAATCCACTGTCCTGCAAGCGAAGAGCCCAGCACAGAGAGCTGGATGGCCCAGTGGCACA
GCGAAGCCATCAGCTCTCCAGAAATACCCAAGGGAGTCACTGTTATTGCAAGCACCAACCCAGAGCTGAGA
AGACCTCGTTCTGAACCCTCTAATTACTACAGCAGTGAGAGCCACAAAGATTATCCGGCTCCCAAAAAGCAT
AAATTGAACCCTGAGTACTTCCAGACAAGGCAGGAGAAGCTGCTTCCCACTGCACTGAGTCTGGAAGAGCCA
AATATCAGGAAGCAAAGCCCTAGTTCTAAGCAGTCTGTCCCCGAGACACTCAGCCCCAGTGAAGGAGTGAG
GGACTTCAGCCGGGAACTCTCCCCTCCCACTCCAGAGACTGCAGCATTTCAAGCCTCTGGATCTCAGCCTGTA
GGAAAGTGGAATTCCAAAGATCTTTACATTGGTGTGTCTACAGTACAGGTGACTGGAAATCCGAAGGGGACC
AGTGTAGGAAAGGAGGCAGCACCTTCACAGGTGCGTCCACGGGAACCAATGAGTGTCCTGATGATGGCTAA
CAGAGAGGTGGTGAATACAGAGCTGGGGTCCTACCGTGATAGTGCAGAAAATGAAGAATGCGGCCAGCCCA
TGGATGACATACAGGTGAACATGATGACCTTGGCAGAACACATTATTGAAGCCACACCTGACCGAATCAAGC
AGGAGAATTTTGTGCCCATGGAGTCCTCAGGATTGGAAAGAACAGACCCTGCCACCATTAGCAGTACAATGA
GCTGGCTGGCCAGTTATCTAGCGGATGCTGACTGCCTTCCCAGTGCTGCCCAGATCCGAAGTGCATATAACG
AGCCTCTAACCCCTTCTTCTAATACCAGCTTGAGCCCTGTTGGCTCTCCCGTCAGTGAAATCGCTTTCGAGAA
ACCTAACCTTCCCTCCGCCGCGGATTGGTCAGAATTCCTGAGTGCATCTACCAGTGAGAAGGTAGAGAATGA
GTTTGCTCAGCTCACTCTGTCTGATCATGAACAGAGAGAACTCTATGAGGCTGCCAGGCTTGTCCAGACAGCT
TTCCGGAAATACAAGGGCCGACCCTTGCGGGAACAGCAAGAAGTAGCTGCTGCTGTTATTCAGCGTTGTTAC
AGAAAATATAAACAGTACGCACTTTATAAAAAGATGACACAGGCTGCCATCCTTATCCAGAGCAAATTCCGA
AGTTACTATGAACAAAAAAAATTCCAGCAGAGCCGACGGGCTGCTGTGCTCATCCAAAAGTACTACCGAAGT
TATAAGAAATGTGGCAAAAGACGGCAGGCTCGCCGGACGGCTGTGATTGTACAACAGAAACTCAGGAGCAG

TTTGCTAACCAAAAAGCAGGATCAAGCTGCTCGAAAAATAATGAGGTTTCTTCGCCGCTGTCGCCACAGCCC
CCTGGTGGACCATAGGCTGTACAAAAGGAGTGAAAGAATTGAAAAAGGCCAAGGAACTTGAGTCGAC

EGFP STOP CAMTA1 SalI EcoRI

GTCGACAATGAGAAGGGTGTCTCAATCTATGGGTATTTCCTGTTCCACACAATCTGGTTTCCTGTCAGGTTTC
CTTTTCCTCCTGAAACAAAAGACAGGAATGCCCTCTGTATAAAATAGCACAGCGCTTTTAATGGGTCTCTGTA
CATCCCGACCTCATGACGCATCTTCTGCGGGACAGCCAATCACGATCAAGTTGGCTTATGAAAACAGTTTTTT
GTCCCCCTGTTAAGTTAAAAGCACGGTAGCATACATGCATTATTCATCATGCAGCATATTCAGCAGTACAAA
AGATGAGCTCTTGACACACCTCAGCGTAAAATCTCTATTCCAGCGTAATCCTGCGGTTCTGGATGGTTAAGCG
AGCCTTGCAAACACGGCCAATTTATAGCCATGTTGAAAATAGCAGCTTTGTGAGCATTTCGACCTCAATGTAC
CAAGAATGCGTGCTCGGTAACTGAAAAAGAGGGGGTGGAGATTTTGGATTTAGAGATGGAATCACATGCAC
GCTGTATATGCTATATAAAAATAGCAGGCATTTAATGCATGCAAAATATGTTTCGACACTAAACACTACAAG
TCGGAAATATATCTATTTTTCTTTTTTTAACGAAATGAGACATTTAATGCGCAGTAAATGTAGTCTAACACGC
ACAATATTCCTATTATTGTCCATGAAAAATGTGAGGTCTATGCTACTGATTTAAAGAAAATGTTGAACAGGC
ACAGCACACAAGAGGTATCAGCCTCTCTATATGGTCCATACAGCACCAGGCTCGCTGCGTTCATGTGCATTC
AGAGGCGCGCACACGTGTGGAGCAGACAGACTCGACGCAGCGGGCTTTGCTTTTTATTCATGGAAGCCCATT
TTAGAAGAAGCTCGGGCAGACTCGTCACATTCTTCACTTCACCATAGGTAGATCAAATCAAAGTTATTGGAT
ATAACGGAACAATATTCATCATATTATGAGATTATTATTAGACCGAGTGCATTAGACATATTTGTATTCGATC
GTTGAAAAAGTATATATTTTATTTTAGCCTTAAACTATGGTTAGCCTATATTAATCAGCATAATCTGTTATTTC
AGACGTTGTATTAATGATTATTTCTAGCACAGCTTTGATGCATCAATGCAATGTTTCTACAAACCCGCCTTGT
TTAATGTCGGAAAAAAAGCGCAACAAATGTAAAGAGTTGGCAGGCATTCTGTAAATATTTCCAGGCAAAAA
CATGCACAAAGGAAAGAAACACCATTGTTTTGGTGTCTTATCTTCGCTGGACAAATATCCTGCTTTGGGTGCC
GTAATGAAGGCAGGGCCAGTGACACACACACATACACACACACACATACACGCATACACGGCTTCCTTCTCA
AGCGCAGTGACTTCACTTCCCAAATTTAGAGGAAAAAAAACCATCCGGCGAAACTGTCTCTGTCTCTCCGCC
ACATATCGGGGGCTGGAATTAATTCAGACGCGCAAGTTTGTACAAAAAAGCAGGCTGGACCATGGTGAGCA
AGGGCGAGGAGCTGTTCACCGGGGTGGTGCCCATCCTGGTCGAGCTGGACGGCGACGTAAACGGCCACAAG
TTCAGCGTGTCCGGCGAGGGCGAGGGCGATGCCACCTACGGCAAGCTGACCCTGAAGTTCATCTGCACCACC
GGCAAGCTGCCCGTGCCCTGGCCCACCCTCGTGACCACCCTGACCTACGGCGTGCAGTGCTTCAGCCGCTAC
CCCGACCACATGAAGCAGCACGACTTCTTCAAGTCCGCCATGCCCGAAGGCTACGTCCAGGAGCGCACCATC
TTCTTCAAGGACGACGGCAACTACAAGACCCGCGCCGAGGTGAAGTTCGAGGGCGACACCCTGGTGAACCG
CATCGAGCTGAAGGGCATCGACTTCAAGGAGGACGGCAACATCCTGGGGCACAAGCTGGAGTACAACTACA
ACAGCCACAACGTCTATATCATGGCCGACAAGCAGAAGAACGGCATCAAGGTGAACTTCAAGATCCGCCAC
AACATCGAGGACGGCAGCGTGCAGCTCGCCGACCACTACCAGCAGAACACCCCCATCGGCGACGGCCCCGT
GCTGCTGCCCGACAACCACTACCTGAGCACCCAGTCCGCCCTGAGCAAAGACCCCAACGAGAAGCGCGATC
ACATGGTCCTGCTGGAGTTCGTGACCGCCGCCGGGATCACTCTCGGCATGGACGAGCTGTACAAGGGCGGTG
GAAGATGAATTC

HindIII MfeI nls-mCherry (zebrafish opt.)

AAGCTTATAACTTCGTATAGCATACATTATACGAAGTTATCCGGTCGCCACCATGGCTCCTAAGAAGAAGAG
AAAGGTGATGGTGAGCAAGGGAGAGGAGGACAACATGGCTATCATCAAGGAGTTCATGAGATTCAAGGTGC
ACATGGAGGGAAGCGTGAACGGACACGAGTTCGAGATCGAGGGAGAGGGAGAGGGAAGACCTTACGAGGG
AACACAGACAGCTAAGCTGAAGGTGACAAAGGGAGGACCTCTGCCTTTCGCTTGGGACATCCTGAGCCCTCA
GTTCATGTACGGAAGCAAGGCTTACGTGAAGCACCCTGCTGACATCCCTGACTACCTGAAGCTGAGCTTCCC
TGAGGGATTCAAGTGGGAGAGAGTGATGAACTTCGAGGACGGAGGAGTGGTGACAGTGACACAAGACAGCA
GCCTGCAAGACGGAGAGTTCATCTACAAGGTGAAGCTGAGAGGAACAAACTTCCCTAGCGACGGACCTGTG
ATGCAGAAGAAGACAATGGGATGGGAGGCTAGCAGCGAGAGAATGTACCCTGAGGACGGAGCTCTGAAGG
GAGAGATCAAGCAGAGACTGAAGCTGAAGGACGGAGGACACTACGACGCTGAGGTGAAGACAACATACAA
GGCTAAGAAGCCTGTGCAGCTGCCTGGAGCTTACAACGTGAACATCAAGCTGGACATCACAAGCCACAACG
AGGACTACACAATCGTGGAGCAGTACGAGAGAGCTGAGGGAAGACACAGCACCGGAGGAATGGACGAGCT
GTACAAGTGAAGCGGCCGCGACTCTAGATCATAATCAGCCATACCACATTTGTAGAGGTTTTACTTGCTTTAA
AAAACCTCCCACACCTCCCCGTGAACGTGAAACATAAAATGAATGCAATTG

StuI XhoI YAP1-TFE3 (with STOP)

AGGCCTGCAACAATGGATCCGAACCAGCACAACCCTCCAGCCGGCCACCAGATCGTCCATGTTCGGGGAGAC
TCCGAGACCGATCTGGAGGCTCTTTTTAACGCTGTGATGAACCCGAAAAACACCATCGTCCCCCCTTCCGTGC
CGATGAGGTTGAGAAAGCTGCCAGACTCATTCTTCACGCCGCCAGAGCCAAAGTCCCACTCCAGACAAGTTC

AGACTCACTTGGAAAATCCAACTAAGTACCACATCCAGCAGGCTCAGAGGCAGCAAGTCAAGCAATACCTGT
CTCACACCCTGGGCAATAAAATAGCCAGTCAGACACTGGCAACGTCGACCCCACCACAGCCCTCATCCGCCC
CTGAGCTGGCACCTGCCGCCAGTAGCACTCCTAGCAGCCCGCTTGCTGTGCTCAGCCTGGGGTCCAACAAAG
AAGAGATCGAAGACGTCATCGATGACATCATCAGCCTGGAGTCGAGTTTAAACGATGAATTTATGACGCTGA
TCGACTCGGGTTTGCAGCTTCCCAGCACGCTGCCAGTCTCAGGGAACCTCCTGGATGTGTACAGCAGTCAGG
GCATGGCGGCGCCCACCATCACCGTCAGCAACTCCTGCCCCGCAGACCTGCAGAATGTCAAGAGAGAAATG
AGCGATGCTGAGGCAAAAGCTATTATGAAGGAGAGGCAGAAGAAAGACAACCATAACCTGATTGAGAGAA
GAAGAAGGTTCAACATTAATGACCGCATTAAGGAACTTGGAGCTCTGATTCCAAAGTCCTCTGACCCGGAGT
TGCGCTGGAACAAGGGCACCATATTAAAGGCGTCAGTCGACTACATCCGCAAGCTGCAAAAGGAGCAGCAG
AGATCCAAAGAGATGGAGACCAGACAGAAGAAACTCGAACACGCAAACCGCAGTCTGATGCTGCGCATTCA
GGAACTGGAAATGCAAGCTCGGCTCCATGGCCTCTCGTCATCTCAGCTCTCAGACTCTCTGACCCAAACACA
GACTTTAACACTGGAGCACAACCCCAACACTGACCTCTCCAAAACCCTCCTGTCAATCACCCAGACCACACC
CTCTTCCTTCCTGTCTCCGCCCTCCTCCACCTCATCAGTTGGCGGGACGGTCACCAGTCCTTTAGAGCTTGGCA
CACTCAGTTTCGGAGAGTTGGACGACCACACGGCCTCCGTCTTCAGTCCAGCCCTGATGGCCGATATGGGCTT
AGGGGATATTCTGATGGATGACACCGGTGCTCTTTCACCCGTAGGAGGCGCTGATCCCCTCCTTTCCGCGGTT
TCTCCAGGAGCCTCAAAAACAAGCAGTCGTAGAAGTAGCTTCAGCATGGAGGAAGACTTGTGACTCGAG

<u>BstBI AatII YAP1-TFE3 (to remove extra ATG) (1st piece)</u>

TTCGAATTCAAGGCCTGCCACCATGGATCCGAACCAGCACAACCCTCCAGCCGGCCACCAGATCGTCCATGT
TCGGGGAGACTCCGAGACCGATCTGGAGGCTCTTTTTAACGCTGTGATGAACCCGAAAAACACCATCGTCCC
CCCTTCCGTGCCGATGAGGTTGAGAAAGCTGCCAGACTCATTCTTCACGCCGCCAGAGCCAAAGTCCCACTC
CAGACAAGTTCAGACTCACTTGGAAAATCCAACTAAGTACCACATCCAGCAGGCTCAGAGGCAGCAAGTCA
AGCAATACCTGTCTCACACCCTGGGCAATAAAATAGCCAGTCAGACACTGGCAACGTCGACCCCACCACAGC
CCTCATCCGCCCCTGAGCTGGCACCTGCCGCCAGTAGCACTCCTAGCAGCCCGCTTGCTGTGCTCAGCCTGGG
GTCCAACAAAGAAGAGATCGAAGACGTC

<u>AgeI PvuI YAP1-TFE3 (to remove STOP) (2nd piece)</u>

ACCGGTGCTCTTTCACCCGTAGGAGGCGCTGATCCCCTCCTTTCCGCGGTTTCTCCAGGAGCCTCAAAAACAA
GCAGTCGTAGAAGTAGCTTCAGCATGGAGGAAGACTTGAACCCAGCTTTCTTGTACAAAGTTGGCATTATAA
GAAAGCATTGCTTATCAATTTGTTGCAACGAACAGGTCACTATCAGTCAAAATAAAATCATTATTTGCCATCC
AGCTGATATCCCCTATAGTGAGTCGTATTACATGGTCATAGCTGTTTCCTGGCAGCTCTGGCCCGTGTCTCAA
AATCTCTGATGTTACATTGCACAAGATAAAATAATATCATCATGAACAATAAAACTGTCTGCTTACATAAAC
AGTAATACAAGGGGTGTTATGAGCCATATTCAACGGGAAACGTCGAGGCCGCGATTAAATTCCAACATGGAT
GCTGATTTATATGGGTATAAATGGGCTCGCGATAATGTCGGGCAATCAGGTGCGACAATCTATCGCTTGTAT
GGGAAGCCCGATGCGCCAGAGTTGTTTCTGAAACATGGCAAAGGTAGCGTTGCCAATGATGTTACAGATGAG
ATGGTCAGACTAAACTGGCTGACGGAATTTATGCCTCTTCCGACCATCAAGCATTTTATCCGTACTCCTGATG
ATGCATGGTTACTCACCACTGCGATCCCCGGAAAAACAGCATTCCAGGTATTAGAAGAATATCCTGATTCAG
GTGAAAATATTGTTGATGCGCTGGCAGTGTTCCTGCGCCGGTTGCATTCGATTCCTGTTTGTAATTGTCCTTTT
AACAGCGATCG

<u>pCS2+ YT S94A EcoRI PstI piece</u>

GAATTCAAGGCCTGCCACCATGGATCCGAACCAGCACAACCCTCCAGCCGGCCACCAGATCGTCCATGTTCG
GGGAGACTCCGAGACCGATCTGGAGGCTCTTTTTAACGCTGTGATGAACCCGAAAAACACCATCGTCCCCCC
TTCCGTGCCGATGAGGTTGAGAAAGCTGCCAGACGCCTTCTTCACGCCGCCAGAGCCAAAGTCCCACTCCAG
ACAAGTTCAGACTCACTTGGAAAATCCAACTAAGTACCACATCCAGCAGGCTCAGAGGCAGCAAGTCAAGC
AATACCTGTCTCACACCCTGGGCAATAAAATAGCCAGTCAGACACTGGCAACGTCGACCCCACCACAGCCCT
CATCCGCCCCTGAGCTGGCACCTGCCGCCAGTAGCACTCCTAGCAGCCCGCTTGCTGTGCTCAGCCTGGGGTC
CAACAAAGAAGAGATCGAAGACGTCATCGATGACATCATCAGCCTGGAGTCGAGTTTAAACGATGAATTTAT
GACGCTGATCGACTCGGGTTTGCAGCTTCCCAGCACGCTGCCAGTCTCAGGGAACCTCCTGGATGTGTACAG
CAGTCAGGGCATGGCGGCGCCCACCATCACCGTCAGCAACTCCTGCCCCGCAGACCTGCAG

<u>TAZ-CAMTA1 Exon 15 1st piece BamHI BanI</u>
GGATCCCATCGGATCAGCCACCATGGACTATAAAGACGACGACGACAAGGGAGCTGACTACAAGGATGATG
ATGACAAGAACCCTGCTTCTGCTCCTCCTCCTCTGCCTCCTCCTGGACAGCAGGTGATCCATGTGACCCAGGA
CCTGGACACTGACCTGGAGGCTCTGTTCAACTCTGTGATGAACCCAAAGCCTTCTTCTTGGAGAAAGAAGAT

CCTGCCTGAGTCTTTCTTCAAGGAGCCTGACTCTGGATCTCACAGCAGACAGTCTTCTACTGACTCTTCTGGA
GGACACCCTGGCCCAAGACTGGCTGGAGGCGCTCAGCATGTGCGCTCTCACTCTTCTCCTGCTTCTCTCCAGC
TGGGAACTGGAGCTGGAGCCGCTGGATCTCCTGCTCAGCAGCATGCTCATCTGAGACAGCAATCTTATGATG
TCACTGATGAGCTGCCTCTGCCTCCTGGATGGGAAATGACCTTTACCGCTACTGGACAGAGATACTTTCTGAA
CCACATTGAGAAGATCACCACCTGGCAGGACCCAAGAAAGGCCATGAATCAGCCTCTGAACCACATGAACC
TCCACCCAGCTGTGTCTAGCACCCCTGTCCCTCAGAGAAGCATGGCTGTGTCTCAGCCAAACCTGGGAGCTG
GAGGATCTGTCCACCACAAGTGCAACTCTGCCAAACACAGAATTATCTCTCCAAAGGTGGAGCCAAGAACTG
GAGGATATGGATCTCACTCTGAGGTGCAACACAATGATGTGTCTGAGGGAAAGCATGAGCACTCTCACAGCA
AGGGATCTTCTCGCGAGAAGAGAAATGGAAAGGTGGCCAAGCCTGTCCTCCTCCACCAGTCTTCTACTGAGG
TGTCTAGCACCAACCAGGTGGAGGTGCC

TC Ex15 Bsu36I AccI 2nd piece
CCTGAGGGAGGAGTGAAGGTGCTGATTACCGGACCTTGGCAGGAGGCTAGCAACAACTACTCTTGCCTGTTT
GATCAAATCTCTGTGCCTGCTTCTCTGATTCAGCCTGGAGTGCTGAGATGCTACTGCCCTGCTCATGATACTG
GACTGGTGACCCTCCAGGTGGCTTTCAACAACCAGATCATCAGCAACTCTGTGGTGTTTGAGTACAAGGCCC
GCGCTCTGCCAACCCTGCCTTCTTCTCAGCATGACTGGCTGTCTCTGGATGACAACCAGTTCAGAATGAGCAT
CCTGGAGAGACTGGAGCAGATGGAGAGAAGAATGGCTGAGATGACTGGATCTCAGCAACATAAGCAGGCTT
CTGGAGGAGGATCTTCTGGAGGAGGATCTGGATCTGGAAATGGAGGATCTCAGGCTCAGTGTGCTTCTGGAA
CTGGCGCTCTGGGCTCTTGTTTTGAGAGCAGAGTGGTGGTGGTGTGTGAGAAGATGATGAGCAGAGCTTGCT
GGGCCAAGAGCAAGCACCTGATCCACAGCAAGACCTTCAGAGGAATGACCCTCCTCCACCTGGCTGCTGCCC
AGGGATATGCCACCCTGATCCAGACCCTGATCAAGTGGCGTTTATAATATTCTGGTGTTTCCTTTTAACGGTG
GTGAATAGTGTGGTAATTTCTGGTGCTCTCCCTTATAGTACAAAGCACGCGGATAGCATTGACCTGGAACTG
GAAGTTGACCCCTTGAATGTGGACCACTTCTCCTGTACTCCTCTGGTAAGGAATGGATTCCTGTAGCCCCCCC
TTGCTGTTCTTCCAGTCTGGCATAGGATTTGCCTGGTTCCCACCGTTGTCTCTTGCTGACACATGGCATGTTTC
GGAGATACTTTGGGATGGGAATCTTCAATGGCCCCACCGAGATTGCCAGCAAGGACCAGTTTGTCAGTTGGC
AGCAATGGCAAAAGTCAGGTCTGGTCTTGACCTCTGATTGAGAACGCTTGCTGTGTCTCCCTGTCTTCTAGAT
GTGGGCGTGTGCCCTAGGGCACTTGGAAGCTGCCGTCGTGCTGTACAAGTGGGACCGTCGGGCCATCTCGAT
TCCCGACTCTCTAGGAAGGCTGCCTTTGGGAATTGCCAGGTCACGGGGTCATGTGAAATTAGCAGAGTGTCT
GGAGCACCTGCAGAGAGATGAGCAGGCTCAGCTGGGACAGAACCCCAGAATCCACTGTCCTGCAAGCGAAG
AGCCCAGCACAGAGAGCTGGATGGCCCAGTGGCACAGCGAAGCCATCAGCTCTCCAGAAATACCCAAGGGA
GTCACTGTTATTGCAAGCACCAACCCAGGTAAGAATTCAGAATCATGACATCTCAGAGCTTGACAGAGATCC
CGTTTGCTTTCATGCAGCTGCCCTCAGCAGAGTCCATAGGATAGTCACATACATTTCAGTTTTTTTGTTAATGT
TTCTGATTTTTCTTTAAGAATGCCTAGTGCTGCCCCCTCCCCCAGTACAGAAGAAAGTAGCAAAAATTCTATG
TTCATGCAAGAAATACATAATTTTGGAGGAGGAAGATCTGAATCTGGTGTATGCTACTGGGGATATTTAAAT
GTTAGGGACGTGTCTTGAGTTCCGGCTTTGCACTTTGTGTCTCTCAGGCATAGAGAAAGTGTTGATTCTTGAG
GATTCCTAGTTGTATCTCCTGTCCTGACTATCCTTTCTACTGTACTTTTCAGAGCTGAGAAGACCTCGTTCTGA
ACCCTCTAATTACTACAGCAGTGAGAGCCACAAAGATTATCCGGCTCCCAAAAAGCATAAATTGAACCCTGA
GTACTTCCAGACAAGGCAGGAGAAGCTGCTTCCCACTGCACTGAGTCTGGAAGAGCCAAACATCAGAAAGC
AGTCTCCTTCTAGCAAGCAGTCTGTGCCAGAGACCCTGTCTCCTTCTGAGGGAGTGAGAGACTTCTCTAGAGA
GCTGTCTCCTCCAACCCCAGAGACTGCTGCTTTCCAGGCTTCTGGATCTCAGCCTGTGGGAAAGTGGAACAGC
AAGGACCTGTACATTGGAGTGTCTAC

# References


https://usegalaxy.org/

https://tinyurl.com/yckdcr6x

https://chopchop.cbu.uib.no/

https://tinyurl.com/2tkverhf

https://tinyurl.com/5bfxt4kz

ABE, G., SUSTER, M. L. & KAWAKAMI, K. 2011. Tol2-mediated transgenesis, gene trapping, enhancer trapping, and the Gal4-UAS system. *Methods Cell Biol,* 104**,** 23-49.

AGULNIK, M., YARBER, J. L., OKUNO, S. H., VON MEHREN, M., JOVANOVIC, B. D., BROCKSTEIN, B. E., EVENS, A. M. & BENJAMIN, R. S. 2013. An open-label, multicenter, phase II study of bevacizumab for the treatment of angiosarcoma and epithelioid hemangioendotheliomas. *Ann Oncol,* 24**,** 257-63.

AKITAKE, C. M., MACURAK, M., HALPERN, M. E. & GOLL, M. G. 2011. Transgenerational analysis of transcriptional silencing in zebrafish. *Dev Biol,* 352**,** 191-201.

AKWII, R. G., SAJIB, M. S., ZAHRA, F. T. & MIKELIS, C. M. 2019. Role of Angiopoietin-2 in Vascular Physiology and Pathophysiology. *Cells,* 8.

ALARCON, C., ZAROMYTIDOU, A. I., XI, Q., GAO, S., YU, J., FUJISAWA, S., BARLAS, A., MILLER, A. N., MANOVA-TODOROVA, K., MACIAS, M. J., SAPKOTA, G., PAN, D. & MASSAGUE, J. 2009. Nuclear CDKs drive Smad transcriptional activation and turnover in BMP and TGF-beta pathways. *Cell,* 139**,** 757-69.

ALBIG, A. R., NEIL, J. R. & SCHIEMANN, W. P. 2006. Fibulins 3 and 5 antagonize tumor angiogenesis in vivo. *Cancer Res,* 66**,** 2621-9.

ALBIG, A. R. & SCHIEMANN, W. P. 2004. Fibulin-5 antagonizes vascular endothelial growth factor (VEGF) signaling and angiogenic sprouting by endothelial cells. *DNA Cell Biol,* 23**,** 367-79.

ALBIG, A. R. & SCHIEMANN, W. P. 2005. Fibulin-5 function during tumorigenesis. *Future Oncol,* 1**,** 23-35.

ALGRAIN, M., ARPIN, M. & LOUVARD, D. 1993. Wizardry at the cell cortex. *Curr Biol,* 3**,** 451-4.

ANDERSON, J. M., VAN ITALLIE, C. M. & FANNING, A. S. 2004. Setting up a selective barrier at the apical junction complex. *Curr Opin Cell Biol,* 16**,** 140-5.

ANDREASEN PA, KJOLLER L, CHRISTENSEN L, DUFFY MJ. The urokinase-type plasminogen activator system in cancer metastasis: a review. Int J Cancer. 1997 Jul 3;72(1):1-22.

ANTONESCU, C. R., LE LOARER, F., MOSQUERA, J. M., SBONER, A., ZHANG, L., CHEN, C. L., CHEN, H. W., PATHAN, N., KRAUSZ, T., DICKSON, B. C., WEINREB, I., RUBIN, M. A., HAMEED, M. & FLETCHER, C. D. 2013. Novel YAP1-TFE3 fusion defines a distinct subset of epithelioid hemangioendothelioma. *Genes Chromosomes Cancer,* 52**,** 775-84.

AO, W., GAUDET, J., KENT, W. J., MUTTUMU, S. & MANGO, S. E. 2004. Environmentally induced foregut remodeling by PHA-4/FoxA and DAF-12/NHR. *Science,* 305**,** 1743-6.

ARAGONA, M., PANCIERA, T., MANFRIN, A., GIULITTI, S., MICHIELIN, F., ELVASSORE, N., DUPONT, S. & PICCOLO, S. 2013. A mechanical checkpoint controls multicellular growth through YAP/TAZ regulation by actin-processing factors. *Cell,* 154**,** 1047-1059.

ARGOS, P., LANDY, A., ABREMSKI, K., EGAN, J. B., HAGGARD-LJUNGQUIST, E., HOESS, R. H., KAHN, M. L., KALIONIS, B., NARAYANA, S. V., PIERSON, L. S., 3RD & ET AL. 1986. The integrase family of site-specific recombinases: regional similarities and global diversity. *EMBO J,* 5**,** 433-40.

ARGRAVES, W. S., GREENE, L. M., COOLEY, M. A. & GALLAGHER, W. M. 2003. Fibulins: physiological and disease perspectives. *EMBO Rep,* 4**,** 1127-31.

ASAKAWA, K., SUSTER, M. L., MIZUSAWA, K., NAGAYOSHI, S., KOTANI, T., URASAKI, A., KISHIMOTO, Y., HIBI, M. & KAWAKAMI, K. 2008. Genetic dissection of neural circuits by Tol2 transposon-mediated Gal4 gene and enhancer trapping in zebrafish. *Proc Natl Acad Sci U S A,* 105**,** 1255-60.

ASRANI, K. H., FARELLI, J. D., STAHLEY, M. R., MILLER, R. L., CHENG, C. J., SUBRAMANIAN, R. R. & BROWN, J. M. 2018. Optimization of mRNA untranslated regions for improved expression of therapeutic mRNA. *RNA Biol,* 15**,** 756-762.

AZAD, T., JANSE VAN RENSBURG, H. J., LIGHTBODY, E. D., NEVEU, B., CHAMPAGNE, A., GHAFFARI, A., KAY, V. R., HAO, Y., SHEN, H., YEUNG, B., CROY, B. A., GUAN, K. L., POULIOT, F., ZHANG, J., NICOL, C. J. B. & YANG, X. 2018. A LATS biosensor screen identifies VEGFR as a regulator of the Hippo pathway in angiogenesis. *Nat Commun,* 9**,** 1061.

BABENDURE, J. R., BABENDURE, J. L., DING, J. H. & TSIEN, R. Y. 2006. Control of mammalian translation by mRNA structure near caps. *RNA,* 12**,** 851-61.

BAGAN, P., HASSAN, M., LE PIMPEC BARTHES, F., PEYRARD, S., SOUILAMAS, R., DANEL, C. & RIQUET, M. 2006. Prognostic factors and surgical indications of pulmonary epithelioid hemangioendothelioma: a review of the literature. *Ann Thorac Surg,* 82**,** 2010-3.

BAIA, G. S., CABALLERO, O. L., ORR, B. A., LAL, A., HO, J. S., COWDREY, C., TIHAN, T., MAWRIN, C. & RIGGINS, G. J. 2012. Yes-associated protein 1 is activated and functions as an oncogene in meningiomas. *Mol Cancer Res,* 10**,** 904-13.

BAILEY, T. L. & ELKAN, C. 1994. Fitting a mixture model by expectation maximization to discover motifs in biopolymers. *Proc Int Conf Intell Syst Mol Biol,* 2**,** 28-36.

BAR-SHAVIT, R., TURM, H., SALAH, Z., MAOZ, M., COHEN, I., WEISS, E., UZIELY, B. & GRISARU-GRANOVSKY, S. 2011. PAR1 plays a role in epithelial malignancies: transcriptional regulation and novel signaling pathway. *IUBMB Life,* 63**,** 397-402.

BARBASHINA, V., SALAZAR, P., HOLLAND, E. C., ROSENBLUM, M. K. & LADANYI, M. 2005. Allelic losses at 1p36 and 19q13 in gliomas: correlation with histologic classification, definition of a 150-kb minimal deleted region on 1p36, and evaluation of CAMTA1 as a candidate tumor suppressor gene. *Clin Cancer Res,* 11**,** 1119-28.

BARRY, E. R., MORIKAWA, T., BUTLER, B. L., SHRESTHA, K., DE LA ROSA, R., YAN, K. S., FUCHS, C. S., MAGNESS, S. T., SMITS, R., OGINO, S., KUO, C. J. & CAMARGO, F. D. 2013. Restriction of intestinal stem cell expansion and the regenerative response by YAP. *Nature,* 493**,** 106-10.

BARTUCCI, M., DATTILO, R., MORICONI, C., PAGLIUCA, A., MOTTOLESE, M., FEDERICI, G., BENEDETTO, A. D., TODARO, M., STASSI, G., SPERATI, F., AMABILE, M. I., PILOZZI, E., PATRIZII, M., BIFFONI, M., MAUGERI-SACCA, M., PICCOLO, S. & DE MARIA, R. 2015. TAZ is required for metastatic activity and chemoresistance of breast cancer stem cells. *Oncogene,* 34**,** 681-90.

BASHIRULLAH, A., COOPERSTOCK, R. L. & LIPSHITZ, H. D. 2001. Spatial and temporal control of RNA stability. *Proc Natl Acad Sci U S A,* 98**,** 7025-8.

BASU-ROY, U., BAYIN, N. S., RATTANAKORN, K., HAN, E., PLACANTONAKIS, D. G., MANSUKHANI, A. & BASILICO, C. 2015. Sox2 antagonizes the Hippo pathway to maintain stemness in cancer cells. *Nat Commun,* 6**,** 6411.

BATTILANA, G., ZANCONATO, F. & PICCOLO, S. 2021. Mechanisms of YAP/TAZ transcriptional control. *Cell Stress,* 5**,** 167-172.

BEYER, K., DANDEKAR, T. & KELLER, W. 1997. RNA ligands selected by cleavage stimulation factor contain distinct sequence motifs that function as downstream elements in 3'-end processing of pre-mRNA. *J Biol Chem,* 272**,** 26769-79.

BHAYA, D., DAVISON, M. & BARRANGOU, R. 2011. CRISPR-Cas systems in bacteria and archaea: versatile small RNAs for adaptive defense and regulation. *Annu Rev Genet,* 45**,** 273-97.

BHOWMICK, N. A., ZENT, R., GHIASSI, M., MCDONNELL, M. & MOSES, H. L. 2001. Integrin beta 1 signaling is necessary for transforming growth factor-beta activation of p38MAPK and epithelial plasticity. *J Biol Chem,* 276**,** 46707-13.

BOCKSTAELE, L., COULONVAL, K., KOOKEN, H., PATERNOT, S. & ROGER, P. P. 2006. Regulation of CDK4. *Cell Div,* 1**,** 25.

BOOPATHY, G. T. K. & HONG, W. 2019. Role of Hippo Pathway-YAP/TAZ Signaling in Angiogenesis. *Front Cell Dev Biol,* 7**,** 49.

BOREIKAITE, V. & PASSMORE, L. A. 2023. 3'-End Processing of Eukaryotic mRNA: Machinery, Regulation, and Impact on Gene Expression. *Annu Rev Biochem,* 92**,** 199-225.

BOWER, N. I., VOGRIN, A. J., LE GUEN, L., CHEN, H., STACKER, S. A., ACHEN, M. G. & HOGAN, B. M. 2017. Vegfd modulates both angiogenesis and lymphangiogenesis during zebrafish embryonic development. *Development,* 144**,** 507-518.

BRACKENRIDGE, S. & PROUDFOOT, N. J. 2000. Recruitment of a basal polyadenylation factor by the upstream sequence element of the human lamin B2 polyadenylation signal. *Mol Cell Biol,* 20**,** 2660-9.

BRATT, A., WILSON, W. J., TROYANOVSKY, B., AASE, K., KESSLER, R., VAN MEIR, E. G. & HOLMGREN, L. 2002. Angiomotin belongs to a novel protein family with conserved coiled-coil and PDZ binding domains. *Gene,* 298**,** 69-77.

BRINSTER, R. L., ALLEN, J. M., BEHRINGER, R. R., GELINAS, R. E. & PALMITER, R. D. 1988. Introns increase transcriptional efficiency in transgenic mice. *Proc Natl Acad Sci U S A,* 85**,** 836-40.

BROWN, J. C. 2021. Role of Gene Length in Control of Human Gene Expression: Chromosome-Specific and Tissue-Specific Effects. *Int J Genomics,* 2021**,** 8902428.

BURGER, A., LINDSAY, H., FELKER, A., HESS, C., ANDERS, C., CHIAVACCI, E., ZAUGG, J., WEBER, L. M., CATENA, R., JINEK, M., ROBINSON, M. D. & MOSIMANN, C. 2016. Maximizing mutagenesis with solubilized CRISPR-Cas9 ribonucleoprotein complexes. *Development,* 143**,** 2025-37.

CALLIS, J., FROMM, M. & WALBOT, V. 1987. Introns increase gene expression in cultured maize cells. *Genes Dev,* 1**,** 1183-200.

CALLUS, B. A., VERHAGEN, A. M. & VAUX, D. L. 2006. Association of mammalian sterile twenty kinases, Mst1 and Mst2, with hSalvador via C-terminal coiled-coil domains, leads to its stabilization and phosphorylation. *FEBS J,* 273**,** 4264-76.

CAMPISI, J. & D'ADDA DI FAGAGNA, F. 2007. Cellular senescence: when bad things happen to good cells. *Nat Rev Mol Cell Biol,* 8**,** 729-40.

CANDAU, R., MOORE, P. A., WANG, L., BARLEV, N., YING, C. Y., ROSEN, C. A. & BERGER, S. L. 1996. Identification of human proteins functionally conserved with the yeast putative adaptors ADA2 and GCN5. *Mol Cell Biol,* 16**,** 593-602.

CARMELIET, P., LAMPUGNANI, M. G., MOONS, L., BREVIARIO, F., COMPERNOLLE, V., BONO, F., BALCONI, G., SPAGNUOLO, R., OOSTHUYSE, B., DEWERCHIN, M., ZANETTI, A., ANGELLILO, A., MATTOT, V., NUYENS, D., LUTGENS, E., CLOTMAN, F., DE RUITER, M. C., GITTENBERGER-DE GROOT, A., POELMANN, R., LUPU, F., HERBERT, J. M., COLLEN, D. & DEJANA, E. 1999. Targeted deficiency or cytosolic truncation of the VE-cadherin gene in mice impairs VEGF-mediated endothelial survival and angiogenesis. *Cell,* 98**,** 147-57.

CARSWELL, S. & ALWINE, J. C. 1989. Efficiency of utilization of the simian virus 40 late

polyadenylation site: effects of upstream sequences. *Mol Cell Biol,* 9**,** 4248-58
CASTILLO-DAVIS, C. I., MEKHEDOV, S. L., HARTL, D. L., KOONIN, E. V. & KONDRASHOV, F. A. 2002. Selection for short introns in highly expressed genes. *Nat Genet,* 31**,** 415-8.
CHAFFER, C. L. & WEINBERG, R. A. 2011. A perspective on cancer cell metastasis. *Science,* 331**,** 1559-64.
CHAN, E. H., NOUSIAINEN, M., CHALAMALASETTY, R. B., SCHAFER, A., NIGG, E. A. & SILLJE, H. H. 2005. The Ste20-like kinase Mst2 activates the human large tumor suppressor kinase Lats1. *Oncogene,* 24**,** 2076-86.
CHAN, P., HAN, X., ZHENG, B., DERAN, M., YU, J., JARUGUMILLI, G. K., DENG, H., PAN, D., LUO, X. & WU, X. 2016. Autopalmitoylation of TEAD proteins regulates transcriptional output of the Hippo pathway. *Nat Chem Biol,* 12**,** 282-9.
CHAN, S. W., LIM, C. J., CHONG, Y. F., POBBATI, A. V., HUANG, C. & HONG, W. 2011. Hippo pathway-independent restriction of TAZ and YAP by angiomotin. *J Biol Chem,* 286**,** 7018-26.
CHAN, S. W., LIM, C. J., LOO, L. S., CHONG, Y. F., HUANG, C. & HONG, W. 2009. TEADs mediate nuclear retention of TAZ to promote oncogenic transformation. *J Biol Chem,* 284**,** 14347-58.
CHANG, L. & KARIN, M. 2001. Mammalian MAP kinase signalling cascades. *Nature,* 410**,** 37-40.
CHAPMAN, A., FERNANDEZ DEL AMA, L., FERGUSON, J., KAMARASHEV, J., WELLBROCK, C. & HURLSTONE, A. 2014. Heterogeneous tumor subpopulations cooperate to drive invasion. *Cell Rep,* 8**,** 688-95.
CHEN, F., MACDONALD, C. C. & WILUSZ, J. 1995. Cleavage site determinants in the mammalian polyadenylation signal. *Nucleic Acids Res,* 23**,** 2614-20.
CHEN, L., CHAN, S. W., ZHANG, X., WALSH, M., LIM, C. J., HONG, W. & SONG, H. 2010. Structural basis of YAP recognition by TEAD4 in the hippo pathway. *Genes Dev,* 24**,** 290-300.
CHEN, X., LI, Y., YAO, T. & JIA, R. 2021. Benefits of Zebrafish Xenograft Models in Cancer Research. *Front Cell Dev Biol,* 9**,** 616551.
CHEO, D. L., TITUS, S. A., BYRD, D. R., HARTLEY, J. L., TEMPLE, G. F. & BRASCH, M. A. 2004. Concerted assembly and cloning of multiple DNA segments using in vitro site-specific recombination: functional analysis of multi-segment expression clones. *Genome Res,* 14**,** 2111-20.
CHEVREAU, C., LE CESNE, A., RAY-COQUARD, I., ITALIANO, A., CIOFFI, A., ISAMBERT, N., ROBIN, Y. M., FOURNIER, C., CLISANT, S., CHAIGNEAU, L., BAY, J. O., BOMPAS, E., GAUTHIER, E., BLAY, J. Y. & PENEL, N. 2013. Sorafenib in patients with progressive epithelioid hemangioendothelioma: a phase 2 study by the French Sarcoma Group (GSF/GETO). *Cancer,* 119**,** 2639-44.
CHIAROMONTE, F., MILLER, W. & BOUHASSIRA, E. E. 2003. Gene length and proximity to neighbors affect genome-wide expression levels. *Genome Res,* 13**,** 2602-8.
CHIU, J. J. & CHIEN, S. 2011. Effects of disturbed flow on vascular endothelium: pathophysiological basis and clinical perspectives. *Physiol Rev,* 91**,** 327-87.
CHOI, H. J., ZHANG, H., PARK, H., CHOI, K. S., LEE, H. W., AGRAWAL, V., KIM, Y. M. & KWON, Y. G. 2015. Yes-associated protein regulates endothelial cell contact-mediated expression of angiopoietin-2. *Nat Commun,* 6**,** 6943.
CLAESSON-WELSH, L., WELSH, M., ITO, N., ANAND-APTE, B., SOKER, S., ZETTER, B., O'REILLY, M. & FOLKMAN, J. 1998. Angiostatin induces endothelial cell apoptosis and activation of focal adhesion kinase independently of the integrin-binding motif RGD. *Proc Natl Acad Sci U S A,* 95**,** 5579-83.
COHEN, E. E., WU, K., HARTFORD, C., KOCHERGINSKY, M., EATON, K. N., ZHA, Y., NALLARI, A., MAITLAND, M. L., FOX-KAY, K., MOSHIER, K., HOUSE, L., RAMIREZ, J., UNDEVIA, S. D., FLEMING, G. F., GAJEWSKI, T. F. & RATAIN, M. J. 2012. Phase I studies of sirolimus alone or in combination with pharmacokinetic modulators in advanced cancer patients. *Clin Cancer Res,*

18**,** 4785-93.
COLLIER, T. S., DIRAVIYAM, K., MONSEY, J., SHEN, W., SEPT, D. & BOSE, R. 2013. Carboxyl group footprinting mass spectrometry and molecular dynamics identify key interactions in the HER2-HER3 receptor tyrosine kinase interface. *J Biol Chem,* 288**,** 25254-25264.
CONG, L., RAN, F. A., COX, D., LIN, S., BARRETTO, R., HABIB, N., HSU, P. D., WU, X., JIANG, W., MARRAFFINI, L. A. & ZHANG, F. 2013. Multiplex genome engineering using CRISPR/Cas systems. *Science,* 339**,** 819-23.
CORDENONSI, M., ZANCONATO, F., AZZOLIN, L., FORCATO, M., ROSATO, A., FRASSON, C., INUI, M., MONTAGNER, M., PARENTI, A. R., POLETTI, A., DAIDONE, M. G., DUPONT, S., BASSO, G., BICCIATO, S. & PICCOLO, S. 2011. The Hippo transducer TAZ confers cancer stem cell-related traits on breast cancer cells. *Cell,* 147**,** 759-72.
CORKERY, D. P., DELLAIRE, G. & BERMAN, J. N. 2011. Leukaemia xenotransplantation in zebrafish--chemotherapy response assay in vivo. *Br J Haematol,* 153**,** 786-9.
COTTINI, F., HIDESHIMA, T., XU, C., SATTLER, M., DORI, M., AGNELLI, L., TEN HACKEN, E., BERTILACCIO, M. T., ANTONINI, E., NERI, A., PONZONI, M., MARCATTI, M., RICHARDSON, P. G., CARRASCO, R., KIMMELMAN, A. C., WONG, K. K., CALIGARIS-CAPPIO, F., BLANDINO, G., KUEHL, W. M., ANDERSON, K. C. & TONON, G. 2014. Rescue of Hippo coactivator YAP1 triggers DNA damage-induced apoptosis in hematological cancers. *Nat Med,* 20**,** 599-606.
CUI, C. B., COOPER, L. F., YANG, X., KARSENTY, G. & AUKHIL, I. 2003. Transcriptional coactivation of bone-specific transcription factor Cbfa1 by TAZ. *Mol Cell Biol,* 23**,** 1004-13.
CUI, Y., GROTH, S., TROUTMAN, S., CARLSTEDT, A., SPERKA, T., RIECKEN, L. B., KISSIL, J. L., JIN, H. & MORRISON, H. 2019. The NF2 tumor suppressor merlin interacts with Ras and RasGAP, which may modulate Ras signaling. *Oncogene,* 38**,** 6370-6381.
CURRAN, T. & FRANZA, B. R., JR. 1988. Fos and Jun: the AP-1 connection. *Cell,* 55**,** 395-7.
DAI, X., LIU, H., SHEN, S., GUO, X., YAN, H., JI, X., LI, L., HUANG, J., FENG, X. H. & ZHAO, B. 2015. YAP activates the Hippo pathway in a negative feedback loop. *Cell Res,* 25**,** 1175-8.
DANCKWARDT, S., KAUFMANN, I., GENTZEL, M., FOERSTNER, K. U., GANTZERT, A. S., GEHRING, N. H., NEU-YILIK, G., BORK, P., KELLER, W., WILM, M., HENTZE, M. W. & KULOZIK, A. E. 2007. Splicing factors stimulate polyadenylation via USEs at non-canonical 3' end formation signals. *EMBO J,* 26**,** 2658-69.
DELLA CHIARA, G., GERVASONI, F., FAKIOLA, M., GODANO, C., D'ORIA, C., AZZOLIN, L., BONNAL, R. J. P., MORENI, G., DRUFUCA, L., ROSSETTI, G., RANZANI, V., BASON, R., DE SIMONE, M., PANARIELLO, F., FERRARI, I., FABBRIS, T., ZANCONATO, F., FORCATO, M., ROMANO, O., CAROLI, J., GRUARIN, P., SARNICOLA, M. L., CORDENONSI, M., BARDELLI, A., ZUCCHINI, N., CERETTI, A. P., MARIANI, N. M., CASSINGENA, A., SARTORE-BIANCHI, A., TESTA, G., GIANOTTI, L., OPOCHER, E., PISATI, F., TRIPODO, C., MACINO, G., SIENA, S., BICCIATO, S., PICCOLO, S. & PAGANI, M. 2021. Epigenomic landscape of human colorectal cancer unveils an aberrant core of pan-cancer enhancers orchestrated by YAP/TAZ. *Nat Commun,* 12**,** 2340.
DENG, H., WANG, W., YU, J., ZHENG, Y., QING, Y. & PAN, D. 2015. Spectrin regulates Hippo signaling by modulating cortical actomyosin activity. *Elife,* 4**,** e06567.
DENG, X. & FANG, L. 2018. VGLL4 is a transcriptional cofactor acting as a novel tumor suppressor via interacting with TEADs. *Am J Cancer Res,* 8**,** 932-943.
DENG, Y., PANG, A. & WANG, J. H. 2003. Regulation of mammalian STE20-like kinase 2 (MST2) by protein phosphorylation/dephosphorylation and proteolysis. *J Biol Chem,* 278**,** 11760-7.
DEYRUP, A. T., TIGHIOUART, M., MONTAG, A. G. & WEISS, S. W. 2008. Epithelioid hemangioendothelioma of soft tissue: a proposal for risk stratification based on 49 cases. *Am J Surg Pathol,* 32**,** 924-7.DERYNCK R, AKHURST RJ, BALMAIN A. TGF-beta signaling in tumor

suppression and cancer progression. *Nat Genet*. 2001 Oct;29(2):117-29.DEZAZZO, J. D., KILPATRICK, J. E. & IMPERIALE, M. J. 1991. Involvement of long terminal repeat U3 sequences overlapping the transcription control region in human immunodeficiency virus type 1 mRNA 3' end formation. *Mol Cell Biol,* 11**,** 1624-30.

DHAR, A. & RAY, A. 2010. The CCN family proteins in carcinogenesis. *Exp Oncol,* 32**,** 2-9.

DIAZ-MARTIN, J., LOPEZ-GARCIA, M. A., ROMERO-PEREZ, L., ATIENZA-AMORES, M. R., PECERO, M. L., CASTILLA, M. A., BISCUOLA, M., SANTON, A. & PALACIOS, J. 2015. Nuclear TAZ expression associates with the triple-negative phenotype in breast cancer. *Endocr Relat Cancer,* 22**,** 443-54.

DONG, J., FELDMANN, G., HUANG, J., WU, S., ZHANG, N., COMERFORD, S. A., GAYYED, M. F., ANDERS, R. A., MAITRA, A. & PAN, D. 2007. Elucidation of a universal size-control mechanism in Drosophila and mammals. *Cell,* 130**,** 1120-33.

DONGRE, A. & WEINBERG, R. A. 2019. New insights into the mechanisms of epithelial-mesenchymal transition and implications for cancer. *Nat Rev Mol Cell Biol,* 20**,** 69-84.

DRISKILL, J. H., ZHENG, Y., WU, B. K., WANG, L., CAI, J., RAKHEJA, D., DELLINGER, M. & PAN, D. 2021. WWTR1(TAZ)-CAMTA1 reprograms endothelial cells to drive epithelioid hemangioendothelioma. *Genes Dev,* 35**,** 495-511.

DUPONT, S., MORSUT, L., ARAGONA, M., ENZO, E., GIULITTI, S., CORDENONSI, M., ZANCONATO, F., LE DIGABEL, J., FORCATO, M., BICCIATO, S., ELVASSORE, N. & PICCOLO, S. 2011. Role of YAP/TAZ in mechanotransduction. *Nature,* 474**,** 179-83.

DYSON, N. 1998. The regulation of E2F by pRB-family proteins. *Genes Dev,* 12**,** 2245-62.

EAGLE, H. & LEVINE, E. M. 1967. Growth regulatory effects of cellular interaction. *Nature,* 213**,** 1102-6.

ECK, S. M., BLACKBURN, J. S., SCHMUCKER, A. C., BURRAGE, P. S. & BRINCKERHOFF, C. E. 2009. Matrix metalloproteinase and G protein coupled receptors: co-conspirators in the pathogenesis of autoimmune disease and cancer. *J Autoimmun,* 33**,** 214-21.

EHMER, U. & SAGE, J. 2016. Control of Proliferation and Cancer Growth by the Hippo Signaling Pathway. *Mol Cancer Res,* 14**,** 127-40.

ENGEL, E. R., COURNOYER, E., ADAMS, D. M. & STAPLETON, S. 2020. A Retrospective Review of the Use of Sirolimus for Pediatric Patients With Epithelioid Hemangioendothelioma. *J Pediatr Hematol Oncol,* 42**,** e826-e829.

ERRANI, C., ZHANG, L., SUNG, Y. S., HAJDU, M., SINGER, S., MAKI, R. G., HEALEY, J. H. & ANTONESCU, C. R. 2011. A novel WWTR1-CAMTA1 gene fusion is a consistent abnormality in epithelioid hemangioendothelioma of different anatomic sites. *Genes Chromosomes Cancer,* 50**,** 644-53.

ESTELLER, M., CORN, P. G., BAYLIN, S. B. & HERMAN, J. G. 2001. A gene hypermethylation profile of human cancer. *Cancer Res,* 61**,** 3225-9.

EVANS, D. G. 2009. Neurofibromatosis type 2 (NF2): a clinical and molecular review. *Orphanet J Rare Dis,* 4**,** 16.

EWEN, M. E. 1994. The cell cycle and the retinoblastoma protein family. *Cancer Metastasis Rev,* 13**,** 45-66.

FENG, S., COKUS, S. J., ZHANG, X., CHEN, P. Y., BOSTICK, M., GOLL, M. G., HETZEL, J., JAIN, J., STRAUSS, S. H., HALPERN, M. E., UKOMADU, C., SADLER, K. C., PRADHAN, S., PELLEGRINI, M. &
JACOBSEN, S. E. 2010. Conservation and divergence of methylation patterning in plants and animals. *Proc Natl Acad Sci U S A,* 107**,** 8689-94.

FLUCKE, U., VOGELS, R. J., DE SAINT AUBAIN SOMERHAUSEN, N., CREYTENS, D. H., RIEDL, R. G., VAN GORP, J. M., MILNE, A. N., HUYSENTRUYT, C. J., VERDIJK, M. A., VAN ASSELDONK, M. M.,

SUURMEIJER, A. J., BRAS, J., PALMEDO, G., GROENEN, P. J. & MENTZEL, T. 2014. Epithelioid Hemangioendothelioma: clinicopathologic, immunhistochemical, and molecular genetic analysis of 39 cases. *Diagn Pathol,* 9**,** 131.

FORRESTER, A. M., GRABHER, C., MCBRIDE, E. R., BOYD, E. R., VIGERSTAD, M. H., EDGAR, A., KAI, F. B., DA'AS, S. I., PAYNE, E., LOOK, A. T. & BERMAN, J. N. 2011. NUP98-HOXA9-transgenic zebrafish develop a myeloproliferative neoplasm and provide new insight into mechanisms of myeloid leukaemogenesis. *Br J Haematol,* 155**,** 167-81.

FRIESS, H., YAMANAKA, Y., KOBRIN, M. S., DO, D. A., BUCHLER, M. W. & KORC, M. 1995. Enhanced erbB-3 expression in human pancreatic cancer correlates with tumor progression. *Clin Cancer Res,* 1**,** 1413-20.

FURGER, A., O'SULLIVAN, J. M., BINNIE, A., LEE, B. A. & PROUDFOOT, N. J. 2002. Promoter proximal splice sites enhance transcription. *Genes Dev,* 16**,** 2792-9.

GALAN, J. A. & AVRUCH, J. 2016. MST1/MST2 Protein Kinases: Regulation and Physiologic Roles. *Biochemistry,* 55**,** 5507-5519.

GALAXY, C. 2022. The Galaxy platform for accessible, reproducible and collaborative biomedical analyses: 2022 update. *Nucleic Acids Res,* 50**,** W345-W351.

GALLI, G. G., CARRARA, M., YUAN, W. C., VALDES-QUEZADA, C., GURUNG, B., PEPE-MOONEY, B., ZHANG, T., GEEVEN, G., GRAY, N. S., DE LAAT, W., CALOGERO, R. A. & CAMARGO, F. D. 2015. YAP Drives Growth by Controlling Transcriptional Pause Release from Dynamic Enhancers. *Mol Cell,* 60**,** 328-37.

GANDULLO-SANCHEZ, L., OCANA, A. & PANDIELLA, A. 2022. HER3 in cancer: from the bench to the bedside. *J Exp Clin Cancer Res,* 41**,** 310.

GARCIA, K., GINGRAS, A. C., HARVEY, K. F. & TANAS, M. R. 2022. TAZ/YAP fusion proteins: mechanistic insights and therapeutic opportunities. *Trends Cancer,* 8**,** 1033-1045.

GASZNER, M. & FELSENFELD, G. 2006. Insulators: exploiting transcriptional and epigenetic mechanisms. *Nat Rev Genet,* 7**,** 703-13.

GAUDENZI, G., ALBERTELLI, M., DICITORE, A., WURTH, R., GATTO, F., BARBIERI, F., COTELLI, F., FLORIO, T., FERONE, D., PERSANI, L. & VITALE, G. 2017. Patient-derived xenograft in zebrafish embryos: a new platform for translational research in neuroendocrine tumors. *Endocrine,* 57**,** 214-219.

GAUTIER, P., NARANJO-GOLBORNE, C., TAYLOR, M. S., JACKSON, I. J. & SMYTH, I. 2008. Expression of the fras1/frem gene family during zebrafish development and fin morphogenesis. *Dev Dyn,* 237**,** 3295-304.

GEYER, P. K. & CORCES, V. G. 1992. DNA position-specific repression of transcription by a Drosophila zinc finger protein. *Genes Dev,* 6**,** 1865-73.

GHOTRA, V. P., HE, S., DE BONT, H., VAN DER ENT, W., SPAINK, H. P., VAN DE WATER, B., SNAAR-JAGALSKA, B. E. & DANEN, E. H. 2012. Automated whole animal bio-imaging assay for human cancer dissemination. *PLoS One,* 7**,** e31281.

GIL, A. & PROUDFOOT, N. J. 1984. A sequence downstream of AAUAAA is required for rabbit beta-globin mRNA 3'-end formation. *Nature,* 312**,** 473-4.

GIL, A. & PROUDFOOT, N. J. 1987. Position-dependent sequence elements downstream of AAUAAA are required for efficient rabbit beta-globin mRNA 3' end formation. *Cell,* 49**,** 399-406.

GOLL, M. G., ANDERSON, R., STAINIER, D. Y., SPRADLING, A. C. & HALPERN, M. E. 2009. Transcriptional silencing and reactivation in transgenic zebrafish. *Genetics,* 182**,** 747-55.

GONZALEZ, S. & SERRANO, M. 2006. A new mechanism of inactivation of the INK4/ARF locus. *Cell Cycle,* 5**,** 1382-4.

GOSSEN, M., FREUNDLIEB, S., BENDER, G., MULLER, G., HILLEN, W. & BUJARD, H. 1995.

Transcriptional activation by tetracyclines in mammalian cells. *Science,* 268**,** 1766-9.
GRABUNDZIJA, I., IRGANG, M., MATES, L., BELAY, E., MATRAI, J., GOGOL-DORING, A., KAWAKAMI, K., CHEN, W., RUIZ, P., CHUAH, M. K., VANDENDRIESSCHE, T., IZSVAK, Z. & IVICS, Z. 2010. Comparative analysis of transposable element vector systems in human cells. *Mol Ther,* 18**,** 1200-9.
GRANT, P. A., DUGGAN, L., COTE, J., ROBERTS, S. M., BROWNELL, J. E., CANDAU, R., OHBA, R., OWEN-HUGHES, T., ALLIS, C. D., WINSTON, F., BERGER, S. L. & WORKMAN, J. L. 1997. Yeast Gcn5 functions in two multisubunit complexes to acetylate nucleosomal histones: characterization of an Ada complex and the SAGA (Spt/Ada) complex. *Genes Dev,* 11**,** 1640-50.
GUO, X., ZHAO, Y., YAN, H., YANG, Y., SHEN, S., DAI, X., JI, X., JI, F., GONG, X. G., LI, L., BAI, X., FENG, X. H., LIANG, T., JI, J., CHEN, L., WANG, H. & ZHAO, B. 2017. Single tumor-initiating cells evade immune clearance by recruiting type II macrophages. *Genes Dev,* 31**,** 247-259.
GUO, Y., PAN, Q., ZHANG, J., XU, X., LIU, X., WANG, Q., YI, R., XIE, X., YAO, L., LIU, W. & SHEN, L. 2015. Functional and clinical evidence that TAZ is a candidate oncogene in hepatocellular carcinoma. *J Cell Biochem,* 116**,** 2465-75.
GUO, Y. J., PAN, W. W., LIU, S. B., SHEN, Z. F., XU, Y. & HU, L. L. 2020. ERK/MAPK signalling pathway and tumorigenesis. *Exp Ther Med,* 19**,** 1997-2007.
GUPTA, D., BHATTACHARJEE, O., MANDAL, D., SEN, M. K., DEY, D., DASGUPTA, A., KAZI, T. A., GUPTA, R., SINHAROY, S., ACHARYA, K., CHATTOPADHYAY, D., RAVICHANDIRAN, V., ROY, S. & GHOSH, D. 2019. CRISPR-Cas9 system: A new-fangled dawn in gene editing. *Life Sci,* 232**,** 116636.
HAHN, C. & SCHWARTZ, M. A. 2009. Mechanotransduction in vascular physiology and atherogenesis. *Nat Rev Mol Cell Biol,* 10**,** 53-62.
HALDER, G. & JOHNSON, R. L. 2011. Hippo signaling: growth control and beyond. *Development,* 138**,** 9-22.
HALDI, M., TON, C., SENG, W. L. & MCGRATH, P. 2006. Human melanoma cells transplanted into zebrafish proliferate, migrate, produce melanin, form masses and stimulate angiogenesis in zebrafish. *Angiogenesis,* 9**,** 139-51.
HALL, M., BATES, S. & PETERS, G. 1995. Evidence for different modes of action of cyclin-dependent kinase inhibitors: p15 and p16 bind to kinases, p21 and p27 bind to cyclins. *Oncogene,* 11**,** 1581-8.
HALL, R. N., MEERS, J., FOWLER, E. & MAHONY, T. 2012. Back to BAC: the use of infectious clone technologies for viral mutagenesis. *Viruses,* 4**,** 211-35.
HAMARATOGLU, F., WILLECKE, M., KANGO-SINGH, M., NOLO, R., HYUN, E., TAO, C., JAFAR-NEJAD, H. & HALDER, G. 2006. The tumour-suppressor genes NF2/Merlin and Expanded act through Hippo signalling to regulate cell proliferation and apoptosis. *Nat Cell Biol,* 8**,** 27-36.
HAN, Y. 2019. Analysis of the role of the Hippo pathway in cancer. *J Transl Med,* 17**,** 116.
HARTLEY, J. L., TEMPLE, G. F. & BRASCH, M. A. 2000. DNA cloning using in vitro site-specific recombination. *Genome Res,* 10**,** 1788-95.
HARVEY, K. & TAPON, N. 2007. The Salvador-Warts-Hippo pathway - an emerging tumour-suppressor network. *Nat Rev Cancer,* 7**,** 182-91.
HARVEY, K. F., ZHANG, X. & THOMAS, D. M. 2013. The Hippo pathway and human cancer. *Nat Rev Cancer,* 13**,** 246-57.
HASON, M. & BARTUNEK, P. 2019. Zebrafish Models of Cancer-New Insights on Modeling Human Cancer in a Non-Mammalian Vertebrate. *Genes (Basel),* 10.
HE, S., LAMERS, G. E., BEENAKKER, J. W., CUI, C., GHOTRA, V. P., DANEN, E. H., MEIJER, A. H., SPAINK, H. P. & SNAAR-JAGALSKA, B. E. 2012. Neutrophil-mediated experimental metastasis is enhanced by VEGFR inhibition in a zebrafish xenograft model. *J Pathol,* 227**,** 431-45.

HENNEY, J. E. 2000. From the Food and Drug Administration. *JAMA,* 284**,** 2178.

HENRICH, K. O., BAUER, T., SCHULTE, J., EHEMANN, V., DEUBZER, H., GOGOLIN, S., MUTH, D., FISCHER, M., BENNER, A., KONIG, R., SCHWAB, M. & WESTERMANN, F. 2011. CAMTA1, a 1p36 tumor suppressor candidate, inhibits growth and activates differentiation programs in neuroblastoma cells. *Cancer Res,* 71**,** 3142-51.

HENRICH, K. O., SCHWAB, M. & WESTERMANN, F. 2012. 1p36 tumor suppression--a matter of dosage? *Cancer Res,* 72**,** 6079-88.

HERGOVICH, A., SCHMITZ, D. & HEMMINGS, B. A. 2006. The human tumour suppressor LATS1 is activated by human MOB1 at the membrane. *Biochem Biophys Res Commun,* 345**,** 50-8.

HIEMER, S. E., SZYMANIAK, A. D. & VARELAS, X. 2014. The transcriptional regulators TAZ and YAP direct transforming growth factor beta-induced tumorigenic phenotypes in breast cancer cells. *J Biol Chem,* 289**,** 13461-74.

HOESS, R. H. & ABREMSKI, K. 1984. Interaction of the bacteriophage P1 recombinase Cre with the recombining site loxP. *Proc Natl Acad Sci U S A,* 81**,** 1026-9.

HOESS, R. H., ZIESE, M. & STERNBERG, N. 1982. P1 site-specific recombination: nucleotide sequence of the recombining sites. *Proc Natl Acad Sci U S A,* 79**,** 3398-402.

HOLLSTEIN, M., SIDRANSKY, D., VOGELSTEIN, B. & HARRIS, C. C. 1991. p53 mutations in human cancers. *Science,* 253**,** 49-53.

HONG, A. W., MENG, Z. & GUAN, K. L. 2016. The Hippo pathway in intestinal regeneration and disease. *Nat Rev Gastroenterol Hepatol,* 13**,** 324-37.

HONG, A. W., MENG, Z., PLOUFFE, S. W., LIN, Z., ZHANG, M. & GUAN, K. L. 2020. Critical roles of phosphoinositides and NF2 in Hippo pathway regulation. *Genes Dev,* 34**,** 511-525.

HONG, D. & JEONG, S. 2023. 3'UTR Diversity: Expanding Repertoire of RNA Alterations in Human mRNAs. *Mol Cells,* 46**,** 48-56.

HONG, J. H., HWANG, E. S., MCMANUS, M. T., AMSTERDAM, A., TIAN, Y., KALMUKOVA, R., MUELLER, E., BENJAMIN, T., SPIEGELMAN, B. M., SHARP, P. A., HOPKINS, N. & YAFFE, M. B. 2005. TAZ, a transcriptional modulator of mesenchymal stem cell differentiation. *Science,* 309**,** 1074-8.

HORSTICK, E. J., JORDAN, D. C., BERGERON, S. A., TABOR, K. M., SERPE, M., FELDMAN, B. & BURGESS, H. A. 2015. Increased functional protein expression using nucleotide sequence features enriched in highly expressed genes in zebrafish. *Nucleic Acids Res,* 43**,** e48.

HOWE, K., CLARK, M. D., TORROJA, C. F., TORRANCE, J., BERTHELOT, C., MUFFATO, M., COLLINS, J. E., HUMPHRAY, S., MCLAREN, K., MATTHEWS, L., MCLAREN, S., SEALY, I., CACCAMO, M., CHURCHER, C., SCOTT, C., BARRETT, J. C., KOCH, R., RAUCH, G. J., WHITE, S., CHOW, W., KILIAN, B., QUINTAIS, L. T., GUERRA-ASSUNCAO, J. A., ZHOU, Y., GU, Y., YEN, J., VOGEL, J. H., EYRE, T., REDMOND, S., BANERJEE, R., CHI, J., FU, B., LANGLEY, E., MAGUIRE, S. F., LAIRD, G. K., LLOYD, D., KENYON, E., DONALDSON, S., SEHRA, H., ALMEIDA-KING, J., LOVELAND, J., TREVANION, S., JONES, M., QUAIL, M., WILLEY, D., HUNT, A., BURTON, J., SIMS, S., MCLAY, K., PLUMB, B., DAVIS, J., CLEE, C., OLIVER, K., CLARK, R., RIDDLE, C., ELLIOT, D., THREADGOLD, G., HARDEN, G., WARE, D., BEGUM, S., MORTIMORE, B., KERRY, G., HEATH, P., PHILLIMORE, B., TRACEY, A., CORBY, N., DUNN, M., JOHNSON, C., WOOD, J., CLARK, S., PELAN, S., GRIFFITHS, G., SMITH, M., GLITHERO, R., HOWDEN, P., BARKER, N., LLOYD, C., STEVENS, C., HARLEY, J., HOLT, K., PANAGIOTIDIS, G., LOVELL, J., BEASLEY, H., HENDERSON, C., GORDON, D., AUGER, K., WRIGHT, D., COLLINS, J., RAISEN, C., DYER, L., LEUNG, K., ROBERTSON, L., AMBRIDGE, K., LEONGAMORNLERT, D., MCGUIRE, S., GILDERTHORP, R., GRIFFITHS, C., MANTHRAVADI, D., NICHOL, S., BARKER, G., et al. 2013. The zebrafish reference genome sequence and its relationship to the human genome. *Nature,* 496**,** 498-503.

HRUSCHA, A., KRAWITZ, P., RECHENBERG, A., HEINRICH, V., HECHT, J., HAASS, C. & SCHMID, B. 2013. Efficient CRISPR/Cas9 genome editing with low off-target effects in zebrafish. *Development,* 140**,** 4982-7.

HU, X., WANG, Q., TANG, M., BARTHEL, F., AMIN, S., YOSHIHARA, K., LANG, F. M., MARTINEZ-LEDESMA, E., LEE, S. H., ZHENG, S. & VERHAAK, R. G. W. 2018. TumorFusions: an integrative resource for cancer-associated transcript fusions. *Nucleic Acids Res,* 46**,** D1144-D1149.

HU, X., XIN, Y., XIAO, Y. & ZHAO, J. 2014. Overexpression of YAP1 is correlated with progression, metastasis and poor prognosis in patients with gastric carcinoma. *Pathol Oncol Res,* 20**,** 805-11.

HUANG, Y. T., LAN, Q., LORUSSO, G., DUFFEY, N. & RUEGG, C. 2017. The matricellular protein CYR61 promotes breast cancer lung metastasis by facilitating tumor cell extravasation and suppressing anoikis. *Oncotarget,* 8**,** 9200-9215.

JAHNER, D., STUHLMANN, H., STEWART, C. L., HARBERS, K., LOHLER, J., SIMON, I. & JAENISCH, R. 1982. De novo methylation and expression of retroviral genomes during mouse embryogenesis. *Nature,* 298**,** 623-8.

JANSE VAN RENSBURG, H. J., AZAD, T., LING, M., HAO, Y., SNETSINGER, B., KHANAL, P., MINASSIAN, L. M., GRAHAM, C. H., RAUH, M. J. & YANG, X. 2018. The Hippo Pathway Component TAZ Promotes Immune Evasion in Human Cancer through PD-L1. *Cancer Res,* 78**,** 1457-1470.

JENNE, D. E., REIMANN, H., NEZU, J., FRIEDEL, W., LOFF, S., JESCHKE, R., MULLER, O., BACK, W. & ZIMMER, M. 1998. Peutz-Jeghers syndrome is caused by mutations in a novel serine threonine kinase. *Nat Genet,* 18**,** 38-43.

JI, W. R., CASTELLINO, F. J., CHANG, Y., DEFORD, M. E., GRAY, H., VILLARREAL, X., KONDRI, M. E., MARTI, D. N., LLINAS, M., SCHALLER, J., KRAMER, R. A. & TRAIL, P. A. 1998. Characterization of kringle domains of angiostatin as antagonists of endothelial cell migration, an important process in angiogenesis. *FASEB J,* 12**,** 1731-8.

JUSTICE, R. W., ZILIAN, O., WOODS, D. F., NOLL, M. & BRYANT, P. J. 1995. The Drosophila tumor suppressor gene warts encodes a homolog of human myotonic dystrophy kinase and is required for the control of cell shape and proliferation. *Genes Dev,* 9**,** 534-46.

KALEV-ZYLINSKA, M. L., HORSFIELD, J. A., FLORES, M. V., POSTLETHWAIT, J. H., VITAS, M. R., BAAS, A. M., CROSIER, P. S. & CROSIER, K. E. 2002. Runx1 is required for zebrafish blood and vessel development and expression of a human RUNX1-CBF2T1 transgene advances a model for studies of leukemogenesis. *Development,* 129**,** 2015-30.

KANAI, F., MARIGNANI, P. A., SARBASSOVA, D., YAGI, R., HALL, R. A., DONOWITZ, M., HISAMINATO, A., FUJIWARA, T., ITO, Y., CANTLEY, L. C. & YAFFE, M. B. 2000. TAZ: a novel transcriptional co-activator regulated by interactions with 14-3-3 and PDZ domain proteins. *EMBO J,* 19**,** 6778-91.

KAPOOR, A., YAO, W., YING, H., HUA, S., LIEWEN, A., WANG, Q., ZHONG, Y., WU, C. J., SADANANDAM, A., HU, B., CHANG, Q., CHU, G. C., AL-KHALIL, R., JIANG, S., XIA, H., FLETCHER-SANANIKONE, E., LIM, C., HORWITZ, G. I., VIALE, A., PETTAZZONI, P., SANCHEZ, N., WANG, H., PROTOPOPOV, A., ZHANG, J., HEFFERNAN, T., JOHNSON, R. L., CHIN, L., WANG, Y. A., DRAETTA, G. & DEPINHO, R. A. 2014. Yap1 activation enables bypass of oncogenic Kras addiction in pancreatic cancer. *Cell,* 158**,** 185-197.

KARAMAN, R. & HALDER, G. 2018. Cell Junctions in Hippo Signaling. *Cold Spring Harb Perspect Biol,* 10.

KAUFFMAN, E. C., RICKETTS, C. J., RAIS-BAHRAMI, S., YANG, Y., MERINO, M. J., BOTTARO, D. P., SRINIVASAN, R. & LINEHAN, W. M. 2014. Molecular genetics and cellular features of TFE3 and TFEB fusion kidney cancers. *Nat Rev Urol,* 11**,** 465-75.

KAWAKAMI, K., TAKEDA, H., KAWAKAMI, N., KOBAYASHI, M., MATSUDA, N. & MISHINA, M. 2004. A transposon-mediated gene trap approach identifies developmentally regulated genes in zebrafish. *Dev Cell,* 7**,** 133-44.

KELLUM, R. & SCHEDL, P. 1991. A position-effect assay for boundaries of higher order chromosomal domains. *Cell,* 64**,** 941-50.

KELLY-SPRATT, K. S., GURLEY, K. E., YASUI, Y. & KEMP, C. J. 2004. p19Arf suppresses growth, progression, and metastasis of Hras-driven carcinomas through p53-dependent and -independent pathways. *PLoS Biol,* 2**,** E242.

KENDALL, G. C., WATSON, S., XU, L., LAVIGNE, C. A., MURCHISON, W., RAKHEJA, D., SKAPEK, S. X., TIRODE, F., DELATTRE, O. & AMATRUDA, J. F. 2018. PAX3-FOXO1 transgenic zebrafish models identify HES3 as a mediator of rhabdomyosarcoma tumorigenesis. *Elife,* 7.

KESHET, I., LIEMAN-HURWITZ, J. & CEDAR, H. 1986. DNA methylation affects the formation of active chromatin. *Cell,* 44**,** 535-43.

KESHET, Y. & SEGER, R. 2010. The MAP kinase signaling cascades: a system of hundreds of components regulates a diverse array of physiological functions. *Methods Mol Biol,* 661**,** 3-38.

KIAVUE, N., CABEL, L., MELAABI, S., BATAILLON, G., CALLENS, C., LEREBOURS, F., PIERGA, J. Y. & BIDARD, F. C. 2020. ERBB3 mutations in cancer: biological aspects, prevalence and therapeutics. *Oncogene,* 39**,** 487-502.

KIM, J., KWON, H., SHIN, Y. K., SONG, G., LEE, T., KIM, Y., JEONG, W., LEE, U., ZHANG, X., NAM, G., JEUNG, H. C., KIM, W. & JHO, E. H. 2020. MAML1/2 promote YAP/TAZ nuclear localization and tumorigenesis. *Proc Natl Acad Sci U S A,* 117**,** 13529-13540.

KIM, M. H., KIM, C. G., KIM, S. K., SHIN, S. J., CHOE, E. A., PARK, S. H., SHIN, E. C. & KIM, J. 2018. YAP-Induced PD-L1 Expression Drives Immune Evasion in BRAFi-Resistant Melanoma. *Cancer Immunol Res,* 6**,** 255-266.

KIM, N. G., KOH, E., CHEN, X. & GUMBINER, B. M. 2011. E-cadherin mediates contact inhibition of proliferation through Hippo signaling-pathway components. *Proc Natl Acad Sci U S A,* 108**,** 11930-5.

KIM, W., CHO, Y. S., WANG, X., PARK, O., MA, X., KIM, H., GAN, W., JHO, E. H., CHA, B., JEUNG, Y. J., ZHANG, L., GAO, B., WEI, W., JIANG, J., CHUNG, K. S. & YANG, Y. 2019. Hippo signaling is intrinsically regulated during cell cycle progression by APC/C(Cdh1). *Proc Natl Acad Sci U S A,* 116**,** 9423-9432.

KIMMEL, C. B., BALLARD, W. W., KIMMEL, S. R., ULLMANN, B. & SCHILLING, T. F. 1995. Stages of embryonic development of the zebrafish. *Dev Dyn,* 203**,** 253-310.

KIRCHBERGER, S., STURTZEL, C., PASCOAL, S. & DISTEL, M. 2017. Quo natas, Danio?-Recent Progress in Modeling Cancer in Zebrafish. *Front Oncol,* 7**,** 186.

KIREEVA, M. L., LATINKIC, B. V., KOLESNIKOVA, T. V., CHEN, C. C., YANG, G. P., ABLER, A. S. & LAU, L. F. 1997. Cyr61 and Fisp12 are both ECM-associated signaling molecules: activities, metabolism, and localization during development. *Exp Cell Res,* 233**,** 63-77.

KIYOZUMI, D., TAKEICHI, M., NAKANO, I., SATO, Y., FUKUDA, T. & SEKIGUCHI, K. 2012. Basement membrane assembly of the integrin alpha8beta1 ligand nephronectin requires Fraser syndrome-associated proteins. *J Cell Biol,* 197**,** 677-89.

KLEER, C. G. 2016. Dual roles of CCN proteins in breast cancer progression. *J Cell Commun Signal,* 10**,** 217-222.

KOGA, A., SUZUKI, M., INAGAKI, H., BESSHO, Y. & HORI, H. 1996. Transposable element in fish. *Nature,* 383**,** 30.

KOLLAR, A., JONES, R. L., STACCHIOTTI, S., GELDERBLOM, H., GUIDA, M., GRIGNANI, G., STEEGHS, N., SAFWAT, A., KATZ, D., DUFFAUD, F., SLEIJFER, S., VAN DER GRAAF, W. T., TOUATI, N., LITIERE,

S., MARREAUD, S., GRONCHI, A. & KASPER, B. 2017. Pazopanib in advanced vascular sarcomas: an EORTC Soft Tissue and Bone Sarcoma Group (STBSG) retrospective analysis. *Acta Oncol,* 56**,** 88-92.

KOMATA, T., KANZAWA, T., TAKEUCHI, H., GERMANO, I. M., SCHREIBER, M., KONDO, Y. & KONDO, S. 2003. Antitumour effect of cyclin-dependent kinase inhibitors (p16(INK4A), p18(INK4C), p19(INK4D), p21(WAF1/CIP1) and p27(KIP1)) on malignant glioma cells. *Br J Cancer,* 88**,** 1277-80.

KOMURO, A., NAGAI, M., NAVIN, N. E. & SUDOL, M. 2003. WW domain-containing protein YAP associates with ErbB-4 and acts as a co-transcriptional activator for the carboxyl-terminal fragment of ErbB-4 that translocates to the nucleus. *J Biol Chem,* 278**,** 33334-41.

KOZAK, M. 1986. Influences of mRNA secondary structure on initiation by eukaryotic ribosomes. *Proc Natl Acad Sci U S A,* 83**,** 2850-4.

KOZAK, M. 2005. Regulation of translation via mRNA structure in prokaryotes and eukaryotes. *Gene,* 361**,** 13-37.

KRIZHANOVSKY, V., XUE, W., ZENDER, L., YON, M., HERNANDO, E. & LOWE, S. W. 2008. Implications of cellular senescence in tissue damage response, tumor suppression, and stem cell biology. *Cold Spring Harb Symp Quant Biol,* 73**,** 513-22.

KRONE, P. H., LELE, Z. & SASS, J. B. 1997. Heat shock genes and the heat shock response in zebrafish embryos. *Biochem Cell Biol,* 75**,** 487-97.

KWAN, K. M., FUJIMOTO, E., GRABHER, C., MANGUM, B. D., HARDY, M. E., CAMPBELL, D. S., PARANT, J. M., YOST, H. J., KANKI, J. P. & CHIEN, C. B. 2007. The Tol2kit: a multisite gateway-based construction kit for Tol2 transposon transgenesis constructs. *Dev Dyn,* 236**,** 3088-99.

KWON, H., KIM, J. & JHO, E. H. 2022. Role of the Hippo pathway and mechanisms for controlling cellular localization of YAP/TAZ. *FEBS J,* 289**,** 5798-5818.

LA SPINA, M., CONTRERAS, P. S., RISSONE, A., MEENA, N. K., JEONG, E. & MARTINA, J. A. 2020. MiT/TFE Family of Transcription Factors: An Evolutionary Perspective. *Front Cell Dev Biol,* 8**,** 609683.

LADWA, R., PRINGLE, H., KUMAR, R. & WEST, K. 2011. Expression of CTGF and Cyr61 in colorectal cancer. *J Clin Pathol,* 64**,** 58-64.

LAI, D., HO, K. C., HAO, Y. & YANG, X. 2011. Taxol resistance in breast cancer cells is mediated by the hippo pathway component TAZ and its downstream transcriptional targets Cyr61 and CTGF. *Cancer Res,* 71**,** 2728-38.

LALLEMAND, D., CURTO, M., SAOTOME, I., GIOVANNINI, M. & MCCLATCHEY, A. I. 2003. NF2 deficiency promotes tumorigenesis and metastasis by destabilizing adherens junctions. *Genes Dev,* 17**,** 1090-100.

LAMAR, J. M., STERN, P., LIU, H., SCHINDLER, J. W., JIANG, Z. G. & HYNES, R. O. 2012. The Hippo pathway target, YAP, promotes metastasis through its TEAD-interaction domain. *Proc Natl Acad Sci U S A,* 109**,** E2441-50.

LANG, J. C., BORCHERS, J., DANAHEY, D., SMITH, S., STOVER, D. G., AGRAWAL, A., MALONE, J. P., SCHULLER, D. E., WEGHORST, C. M., HOLINGA, A. J., LINGAM, K., PATEL, C. R. & ESHAM, B. 2002. Mutational status of overexpressed p16 in head and neck cancer: evidence for germline mutation of p16/p14ARF. *Int J Oncol,* 21**,** 401-8.

LANGENAU, D. M., FENG, H., BERGHMANS, S., KANKI, J. P., KUTOK, J. L. & LOOK, A. T. 2005. Cre/lox-regulated transgenic zebrafish model with conditional myc-induced T cell acute lymphoblastic leukemia. *Proc Natl Acad Sci U S A,* 102**,** 6068-73.

LANGENAU, D. M., TRAVER, D., FERRANDO, A. A., KUTOK, J. L., ASTER, J. C., KANKI, J. P., LIN, S., PROCHOWNIK, E., TREDE, N. S., ZON, L. I. & LOOK, A. T. 2003. Myc-induced T cell leukemia in

transgenic zebrafish. *Science,* 299**,** 887-90.
LATIFI, A., ABUBAKER, K., CASTRECHINI, N., WARD, A. C., LIONGUE, C., DOBILL, F., KUMAR, J., THOMPSON, E. W., QUINN, M. A., FINDLAY, J. K. & AHMED, N. 2011. Cisplatin treatment of.primary and metastatic epithelial ovarian carcinomas generates residual cells with mesenchymal stem cell-like profile. *J Cell Biochem,* 112**,** 2850-64.
LAU, K., MASSAD, M., POLLAK, C., RUBIN, C., YEH, J., WANG, J., EDELMAN, G., YEH, J., PRASAD, S. & WEINBERG, G. 2011. Clinical patterns and outcome in epithelioid hemangioendothelioma with or without pulmonary involvement: insights from an internet registry in the study of a rare cancer. *Chest,* 140**,** 1312-1318.
LAWRENCE, M. C., JIVAN, A., SHAO, C., DUAN, L., GOAD, D., ZAGANJOR, E., OSBORNE, J., MCGLYNN, K., STIPPEC, S., EARNEST, S., CHEN, W. & COBB, M. H. 2008. The roles of MAPKs in disease. *Cell Res,* 18**,** 436-42.
LAWSON, N. D. & WEINSTEIN, B. M. 2002. In vivo imaging of embryonic vascular development using transgenic zebrafish. *Dev Biol,* 248**,** 307-18.
LE GALL, A., VALERI, A. & NOLLMANN, M. 2015. Roles of chromatin insulators in the formation of long-range contacts. *Nucleus,* 6**,** 118-22.
LEACOCK, S. W., BASSE, A. N., CHANDLER, G. L., KIRK, A. M., RAKHEJA, D. & AMATRUDA, J. F. 2012. A zebrafish transgenic model of Ewing's sarcoma reveals conserved mediators of EWS-FLI1 tumorigenesis. *Dis Model Mech,* 5**,** 95-106.
LEE, H. J., DIAZ, M. F., PRICE, K. M., OZUNA, J. A., ZHANG, S., SEVICK-MURACA, E. M., HAGAN, J. P. & WENZEL, P. L. 2017. Fluid shear stress activates YAP1 to promote cancer cell motility. *Nat Commun,* 8**,** 14122.
LEE, H. J., EWERE, A., DIAZ, M. F. & WENZEL, P. L. 2018. TAZ responds to fluid shear stress to regulate the cell cycle. *Cell Cycle,* 17**,** 147-153.
LEE, Y. H., ALBIG, A. R., REGNER, M., SCHIEMANN, B. J. & SCHIEMANN, W. P. 2008. Fibulin-5 initiates epithelial-mesenchymal transition (EMT) and enhances EMT induced by TGF-beta in mammary epithelial cells via a MMP-dependent mechanism. *Carcinogenesis,* 29**,** 2243-51.
LEI, Q. Y., ZHANG, H., ZHAO, B., ZHA, Z. Y., BAI, F., PEI, X. H., ZHAO, S., XIONG, Y. & GUAN, K. L. 2008. TAZ promotes cell proliferation and epithelial-mesenchymal transition and is inhibited by the hippo pathway. *Mol Cell Biol,* 28**,** 2426-36.
LERUT, J. P., ORLANDO, G., ADAM, R., SCHIAVO, M., KLEMPNAUER, J., MIRZA, D., BOLESLAWSKI, E., BURROUGHS, A., SELLES, C. F., JAECK, D., PFITZMANN, R., SALIZZONI, M., SODERDAHL, G., STEININGER, R., WETTERGREN, A., MAZZAFERRO, V., LE TREUT, Y. P., KARAM, V. & EUROPEAN LIVER TRANSPLANT, R. 2007. The place of liver transplantation in the treatment of hepatic epitheloid hemangioendothelioma: report of the European liver transplant registry. *Ann Surg,* 246**,** 949-57; discussion 957.
LEUNG, H. Y., WESTON, J., GULLICK, W. J. & WILLIAMS, G. 1997. A potential autocrine loop between heregulin-alpha and erbB-3 receptor in human prostatic adenocarcinoma. *Br J Urol,* 79**,** 212-6.
LEVCHENKO, T., BRATT, A., ARBISER, J. L. & HOLMGREN, L. 2004. Angiomotin expression promotes hemangioendothelioma invasion. *Oncogene,* 23**,** 1469-73.
LI, E. & ZHANG, Y. 2014. DNA methylation in mammals. *Cold Spring Harb Perspect Biol,* 6**,** a019133.
LI, J., MAHAJAN, A. & TSAI, M. D. 2006. Ankyrin repeat: a unique motif mediating protein-protein interactions. *Biochemistry,* 45**,** 15168-78.
LI, J., POI, M. J. & TSAI, M. D. 2011. Regulatory mechanisms of tumor suppressor P16(INK4A) and their relevance to cancer. *Biochemistry,* 50**,** 5566-82.
LI, Y., ZHOU, H., LI, F., CHAN, S. W., LIN, Z., WEI, Z., YANG, Z., GUO, F., LIM, C. J., XING, W., SHEN, Y., HONG, W., LONG, J. & ZHANG, M. 2015. Angiomotin binding-induced activation of Merlin/NF2

in the Hippo pathway. *Cell Res,* 25**,** 801-17.
LI, Z., ZHAO, B., WANG, P., CHEN, F., DONG, Z., YANG, H., GUAN, K. L. & XU, Y. 2010. Structural insights into the YAP and TEAD complex. *Genes Dev,* 24**,** 235-40.
LIN, H. S., HUANG, Y. L., WANG, Y. S., HSIAO, E., HSU, T. A., SHIAO, H. Y., JIAANG, W. T., SAMPURNA,B. P., LIN, K. H., WU, M. S., LAI, G. M. & YUH, C. H. 2019. Identification of Novel Anti-Liver Cancer Small Molecules with Better Therapeutic Index than Sorafenib via Zebrafish Drug Screening Platform. *Cancers (Basel),* 11.
LIN, Z., GUO, H., CAO, Y., ZOHRABIAN, S., ZHOU, P., MA, Q., VANDUSEN, N., GUO, Y., ZHANG, J., STEVENS, S. M., LIANG, F., QUAN, Q., VAN GORP, P. R., LI, A., DOS REMEDIOS, C., HE, A., BEZZERIDES, V. J. & PU, W. T. 2016. Acetylation of VGLL4 Regulates Hippo-YAP Signaling and Postnatal Cardiac Growth. *Dev Cell,* 39**,** 466-479.
LIPSON, K. E., WONG, C., TENG, Y. & SPONG, S. 2012. CTGF is a central mediator of tissue remodeling and fibrosis and its inhibition can reverse the process of fibrosis. *Fibrogenesis Tissue Repair,* 5**,** S24.
LITTLEFIELD, P., LIU, L., MYSORE, V., SHAN, Y., SHAW, D. E. & JURA, N. 2014. Structural analysis of the EGFR/HER3 heterodimer reveals the molecular basis for activating HER3 mutations. *Sci Signal,* 7**,** ra114.
LIU, C. Y., ZHA, Z. Y., ZHOU, X., ZHANG, H., HUANG, W., ZHAO, D., LI, T., CHAN, S. W., LIM, C. J., HONG, W., ZHAO, S., XIONG, Y., LEI, Q. Y. & GUAN, K. L. 2010. The hippo tumor pathway promotes TAZ degradation by phosphorylating a phosphodegron and recruiting the SCF(Zhu et al.)-TrCP E3 ligase. *J Biol Chem,* 285**,** 37159-69.
LIU, X., LI, H., RAJURKAR, M., LI, Q., COTTON, J. L., OU, J., ZHU, L. J., GOEL, H. L., MERCURIO, A. M., PARK, J. S., DAVIS, R. J. & MAO, J. 2016. Tead and AP1 Coordinate Transcription and Motility. *Cell Rep,* 14**,** 1169-1180.
LIU-CHITTENDEN, Y., HUANG, B., SHIM, J. S., CHEN, Q., LEE, S. J., ANDERS, R. A., LIU, J. O. & PAN, D. 2012. Genetic and pharmacological disruption of the TEAD-YAP complex suppresses the oncogenic activity of YAP. *Genes Dev,* 26**,** 1300-5.
LO SARDO, F., STRANO, S. & BLANDINO, G. 2018. YAP and TAZ in Lung Cancer: Oncogenic Role and Clinical Targeting. *Cancers (Basel),* 10.
LOW, B. C., PAN, C. Q., SHIVASHANKAR, G. V., BERSHADSKY, A., SUDOL, M. & SHEETZ, M. 2014. YAP/TAZ as mechanosensors and mechanotransducers in regulating organ size and tumor growth. *FEBS Lett,* 588**,** 2663-70.
LU, Y., WU, T., GUTMAN, O., LU, H., ZHOU, Q., HENIS, Y. I. & LUO, K. 2020. Phase separation of TAZ compartmentalizes the transcription machinery to promote gene expression. *Nat Cell Biol,* 22**,** 453-464.
LUCAS, R., HOLMGREN, L., GARCIA, I., JIMENEZ, B., MANDRIOTA, S. J., BORLAT, F., SIM, B. K., WU, Z., GRAU, G. E., SHING, Y., SOFF, G. A., BOUCK, N. & PEPPER, M. S. 1998. Multiple forms of angiostatin induce apoptosis in endothelial cells. *Blood,* 92**,** 4730-41.
LUO, J., DENG, L., ZOU, H., GUO, Y., TONG, T., HUANG, M., LING, G. & LI, P. 2023. New insights into the ambivalent role of YAP/TAZ in human cancers. *J Exp Clin Cancer Res,* 42**,** 130.
LV, M., SHEN, Y., YANG, J., LI, S., WANG, B., CHEN, Z., LI, P., LIU, P. & YANG, J. 2017. Angiomotin Family Members: Oncogenes or Tumor Suppressors? *Int J Biol Sci,* 13**,** 772-781.
MA, S., KANAI, R., POBBATI, A. V., LI, S., CHE, K., SEAVEY, C. N., HALLETT, A., BURTSCHER, A., LAMAR, J. M. & RUBIN, B. P. 2022. The TAZ-CAMTA1 Fusion Protein Promotes Tumorigenesis via Connective Tissue Growth Factor and Ras-MAPK Signaling in Epithelioid Hemangioendothelioma. *Clin Cancer Res,* 28**,** 3116-3126.
MA, S., MENG, Z., CHEN, R. & GUAN, K. L. 2019. The Hippo Pathway: Biology and Pathophysiology.

*Annu Rev Biochem,* 88**,** 577-604.
MACARA, I. G. 2004. Parsing the polarity code. *Nat Rev Mol Cell Biol,* 5**,** 220-31.
MACHNICKA, B., GROCHOWALSKA, R., BOGUSLAWSKA, D. M., SIKORSKI, A. F. & LECOMTE, M. C. 2012. Spectrin-based skeleton as an actor in cell signaling. *Cell Mol Life Sci,* 69**,** 191-201.
MACRAE, C. A. & PETERSON, R. T. 2015. Zebrafish as tools for drug discovery. *Nat Rev Drug Discov,* 14**,** 721-31.
MAISONPIERRE, P. C., SURI, C., JONES, P. F., BARTUNKOVA, S., WIEGAND, S. J., RADZIEJEWSKI, C., COMPTON, D., MCCLAIN, J., ALDRICH, T. H., PAPADOPOULOS, N., DALY, T. J., DAVIS, S., SATO, T. N. & YANCOPOULOS, G. D. 1997. Angiopoietin-2, a natural antagonist for Tie2 that disrupts in vivo angiogenesis. *Science,* 277**,** 55-60.
MALI, P., AACH, J., STRANGES, P. B., ESVELT, K. M., MOOSBURNER, M., KOSURI, S., YANG, L. & CHURCH, G. M. 2013a. CAS9 transcriptional activators for target specificity screening and paired nickases for cooperative genome engineering. *Nat Biotechnol,* 31**,** 833-8.
MALI, P., YANG, L., ESVELT, K. M., AACH, J., GUELL, M., DICARLO, J. E., NORVILLE, J. E. & CHURCH, G. M. 2013b. RNA-guided human genome engineering via Cas9. *Science,* 339**,** 823-6.
MANNING, S. A., KROEGER, B. & HARVEY, K. F. 2020. The regulation of Yorkie, YAP and TAZ: new insights into the Hippo pathway. *Development,* 147.
MARCUS, G. A., SILVERMAN, N., BERGER, S. L., HORIUCHI, J. & GUARENTE, L. 1994. Functional similarity and physical association between GCN5 and ADA2: putative transcriptional adaptors. *EMBO J,* 13**,** 4807-15.
MARQUES, I. J., WEISS, F. U., VLECKEN, D. H., NITSCHE, C., BAKKERS, J., LAGENDIJK, A. K., PARTECKE, L. I., HEIDECKE, C. D., LERCH, M. M. & BAGOWSKI, C. P. 2009. Metastatic behaviour of primary human tumours in a zebrafish xenotransplantation model. *BMC Cancer,* 9**,** 128.
MARTIN, F. J., AMODE, M. R., ANEJA, A., AUSTINE-ORIMOLOYE, O., AZOV, A. G., BARNES, I., BECKER, A., BENNETT, R., BERRY, A., BHAI, J., BHURJI, S. K., BIGNELL, A., BODDU, S., BRANCO LINS, P. R., BROOKS, L., RAMARAJU, S. B., CHARKHCHI, M., COCKBURN, A., DA RIN FIORRETTO, L., DAVIDSON, C., DODIYA, K., DONALDSON, S., EL HOUDAIGUI, B., EL NABOULSI, T., FATIMA, R., GIRON, C. G., GENEZ, T., GHATTAORAYA, G. S., MARTINEZ, J. G., GUIJARRO, C., HARDY, M., HOLLIS, Z., HOURLIER, T., HUNT, T., KAY, M., KAYKALA, V., LE, T., LEMOS, D., MARQUES-COELHO, D., MARUGAN, J. C., MERINO, G. A., MIRABUENO, L. P., MUSHTAQ, A., HOSSAIN, S. N., OGEH, D. N., SAKTHIVEL, M. P., PARKER, A., PERRY, M., PILIZOTA, I., PROSOVETSKAIA, I., PEREZ-SILVA, J. G., SALAM, A. I. A., SARAIVA-AGOSTINHO, N., SCHUILENBURG, H., SHEPPARD, D., SINHA, S., SIPOS, B., STARK, W., STEED, E., SUKUMARAN, R., SUMATHIPALA, D., SUNER, M. M., SURAPANENI, L., SUTINEN, K., SZPAK, M., TRICOMI, F. F., URBINA-GOMEZ, D., VEIDENBERG, A., WALSH, T. A., WALTS, B., WASS, E., WILLHOFT, N., ALLEN, J., ALVAREZ-JARRETA, J., CHAKIACHVILI, M., FLINT, B., GIORGETTI, S., HAGGERTY, L., ILSLEY, G. R., LOVELAND, J. E., MOORE, B., MUDGE, J. M., TATE, J., THYBERT, D., TREVANION, S. J., WINTERBOTTOM, A., FRANKISH, A., HUNT, S. E., RUFFIER, M., CUNNINGHAM, F., DYER, S., FINN, R. D., HOWE, K. L., HARRISON, P. W., YATES, A. D. & FLICEK, P. 2023. Ensembl 2023. *Nucleic Acids Res,* 51**,** D933-D941.
MASCARENHAS, D., METTLER, I. J., PIERCE, D. A. & LOWE, H. W. 1990. Intron-mediated enhancement of heterologous gene expression in maize. *Plant Mol Biol,* 15**,** 913-20.
MATTER, K., AIJAZ, S., TSAPARA, A. & BALDA, M. S. 2005. Mammalian tight junctions in the regulation of epithelial differentiation and proliferation. *Curr Opin Cell Biol,* 17**,** 453-8.
MATTICK, J. S. & MAKUNIN, I. V. 2006. Non-coding RNA. *Hum Mol Genet,* 15 Spec No 1**,** R17-29.
MAYDEN, R. L., TANG, K. L., CONWAY, K. W., FREYHOF, J., CHAMBERLAIN, S., HASKINS, M., SCHNEIDER, L., SUDKAMP, M., WOOD, R. M., AGNEW, M., BUFALINO, A., SULAIMAN, Z., MIYA,

M., SAITOH, K. & HE, S. 2007. Phylogenetic relationships of Danio within the order Cypriniformes: a framework for comparative and evolutionary studies of a model species. *J Exp Zool B Mol Dev Evol,* 308**,** 642-54.

MCGREGOR, L., MAKELA, V., DARLING, S. M., VRONTOU, S., CHALEPAKIS, G., ROBERTS, C., SMART, N., RUTLAND, P., PRESCOTT, N., HOPKINS, J., BENTLEY, E., SHAW, A., ROBERTS, E., MUELLER, R., JADEJA, S., PHILIP, N., NELSON, J., FRANCANNET, C., PEREZ-AYTES, A., MEGARBANE, A., KERR, B., WAINWRIGHT, B., WOOLF, A. S., WINTER, R. M. & SCAMBLER, P. J. 2003. Fraser syndrome and mouse blebbed phenotype caused by mutations in FRAS1/Fras1 encoding a putative extracellular matrix protein. *Nat Genet,* 34**,** 203-8.

MCLAUCHLAN, J., GAFFNEY, D., WHITTON, J. L. & CLEMENTS, J. B. 1985. The consensus sequence YGTGTTYY located downstream from the AATAAA signal is required for efficient formation of mRNA 3' termini. *Nucleic Acids Res,* 13**,** 1347-68.

MCMAHON BJ, KWAAN HC. Components of the Plasminogen-Plasmin System as Biologic Markers for Cancer. *Adv Exp Med Biol*. 2015;867:145-56.

MEHENNI, H., GEHRIG, C., NEZU, J., OKU, A., SHIMANE, M., ROSSIER, C., GUEX, N., BLOUIN, J. L., SCOTT, H. S. & ANTONARAKIS, S. E. 1998. Loss of LKB1 kinase activity in Peutz-Jeghers syndrome, and evidence for allelic and locus heterogeneity. *Am J Hum Genet,* 63**,** 1641-50.

MENDLICK, M. R., NELSON, M., PICKERING, D., JOHANSSON, S. L., SEEMAYER, T. A., NEFF, J. R., VERGARA, G., ROSENTHAL, H. & BRIDGE, J. A. 2001. Translocation t(1;3)(p36.3;q25) is a nonrandom aberration in epithelioid hemangioendothelioma. *Am J Surg Pathol,* 25**,** 684-7.

MENG, Z., MOROISHI, T. & GUAN, K. L. 2016. Mechanisms of Hippo pathway regulation. *Genes Dev,* 30**,** 1-17.

MENG, Z., MOROISHI, T., MOTTIER-PAVIE, V., PLOUFFE, S. W., HANSEN, C. G., HONG, A. W., PARK, H. W., MO, J. S., LU, W., LU, S., FLORES, F., YU, F. X., HALDER, G. & GUAN, K. L. 2015. MAP4K family kinases act in parallel to MST1/2 to activate LATS1/2 in the Hippo pathway. *Nat Commun,* 6**,** 8357.

MERRITT, N., GARCIA, K., RAJENDRAN, D., LIN, Z. Y., ZHANG, X., MITCHELL, K. A., BORCHERDING, N., FULLENKAMP, C., CHIMENTI, M. S., GINGRAS, A. C., HARVEY, K. F. & TANAS, M. R. 2021. TAZ-CAMTA1 and YAP-TFE3 alter the TAZ/YAP transcriptome by recruiting the ATAC histone acetyltransferase complex. *Elife,* 10.

MERRITT, N. M., FULLENKAMP, C. A., HALL, S. L., QIAN, Q., DESAI, C., THOMASON, J., LAMBERTZ, A. M., DUPUY, A. J., DARBRO, B. & TANAS, M. R. 2018. A comprehensive evaluation of Hippo pathway silencing in sarcomas. *Oncotarget,* 9**,** 31620-31636.

MESSERLE, M., CRNKOVIC, I., HAMMERSCHMIDT, W., ZIEGLER, H. & KOSZINOWSKI, U. H. 1997. Cloning and mutagenesis of a herpesvirus genome as an infectious bacterial artificial chromosome. *Proc Natl Acad Sci U S A,* 94**,** 14759-63.

MEYER, A. & SCHARTL, M. 1999. Gene and genome duplications in vertebrates: the one-to-four (-to-eight in fish) rule and the evolution of novel gene functions. *Curr Opin Cell Biol,* 11**,** 699-704.

MI, W., GUAN, H., LYU, J., ZHAO, D., XI, Y., JIANG, S., ANDREWS, F. H., WANG, X., GAGEA, M., WEN, H., TORA, L., DENT, S. Y. R., KUTATELADZE, T. G., LI, W., LI, H. & SHI, X. 2017. YEATS2 links histone acetylation to tumorigenesis of non-small cell lung cancer. *Nat Commun,* 8**,** 1088.

MI, W., ZHANG, Y., LYU, J., WANG, X., TONG, Q., PENG, D., XUE, Y., TENCER, A. H., WEN, H., LI, W., KUTATELADZE, T. G. & SHI, X. 2018. The ZZ-type zinc finger of ZZZ3 modulates the ATAC complex-mediated histone acetylation and gene activation. *Nat Commun,* 9**,** 3759.

MIESFELD, J. B., GESTRI, G., CLARK, B. S., FLINN, M. A., POOLE, R. J., BADER, J. R., BESHARSE, J. C., WILSON, S. W. & LINK, B. A. 2015. Yap and Taz regulate retinal pigment epithelial cell fate. *Development,* 142**,** 3021-32.

MIRANDA, M. Z., BIALIK, J. F., SPEIGHT, P., DAN, Q., YEUNG, T., SZASZI, K., PEDERSEN, S. F. & KAPUS, A. 2017. TGF-beta1 regulates the expression and transcriptional activity of TAZ protein via a Smad3-independent, myocardin-related transcription factor-mediated mechanism. *J Biol Chem,* 292**,** 14902-14920.

MOHSENI, M., SUN, J., LAU, A., CURTIS, S., GOLDSMITH, J., FOX, V. L., WEI, C., FRAZIER, M., SAMSON, O., WONG, K. K., KIM, C. & CAMARGO, F. D. 2014. A genetic screen identifies an LKB1-MARK signalling axis controlling the Hippo-YAP pathway. *Nat Cell Biol,* 16**,** 108-17.

MOKHTARI, R. B., ASHAYERI, N., BAGHAIE, L., SAMBI, M., SATARI, K., BALUCH, N., BOSYKH, D. A., SZEWCZUK, M. R. & CHAKRABORTY, S. 2023. The Hippo Pathway Effectors YAP/TAZ-TEAD Oncoproteins as Emerging Therapeutic Targets in the Tumor Microenvironment. *Cancers (Basel),* 15.

MONACO, A. P. & LARIN, Z. 1994. YACs, BACs, PACs and MACs: artificial chromosomes as research tools. *Trends Biotechnol,* 12**,** 280-6.

MOON, S. B., KWON, H. J., PARK, K. W., YUN, W. J. & JUNG, S. E. 2009. Clinical experience with infantile hepatic hemangioendothelioma. *World J Surg,* 33**,** 597-602.

MOOTHA, V. K., LINDGREN, C. M., ERIKSSON, K. F., SUBRAMANIAN, A., SIHAG, S., LEHAR, J., PUIGSERVER, P., CARLSSON, E., RIDDERSTRALE, M., LAURILA, E., HOUSTIS, N., DALY, M. J., PATTERSON, N., MESIROV, J. P., GOLUB, T. R., TAMAYO, P., SPIEGELMAN, B., LANDER, E. S., HIRSCHHORN, J. N., ALTSHULER, D. & GROOP, L. C. 2003. PGC-1alpha-responsive genes involved in oxidative phosphorylation are coordinately downregulated in human diabetes. *Nat Genet,* 34**,** 267-73.

MOREIRA, A., WOLLERTON, M., MONKS, J. & PROUDFOOT, N. J. 1995. Upstream sequence elements enhance poly(A) site efficiency of the C2 complement gene and are phylogenetically conserved. *EMBO J,* 14**,** 3809-19.

MOROISHI, T., HANSEN, C. G. & GUAN, K. L. 2015a. The emerging roles of YAP and TAZ in cancer. *Nat Rev Cancer,* 15**,** 73-79.

MOROISHI, T., PARK, H. W., QIN, B., CHEN, Q., MENG, Z., PLOUFFE, S. W., TANIGUCHI, K., YU, F. X., KARIN, M., PAN, D. & GUAN, K. L. 2015b. A YAP/TAZ-induced feedback mechanism regulates Hippo pathway homeostasis. *Genes Dev,* 29**,** 1271-84.

MORRISON, H., SHERMAN, L. S., LEGG, J., BANINE, F., ISACKE, C., HAIPEK, C. A., GUTMANN, D. H., PONTA, H. & HERRLICH, P. 2001. The NF2 tumor suppressor gene product, merlin, mediates contact inhibition of growth through interactions with CD44. *Genes Dev,* 15**,** 968-80.

MOSIMANN, C., KAUFMAN, C. K., LI, P., PUGACH, E. K., TAMPLIN, O. J. & ZON, L. I. 2011. Ubiquitous transgene expression and Cre-based recombination driven by the ubiquitin promoter in zebrafish. *Development,* 138**,** 169-77.

MOSIMANN, C. & ZON, L. I. 2011. Advanced zebrafish transgenesis with Tol2 and application for Cre/lox recombination experiments. *Methods Cell Biol,* 104**,** 173-94.

MURA, M., SWAIN, R. K., ZHUANG, X., VORSCHMITT, H., REYNOLDS, G., DURANT, S., BEESLEY, J. F., HERBERT, J. M., SHELDON, H., ANDRE, M., SANDERSON, S., GLEN, K., LUU, N. T., MCGETTRICK, H. M., ANTCZAK, P., FALCIANI, F., NASH, G. B., NAGY, Z. S. & BICKNELL, R. 2012. Identification and angiogenic role of the novel tumor endothelial marker CLEC14A. *Oncogene,* 31**,** 293-305.

MURAKAMI, M., NAKAGAWA, M., OLSON, E. N. & NAKAGAWA, O. 2005. A WW domain protein TAZ is a critical coactivator for TBX5, a transcription factor implicated in Holt-Oram syndrome. *Proc Natl Acad Sci U S A,* 102**,** 18034-9.

MURAKAMI, M., TOMINAGA, J., MAKITA, R., UCHIJIMA, Y., KURIHARA, Y., NAKAGAWA, O., ASANO, T. & KURIHARA, H. 2006. Transcriptional activity of Pax3 is co-activated by TAZ. *Biochem Biophys Res Commun,* 339**,** 533-9.

NAGY, Z. & TORA, L. 2007. Distinct GCN5/PCAF-containing complexes function as co-activators and are involved in transcription factor and global histone acetylation. *Oncogene,* 26**,** 5341-57.

NAKAJIMA, H. & MOCHIZUKI, N. 2017. Flow pattern-dependent endothelial cell responses through transcriptional regulation. *Cell Cycle,* 16**,** 1893-1901.

NEIL, E., PAREDES, R., POOLEY, O., RUBIN, B. & KOUSKOFF, V. 2023. The oncogenic fusion protein TAZ::CAMTA1 promotes genomic instability and senescence through hypertranscription. *Commun Biol,* 6**,** 1174.

NEVINS, J. R. 1998. Toward an understanding of the functional complexity of the E2F and retinoblastoma families. *Cell Growth Differ,* 9**,** 585-93.

NI, L., ZHENG, Y., HARA, M., PAN, D. & LUO, X. 2015. Structural basis for Mob1-dependent activation of the core Mst-Lats kinase cascade in Hippo signaling. *Genes Dev,* 29**,** 1416-31.

NOLAND, C. L., GIERKE, S., SCHNIER, P. D., MURRAY, J., SANDOVAL, W. N., SAGOLLA, M., DEY, A., HANNOUSH, R. N., FAIRBROTHER, W. J. & CUNNINGHAM, C. N. 2016. Palmitoylation of TEAD Transcription Factors Is Required for Their Stability and Function in Hippo Pathway Signaling. *Structure,* 24**,** 179-186.

O'CONNOR, M., PEIFER, M. & BENDER, W. 1989. Construction of large DNA segments in Escherichia coli. *Science,* 244**,** 1307-12.

OFT M, HEIDER KH, BEUG H. TGFbeta signaling is necessary for carcinoma cell invasiveness and metastasis. *Curr Biol*. 1998 Nov 19;8(23):1243-52.

O'REILLY, M. S., HOLMGREN, L., SHING, Y., CHEN, C., ROSENTHAL, R. A., MOSES, M., LANE, W. S., CAO, Y., SAGE, E. H. & FOLKMAN, J. 1994. Angiostatin: a novel angiogenesis inhibitor that mediates the suppression of metastases by a Lewis lung carcinoma. *Cell,* 79**,** 315-28.

OCANA, A., VERA-BADILLO, F., SERUGA, B., TEMPLETON, A., PANDIELLA, A. & AMIR, E. 2013. HER3 overexpression and survival in solid tumors: a meta-analysis. *J Natl Cancer Inst,* 105**,** 266-73.

OMEROVIC, J., PUGGIONI, E. M., NAPOLETANO, S., VISCO, V., FRAIOLI, R., FRATI, L., GULINO, A. & ALIMANDI, M. 2004. Ligand-regulated association of ErbB-4 to the transcriptional co-activator YAP65 controls transcription at the nuclear level. *Exp Cell Res,* 294**,** 469-79.

ORTEGA, S., MALUMBRES, M. & BARBACID, M. 2002. Cyclin D-dependent kinases, INK4 inhibitors and cancer. *Biochim Biophys Acta,* 1602**,** 73-87.

OVERHOLTZER, M., ZHANG, J., SMOLEN, G. A., MUIR, B., LI, W., SGROI, D. C., DENG, C. X., BRUGGE, J. S. & HABER, D. A. 2006. Transforming properties of YAP, a candidate oncogene on the chromosome 11q22 amplicon. *Proc Natl Acad Sci U S A,* 103**,** 12405-10.

PAJTLER, K. W., WITT, H., SILL, M., JONES, D. T., HOVESTADT, V., KRATOCHWIL, F., WANI, K., TATEVOSSIAN, R., PUNCHIHEWA, C., JOHANN, P., REIMAND, J., WARNATZ, H. J., RYZHOVA, M., MACK, S., RAMASWAMY, V., CAPPER, D., SCHWEIZER, L., SIEBER, L., WITTMANN, A., HUANG, Z., VAN SLUIS, P., VOLCKMANN, R., KOSTER, J., VERSTEEG, R., FULTS, D., TOLEDANO, H., AVIGAD, S., HOFFMAN, L. M., DONSON, A. M., FOREMAN, N., HEWER, E., ZITTERBART, K., GILBERT, M., ARMSTRONG, T. S., GUPTA, N., ALLEN, J. C., KARAJANNIS, M. A., ZAGZAG, D., HASSELBLATT, M., KULOZIK, A. E., WITT, O., COLLINS, V. P., VON HOFF, K., RUTKOWSKI, S., PIETSCH, T., BADER, G., YASPO, M. L., VON DEIMLING, A., LICHTER, P., TAYLOR, M. D., GILBERTSON, R., ELLISON, D. W., ALDAPE, K., KORSHUNOV, A., KOOL, M. & PFISTER, S. M. 2015. Molecular Classification of Ependymal Tumors across All CNS Compartments, Histopathological Grades, and Age Groups. *Cancer Cell,* 27**,** 728-43.

PAJTLER, K. W., WEI, Y., OKONECHNIKOV, K., SILVA, P. B. G., VOURI, M., ZHANG, L., BRABETZ, S., SIEBER, L., GULLEY, M., MAUERMANN, M., WEDIG, T., MACK, N., IMAMURA KAWASAWA, Y., SHARMA, T., ZUCKERMANN, M., ANDREIUOLO, F., HOLLAND, E., MAASS, K., KORKEL-QU, H., LIU, H. K., SAHM, F., CAPPER, D., BUNT, J., RICHARDS, L. J., JONES, D. T. W., KORSHUNOV, A., CHAVEZ, L.,

LICHTER, P., HOSHINO, M., PFISTER, S. M., KOOL, M., LI, W. & KAWAUCHI, D. 2019. YAP1 subgroup supratentorial ependymoma requires TEAD and nuclear factor I-mediated transcriptional programmes for tumorigenesis. *Nat Commun,* 10**,** 3914.

PAN, D. 2010. The hippo signaling pathway in development and cancer. *Dev Cell,* 19**,** 491-505.

PAN, Z., TIAN, Y., CAO, C. & NIU, G. 2019. The Emerging Role of YAP/TAZ in Tumor Immunity. *Mol Cancer Res,* 17**,** 1777-1786.

PAN, Z., TIAN, Y., ZHANG, B., ZHANG, X., SHI, H., LIANG, Z., WU, P., LI, R., YOU, B., YANG, L., MAO, F., QIAN, H. & XU, W. 2017. YAP signaling in gastric cancer-derived mesenchymal stem cells is critical for its promoting role in cancer progression. *Int J Oncol,* 51**,** 1055-1066.

PANETTI, T. S. 2002. Differential effects of sphingosine 1-phosphate and lysophosphatidic acid on endothelial cells. *Biochim Biophys Acta,* 1582**,** 190-6.

PAOLI, P., GIANNONI, E. & CHIARUGI, P. 2013. Anoikis molecular pathways and its role in cancer progression. *Biochim Biophys Acta,* 1833**,** 3481-3498.

PARK, K. S., WHITSETT, J. A., DI PALMA, T., HONG, J. H., YAFFE, M. B. & ZANNINI, M. 2004. TAZ interacts with TTF-1 and regulates expression of surfactant protein-C. *J Biol Chem,* 279**,** 17384-90.

PARKER, M., MOHANKUMAR, K. M., PUNCHIHEWA, C., WEINLICH, R., DALTON, J. D., LI, Y., LEE, R., TATEVOSSIAN, R. G., PHOENIX, T. N., THIRUVENKATAM, R., WHITE, E., TANG, B., ORISME, W., GUPTA, K., RUSCH, M., CHEN, X., LI, Y., NAGAHAWHATTE, P., HEDLUND, E., FINKELSTEIN, D., WU, G., SHURTLEFF, S., EASTON, J., BOGGS, K., YERGEAU, D., VADODARIA, B., MULDER, H. L., BECKSFORT, J., GUPTA, P., HUETHER, R., MA, J., SONG, G., GAJJAR, A., MERCHANT, T., BOOP, F., SMITH, A. A., DING, L., LU, C., OCHOA, K., ZHAO, D., FULTON, R. S., FULTON, L. L., MARDIS, E. R., WILSON, R. K., DOWNING, J. R., GREEN, D. R., ZHANG, J., ELLISON, D. W. & GILBERTSON, R. J. 2014. C11orf95-RELA fusions drive oncogenic NF-kappaB signalling in ependymoma. *Nature,* 506**,** 451-5.

PAVEL, M., RENNA, M., PARK, S. J., MENZIES, F. M., RICKETTS, T., FULLGRABE, J., ASHKENAZI, A., FRAKE, R. A., LOMBARTE, A. C., BENTO, C. F., FRANZE, K. & RUBINSZTEIN, D. C. 2018. Contact inhibition controls cell survival and proliferation via YAP/TAZ-autophagy axis. *Nat Commun,* 9**,** 2961.

PAVLAKIS, E., CHIOTAKI, R. & CHALEPAKIS, G. 2011. The role of Fras1/Frem proteins in the structure and function of basement membrane. *Int J Biochem Cell Biol,* 43**,** 487-95.

PAVLETICH, N. P. 1999. Mechanisms of cyclin-dependent kinase regulation: structures of Cdks, their cyclin activators, and Cip and INK4 inhibitors. *J Mol Biol,* 287**,** 821-8.

PAVON MA, ARROYO-SOLERA I, CESPEDES MV, CASANOVA I, LEON X, MANGUES R. uPA/uPAR and SERPINE1 in head and neck cancer: role in tumor resistance, metastasis, prognosis and therapy. Oncotarget. 2016 Aug 30;7(35):57351-57366.

PAYNE, E. & LOOK, T. 2009. Zebrafish modelling of leukaemias. *Br J Haematol,* 146**,** 247-56.

PEARSON, J. D., HUANG, K., PACAL, M., MCCURDY, S. R., LU, S., AUBRY, A., YU, T., WADOSKY, K. M., ZHANG, L., WANG, T., GREGORIEFF, A., AHMAD, M., DIMARAS, H., LANGILLE, E., COLE, S. P. C., MONNIER, P. P., LOK, B. H., TSAO, M. S., AKENO, N., SCHRAMEK, D., WIKENHEISER-BROKAMP, K. A., KNUDSEN, E. S., WITKIEWICZ, A. K., WRANA, J. L., GOODRICH, D. W. & BREMNER, R. 2021. Binary pan-cancer classes with distinct vulnerabilities defined by pro- or anti-cancer YAP/TEAD activity. *Cancer Cell,* 39**,** 1115-1134 e12.

PETRILLI, A. M. & FERNANDEZ-VALLE, C. 2016. Role of Merlin/NF2 inactivation in tumor biology. *Oncogene,* 35**,** 537-48.

PICCOLO, S., DUPONT, S. & CORDENONSI, M. 2014. The biology of YAP/TAZ: hippo signaling and beyond. *Physiol Rev,* 94**,** 1287-312.

PICCOLO, S., PANCIERA, T., CONTESSOTTO, P. & CORDENONSI, M. 2023. YAP/TAZ as master regulators in cancer: modulation, function and therapeutic approaches. *Nat Cancer,* 4**,** 9-26.

PLOTNIKOV, A., ZEHORAI, E., PROCACCIA, S. & SEGER, R. 2011. The MAPK cascades: signaling components, nuclear roles and mechanisms of nuclear translocation. *Biochim Biophys Acta,* 1813**,** 1619-33.

PRASKOVA, M., KHOKLATCHEV, A., ORTIZ-VEGA, S. & AVRUCH, J. 2004. Regulation of the MST1 kinase by autophosphorylation, by the growth inhibitory proteins, RASSF1 and NORE1, and by Ras. *Biochem J,* 381**,** 453-62.

PRASKOVA, M., XIA, F. & AVRUCH, J. 2008. MOBKL1A/MOBKL1B phosphorylation by MST1 and MST2 inhibits cell proliferation. *Curr Biol,* 18**,** 311-21.

PROUDFOOT, N. J. 2011. Ending the message: poly(A) signals then and now. *Genes Dev,* 25**,** 1770-82.

QUELLE, D. E., ZINDY, F., ASHMUN, R. A. & SHERR, C. J. 1995. Alternative reading frames of the INK4a tumor suppressor gene encode two unrelated proteins capable of inducing cell cycle arrest. *Cell,* 83**,** 993-1000.

RADZIKOWSKA, E., SZCZEPULSKA-WOJCIK, E., CHABOWSKI, M., ONISZH, K., LANGFORT, R. & ROSZKOWSKI, K. 2008. Pulmonary epithelioid haemangioendothelioma--interferon 2-alpha treatment--case report. *Pneumonol Alergol Pol,* 76**,** 281-5.

REDDY KB, HOCEVAR BA, HOWE PH. Inhibition of G1 phase cyclin dependent kinases by transforming growth factor beta 1. *J Cell Biochem*. 1994 Nov;56(3):418-25. doi: 10.1002/jcb.240560318. PMID: 7876335.

REECE-HOYES, J. S. & WALHOUT, A. J. M. 2018. Gateway Recombinational Cloning. *Cold Spring Harb Protoc,* 2018**,** pdb top094912.

REGUE, L., MOU, F. & AVRUCH, J. 2013. G protein-coupled receptors engage the mammalian Hippo pathway through F-actin: F-Actin, assembled in response to Galpha12/13 induced RhoA-GTP, promotes dephosphorylation and activation of the YAP oncogene. *Bioessays,* 35**,** 430-5.

RIOU, S., MORELON, E., GUIBAUD, L., CHOTEL, F., DIJOUD, F. & MAREC-BERARD, P. 2012. Efficacy of rapamycin for refractory hemangioendotheliomas in Maffucci's syndrome. *J Clin Oncol,* 30**,** e213-5.

ROBERTS AB, SPORN MB. Transforming growth factor-beta: potential common mechanisms mediating its effects on embryogenesis, inflammation-repair, and carcinogenesis. *Int J Rad Appl Instrum B*. 1987;14(4):435-9.

ROBINSON, J. T., THORVALDSDOTTIR, H., WINCKLER, W., GUTTMAN, M., LANDER, E. S., GETZ, G. & MESIROV, J. P. 2011. Integrative genomics viewer. *Nat Biotechnol,* 29**,** 24-6.

RONICKE, V., RISAU, W. & BREIER, G. 1996. Characterization of the endothelium-specific murine vascular endothelial growth factor receptor-2 (Flk-1) promoter. *Circ Res,* 79**,** 277-85.

ROSENBAUM, E., JADEJA, B., XU, B., ZHANG, L., AGARAM, N. P., TRAVIS, W., SINGER, S., TAP, W. D. & ANTONESCU, C. R. 2020. Prognostic stratification of clinical and molecular epithelioid hemangioendothelioma subsets. *Mod Pathol,* 33**,** 591-602.

ROSENBERG, A. & AGULNIK, M. 2018. Epithelioid Hemangioendothelioma: Update on Diagnosis and Treatment. *Curr Treat Options Oncol,* 19**,** 19.

ROSS, J. & SULLIVAN, T. D. 1985. Half-lives of beta and gamma globin messenger RNAs and of protein synthetic capacity in cultured human reticulocytes. *Blood,* 66**,** 1149-54.

ROTELLO RJ, LIEBERMAN RC, PURCHIO AF, GERSCHENSON LE. Coordinated regulation of apoptosis and cell proliferation by transforming growth factor beta 1 in cultured uterine epithelial cells. *Proc Natl Acad Sci U S A*. 1991 Apr 15;88(8):3412-5.

ROULEAU, G. A., MEREL, P., LUTCHMAN, M., SANSON, M., ZUCMAN, J., MARINEAU, C., HOANG-XUAN, K., DEMCZUK, S., DESMAZE, C., PLOUGASTEL, B. & ET AL. 1993. Alteration in a new

gene encoding a putative membrane-organizing protein causes neuro-fibromatosis type 2. *Nature,* 363**,** 515-21.

ROUSSEL, M. F. 1999. The INK4 family of cell cycle inhibitors in cancer. *Oncogene,* 18**,** 5311-7.

RUAS, M., BROOKES, S., MCDONALD, N. Q. & PETERS, G. 1999. Functional evaluation of tumour-specific variants of p16INK4a/CDKN2A: correlation with protein structure information. *Oncogene,* 18**,** 5423-34.

RUAS, M. & PETERS, G. 1998. The p16INK4a/CDKN2A tumor suppressor and its relatives. *Biochim Biophys Acta,* 1378**,** F115-77.

SAADA, E., SAINT PAUL, M. C., GUGENHEIM, J., FOLLANA, P. & FRANCOIS, E. 2014. Metastatic hepatic epithelioid hemangio-endothelioma: long-term response to sunitinib malate. *Oncol Res Treat,* 37**,** 124-6.

SABAAWY, H. E., AZUMA, M., EMBREE, L. J., TSAI, H. J., STAROST, M. F. & HICKSTEIN, D. D. 2006. TEL-AML1 transgenic zebrafish model of precursor B cell acute lymphoblastic leukemia. *Proc Natl Acad Sci U S A,* 103**,** 15166-71.

SABIO, G. & DAVIS, R. J. 2014. TNF and MAP kinase signalling pathways. *Semin Immunol,* 26**,** 237-45.

SALISBURY, J., HUTCHISON, K. W. & GRABER, J. H. 2006. A multispecies comparison of the metazoan 3'-processing downstream elements and the CstF-64 RNA recognition motif. *BMC Genomics,* 7**,** 55.

SAMADDER, P., SIVAMANI, E., LU, J., LI, X. & QU, R. 2008. Transcriptional and post-transcriptional enhancement of gene expression by the 5' UTR intron of rice rubi3 gene in transgenic rice cells. *Mol Genet Genomics,* 279**,** 429-39.

SANDBERG, R., NEILSON, J. R., SARMA, A., SHARP, P. A. & BURGE, C. B. 2008. Proliferating cells express mRNAs with shortened 3' untranslated regions and fewer microRNA target sites. *Science,* 320**,** 1643-7.

SANTACRUZ, H., VRIZ, S. & ANGELIER, N. 1997. Molecular characterization of a heat shock cognate cDNA of zebrafish, hsc70, and developmental expression of the corresponding transcripts. *Dev Genet,* 21**,** 223-33.

SARDARO, A., BARDOSCIA, L., PETRUZZELLI, M. F. & PORTALURI, M. 2014. Epithelioid hemangioendothelioma: an overview and update on a rare vascular tumor. *Oncol Rev,* 8**,** 259.

SAVAGNER, P. 2010. The epithelial-mesenchymal transition (EMT) phenomenon. *Ann Oncol,* 21 Suppl 7**,** vii89-92.

SAVITSKY, M., KIM, M., KRAVCHUK, O. & SCHWARTZ, Y. B. 2016. Distinct Roles of Chromatin Insulator Proteins in Control of the Drosophila Bithorax Complex. *Genetics,* 202**,** 601-17.

SCHEER, N. & CAMPOS-ORTEGA, J. A. 1999. Use of the Gal4-UAS technique for targeted gene expression in the zebrafish. *Mech Dev,* 80**,** 153-8.

SCHIEMANN, W. P., BLOBE, G. C., KALUME, D. E., PANDEY, A. & LODISH, H. F. 2002. Context-specific effects of fibulin-5 (DANCE/EVEC) on cell proliferation, motility, and invasion. Fibulin-5 is induced by transforming growth factor-beta and affects protein kinase cascades. *J Biol Chem,* 277**,** 27367-77.

SCHRAIVOGEL, D., WEINMANN, L., BEIER, D., TABATABAI, G., EICHNER, A., ZHU, J. Y., ANTON, M., SIXT, M., WELLER, M., BEIER, C. P. & MEISTER, G. 2011. CAMTA1 is a novel tumour suppressor regulated by miR-9/9* in glioblastoma stem cells. *EMBO J,* 30**,** 4309-22.

SCHUETZE, S. M., BALLMAN, K. V., HEISE, R., GANJOO, K. N., DAVIS, E. J., GEORGE, S., BURGESS, M. A., CHOY, E., SHEPARD, D. R., TINOCO, G., HIRBE, A., KELLY, C. M., ATTIA, S., DESHPANDE, H. A., SCHWARTZ, G. K., SIONTIS, B. L., RIEDEL, R. F., VON MEHREN, M., KOZLOWSKI, E., CHEN, H. X., ASTBURY, C. & RUBIN, B. P. 2024. A Single Arm Phase 2 Trial of Trametinib in Patients With Locally Advanced or Metastatic Epithelioid Hemangioendothelioma. *Clin Cancer Res*.

SCHWERK, J. & SAVAN, R. 2015. Translating the Untranslated Region. *J Immunol,* 195**,** 2963-71.
SEAVEY, C. N., HALLETT, A., LI, S., CHE, K., POBBATI, A. V., MA, S., BURTSCHER, A., KANAI, R., LAMAR, J. M. & RUBIN, B. P. 2023. Loss of CDKN2A cooperates with WWTR1(TAZ)-CAMTA1 gene fusion to promote tumor progression in epithelioid hemangioendothelioma. *Clin Cancer Res*.
SEAVEY, C. N., POBBATI, A. V., HALLETT, A., MA, S., REYNOLDS, J. P., KANAI, R., LAMAR, J. M. & RUBIN, B. P. 2021. WWTR1(TAZ)-CAMTA1 gene fusion is sufficient to dysregulate YAP/TAZ signaling and drive epithelioid hemangioendothelioma tumorigenesis. *Genes Dev,* 35**,** 512-527.
SELIGSON, N. D., AWASTHI, A., MILLIS, S. Z., TURPIN, B. K., MEYER, C. F., GRAND'MAISON, A., LIEBNER, D. A., HAYS, J. L. & CHEN, J. L. 2019. Common Secondary Genomic Variants Associated With Advanced Epithelioid Hemangioendothelioma. *JAMA Netw Open,* 2**,** e1912416.
SERRA, S. & CHETTY, R. 2018. p16. *J Clin Pathol,* 71**,** 853-858.
SERRANO, M. 1997. The tumor suppressor protein p16INK4a. *Exp Cell Res,* 237**,** 7-13.
SERRANO, M., LIN, A. W., MCCURRACH, M. E., BEACH, D. & LOWE, S. W. 1997. Oncogenic ras provokes premature cell senescence associated with accumulation of p53 and p16INK4a. *Cell,* 88**,** 593-602.
SHANER, N. C., LAMBERT, G. G., CHAMMAS, A., NI, Y., CRANFILL, P. J., BAIRD, M. A., SELL, B. R., ALLEN, J. R., DAY, R. N., ISRAELSSON, M., DAVIDSON, M. W. & WANG, J. 2013. A bright monomeric green fluorescent protein derived from Branchiostoma lanceolatum. *Nat Methods,* 10**,** 407-9.
SHAUL, O. 2017. How introns enhance gene expression. *Int J Biochem Cell Biol,* 91**,** 145-155.
SHEETS, M. D., OGG, S. C. & WICKENS, M. P. 1990. Point mutations in AAUAAA and the poly (A) addition site: effects on the accuracy and efficiency of cleavage and polyadenylation in vitro. *Nucleic Acids Res,* 18**,** 5799-805.
SHERR, C. J. & ROBERTS, J. M. 1995. Inhibitors of mammalian G1 cyclin-dependent kinases. *Genes Dev,* 9**,** 1149-63.
SHI, F., TELESCO, S. E., LIU, Y., RADHAKRISHNAN, R. & LEMMON, M. A. 2010. ErbB3/HER3 intracellular domain is competent to bind ATP and catalyze autophosphorylation. *Proc Natl Acad Sci U S A,* 107**,** 7692-7.
SHIBA, S., IMAOKA, H., SHIOJI, K., SUZUKI, E., HORIGUCHI, S., TERASHIMA, T., KOJIMA, Y., OKUNO, T., SUKAWA, Y., TSUJI, K., UMEMOTO, K., ASAGI, A., TODAKA, A., UENO, M., IKEDA, M., MORIZANE, C. & FURUSE, J. 2018. Clinical characteristics of Japanese patients with epithelioid hemangioendothelioma: a multicenter retrospective study. *BMC Cancer,* 18**,** 993.
SHIBUE, T. & WEINBERG, R. A. 2017. EMT, CSCs, and drug resistance: the mechanistic link and clinical implications. *Nat Rev Clin Oncol,* 14**,** 611-629.
SHIZUYA, H., BIRREN, B., KIM, U. J., MANCINO, V., SLEPAK, T., TACHIIRI, Y. & SIMON, M. 1992. Cloning and stable maintenance of 300-kilobase-pair fragments of human DNA in Escherichia coli using an F-factor-based vector. *Proc Natl Acad Sci U S A,* 89**,** 8794-7.
SIDOR, C., BORREGUERO-MUNOZ, N., FLETCHER, G. C., ELBEDIWY, A., GUILLERMIN, O. & THOMPSON, B. J. 2019. Mask family proteins ANKHD1 and ANKRD17 regulate YAP nuclear import and stability. *Elife,* 8.
SIMONE TM, HIGGINS PJ. Small Molecule PAI-1 Functional Inhibitor Attenuates Vascular Smooth Muscle Cell Migration and Survival: Implications for the Therapy of Vascular Disease. *New Horiz Transl Med.* 2014 Sep 1;2(1):16-19.
SIMONE TM, LONGMATE WM, LAW BK, HIGGINS PJ. Targeted Inhibition of PAI-1 Activity Impairs Epithelial Migration and Wound Closure Following Cutaneous Injury. *Adv Wound Care* (New Rochelle). 2015 Jun 1;4(6):321-328.
SIMPSON, C. D., ANYIWE, K. & SCHIMMER, A. D. 2008. Anoikis resistance and tumor metastasis.

*Cancer Lett,* 272**,** 177-85.
SITHANANDAM, G. & ANDERSON, L. M. 2008. The ERBB3 receptor in cancer and cancer gene therapy. *Cancer Gene Ther,* 15**,** 413-48.
SLESAK, B., HARLOZINSKA, A., POREBSKA, I., BOJAROWSKI, T., LAPINSKA, J., RZESZUTKO, M. & WOJNAR, A. 1998. Expression of epidermal growth factor receptor family proteins (EGFR, c-erbB-2 and c-erbB-3) in gastric cancer and chronic gastritis. *Anticancer Res,* 18**,** 2727-32.
SMITH, M. P., FERGUSON, J., AROZARENA, I., HAYWARD, R., MARAIS, R., CHAPMAN, A., HURLSTONE, A. & WELLBROCK, C. 2013. Effect of SMURF2 targeting on susceptibility to MEK inhibitors in melanoma. *J Natl Cancer Inst,* 105**,** 33-46.
SOAPE, M. P., VERMA, R., PAYNE, J. D., WACHTEL, M., HARDWICKE, F. & COBOS, E. 2015. Treatment of Hepatic Epithelioid Hemangioendothelioma: Finding Uses for Thalidomide in a New Era of Medicine. *Case Rep Gastrointest Med,* 2015**,** 326795.
SONENBERG, N. & HINNEBUSCH, A. G. 2009. Regulation of translation initiation in eukaryotes: mechanisms and biological targets. *Cell,* 136**,** 731-45.
SONG, S., AJANI, J. A., HONJO, S., MARU, D. M., CHEN, Q., SCOTT, A. W., HEALLEN, T. R., XIAO, L., HOFSTETTER, W. L., WESTON, B., LEE, J. H., WADHWA, R., SUDO, K., STROEHLEIN, J. R., MARTIN, J. F., HUNG, M. C. & JOHNSON, R. L. 2014. Hippo coactivator YAP1 upregulates SOX9 and endows esophageal cancer cells with stem-like properties. *Cancer Res,* 74**,** 4170-82.
SORRENTINO, G., RUGGERI, N., ZANNINI, A., INGALLINA, E., BERTOLIO, R., MAROTTA, C., NERI, C., CAPPUZZELLO, E., FORCATO, M., ROSATO, A., MANO, M., BICCIATO, S. & DEL SAL, G. 2017. Glucocorticoid receptor signalling activates YAP in breast cancer. *Nat Commun,* 8**,** 14073.
STACCHIOTTI, S., MIAH, A. B., FREZZA, A. M., MESSIOU, C., MOROSI, C., CARACENI, A., ANTONESCU, C. R., BAJPAI, J., BALDINI, E., BAUER, S., BIAGINI, R., BIELACK, S., BLAY, J. Y., BONVALOT, S., BOUKOVINAS, I., BOVEE, J., BOYE, K., BRODOWICZ, T., CALLEGARO, D., DE ALAVA, E., DEORAS-SUTLIFF, M., DUFRESNE, A., ERIKSSON, M., ERRANI, C., FEDENKO, A., FERRARESI, V., FERRARI, A., FLETCHER, C. D. M., GARCIA DEL MURO, X., GELDERBLOM, H., GLADDY, R. A., GOUIN, F., GRIGNANI, G., GUTKOVICH, J., HAAS, R., HINDI, N., HOHENBERGER, P., HUANG, P., JOENSUU, H., JONES, R. L., JUNGELS, C., KASPER, B., KAWAI, A., LE CESNE, A., LE GRANGE, F., LEITHNER, A., LEONARD, H., LOPEZ POUSA, A., MARTIN BROTO, J., MERIMSKY, O., MERRIAM, P., MICELI, R., MIR, O., MOLINARI, M., MONTEMURRO, M., OLDANI, G., PALMERINI, E., PANTALEO, M. A., PATEL, S., PIPERNO-NEUMANN, S., RAUT, C. P., RAVI, V., RAZAK, A. R. A., REICHARDT, P., RUBIN, B. P., RUTKOWSKI, P., SAFWAT, A. A., SANGALLI, C., SAPISOCHIN, G., SBARAGLIA, M., SCHEIPL, S., SCHOFFSKI, P., STRAUSS, D., STRAUSS, S. J., SUNDBY HALL, K., TAP, W. D., TRAMA, A., TWEDDLE, A., VAN DER GRAAF, W. T. A., VAN DE SANDE, M. A. J., VAN HOUDT, W., VAN OORTMERSSEN, G., WAGNER, A. J., WARTENBERG, M., WOOD, J., ZAFFARONI, N., ZIMMERMANN, C., CASALI, P. G., DEI TOS, A. P. & GRONCHI, A. 2021a. Epithelioid hemangioendothelioma, an ultra-rare cancer: a consensus paper from the community of experts. *ESMO Open,* 6**,** 100170.
STACCHIOTTI, S., SIMEONE, N., LO VULLO, S., BALDI, G. G., BRUNELLO, A., VINCENZI, B., PALASSINI, E., DAGRADA, G., COLLINI, P., MOROSI, C., GRECO, F. G., SBARAGLIA, M., DEI TOS, A. P., MARIANI, L., FREZZA, A. M. & CASALI, P. G. 2021b. Activity of sirolimus in patients with progressive epithelioid hemangioendothelioma: A case-series analysis within the Italian Rare Cancer Network. *Cancer,* 127**,** 569-576.
STACCHIOTTI, S., TAP, W., LEONARD, H., ZAFFARONI, N. & BALDI, G. G. 2023. New Molecular Insights, and the Role of Systemic Therapies and Collaboration for Treatment of Epithelioid Hemangioendothelioma (EHE). *Curr Treat Options Oncol,* 24**,** 667-679.
STEIN, C., BARDET, A. F., ROMA, G., BERGLING, S., CLAY, I., RUCHTI, A., AGARINIS, C., SCHMELZLE, T.,

BOUWMEESTER, T., SCHUBELER, D. & BAUER, A. 2015. YAP1 Exerts Its Transcriptional Control via TEAD-Mediated Activation of Enhancers. *PLoS Genet,* 11**,** e1005465.

STERNBERG, N., SAUER, B., HOESS, R. & ABREMSKI, K. 1986. Bacteriophage P1 cre gene and its regulatory region. Evidence for multiple promoters and for regulation by DNA methylation. *J Mol Biol,* 187**,** 197-212.

STEWART, C. L., STUHLMANN, H., JAHNER, D. & JAENISCH, R. 1982. De novo methylation, expression, and infectivity of retroviral genomes introduced into embryonal carcinoma cells. *Proc Natl Acad Sci U S A,* 79**,** 4098-102.

STRANO, S., MUNARRIZ, E., ROSSI, M., CASTAGNOLI, L., SHAUL, Y., SACCHI, A., OREN, M., SUDOL, M., CESARENI, G. & BLANDINO, G. 2001. Physical interaction with Yes-associated protein enhances p73 transcriptional activity. *J Biol Chem,* 276**,** 15164-73.

STREISINGER, G., WALKER, C., DOWER, N., KNAUBER, D. & SINGER, F. 1981. Production of clones of homozygous diploid zebra fish (Brachydanio rerio). *Nature,* 291**,** 293-6.

SUBRAMANIAN, A., TAMAYO, P., MOOTHA, V. K., MUKHERJEE, S., EBERT, B. L., GILLETTE, M. A., PAULOVICH, A., POMEROY, S. L., GOLUB, T. R., LANDER, E. S. & MESIROV, J. P. 2005. Gene set enrichment analysis: a knowledge-based approach for interpreting genome-wide expression profiles. *Proc Natl Acad Sci U S A,* 102**,** 15545-50.

SUETSUGU, Y., FUTAHASHI, R., KANAMORI, H., KADONO-OKUDA, K., SASANUMA, S., NARUKAWA, J., AJIMURA, M., JOURAKU, A., NAMIKI, N., SHIMOMURA, M., SEZUTSU, H., OSANAI-FUTAHASHI, M., SUZUKI, M. G., DAIMON, T., SHINODA, T., TANIAI, K., ASAOKA, K., NIWA, R., KAWAOKA, S., KATSUMA, S., TAMURA, T., NODA, H., KASAHARA, M., SUGANO, S., SUZUKI, Y., FUJIWARA, H., KATAOKA, H., ARUNKUMAR, K. P., TOMAR, A., NAGARAJU, J., GOLDSMITH, M. R., FENG, Q., XIA, Q., YAMAMOTO, K., SHIMADA, T. & MITA, K. 2013. Large scale full-length cDNA sequencing reveals a unique genomic landscape in a lepidopteran model insect, Bombyx mori. *G3 (Bethesda),* 3**,** 1481-92.

SUHAIL, Y., CAIN, M. P., VANAJA, K., KURYWCHAK, P. A., LEVCHENKO, A., KALLURI, R. & KSHITIZ 2019. Systems Biology of Cancer Metastasis. *Cell Syst,* 9**,** 109-127.

SUN, F. L. & ELGIN, S. C. 1999. Putting boundaries on silence. *Cell,* 99**,** 459-62.

SUSTER, M. L., ABE, G., SCHOUW, A. & KAWAKAMI, K. 2011. Transposon-mediated BAC transgenesis in zebrafish. *Nat Protoc,* 6**,** 1998-2021.

SUURMEIJER, A. J. H., DICKSON, B. C., SWANSON, D., SUNG, Y. S., ZHANG, L. & ANTONESCU, C. R. 2020. Variant WWTR1 gene fusions in epithelioid hemangioendothelioma-A genetic subset associated with cardiac involvement. *Genes Chromosomes Cancer,* 59**,** 389-395.

SZULZEWSKY, F., ARORA, S., HOELLERBAUER, P., KING, C., NATHAN, E., CHAN, M., CIMINO, P. J., OZAWA, T., KAWAUCHI, D., PAJTLER, K. W., GILBERTSON, R. J., PADDISON, P. J., VASIOUKHIN, V., GUJRAL, T. S. & HOLLAND, E. C. 2020. Comparison of tumor-associated YAP1 fusions identifies a recurrent set of functions critical for oncogenesis. *Genes Dev,* 34**,** 1051-1064.

SZULZEWSKY, F., HOLLAND, E. C. & VASIOUKHIN, V. 2021. YAP1 and its fusion proteins in cancer initiation, progression and therapeutic resistance. *Dev Biol,* 475**,** 205-221.

TAKAGAKI, Y. & MANLEY, J. L. 1997. RNA recognition by the human polyadenylation factor CstF. *Mol Cell Biol,* 17**,** 3907-14.

TALBOT, J. C., WALKER, M. B., CARNEY, T. J., HUYCKE, T. R., YAN, Y. L., BREMILLER, R. A., GAI, L., DELAURIER, A., POSTLETHWAIT, J. H., HAMMERSCHMIDT, M. & KIMMEL, C. B. 2012. fras1 shapes endodermal pouch 1 and stabilizes zebrafish pharyngeal skeletal development. *Development,* 139**,** 2804-13.

TAMURA, R. 2021. Current Understanding of Neurofibromatosis Type 1, 2, and Schwannomatosis. *Int J Mol Sci,* 22.

TANAS, M. R., MA, S., JADAAN, F. O., NG, C. K., WEIGELT, B., REIS-FILHO, J. S. & RUBIN, B. P. 2016. Mechanism of action of a WWTR1(TAZ)-CAMTA1 fusion oncoprotein. *Oncogene,* 35**,** 929-38.

TANAS, M. R., SBONER, A., OLIVEIRA, A. M., ERICKSON-JOHNSON, M. R., HESPELT, J., HANWRIGHT, P. J., FLANAGAN, J., LUO, Y., FENWICK, K., NATRAJAN, R., MITSOPOULOS, C., ZVELEBIL, M., HOCH, B. L., WEISS, S. W., DEBIEC-RYCHTER, M., SCIOT, R., WEST, R. B., LAZAR, A. J., ASHWORTH, A., REIS-FILHO, J. S., LORD, C. J., GERSTEIN, M. B., RUBIN, M. A. & RUBIN, B. P. 2011. Identification of a disease-defining gene fusion in epithelioid hemangioendothelioma. *Sci Transl Med,* 3**,** 98ra82.

TANG, J. C., XIE, A. Y. & CAI, X. J. 2014. [Diverse functions of fibulin-5 in tumors]. *Mol Biol (Mosk),* 48**,** 875-80.

TERNS, M. P. & TERNS, R. M. 2011. CRISPR-based adaptive immune systems. *Curr Opin Microbiol,* 14**,** 321-7.

THIERY, J. P., ACLOQUE, H., HUANG, R. Y. & NIETO, M. A. 2009. Epithelial-mesenchymal transitions in development and disease. *Cell,* 139**,** 871-90.

THISSE, C. & THISSE, B. 2008. High-resolution in situ hybridization to whole-mount zebrafish embryos. *Nat Protoc,* 3**,** 59-69.

THOMPSON, W., ROUCHKA, E. C. & LAWRENCE, C. E. 2003. Gibbs Recursive Sampler: finding transcription factor binding sites. *Nucleic Acids Res,* 31**,** 3580-5.

TIAN, B. & GRABER, J. H. 2012. Signals for pre-mRNA cleavage and polyadenylation. *Wiley Interdiscip Rev RNA,* 3**,** 385-96.

TIMPL, R., SASAKI, T., KOSTKA, G. & CHU, M. L. 2003. Fibulins: a versatile family of extracellular matrix proteins. *Nat Rev Mol Cell Biol,* 4**,** 479-89.

TROFATTER, J. A., MACCOLLIN, M. M., RUTTER, J. L., MURRELL, J. R., DUYAO, M. P., PARRY, D. M., ELDRIDGE, R., KLEY, N., MENON, A. G., PULASKI, K. & ET AL. 1993. A novel moesin-, ezrin-, radixin-like gene is a candidate for the neurofibromatosis 2 tumor suppressor. *Cell,* 72**,** 791-800.

TSUKITA, S., OISHI, K., SATO, N., SAGARA, J., KAWAI, A. & TSUKITA, S. 1994. ERM family members as molecular linkers between the cell surface glycoprotein CD44 and actin-based cytoskeletons. *J Cell Biol,* 126**,** 391-401.

URRUTIA, A. O. & HURST, L. D. 2003. The signature of selection mediated by expression on human genes. *Genome Res,* 13**,** 2260-4.

VALASTYAN, S. & WEINBERG, R. A. 2011. Tumor metastasis: molecular insights and evolving paradigms. *Cell,* 147**,** 275-92.

VALSAMAKIS, A., ZEICHNER, S., CARSWELL, S. & ALWINE, J. C. 1991. The human immunodeficiency virus type 1 polyadenylylation signal: a 3' long terminal repeat element upstream of the AAUAAA necessary for efficient polyadenylylation. *Proc Natl Acad Sci U S A,* 88**,** 2108-12.

VAN DER VELDEN, A. W. & THOMAS, A. A. 1999. The role of the 5' untranslated region of an mRNA in translation regulation during development. *Int J Biochem Cell Biol,* 31**,** 87-106.

VARELAS, X. 2014. The Hippo pathway effectors TAZ and YAP in development, homeostasis and disease. *Development,* 141**,** 1614-26.

VARELAS, X., SAKUMA, R., SAMAVARCHI-TEHRANI, P., PEERANI, R., RAO, B. M., DEMBOWY, J., YAFFE, M. B., ZANDSTRA, P. W. & WRANA, J. L. 2008. TAZ controls Smad nucleocytoplasmic shuttling and regulates human embryonic stem-cell self-renewal. *Nat Cell Biol,* 10**,** 837-48.

VARELAS, X. & WRANA, J. L. 2012. Coordinating developmental signaling: novel roles for the Hippo pathway. *Trends Cell Biol,* 22**,** 88-96.

VASSILEV, A., KANEKO, K. J., SHU, H., ZHAO, Y. & DEPAMPHILIS, M. L. 2001. TEAD/TEF transcription factors utilize the activation domain of YAP65, a Src/Yes-associated protein localized in the

cytoplasm. *Genes Dev,* 15**,** 1229-41.
VAUGHAN, L., TAN, C. T., CHAPMAN, A., NONAKA, D., MACK, N. A., SMITH, D., BOOTON, R., HURLSTONE, A. F. & MALLIRI, A. 2015. HUWE1 ubiquitylates and degrades the RAC activator TIAM1 promoting cell-cell adhesion disassembly, migration, and invasion. *Cell Rep,* 10**,** 88-102.
VEINOTTE, C. J., DELLAIRE, G. & BERMAN, J. N. 2014. Hooking the big one: the potential of zebrafish xenotransplantation to reform cancer drug screening in the genomic era. *Dis Model Mech,* 7**,** 745-54.
VENKATARAMAN, K., BROWN, K. M. & GILMARTIN, G. M. 2005. Analysis of a noncanonical poly(A) site reveals a tripartite mechanism for vertebrate poly(A) site recognition. *Genes Dev,* 19**,** 1315-27.
VILLEFRANC, J. A., AMIGO, J. & LAWSON, N. D. 2007. Gateway compatible vectors for analysis of gene function in the zebrafish. *Dev Dyn,* 236**,** 3077-87.
VITOLO, M. I., ANGLIN, I. E., MAHONEY, W. M., JR., RENOUD, K. J., GARTENHAUS, R. B., BACHMAN, K. E. & PASSANITI, A. 2007. The RUNX2 transcription factor cooperates with the YES-associated protein, YAP65, to promote cell transformation. *Cancer Biol Ther,* 6**,** 856-63.
VOLLOCH, V. & HOUSMAN, D. 1981. Stability of globin mRNA in terminally differentiating murine erythroleukemia cells. *Cell,* 23**,** 509-14.
WADA, K., ITOGA, K., OKANO, T., YONEMURA, S. & SASAKI, H. 2011. Hippo pathway regulation by cell morphology and stress fibers. *Development,* 138**,** 3907-14.
WAGNER, E. F. 2001. AP-1--Introductory remarks. *Oncogene,* 20**,** 2334-5.
WANG, G., LU, X., DEY, P., DENG, P., WU, C. C., JIANG, S., FANG, Z., ZHAO, K., KONAPARTHI, R., HUA, S., ZHANG, J., LI-NING-TAPIA, E. M., KAPOOR, A., WU, C. J., PATEL, N. B., GUO, Z., RAMAMOORTHY, V., TIEU, T. N., HEFFERNAN, T., ZHAO, D., SHANG, X., KHADKA, S., HOU, P., HU, B., JIN, E. J., YAO, W., PAN, X., DING, Z., SHI, Y., LI, L., CHANG, Q., TRONCOSO, P., LOGOTHETIS, C. J., MCARTHUR, M. J., CHIN, L., WANG, Y. A. & DEPINHO, R. A. 2016a. Targeting YAP-Dependent MDSC Infiltration Impairs Tumor Progression. *Cancer Discov,* 6**,** 80- 95.
WANG, G., WANG, Z., LU, H., ZHAO, Z., GUO, L., KONG, F., WANG, A. & ZHAO, S. 2022. Comprehensive analysis of FRAS1/FREM family as potential biomarkers and therapeutic targets in renal clear cell carcinoma. *Front Pharmacol,* 13**,** 972934.
WANG, K. C., YEH, Y. T., NGUYEN, P., LIMQUECO, E., LOPEZ, J., THOROSSIAN, S., GUAN, K. L., LI, Y. J. & CHIEN, S. 2016b. Flow-dependent YAP/TAZ activities regulate endothelial phenotypes and atherosclerosis. *Proc Natl Acad Sci U S A,* 113**,** 11525-11530.
WANG, L., ZHANG, Z., YU, X., HUANG, X., LIU, Z., CHAI, Y., YANG, L., WANG, Q., LI, M., ZHAO, J., HOU, J. & LI, F. 2019. Unbalanced YAP-SOX9 circuit drives stemness and malignant progression in esophageal squamous cell carcinoma. *Oncogene,* 38**,** 2042-2055.
WANG, W., HUANG, J. & CHEN, J. 2011. Angiomotin-like proteins associate with and negatively regulate YAP1. *J Biol Chem,* 286**,** 4364-70.
WANG, X., FREIRE VALLS, A., SCHERMANN, G., SHEN, Y., MOYA, I. M., CASTRO, L., URBAN, S., SOLECKI, G. M., WINKLER, F., RIEDEMANN, L., JAIN, R. K., MAZZONE, M., SCHMIDT, T., FISCHER, T., HALDER, G. & RUIZ DE ALMODOVAR, C. 2017. YAP/TAZ Orchestrate VEGF Signaling during Developmental Angiogenesis. *Dev Cell,* 42**,** 462-478 e7.
WANG, Z., GERSTEIN, M. & SNYDER, M. 2009. RNA-Seq: a revolutionary tool for transcriptomics. *Nat Rev Genet,* 10**,** 57-63.
WARNER, L. E., MANCIAS, P., BUTLER, I. J., MCDONALD, C. M., KEPPEN, L., KOOB, K. G. & LUPSKI, J. R. 1998. Mutations in the early growth response 2 (EGR2) gene are associated with hereditary myelinopathies. *Nat Genet,* 18**,** 382-4.

WEI, H., WANG, F., WANG, Y., LI, T., XIU, P., ZHONG, J., SUN, X. & LI, J. 2017. Verteporfin suppresses cell survival, angiogenesis and vasculogenic mimicry of pancreatic ductal adenocarcinoma via disrupting the YAP-TEAD complex. *Cancer Sci,* 108**,** 478-487.

WEINBERG, R. A. 1995. The retinoblastoma protein and cell cycle control. *Cell,* 81**,** 323-30.

WEISS, F. U., MARQUES, I. J., WOLTERING, J. M., VLECKEN, D. H., AGHDASSI, A., PARTECKE, L. I., HEIDECKE, C. D., LERCH, M. M. & BAGOWSKI, C. P. 2009. Retinoic acid receptor antagonists inhibit miR-10a expression and block metastatic behavior of pancreatic cancer. *Gastroenterology,* 137**,** 2136-45 e1-7.

WEISS, S. W. & ENZINGER, F. M. 1982. Epithelioid hemangioendothelioma: a vascular tumor often mistaken for a carcinoma. *Cancer,* 50**,** 970-81.

WEST, A. G., GASZNER, M. & FELSENFELD, G. 2002. Insulators: many functions, many mechanisms. *Genes Dev,* 16**,** 271-88.

WIEDENHEFT, B., STERNBERG, S. H. & DOUDNA, J. A. 2012. RNA-guided genetic silencing systems in bacteria and archaea. *Nature,* 482**,** 331-8.

WIERSON, W. A., WELKER, J. M., ALMEIDA, M. P., MANN, C. M., WEBSTER, D. A., TORRIE, M. E., WEISS, T. J., KAMBAKAM, S., VOLLBRECHT, M. K., LAN, M., MCKEIGHAN, K. C., LEVEY, J., MING, Z., WEHMEIER, A., MIKELSON, C. S., HALTOM, J. A., KWAN, K. M., CHIEN, C. B., BALCIUNAS, D., EKKER, S. C., CLARK, K. J., WEBBER, B. R., MORIARITY, B. S., SOLIN, S. L., CARLSON, D. F., DOBBS, D. L., MCGRAIL, M. & ESSNER, J. 2020. Efficient targeted integration directed by short homology in zebrafish and mammalian cells. *Elife,* 9.

WILLETT, C. E., CORTES, A., ZUASTI, A. & ZAPATA, A. G. 1999. Early hematopoiesis and developing lymphoid organs in the zebrafish. *Dev Dyn,* 214**,** 323-36.

WLAZLINSKI, A., ENGERS, R., HOFFMANN, M. J., HADER, C., JUNG, V., MULLER, M. & SCHULZ, W. A. 2007. Downregulation of several fibulin genes in prostate cancer. *Prostate,* 67**,** 1770-80.

WONG, C. W., HAN, H. W., TIEN, Y. W. & HSU, S. H. 2019. Biomaterial substrate-derived compact cellular spheroids mimicking the behavior of pancreatic cancer and microenvironment. *Biomaterials,* 213**,** 119202.

WONG, K. K., LI, W., AN, Y., DUAN, Y., LI, Z., KANG, Y. & YAN, Y. 2015. beta-Spectrin regulates the hippo signaling pathway and modulates the basal actin network. *J Biol Chem,* 290**,** 6397-407.

WU, R. S., LAM, II, CLAY, H., DUONG, D. N., DEO, R. C. & COUGHLIN, S. R. 2018. A Rapid Method for Directed Gene Knockout for Screening in G0 Zebrafish. *Dev Cell,* 46**,** 112-125 e4.

WU, S., HUANG, J., DONG, J. & PAN, D. 2003. hippo encodes a Ste-20 family protein kinase that restricts cell proliferation and promotes apoptosis in conjunction with salvador and warts. *Cell,* 114**,** 445-56.

XIAO, H., JIANG, N., ZHOU, B., LIU, Q. & DU, C. 2015. TAZ regulates cell proliferation and epithelial-mesenchymal transition of human hepatocellular carcinoma. *Cancer Sci,* 106**,** 151-9.

XIE, D., CUI, J., XIA, T., JIA, Z., WANG, L., WEI, W., ZHU, A., GAO, Y., XIE, K. & QUAN, M. 2015. Hippo transducer TAZ promotes epithelial mesenchymal transition and supports pancreatic cancer progression. *Oncotarget,* 6**,** 35949-63.

XIE, D., YIN, D., WANG, H. J., LIU, G. T., ELASHOFF, R., BLACK, K. & KOEFFLER, H. P. 2004. Levels of expression of CYR61 and CTGF are prognostic for tumor progression and survival of individuals with gliomas. *Clin Cancer Res,* 10**,** 2072-81.

XIE, M., ZHANG, L., HE, C. S., HOU, J. H., LIN, S. X., HU, Z. H., XU, F. & ZHAO, H. Y. 2012. Prognostic significance of TAZ expression in resected non-small cell lung cancer. *J Thorac Oncol,* 7**,** 799-807.

XU, H. M. & GUTMANN, D. H. 1998. Merlin differentially associates with the microtubule and actin cytoskeleton. *J Neurosci Res,* 51**,** 403-15.

XU, M., YE, Y., YE, Z., XU, S., LIU, W., XU, J., ZHANG, Y., LIU, Q., HUANG, Z. & ZHANG, W. 2020. Human

BCR/ABL1 induces chronic myeloid leukemia-like disease in zebrafish. *Haematologica,* 105**,** 674-686.

YAMAGUCHI, H. & TAOUK, G. M. 2020. A Potential Role of YAP/TAZ in the Interplay Between Metastasis and Metabolic Alterations. *Front Oncol,* 10**,** 928.

YANG, S. & LIU, G. 2017. Targeting the Ras/Raf/MEK/ERK pathway in hepatocellular carcinoma. *Oncol Lett,* 13**,** 1041-1047.

YANG, S., ZHANG, L., PUROHIT, V., SHUKLA, S. K., CHEN, X., YU, F., FU, K., CHEN, Y., SOLHEIM, J., SINGH, P. K., SONG, W. & DONG, J. 2015. Active YAP promotes pancreatic cancer cell motility, invasion and tumorigenesis in a mitotic phosphorylation-dependent manner through LPAR3. *Oncotarget,* 6**,** 36019-31.

YE, X. & WEINBERG, R. A. 2015. Epithelial-Mesenchymal Plasticity: A Central Regulator of Cancer Progression. *Trends Cell Biol,* 25**,** 675-686.

YEH, J. R., MUNSON, K. M., CHAO, Y. L., PETERSON, Q. P., MACRAE, C. A. & PETERSON, R. T. 2008. AML1-ETO reprograms hematopoietic cell fate by downregulating scl expression. *Development,* 135**,** 401-10.

YI, E. S., HARCLERODE, D., GONDO, M., STEPHENSON, M., BROWN, R. W., YOUNES, M. & CAGLE, P. T. 1997. High c-erbB-3 protein expression is associated with shorter survival in advanced non-small cell lung carcinomas. *Mod Pathol,* 10**,** 142-8.

YOUSAF, N., MARUZZO, M., JUDSON, I., AL-MUDERIS, O., FISHER, C. & BENSON, C. 2015. Systemic treatment options for epithelioid haemangioendothelioma: the Royal Marsden Hospital experience. *Anticancer Res,* 35**,** 473-80.

YU, F. X., MENG, Z., PLOUFFE, S. W. & GUAN, K. L. 2015a. Hippo pathway regulation of gastrointestinal tissues. *Annu Rev Physiol,* 77**,** 201-27.

YU, F. X., ZHAO, B. & GUAN, K. L. 2015b. Hippo Pathway in Organ Size Control, Tissue Homeostasis, and Cancer. *Cell,* 163**,** 811-28.

YU, F. X., ZHAO, B., PANUPINTHU, N., JEWELL, J. L., LIAN, I., WANG, L. H., ZHAO, J., YUAN, H., TUMANENG, K., LI, H., FU, X. D., MILLS, G. B. & GUAN, K. L. 2012. Regulation of the Hippo-YAP pathway by G-protein-coupled receptor signaling. *Cell,* 150**,** 780-91.

YU, P., YE, L., WANG, H., DU, G., ZHANG, J., ZHANG, J. & TIAN, J. 2015c. NSK-01105 inhibits proliferation and induces apoptosis of prostate cancer cells by blocking the Raf/MEK/ERK and PI3K/Akt/mTOR signal pathways. *Tumour Biol,* 36**,** 2143-53.

YUE, W., SUN, Q., LANDRENEAU, R., WU, C., SIEGFRIED, J. M., YU, J. & ZHANG, L. 2009. Fibulin-5 suppresses lung cancer invasion by inhibiting matrix metalloproteinase-7 expression. *Cancer Res,* 69**,** 6339-46.

ZANCONATO, F., BATTILANA, G., CORDENONSI, M. & PICCOLO, S. 2016a. YAP/TAZ as therapeutic targets in cancer. *Curr Opin Pharmacol,* 29**,** 26-33.

ZANCONATO, F., BATTILANA, G., FORCATO, M., FILIPPI, L., AZZOLIN, L., MANFRIN, A., QUARANTA, E., DI BIAGIO, D., SIGISMONDO, G., GUZZARDO, V., LEJEUNE, P., HAENDLER, B., KRIJGSVELD, J., FASSAN, M., BICCIATO, S., CORDENONSI, M. & PICCOLO, S. 2018. Transcriptional addiction in cancer cells is mediated by YAP/TAZ through BRD4. *Nat Med,* 24**,** 1599-1610.

ZANCONATO, F., CORDENONSI, M. & PICCOLO, S. 2016b. YAP/TAZ at the Roots of Cancer. *Cancer Cell,* 29**,** 783-803.

ZANCONATO, F., FORCATO, M., BATTILANA, G., AZZOLIN, L., QUARANTA, E., BODEGA, B., ROSATO, A., BICCIATO, S., CORDENONSI, M. & PICCOLO, S. 2015. Genome-wide association between YAP/TAZ/TEAD and AP-1 at enhancers drives oncogenic growth. *Nat Cell Biol,* 17**,** 1218-27.

ZARGHAMPOOR, F., AZARPIRA, N., KHATAMI, S. R., BEHZAD-BEHBAHANI, A. & FOROUGHMAND, A. M. 2019. Improved translation efficiency of therapeutic mRNA. *Gene,* 707**,** 231-238.

ZHAN, L., ROSENBERG, A., BERGAMI, K. C., YU, M., XUAN, Z., JAFFE, A. B., ALLRED, C. & MUTHUSWAMY, S. K. 2008. Deregulation of scribble promotes mammary tumorigenesis and reveals a role for cell polarity in carcinoma. *Cell,* 135**,** 865-78.

ZHANG, H., LIU, C. Y., ZHA, Z. Y., ZHAO, B., YAO, J., ZHAO, S., XIONG, Y., LEI, Q. Y. & GUAN, K. L. 2009. TEAD transcription factors mediate the function of TAZ in cell growth and epithelial-mesenchymal transition. *J Biol Chem,* 284**,** 13355-13362.

ZHANG, H., PASOLLI, H. A. & FUCHS, E. 2011. Yes-associated protein (YAP) transcriptional coactivator functions in balancing growth and differentiation in skin. *Proc Natl Acad Sci U S A,* 108**,** 2270-5.

ZHANG, J., ZHANG, Y. Z., JIANG, J. & DUAN, C. G. 2020. The Crosstalk Between Epigenetic Mechanisms and Alternative RNA Processing Regulation. *Front Genet,* 11**,** 998.

ZHANG, W., GAO, Y., LI, F., TONG, X., REN, Y., HAN, X., YAO, S., LONG, F., YANG, Z., FAN, H., ZHANG, L. & JI, H. 2015. YAP promotes malignant progression of Lkb1-deficient lung adenocarcinoma through downstream regulation of survivin. *Cancer Res,* 75**,** 4450-7.

ZHAO, B., LI, L., LU, Q., WANG, L. H., LIU, C. Y., LEI, Q. & GUAN, K. L. 2011. Angiomotin is a novel Hippo pathway component that inhibits YAP oncoprotein. *Genes Dev,* 25**,** 51-63.

ZHAO, B., LI, L., TUMANENG, K., WANG, C. Y. & GUAN, K. L. 2010. A coordinated phosphorylation by Lats and CK1 regulates YAP stability through SCF(beta-TRCP). *Genes Dev,* 24**,** 72-85.

ZHAO, B., LI, L., WANG, L., WANG, C. Y., YU, J. & GUAN, K. L. 2012. Cell detachment activates the Hippo pathway via cytoskeleton reorganization to induce anoikis. *Genes Dev,* 26**,** 54-68.

ZHAO, B., WEI, X., LI, W., UDAN, R. S., YANG, Q., KIM, J., XIE, J., IKENOUE, T., YU, J., LI, L., ZHENG, P., YE, K., CHINNAIYAN, A., HALDER, G., LAI, Z. C. & GUAN, K. L. 2007. Inactivation of YAP oncoprotein by the Hippo pathway is involved in cell contact inhibition and tissue growth control. *Genes Dev,* 21**,** 2747-61.

ZHAO, B., YE, X., YU, J., LI, L., LI, W., LI, S., YU, J., LIN, J. D., WANG, C. Y., CHINNAIYAN, A. M., LAI, Z. C. & GUAN, K. L. 2008. TEAD mediates YAP-dependent gene induction and growth control. *Genes Dev,* 22**,** 1962-71.

ZHAO, H., TANG, C., CUI, K., ANG, B. T. & WONG, S. T. 2009. A screening platform for glioma growth and invasion using bioluminescence imaging. Laboratory investigation. *J Neurosurg,* 111**,** 238- 46.

ZHENG, B., SUN, W., YI, K., ZHANG, Y., WANG, L., LAN, H., ZHANG, C., XIAN, H. & LI, R. 2021. Integrated Transcriptomic Analysis Reveals a Distinctive Role of YAP1 in Extramedullary Invasion and Therapeutic Sensitivity of Multiple Myeloma. *Front Oncol,* 11**,** 787814.

ZHENG, Y. & PAN, D. 2019. The Hippo Signaling Pathway in Development and Disease. *Dev Cell,* 50**,** 264-282.

ZHENG, Y., WANG, W., LIU, B., DENG, H., USTER, E. & PAN, D. 2015. Identification of Happyhour/MAP4K as Alternative Hpo/Mst-like Kinases in the Hippo Kinase Cascade. *Dev Cell,* 34**,** 642-55.

ZHENG, Z., WANG, H., JIANG, H., CHEN, E., ZHANG, J. & XIE, X. 2017. Apatinib for the treatment of pulmonary epithelioid hemangioendothelioma: A case report and literature review. *Medicine (Baltimore),* 96**,** e8507.

ZHOU, X., WANG, S., WANG, Z., FENG, X., LIU, P., LV, X. B., LI, F., YU, F. X., SUN, Y., YUAN, H., ZHU, H., XIONG, Y., LEI, Q. Y. & GUAN, K. L. 2015. Estrogen regulates Hippo signaling via GPER in breast cancer. *J Clin Invest,* 125**,** 2123-35.

ZHOU, Z. Q., CAO, W. H., XIE, J. J., LIN, J., SHEN, Z. Y., ZHANG, Q. Y., SHEN, J. H., XU, L. Y. & LI, E. M. 2009. Expression and prognostic significance of THBS1, Cyr61 and CTGF in esophageal squamous cell carcinoma. *BMC Cancer,* 9**,** 291.

ZHU, C., CHEN, X., LIU, T. Q., CHENG, L., CHENG, W., CHENG, P. & WU, A. H. 2024. Hexosaminidase B-

driven cancer cell-macrophage co-dependency promotes glycolysis addiction and tumorigenesis in glioblastoma. *Nat Commun,* 15**,** 8506.

ZHURAVLEVA, J., PAGGETTI, J., MARTIN, L., HAMMANN, A., SOLARY, E., BASTIE, J. N. & DELVA, L. 2008. MOZ/TIF2-induced acute myeloid leukaemia in transgenic fish. *Br J Haematol,* 143**,** 378-82.

ZIGLER, M., KAMIYA, T., BRANTLEY, E. C., VILLARES, G. J. & BAR-ELI, M. 2011. PAR-1 and thrombin: the ties that bind the microenvironment to melanoma metastasis. *Cancer Res,* 71**,** 6561-6.

ZINATIZADEH, M. R., MIRI, S. R., ZARANDI, P. K., CHALBATANI, G. M., RAPOSO, C., MIRZAEI, H. R., AKBARI, M. E. & MAHMOODZADEH, H. 2021. The Hippo Tumor Suppressor Pathway (YAP/TAZ/TEAD/MST/LATS) and EGFR-RAS-RAF-MEK in cancer metastasis. *Genes Dis,* 8**,** 48-60.